

**Field Measurements of Wind-Driven Rain on Mid - and High - Rise Buildings in Two
Canadian Regions**

Uzzwal Kumar Deb Nath

A Thesis
in
The Department
of
Building, Civil & Environmental Engineering

Presented in partial fulfilment of the requirements for the Degree of Master of Applied
Science (Building Engineering) at
Concordia University
Montreal, Quebec, Canada

December 2015

© Uzzwal Kumar Deb Nath, 2015

CONCORDIA UNIVERSITY
School of Graduate Studies

This is to certify that the thesis prepared

By: **Uzzwal Kumar Deb Nath**

Entitled: **Field Measurements of Wind-Driven Rain on Mid - and High - Rise Buildings in Two Canadian Regions**

and submitted in partial fulfillment of the requirements for the degree of

Master of Applied Science (Building Engineering)

complies with the regulations of the University and meets the accepted standards with respect to originality and quality.

Signed by the final examining committee:

| | |
|---------------------------|--------------------------------|
| _____ | Chair |
| Dr. Theodore Stathopoulos | |
| _____ | Examiner |
| Lucia Tirca | |
| _____ | Examiner External (to program) |
| Dr. Hoi Dick Ng | |
| _____ | Supervisor |
| Dr. Hua Ge | |

Approved by _____
Chair of Department or Graduate Program Director

Dean of Faculty

Date _____

ABSTRACT

Field Measurements of Wind-Driven Rain on Mid - and High - Rise Buildings in Two Canadian Regions

Uzzwal Kumar Deb Nath

Wind-driven rain (WDR) is an important boundary condition for the study of the hygrothermal behaviour and durability of building envelopes. Understanding the WDR characteristics is important for establishing designs that minimize the moisture related issues. The objectives of this study are to generate a unique set of measurements to characterize the WDR distribution on mid- and high-rise buildings for different Canadian climatic regions, to provide data for validating CFD models and to evaluate the accuracy of existing semi-empirical methods used for quantifying WDR loads on building façades. Three buildings located in two Canadian cities (i.e., McLeod House in Fredericton; HB and FB Building in Montreal) have been instrumented with equipment to simultaneously record local weather data of wind speed, wind direction, temperature, relative humidity, horizontal rainfall, and WDR loads on building façades. Onsite data, collected for fourteen months from McLeod House, fifteen months from HB Building, and twelve months from FB Building, has been used for analysis. The historical and onsite wind and rain conditions, spatial distribution of wind-driven rain on façades in terms of catch ratios and wall factors, and comparisons between measured and predicted wind-driven rain using the semi-empirical models are reported for the monitoring periods.

The analysis of field measurements shows that catch ratios vary with rain events with higher values at the corners and edges of the façades. Typically catch ratios are higher at the top of the facades and decrease towards the bottom. The catch ratios are higher for the thirteen story high-rise building compared to the four and seven story mid-rise buildings at the same height below the roofline. Catch ratios are higher when approaching wind is normal to the façade and values increase with the increase of wind speed. Discrepancies between the ISO standard suggested wall factors and wall factors calculated based on measurements are observed for all three test buildings. It is found that the wall factors vary along both the building height and across the building width,

while the ISO standard only suggests two values along the building height with no change across the building width. The ISO semi-empirical model overestimates the WDR at all monitored façade locations on McLeod House and HB Building, and 83% of the monitored façade locations on FB Building. The ASHRAE 160 model overestimates the WDR amount largely for most of the monitored façade locations of the test buildings. The discrepancies between measurements and predictions using semi-empirical models are due to the lack of variation of wall factors across building façade suggested in the standards and limited number of building geometries. The errors associated with WDR measurements vary with rain events with the maximum error contributed by adhesion-water-evaporation, however, the total amount of error is small as compared to WDR amount. To improve the semi-empirical models for estimating WDR on façade, wall factors based on field measurements on buildings with a wider range of building geometries and at more façade locations are needed.

Acknowledgements

It was a great pleasure for me to work with all the amazing people in Department of Building, Civil and Environmental Engineering in Concordia University, Montreal, Quebec. I would like to thank my supervisor Dr. Hua Ge for giving me the opportunity to conduct my Master's degree under her guidance and supervision. Her invaluable support, encouragement, motivation, and continuous guidance throughout the project made its successful completion. During this period, I learned a lot and I am fully confident that this knowledge will help me in future.

A special thanks to my friend and colleague Vincent Chiu for his co-operation throughout the project. I would also like to acknowledge Ali Sehzadeh and my other colleagues for the great time I had with them.

I would like to thank Dr. Y. H. Chui, Mr. Jianhui Zhang and Mr. Dean McCarthy from University of New Brunswick and Mr. Daniel Gauthier, Mr. Patrick Sullivan, Mr. Sylvaine Lalumiere and Mr. Victor of Concordia University for their assistance in setting up the field measurements and the data collection in Fredericton and Montreal respectively.

I would also like to express appreciation to the financial supports from NSERC Strategic Research Network for Engineered Wood-based Building Systems (NEWBuildS), Homeowner Protection Office branch of BC housing, and the Faculty of Engineering and Computer Science of Concordia University.

Last but not least I wish to thank my wife, Shrabani Sarma for her constant mental support and affection, extreme patience, encouragements, criticism and support to finish the project. I would like thank my parents and parents-in-law for taking care of me and supporting my curiosity, ambition and decisions through my entire life.

Table of Contents

| | |
|--|------|
| List of Figures | xii |
| List of Tables..... | xx |
| Nomenclature | xxii |
| Chapter 1 | 1 |
| INTRODUCTION..... | 1 |
| 1.1 BACKGROUND..... | 1 |
| 1.2 KNOWLEDGE GAP..... | 4 |
| 1.3 OBJECTIVES OF THE CURRENT STUDY..... | 5 |
| 1.4 OUTLINE OF THE THESIS | 5 |
| Chapter 2..... | 7 |
| LITERATURE REVIEW..... | 7 |
| 2.1 INTRODUCTION..... | 7 |
| 2.2 EXPERIMENTAL METHOD | 9 |
| 2.3 SEMI-EMPIRICAL METHODS | 14 |
| 2.3.1 ISO model..... | 16 |
| 2.3.1.1 Wall factor..... | 20 |
| 2.3.2 ASHRAE 160 model..... | 22 |
| 2.3.3 Straube and Burnett model..... | 23 |
| 2.4 NUMERICAL METHOD | 28 |
| 2.5 BUILDING GEOMETRY AND WIND-DRIVEN RAIN..... | 31 |
| 2.5.1 Effect of overhang in reducing wind-driven rain..... | 31 |
| 2.6. SUMMARY..... | 33 |
| Chapter 3..... | 36 |
| METHODOLOGY..... | 36 |

| | |
|---|----|
| 3.1 INTRODUCTION | 36 |
| 3.2 BUILDING LOCATION AND DESCRIPTION | 36 |
| 3.2.1 McLeod House | 37 |
| 3.2.2 Hingston Hall B (HB) Building | 43 |
| 3.2.3 Faubourg Tower (FB Building) | 47 |
| 3.3 EQUIPMENT USED | 53 |
| 3.3.1 Wind monitor | 53 |
| 3.3.2 Temperature and relative humidity probe | 53 |
| 3.3.3 Tipping bucket horizontal rain gauge | 53 |
| 3.3.4 Driving rain gauge | 54 |
| 3.4 DATA COLLECTION AND PROCESSING | 55 |
| Chapter 4 | 57 |
| DATA ANALYSIS AND RESULTS | 57 |
| 4.1 INTRODUCTION | 57 |
| 4.2 ANALYSIS OF HISTORICAL DATA | 57 |
| 4.2.1 Prevailing wind direction | 57 |
| 4.2.2 Wind speed | 58 |
| 4.2.3 Rainfall | 59 |
| 4.3 COMPARISON OF ONSITE WEATHER DATA WITH DATA FROM NEARBY WEATHER STATIONS | 60 |
| 4.3.1 McLeod House, Fredericton | 61 |
| 4.3.1.1 Prevailing wind direction | 62 |
| 4.3.1.2 Wind speed | 62 |
| 4.3.2 HB Building, Montreal | 64 |
| 4.3.2.1 Prevailing wind direction | 65 |

| | |
|---|-----|
| 4.3.2.2 Wind speed..... | 66 |
| 4.3.3. FB Building, Montreal..... | 67 |
| 4.3.3.1 Prevailing wind direction..... | 68 |
| 4.3.3.2 Wind speed..... | 69 |
| 4.4 ONSITE WEATHER DATA ANALYSIS..... | 71 |
| 4.4.1 Prevailing wind direction..... | 71 |
| 4.4.2 Wind speed..... | 72 |
| 4.4.3 Rainfall intensity..... | 74 |
| 4.4.4 Wind speed variation with rainfall intensity..... | 74 |
| 4.5 WIND-DRIVEN RAIN ANALYSIS..... | 76 |
| 4.5.1 Error analysis..... | 76 |
| 4.5.2 Spatial distribution of wind-driven rain..... | 84 |
| 4.5.2.1 Catch ratio analysis..... | 85 |
| 4.5.2.2 Frequency analysis of catch ratios..... | 94 |
| 4.5.2.3 Catch ratio as a function of incidence angle..... | 96 |
| 4.5.2.4 Catch ratio as a function of wind speed..... | 101 |
| 4.5.2.5 Catch ratio as a function of horizontal rainfall intensity..... | 102 |
| 4.5.2.7 Summary of weather data and catch ratios for different rain events..... | 104 |
| 4.5.2.8 Wall factor analysis..... | 108 |
| 4.5.2.9 Wall factor as a function of wind speed..... | 114 |
| 4.5.2.10 Wall factor as a function of rainfall intensity..... | 115 |
| 4.5.2.11 Wall factor as a function of incidence angle..... | 115 |
| 4.5.3 Comparison between WDR measured and WDR estimated by semi-empirical models..... | 118 |
| 4.5.3.1 Calculation procedure for the ISO standard..... | 118 |

| | |
|--|-----|
| 4.5.3.2 Calculation procedure for the ASHRAE 160 model..... | 121 |
| 4.5.3.3 Comparison between measured and predicted wind-driven rain | 122 |
| 4.5.3.4 Validity of the ISO suggested wall factor | 125 |
| Chapter 5..... | 128 |
| CONCLUSIONS..... | 128 |
| 5.1 SUMMARY OF FINDINGS..... | 128 |
| 5.1.1 Wind and rain conditions at test sites | 128 |
| 5.1.1.1 Prevailing wind directions..... | 128 |
| 5.1.1.2 Wind speed..... | 129 |
| 5.1.1.3 Rainfall intensity | 130 |
| 5.1.2 Error associated with wind-driven rain measurements..... | 130 |
| 5.1.3 Spatial distribution of wind-driven rain..... | 131 |
| 5.1.3.1 In terms of catch ratios | 131 |
| 5.1.3.2 In terms of wall factors..... | 132 |
| 5.1.4. Comparison between measured and predicted WDR using the semi-empirical models..... | 132 |
| 5.2 CONTRIBUTIONS..... | 134 |
| 5.3 RECOMMENDATIONS FOR FUTURE WORKS..... | 135 |
| REFERENCES..... | 136 |
| APPENDIX A..... | 145 |
| Comparison of weather data obtained from onsite and nearby meteorological stations..... | 145 |
| McLeod House, Fredericton, NB | 145 |
| Comparison of temperature..... | 145 |
| Comparison of relative humidity..... | 146 |
| HB Building, Montreal, QC | 147 |

| | |
|---|-----|
| Comparison of temperature..... | 147 |
| Comparison of relative humidity..... | 148 |
| FB Building, Montreal, QC..... | 149 |
| Comparison of temperature..... | 149 |
| Comparison of relative humidity..... | 150 |
| APPENDIX B..... | 152 |
| Error analysis for major rain events..... | 152 |
| McLeod House, Fredericton, NB..... | 152 |
| Event: From August 14, 2013 to September 16, 2013..... | 152 |
| Event: From September 22, 2013 to September 25, 2013..... | 152 |
| Event: From October 07, 2013 to October 08, 2013..... | 153 |
| Event: From January 25, 2014 to January 27, 2014..... | 153 |
| Event: From April 06, 2014 to April 28, 2014..... | 154 |
| Event: From May 17, 2015 to June 03, 2015..... | 154 |
| HB Building, Montreal, QC..... | 155 |
| Event: From April 26, 2014 to May 04, 2014..... | 155 |
| Event: From June 11, 2014 to June 18, 2014..... | 156 |
| Event: From August 12, 2014 to August 17, 2014..... | 156 |
| Event: From October 04, 2014 to October 09, 2014..... | 157 |
| Event: From November 22, 2014 to November 24, 2014..... | 157 |
| Event: From May 25, 2015 to June 16, 2015..... | 158 |
| FB Building, Montreal, QC..... | 159 |
| Event: From July 26, 2014 to August 07, 2014..... | 159 |
| Event: From August 31, 2014 to September 06, 2014..... | 159 |
| Event: From October 04, 2014 to October 09, 2014..... | 160 |

Event: From November 22, 2014 to November 24, 2014..... 161

Event: From December 23, 2014 to December 28, 2014..... 162

Event: From May 30, 2015 to June 10, 2015..... 162

List of Figures

| | |
|--|----|
| Figure 1.1 : Wind-driven rain on building façade..... | 1 |
| Figure 1.2 : Wind-driven rain (Straube & Burnett, 2000) | 2 |
| Figure 1.3 : Wind-driven rain intensity and horizontal rain intensity (Blocken, B. & Carmeliet, J. 2004) | 3 |
| Figure 2.1 : Schematic representation of the two parts in wind-driven rain research: (a) assessment of the impinging wind-driven rain intensity (before raindrop impact) and (b) assessment of the response of the building wall (at and after raindrop impact). (Blocken, B. & Carmeliet, J., 2012; Blocken, B. et al., 2013) | 7 |
| Figure 2.2 : Methods associated with wind-driven rain measurement | 8 |
| Figure 2.3 : Driving rain gauges | 10 |
| Figure 2.4: Definition of factors determining the topography coefficient (C_T) (source: (NBN EN ISO 15927-3 (2009))..... | 18 |
| Figure 2.5: Factor s for: (a) cliffs and escarpments; and (b) hills and ridges (source: (NBN EN ISO 15927-3 (2009))..... | 19 |
| Figure 2.6 : Wall factors in the ISO standard 15927 (NBN EN ISO 15927-3 (2009)) | 21 |
| Figure 2.7: Values of RDF (Straube, J. & Burnett, E. 2000)..... | 25 |
| Figure 2.8 : Recommended values for EHF (Straube, J. & Burnett, E. 2000)..... | 25 |
| Figure 3.1: Locations of test buildings (Google maps.2015a)..... | 36 |
| Figure 3.2: Satellite image of the surroundings of McLeod House (Google maps.2015b) | 38 |
| Figure 3.3: Photo of wind monitor, temperature and relative humidity probe and the horizontal rain gauge installed on the roof top of McLeod House | 38 |

| | |
|--|----|
| Figure 3.4: Prevailing wind direction at Fredericton obtained from Fredericton airport station data | 39 |
| Figure 3.5: Plan view of McLeod House with driving rain gauge locations | 40 |
| Figure 3.6 : South-west elevation of McLeod House with the driving rain gauge locations | 40 |
| Figure 3.7 : Photo of the south-west façade of McLeod House with driving rain gauges..... | 40 |
| Figure 3.8: South-east elevation of McLeod House with driving rain gauge locations | 41 |
| Figure 3.9 : Photo of the south-east façade of McLeod House with driving rain gauges..... | 41 |
| Figure 3.10 : North-east elevation of McLeod House with driving rain gauge locations | 41 |
| Figure 3.11 : Photo of the north-east façade of McLeod House with driving rain gauges..... | 42 |
| Figure 3.12 : North-west elevation of McLeod House with driving rain gauge locations | 42 |
| Figure 3.13 : Photo of the north-west façade of McLeod House with driving rain gauges..... | 42 |
| Figure 3.14 : Satellite image of the surroundings of HB Building (Google maps.2015c) | 43 |
| Figure 3.15: Prevailing wind direction at Montreal obtained from Montreal international airport station data | 44 |
| Figure 3.16 : Plan view of HB Building with driving rain gauge locations | 44 |
| Figure 3.17 : South-west elevation of HB Building with driving rain gauge locations..... | 45 |
| Figure 3.18 : Photo of the south-west façade of HB Building with driving rain gauges..... | 45 |
| Figure 3.19 : South-east elevation of HB Building with driving rain gauge locations..... | 45 |
| Figure 3.20 : Photo of the south-east façade of HB Building with driving rain gauges..... | 45 |
| Figure 3.21 : North-west elevation of HB Building with driving rain gauge locations..... | 46 |
| Figure 3.22 : Photo of the north-west façade of HB Building with driving rain gauges | 46 |
| Figure 3.23: Photo of: (a) wind monitor, temperature and relative humidity probe; and (b) horizontal rain gauge installed on the roof top of HB Building | 46 |

| | |
|---|----|
| Figure 3.24 : Satellite image of the surroundings of FB Building (Google maps.2015d)..... | 47 |
| Figure 3.25 : Plan view of FB Building with driving rain gauge locations | 48 |
| Figure 3.26 : North-east elevation of FB Building with driving rain gauge locations | 49 |
| Figure 3.27 : Photo of the north-east façade of FB Building with driving rain gauges..... | 49 |
| Figure 3.28 : North-west elevation of FB Building with driving rain gauge locations | 50 |
| Figure 3.29: Photo of the north-west façade of FB Building with driving rain gauge | 50 |
| Figure 3.30 : South-east elevation of FB Building with driving rain gauge locations | 51 |
| Figure 3.31 : Photo of the south-east façade of FB Building with driving rain gauges..... | 51 |
| Figure 3.32 : South-west elevation of FB Building with driving rain gauge locations | 52 |
| Figure 3.33: Photo of the south-west façade of FB Building with driving rain gauges (Source: Google maps)..... | 52 |
| Figure 3.34 : Equipment used for measurements..... | 54 |
| Figure 3.35 : Photos of: (a) data logger; and (b) data Collection | 55 |
| Figure 4.1 : Prevailing wind direction in: (a) Fredericton; and (b) Montreal | 58 |
| Figure 4.2 : Comparison of wind speed frequency in: (a) Fredericton; and (b) Montreal..... | 58 |
| Figure 4.3 : Comparison of total annual rainfall in Fredericton and Montreal..... | 59 |
| Figure 4.4 : Comparison of frequency distribution of rainfall intensity in Fredericton and Montreal..... | 60 |
| Figure 4.5 : Average total rainfall per month in (a) Fredericton; and (b) Montreal | 60 |
| Figure 4.6: Locations of the test building at Fredericton and nearby meteorological stations..... | 61 |
| Figure 4.7: Comparison of prevailing wind direction for all hours obtained from onsite measurements and nearby meteorological stations for the period from August 2013 to March 2014..... | 62 |

| | |
|--|----|
| Figure 4.8 : Comparison of wind speed obtained from the onsite measurements and Fredericton airport station for the period from August 2013 to March 2014..... | 64 |
| Figure 4.9: Locations of HB Building and Montreal international airport station | 65 |
| Figure 4.10: Comparison of prevailing wind direction for all hours obtained from the onsite measurements and Montreal international airport station for the period from April 2014 to June 2014..... | 66 |
| Figure 4.11: Comparison of hourly wind speed obtained from the onsite measurements and Montreal international airport station for the period from May 2014 to September 2014 | 67 |
| Figure 4.12: Locations of FB Building and nearby meteorological stations | 68 |
| Figure 4.13 : Comparison of prevailing wind direction for all hours obtained from the onsite measurements and nearby meteorological stations for the period from July 2014 to August 2014 | 69 |
| Figure 4.14 : Comparison of hourly wind speed obtained from FB Building site and nearby meteorological stations for the period from July 2014 to August2014 | 70 |
| Figure 4.15 : Prevailing wind direction at test building sites: (a) McLeod House, Fredericton; (b) HB Building, Montreal; (c) FB Building, Montreal | 72 |
| Figure 4.16 : Frequency distribution of wind speed at test building sites: (a) McLeod House, Fredericton; (b) HB Building, Montreal; (c) FB Building, Montreal | 73 |
| Figure 4.17 : Frequency distribution of rainfall intensity at test building site: (a) McLeod House, Fredericton; (b) HB Building, Montreal; (c) FB Building, Montreal | 74 |
| Figure 4.18 : Rainfall intensity versus wind speed at test building site: (a) McLeod House, Fredericton; (b) HB Building, Montreal; (c) FB Building, Montreal | 76 |
| Figure 4.19 : Typical spells (NBN EN ISO 15927-3 (2009))..... | 80 |

| | |
|---|----|
| Figure 4.20 : Error as a function of wind-driven rain amount for: (a) McLeod House, Fredericton; (b) HB Building, Montreal; (c) FB Building, Montreal | 83 |
| Figure 4.21 : Horizontal rainfall intensity recorded at test building site in Fredericton: (a) from August 2013 to June 2014 and (b) from April 2015 to June 2015 | 86 |
| Figure 4.22 : (a) Prevailing wind direction during rain hours for the entire monitoring period; (b) Plan view with rain gauge locations of McLeod House in Fredericton..... | 87 |
| Figure 4.23 : Total rainfall, wind-driven rain and catch ratio values at driving rain gauge locations for the entire monitoring period at McLeod House in Fredericton | 87 |
| Figure 4.24 : Catch ratio values on rain gauge locations on the: (a) south-west; (b) north-east; (c) south-east; (d) north-west façade of McLeod House in Fredericton | 88 |
| Figure 4.25 : Horizontal rainfall intensity recorded at HB Building site in Montreal from April 2014 to June 2015 | 89 |
| Figure 4.26 : (a) Prevailing wind direction during rain hours for the entire monitoring period; (b) Plan view with rain gauge locations of HB Building in Montreal..... | 89 |
| Figure 4.27 : Total rainfall, wind-driven rain and catch ratio values at driving rain gauge locations for the entire monitoring period at HB Building in Montreal | 90 |
| Figure 4.28 : Catch ratio values on rain gauge locations on the: (a) south-west; (b) south-east; (c) north-west façade of HB Building in Montreal | 90 |
| Figure 4.29 : Horizontal rainfall intensity recorded at HB Building site in Montreal from July 2014 to June 2015 | 91 |
| Figure 4.30 : (a) Prevailing wind direction during rain hours for the entire monitoring period; (b) Plan view with rain gauge locations of FB Building in Montreal | 92 |

| | |
|--|-----|
| Figure 4.31 : Total rainfall, wind-driven rain and catch ratio values at driving rain gauge locations for the entire monitoring period at FB Building in Montreal | 92 |
| Figure 4.32 : Catch ratio values at rain gauge locations on the: (a) south-west; (b) south-east; (c) north-east; (d) north-west façade of FB Building in Montreal | 93 |
| Figure 4.33 : Incidence angle (θ) | 94 |
| Figure 4.34 : Frequency distribution of catch ratio at different locations on the south-west façade of McLeod House | 95 |
| Figure 4.35 : Frequency distribution of catch ratio at different locations on the south-west façade of HB Building..... | 95 |
| Figure 4.36 : Frequency distribution of catch ratio at different locations on the south-west façade of FB Building | 96 |
| Figure 4.37: Catch ratio variation with incidence angle at locations 0.61 m below the roofline of the south-west façade of: (a) McLeod House; (b) HB Building; (c) FB Building | 97 |
| Figure 4.38: Average catch ratio values over the entire monitoring period at different locations on the south-west façade of McLeod House for different ranges of incidence angles | 98 |
| Figure 4.39: Average catch ratio values over the entire monitoring period at different locations on the south-west façade of HB Building for different ranges of incidence angles | 99 |
| Figure 4.40: Average catch ratio values over the entire monitoring period at different locations on the south-west façade of FB Building for different ranges of incidence angles | 100 |
| Figure 4.41 : Catch ratio variation with wind speed at different locations on the south-west façade of: (a) McLeod House; (b) HB Building; (c) FB Building..... | 101 |
| Figure 4.42: Catch ratio variation with rainfall intensity at locations 0.61 m below the roofline on the south-west façade of: (a) McLeod House; (b) HB Building; and (c) FB Building..... | 102 |

| | |
|---|-----|
| Figure 4.43: Calculated DRF versus rainfall intensity for: (a) McLeod House; (b) HB Building; (c) FB Building | 103 |
| Figure 4.44 : Wall factors (red-ISO, blue-measurements) at driving rain gauge locations on the (a) south-west façade; (b) north-east façade; (c) south-east façade; (d) north-west façade of McLeod House, Fredericton | 110 |
| Figure 4.45 : Wall factors (red-ISO, blue-measurements) at driving rain gauge locations on the (a) south-west façade; (b) south-east façade; (c) north-west façade of HB Building, Montreal | 111 |
| Figure 4.46 : Wall factors (red-ISO, blue-measurements) at wind-driven rain gauge locations on the (a) south-west façade; (b) south-east façade; (c) north-east façade; (d) north-west façade of FB Building, Montreal | 113 |
| Figure 4.47 : Wall factor variation with wind speed at locations 0.61 m below the roofline on the south-west façade of: (a) McLeod House; (b) HB Building; and (c) FB Building..... | 114 |
| Figure 4.48 : Wall factor variation with rainfall intensity at locations 0.61 m below the roofline on the south-west façade of: (a) McLeod House; (b) HB Building; and (c) FB Building..... | 115 |
| Figure 4.49 : Wall factor variation with incidence angle at different locations on the south-west façade of: (a) McLeod House; (b) HB Building; (c) FB Building..... | 117 |
| Figure 4.50 : Comparison between measured wind-driven rain and the estimated wind-driven rain using semi-empirical models for: (a) McLeod House; (b) HB Building; (c) FB Building . | 124 |
| Figure 4.51 : Comparison of estimated wind-driven rain by the ISO standard suggested equation using the ISO suggested wall factors and the measured wall factors with the measured wind- driven rain amount for: (a) McLeod House; (b) HB Building; (c) FB Building | 127 |
| Figure A.1: Comparison of hourly temperature obtained from onsite and nearby meteorological stations for the period from August 2013 to March 2014..... | 146 |

| | |
|--|-----|
| Figure A.2: Comparison of hourly relative humidity obtained from onsite and nearby meteorological stations for the period from August 2013 to March 2014..... | 147 |
| Figure A.3: Comparison of hourly temperature obtained from onsite and Montreal international airport station for the period from April 2014 to June 2014..... | 148 |
| Figure A.4 : Comparison of hourly relative humidity obtained from onsite and Montreal international airport station for the period from April 2014 to June 2014..... | 149 |
| Figure A.5 : Comparison of hourly temperature obtained from FB Building site and nearby meteorological stations for the period from July 2014 to August 2014 | 150 |
| Figure A.6 : Comparison of hourly relative humidity obtained from FB Building site and nearby meteorological stations for the period from July 2014 to August 2014 | 151 |

List of Tables

| | |
|--|-----|
| Table 2.1: Terrain categories and related parameters suggested by the ISO standard (source: (NBN EN ISO 15927-3 (2009))..... | 17 |
| Table 2.2 : Effective length, L_e | 18 |
| Table 2.3 : Obstruction factor (source: (NBN EN ISO 15927-3 (2009)) | 20 |
| Table 2.4: Exposure factor (source: ASHRAE 2009)..... | 22 |
| Table 2.5 : Deposition factor (source: ASHRAE 2009) | 22 |
| Table 3.1: Details of test buildings | 37 |
| Table 3.2: List of different types of data analysis conducted in this study with their purpose..... | 56 |
| Table 4.1: values of gradient height and power law exponents for different terrain categories [Source: (Hutcheon, N. B., & Handergord G.O.P, 1995)]..... | 63 |
| Table 4.2: Error estimation for the accumulated wind-driven rain: (a) McLeod House - for the rain event from October 26 to November 28, 2013; (b) HB Building - for the rain event from May 9to May 17, 2014; (c) FB Building - for the rain event from August 12 to August 17, 2014 | 82 |
| Table 4.3 : Total amount of wind-driven rain registered by each driving rain gauge and total amount of losses during the entire monitoring period for all three test buildings | 84 |
| Table 4.4: Summary of weather data and catch ratios at different locations on the south-west façade of McLeod House for different rain events | 105 |
| Table 4.5: Summary of weather data and catch ratios at different locations on the south-west façade of HB Building for different rain events | 106 |
| Table 4.6 : Summary of weather data and catch ratios at different locations on the south-west façade of FB Building for different rain events | 107 |

| | |
|---|-----|
| Table 4.7: Wall orientation relative to north (θ) for building façades | 108 |
| Table 4.8: Terrain categories and values of related parameters for three test buildings | 118 |
| Table 4.9 : Wall factor, W (source: (NBN EN ISO 15927-3 (2009))..... | 119 |
| Table 4.10 : Values of the correction factors used for estimating wind-driven rain amount at different rain gauge locations of McLeod House using the ISO standard | 119 |
| Table 4.11 : Values of the correction factors used for estimating wind-driven rain amount at different rain gauge locations of HB Building using the ISO standard | 120 |
| Table 4.12 : Values of the correction factors used for estimating wind-driven rain amount at different rain gauge locations of FB Building using the ISO standard..... | 120 |
| Table 4.13: Values of exposure factor (F_E) and the rain deposition factor (F_D) for each façade of three test buildings | 121 |

Nomenclature

| | |
|------------|---|
| C_R | Terrain roughness coefficient |
| C_T | Topography coefficient |
| c_{pa} | Specific heat at constant pressure |
| D | Hourly mean wind direction from north [°] |
| DRF | Driving rain factor |
| E_{AW} | Adhesion-water-evaporation error [mm] |
| E_{EVAP} | Evaporation error from the tipping bucket and collection plate [mm] |
| EHF | Exposure and height factor |
| E_{RW} | Rest-water error [grams of water] |
| E_{TIP} | collection loss during every tip [grams of water] |
| E_{TOT} | Total error in the wind-driven rain measurement [mm] |
| e_{TOT} | Relative error associated with the wind-driven rain measurement [%] |
| E_{UC} | Condensation error [mm] |
| F_D | Rain deposition factor |
| F_E | Rain exposure factor |
| g_v | Vapour flow rate [kg/m ² s] |
| I_A | Airfield index [mm] |
| I_{WA} | Wall indices [mm] |
| k | Wind-driven rain coefficient |
| n | Amount of tips during the rain event |
| O | Obstruction factor |
| p | Vapour pressure in the air [Pa] |
| p_s | Vapour pressure at the surface [Pa] |
| RDF | Rain deposition factor |

| | |
|------------|--|
| R_h | Horizontal rainfall intensity [mm/hr] |
| R_{wdr} | Wind-driven rain intensity [mm/hr] |
| S_{WDR} | Total accumulated wind-driven rain for the rain event [mm] |
| TOF | Topography factor |
| U | Wind speed [m/s] |
| U_{10} | Hourly average wind speed at 10 m [m/s] |
| U_g | Wind speeds at gradient height [m/s] |
| U_z | Wind speeds at height z [m/s] |
| V_{BOWL} | Content of the bowls [grams of water] |
| V_t | Raindrop terminal velocity [m/s] |
| W | Wall factor |
| WDR | Wind-driven rain |
| Z_g | Gradient height [m] |
| α | Power exponent |
| α_c | Convective heat transfer coefficient [J/kgK] |
| β | Moisture transfer coefficient [m/s] |
| η | Catch ratio |
| θ | Wall orientation relative to north [°] |
| ρ_a | Air density [kg/m ³] |

Chapter 1

INTRODUCTION

1.1 BACKGROUND

The aesthetics, occupant's thermal comfort, structural stability and durability of buildings considerably depend upon the performance of building envelopes. One of the most important functions of the building envelope is to protect the inside from wind and precipitation. In order to ensure long-term durability, building envelopes should prevent the penetration of weather elements such as rain. The exterior hygrothermal environmental loads that directly affect the transport of heat and moisture through building envelopes include: ambient temperature, ambient relative humidity, solar diffuse, solar direct, cloud index, wind speed, wind orientation, and horizontal rain precipitation (Karagiozis, A.N. et al., 2003). Among the exterior environmental loads, the most important are those imposed due to wind-driven rain and under some climatic conditions these loads are many times more important than those resulted from vapour and air convection transport. Karagiozis, A.N. et al. (2003) found that in more than 90 percent of cases the effect of wind-driven rain is much more critical than most of the other exterior environmental loads. But, though wind-driven rain loads can influence the moisture and energy performance of the building envelope the most, they are possibly the least understood.

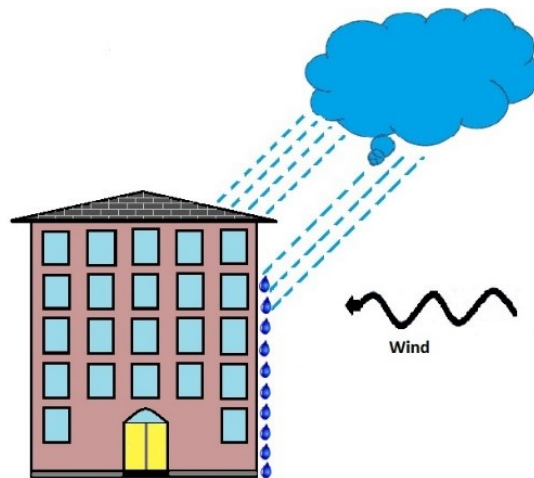


Figure 1.1 : Wind-driven rain on building façade

The effect of wind and rain is very significant on building performance and durability. These two can affect building performance individually or in combination. In a windless condition raindrops fall vertically. But in reality rain is associated with wind as absolutely calm weather during the period of rain is rare. Under the action of wind, raindrop paths are oblique. It has two components, the vertical component is called precipitation and the horizontal component is called wind-driven rain (WDR) or driving rain. Precipitation wets horizontal and sloped surfaces and wind-driven rain humidifies vertical surfaces. So, wind-driven rain is the combination of wind and rain, which describes as the amount of rain passing through a vertical plane. As stated by Abuku, M. et al. (2009), wind-driven rain corresponds to the sum of individual raindrops that impinge on the façade in a temporally and spatially discrete mode. Apart from spreading at impact, they may also splash or bounce off the façade. The quantity of wind-driven rain on a specific location on the building façade depends upon the wind speed, rainfall intensity, raindrop spectrum and building geometry (Blocken, B. & Carmeliet, J., 2000a; Högberg, A.B. et al., 1999).

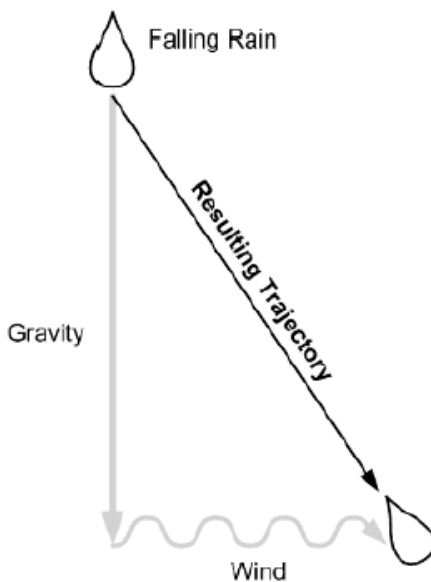


Figure 1.2 : Wind-driven rain (Straube & Burnett, 2000)

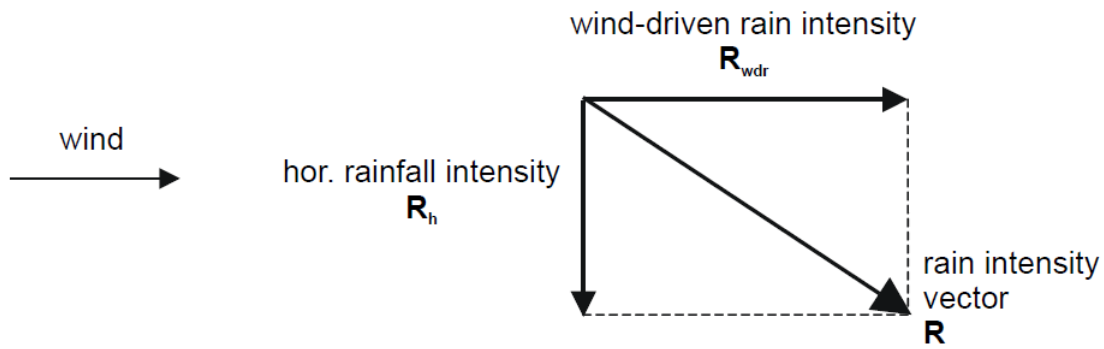


Figure 1.3 : Wind-driven rain intensity and horizontal rain intensity (Blocken, B. & Carmeliet, J. 2004)

Wind-driven rain is an important boundary condition for the study of the hygrothermal behaviour and durability and design of building envelopes (Abuku, M. et al., 2009; Blocken, B. & Carmeliet, J., 2004). It is one of the most important moisture sources affecting building façades. Wind-driven rain can lead to water penetration, frost damage, moisture induced salt migration, discoloration by efflorescence, structural cracking, surface soiling etc. (Blocken, B. & Carmeliet, J., 2002; Blocken, B. et al., 2013; Blocken, B. & Carmeliet, J., 2004). Wind-driven rain is the main factor being responsible for surface erosion or detachment of material from a masonry building façade (Erkal, A. et al., 2012). Precipitation accompanied by wind gusts is mainly responsible for moistening building envelope and penetration of this moisture leads to reduced performance and damage of insulation and other energy saving features of the buildings (Pérez-Bella, J.M. et al., 2013). Understanding wind-driven rain characteristics is the fundamental requirements to establish designs that minimize the moisture related issues. Even though wind-driven rain is a very important parameter, so far knowledge about its magnitude, duration and frequency is relatively little (Straube & Burnett, 2000).

So far a number of methods have been employed to quantify wind-driven rain amounts (Blocken, B. & Carmeliet, J., 2004; Blocken, B. & Carmeliet, J., 2008; Nore, K., 2006; Nore, K. et al., 2007; Rychtáriková, M. & Vargová, A., 2008). Three main categories are: (a) Experimental method; (b) Semi-empirical method; and (c) Numerical method. The experimental method consists of

measuring wind-driven rain with driving rain gauges. It has been the primary tool in wind-driven rain studies and it has provided the basic knowledge that we have on wind-driven rain. Semi-empirical methods use semi-empirical relationships between wind-driven rain and the influencing climatic parameters such as wind speed, wind direction, and horizontal rainfall. Numerical methods comprises the calculation of the wind flow pattern by solving the complex three dimensional Reynolds-averaged Navier-Stokes equations with a CFD code and the calculation of raindrop trajectories in this flow pattern.

In order to ensure long-term durability of highly energy efficient and sustainable buildings, it is important to advance our knowledge on the wind-driven rain load and its impact on the building envelope performance. Wolf and Griffith (Wolf & Griffith, 2008) noted that on many buildings, water intrusion problems are mainly associated with one elevation, which is exposed to the predominant direction of wind-driven rain. They stated that wind-driven rain could be used as both a design tool and construction parameter. By assessing wind-driven rain and its dispersion on the external wall surface and using wind-driven rain intensities as a design parameter the increased service life may be achieved (Nore, K., 2006).

1.2 KNOWLEDGE GAP

A great number of studies have been done so far in the field of wind-driven on building façade. But still there are lots of unanswered questions, some of which are as follows:

- There is very limited experimental datasets on wind-driven rain study. In order to further develop semi-empirical models and validate CFD models, measurements on buildings with various geometries and design details under different climatic conditions are essential.
- The semi-empirical models (such as the ISO Standard 15972 and ASHRAE 160), that estimates wind-driven rain using wind and rain data collected at meteorological stations were developed based on measurements on a limited number of building geometries and façade locations. As a result, wind-driven rain estimated by semi-empirical models may have large deviations from field measurements.

- Various correction factors used in the semi-empirical models need to be revised to improve the predictive performance of these models. For example, the ISO standard suggests only two wall factor values along building height with no change across the building width for a multi-story building, but site measurements show that those widely varies. Moreover, it suggests the same values for all four façades without considering façade orientation. So, based on experimental data the wall factor values need to be revised and values for more façade locations, building types and geometries are required.
- Lack of study to investigate the influence of wind speed, wind direction and rainfall intensity on the spatial distribution of wind-driven rain, i.e. wall factor.

1.3 OBJECTIVES OF THE CURRENT STUDY

The objective of this study is to characterize wind-driven rain load on mid-rise and high-rise buildings in different Canadian climatic regions. More specifically, this study will:

- Generate a unique set of measurements to characterize the wind-driven rain distribution on mid- and high-rise buildings for different Canadian climatic regions.
- Provide data for validating CFD models.
- Evaluate the accuracy of existing semi-empirical methods used for quantifying wind-driven rain loads on building façades.

1.4 OUTLINE OF THE THESIS

This study is presented in five chapters. The background, importance, knowledge gap and objectives for this research work have been stated in the previous sections of Chapter 1.

Chapter 2 reviews previous laboratory and field experiments and numerical works related to wind-driven rain research. The main topics in this chapter includes three different methods for quantifying wind-driven rain loads on building façades (i.e., experimental method, semi-empirical method and numerical method) including catch ratio; wall factor and wall index, effect of building

geometry on wind-driven rain load, effect of roof overhang on reducing wind-driven rain load on building façades etc.

Chapter 3 is the methodology. This chapter describes the study buildings, measurement set up, equipment used for the study and the analyses carried out.

Chapter 4 reports of analyses of historical and experimental data and discussions including wind direction analysis, wind speed analysis, rainfall analysis, spatial distribution of wind-driven rain in terms of catch ratio and wall factor, estimation of wind-driven rain using semi-empirical model, error associated with wind-driven rain measurements etc.

Finally in Chapter 5, conclusions drawn from the analyses are included. Contributions of this study, recommendations and suggestions for further work are also provided.

The references cited in this thesis are listed in the references section.

Chapter 2

LITERATURE REVIEW

2.1 INTRODUCTION

For the adequate design of building façades sufficient knowledge on wind-driven rain is essential. In Building Engineering wind-driven research consists of two parts, the first part is associated with before raindrop impact and the second one is associated with after raindrop impact (M. Abuku, M. et al., 2006; Blocken, B. & Carmeliet, J., 2012; Blocken, B. et al., 2013). The first part includes the assessment of the impinging wind-driven rain on vertical building walls and the second part includes the assessment of the response of the building walls to the impinging rain (Figure 2.1).

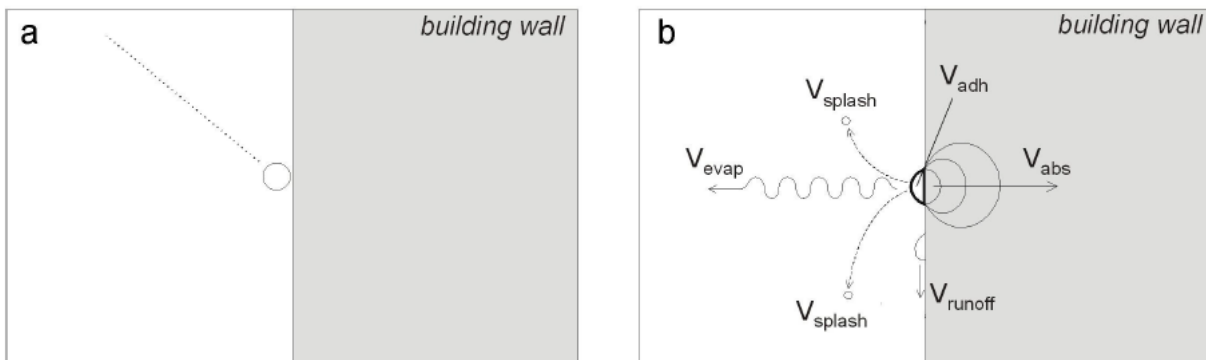


Figure 2.1 : Schematic representation of the two parts in wind-driven rain research: (a) assessment of the impinging wind-driven rain intensity (before raindrop impact) and (b) assessment of the response of the building wall (at and after raindrop impact). (Blocken, B. & Carmeliet, J., 2012; Blocken, B. et al., 2013)

A number of parameters including urban geometry, building geometry, façade detailing, and position on the building façade, and all the relevant meteorological parameters, i.e., wind speed, wind direction, rainfall intensity governs the impinging wind-driven rain intensity (Blocken, B. & Carmeliet, J., 2004; Nore, K. et al., 2007). The complex interaction of the above parameters results in distinct wind-driven rain patterns across the building façades (Blocken, B. et al., 2013; Blocken, B. & Carmeliet, J., 2004). The meteorological parameters, i.e., wind speed, wind direction, rainfall intensity are highly variable in both space and time. As a result, wind-driven rain is also strongly dependent on space and time (Nore, K. et al., 2007). The wetting pattern on a building caused by

wind-driven rain is highly influenced by the wind direction (Nore, K. et al., 2007). It is found that so far less attention has been given to the second part of wind-driven rain research. This is usual because research on the first part of wind-driven rain research is still under full development, while being an essential input to the second part of wind-driven rain research (Blocken, B. & Carmeliet, J., 2012; Blocken, B. et al., 2013).

Wind-driven rain is a too difficult boundary condition to make reliable prediction (Abuku, M. et al., 2006). A standard test method for wind-driven rain that can result in reliable and repeatable test results is still in its development stage (Baheru, T. et al., 2013). Till today most research efforts on wind-driven rain have focused on the first part of wind-driven rain assessment using three categories of methods: (a) experimental methods; (b) semi-empirical methods; and (c) numerical simulation based on Computational Fluid Dynamics (CFD) (Abuku, M. et al., 2009; Blocken, B. & Carmeliet, J., 2012; Blocken, B. et al., 2013; Giarma, C., & Aravantinos, D., 2014; Nore, K. et al., 2007; Rychtáriková, M., & Vargová, A., 2008; Van den Brande, T. et al., 2013).

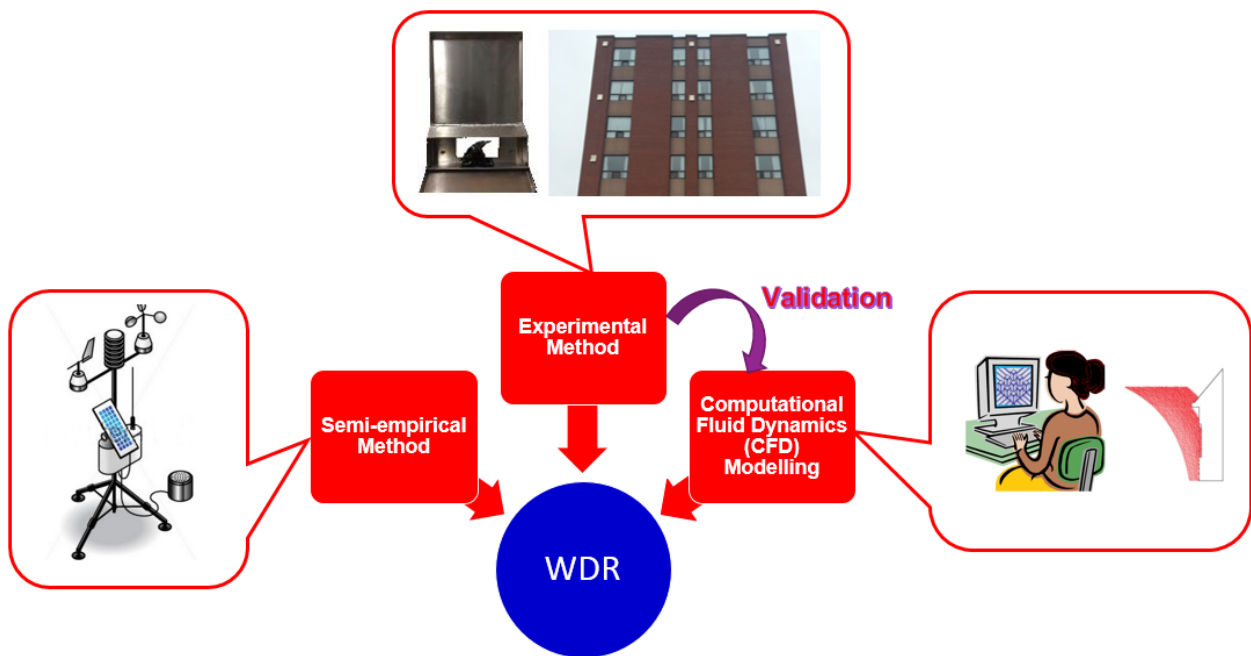


Figure 2.2 : Methods associated with wind-driven rain measurement

2.2 EXPERIMENTAL METHOD

Experimental methods consist of field measurements as well as laboratory experiments. It is considered as the primary tool for wind-driven rain study, which provides the basic knowledge for understanding wind-driven rain (Blocken, B. & Carmeliet, J., 2004). Here wind-driven rain gauges are used to measure wind-driven rain. The difference between horizontal rainfall gauges and driving rain gauges is that horizontal rainfall gauges are equipped with a horizontal aperture to measure rainfall whereas driving rain gauges are characterized by a vertical aperture to collect the amount of wind-driven rain (Blocken, B. & Carmeliet, J., 2004). These gauges have never been industrially manufactured, and as there exists no standard on their design, they vary significantly (Blocken, B. et al., 2009; Blocken, B. & Carmeliet, J., 2000a; Blocken, B. & Carmeliet, J., 2004; Högberg et al., 1999). Almost every research laboratory has designed its own driving rain gauge (B. Blocken et al., 2009). Figure 2.3 shows three different types of driving rain gauges used by different researchers in the past. According to references (Högberg, A. B. et al., 1999; Mook, F., 1998), a traditional driving rain gauge consists normally of:

- a collector (a shallow tray) fixed to the wall of a building. Raindrops hit the tray, drip downwards and are collected by a drainage channel.
- a drainage channel, which supplies the collected rain water to a reservoir or a water flux gauge.
- a water flux gauge enables the measurement of instantaneous driving rain intensities.

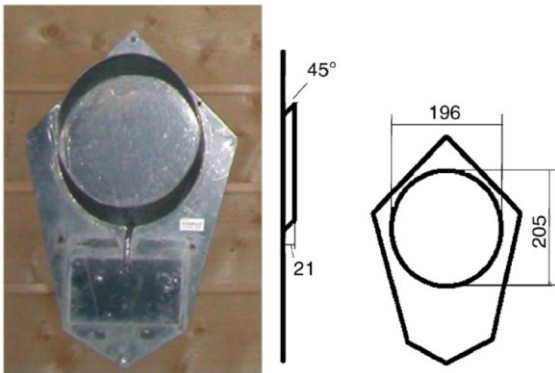
Literature shows two types of measurements with driving rain gauges (Blocken, B. & Carmeliet, J., 2004): (1) measurements of the free wind-driven rain and (2) measurements of the wind-driven rain on buildings. Free driving rain gauges are placed in “free field conditions” and measure the wind-driven rain that is not influenced by the presence of buildings or other obstructions. On the other hand to obtain specific information of the wind-driven rain exposure at certain positions of the façade, wall-mounted driving rain gauges are used.



Source: (Mook, F., 1998)



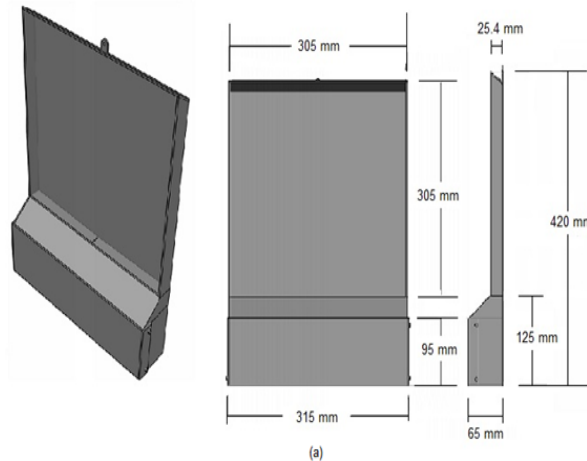
Source: (Blocken, B. & Carmeliet, J., 2005)



Source: (Nore, K. et al., 2007)



Source: (Ge, H. & Krpan, R., 2007)



Source: (Osorio, M. & Ge, H., 2013)

Figure 2.3 : Driving rain gauges

Several studies (Högberg, A. B. et al., 1999; Juras, P. et al., 2014; Mook, F., 1998) have been conducted in the past to evaluate the performance of different types of driving rain gauges that have been used so far for measuring wind-driven rain. Mook, F. (1998) verified that the gauge with a wiper measures two times wind-driven rain than a gauge without a wiper. He carried out wind-driven rain measurements with the driving rain gauges that contains wiper and found that wind driven rain intensity increases with the use of wiper. Hogberg, A.B. et al. (1999) conducted full-scale test at Denmark with four types of driving rain gauges with the aim to evaluate their performance. The first rain gauge had a traditional collector with tipping bucket, second one contained a collector weighted by a strain gauge, third one had traditional collector with reservoir and balance, and the last one contained a rotating wiper. The first and second one was made of Perspex and stainless steel respectively and the third and fourth had Teflon coating. It was found that Teflon coating is not sufficient measure and becomes dirty, but a wiper can serve to keep the surface clean and to improve coagulation and dropping-down of collected raindrops.

There exist numerous drawbacks of experimental methods. Databases of wind-driven rain measurements are not commonly available as wind-driven rain is usually not measured at meteorological stations. Measurements of driving rain are often difficult to carry out. It usually provides limited spatial and temporal information. Wind-driven rain measurements are time consuming and expensive and measurements on a particular building site have very limited application to other sites (Blocken, B. et al., 2009; Blocken, B. & Carmeliet, J., 2007). Also experimental method can suffer from large errors (Blocken, B. & Carmeliet, J., 2006; Högberg, A.B. et al., 1999). A study was conducted to identify and investigate the principal errors that can take place during wind-driven rain measurements (Blocken, B. & Carmeliet, J., 2006). It was found that mainly 5 types of errors may happen during wind-driven rain measurements. These are:

- i) evaporation of adhesion water from the collection area (and from the inner side of the draining tube),
- ii) evaporative losses from the reservoir,
- iii) splashing of drops from the collection area,
- iv) condensation on the collection area, and
- v) wind errors.

During and after the rain, some amount of rain water is adhered to collection area of the gauge. This amount is not collected to the reservoir and hence remains unmeasured. With time this adhesion water evaporates. The error associated with the evaporation of adhesion water from the gauge catch area (or collection area) is the largest (Blocken, B. & Carmeliet, J., 2006). This error can be as high as 100%. It depends not only on the gauge type but also on the type of rain event. Blocken, B. & Carmeliet, J. (2006) suggested some procedures to minimize evaporative losses from the reservoir, such as exposing only a small water surface to the ambient air, to minimize the ventilation rate in the reservoir and to add a few drops of light oil regularly. According to this study splashing errors are expected to be negligible given the low wind speed and the low horizontal rainfall intensity values. The condensation on the gauge during the rain event is negligible and wind errors are expected to be negligible when the wind direction is approximately perpendicular to building façade.

Several experimental studies have been carried out in the past to quantify wind-driven rain on building façades (Abuku, M. et al., 2009; Blocken, B. & Carmeliet, J., 2006; Ge, H. & Krpan, R., 2009; Ge, H. & Krpan, R., 2007; Hens, H., 2010; Kubilay, A. et al., 2014a; Mook, F., 1998; Nore, K., 2006; Nore, K. et al., 2007; Van Mook, F. J., 1999). In this type of study locations of driving rain gauges on the building façades are selected based on prevailing wind direction, building geometry and surrounding conditions. Spatial distribution of wind-driven rain is presented in the form of catch ratios. Almost all the research on wind-driven rain measurements includes catch ratio analysis. Catch ratio is defined as the ratio of the wind-driven rain intensity on vertical surfaces (R_{wdr}) to the horizontal rainfall intensity (R_h) (equation 2.1). The catch ratio is influenced by six basic parameters including: a) building geometry (including environment topology), b) position on the building façade, c) reference wind speed, d) reference wind direction, e) horizontal rainfall intensity, and f) raindrop-size distribution.

$$\eta = \frac{R_{wdr}}{R_h} \quad (2.1)$$

Researchers tried to find out the spatial distribution of wind-driven rain and hence the most vulnerable to façade location. Nore, K. et al. (2006; 2007) measured wind-driven rain distribution on a low-rise test building in Norway. This test building was a block-type test house which is 4.3

m high and 11.2 m long with a roof overhang of 0.34 m on the east and west facing sides. Results showed that the corners and edges of the building façade obtained higher catch ratio values. Ge, H. and Krpan, R. (2009; 2007) conducted wind-driven rain measurement on 8 test buildings of different geometries in British Columbia from 2006 to 2008 and found higher catch ratio values at the corners and edges of the building façades. Recently Kubilay, A. et al. (2014) have conducted wind-driven rain measurements with high spatial and temporal resolution in a test setup consisting of an array of 9 low-rise cubic building models of 2 m height and 2 m apart from each other, located in Dübendorf, Switzerland. The cubes are made of wood panels on a wood structure and finished with protective paint. The roofs are flat and covered with a water resistant polymeric membrane as roofing. The total roof height including the support beneath the cubes is 2.17 m. From the experimental results they have developed a dataset of several rain events and wind-driven rain measurement. These dataset comprise information of: (i) detailed descriptions of the building site, (ii) the building geometry, (iii) the measurement setup, (iv) measurements of the reference wind speed, the reference wind direction and the horizontal rainfall intensity, (v) wind-driven rain measurements at the façades with a sufficiently high resolution in space and time and (vi) error estimates for the wind-driven rain measurements. They also found higher catch ratio values at edges and corner locations on façades. Higher catch ratio values at the corners and edges of the building façades confirms that these locations are most vulnerable to wind-driven rain.

Blocken, B. and Carmeliet, J. (2006) conducted wind-driven rain measurements on the low-rise VLIET test building of the Laboratory of Building Physics, K.U. Leuven. They concluded that the corners and edges of the building façade shows higher catch ratio values but the locations below the overhangs do not follow this classical theory.

Van Mook, F.J. (1999) conducted field experiments to observe how catch ratio varies with rain fall intensity. Experiments was carried out to measure wind-driven rain on the west façade of the Main Building of the Eindhoven University of Technology (TUE), Netherlands. Results showed that driving rain ratios or catch ratios do not depend clearly on horizontal rainfall intensity. Tang, W. et al. (2004) conducted wind-driven rain measurement on the Cathedral of Learning building at University of Pittsburgh, which is a complex high rise building surrounded by several lower building. From measurements they found that high driving rain fluxes are associated with strong

winds and intense rainfall and walls facing prevailing wind directions generally receives higher wind-driven rain.

2.3 SEMI-EMPIRICAL METHODS

To avoid the difficulties associated with the experimental method researchers tried to develop semi-empirical relationships to estimate wind-driven rain from standard weather data. These relationships relate wind-driven rain with the influencing climatic parameters (Blocken, B., & Carmeliet, J., 2004) . Climatic parameters such as wind speed, wind direction, and horizontal rainfall can be obtained from weather stations. As wind-driven rain is usually not measured, it would be useful if information on wind-driven rain could be obtained from standard weather data. The semi-empirical relationships were developed on the basis of the experimental observation that both free field wind-driven rain and wind-driven rain on buildings increase approximately proportionally with wind speed and horizontal rainfall (Blocken, B., & Carmeliet, J., 2004; Nore, K. et al., 2007).

Wind-driven rain relationship is based on a simple theoretical formula. Assuming all raindrops are of the same size and uniform, steady and horizontal wind flow, the intensity of wind-driven rain passing through an imaginary vertical surface can be expressed as (Hoppestad, H., 1955):

$$R_{wdr} = \frac{U}{V_t} \quad (2.2)$$

Where U is the wind speed (m/s) and V_t is the raindrop terminal velocity of fall (m/s). As this equation assumes the wind direction always to be perpendicular to the building façade and no deflection of wind or raindrops by vertical surface, so it measures the free wind-driven rain (Blocken, B., & Carmeliet, J., 2004).

Hoppestad, S. (1955) proposed the following formula based on Equation (2.2):

$$R_{wdr} = k * U * R_h \quad (2.3)$$

Hoppestad defined equation (2.3) as “the wind-driven rain relationship” and the factor k as “the wind-driven rain coefficient”. He conducted measurements using the 4-way free wind-driven rain gauge at four different locations to find out the average values for k . The values of k at four different locations were: Oslo ($k = 0.130$), Bergen ($k = 0.188$), Trondheim ($k = 0.221$) and Tromsø ($k = 0.148$), yielding an average value of 0.180. Lacy, R. E. (1965) modified equation (2.3) which is given by equation (2.4):

$$R_{wdr} = 0.222 * U * R_h^{0.88} \approx 0.222 * U * R_h \quad (2.4)$$

Where 0.222 (s/m) is the wind-driven rain coefficient (average value) that results from the adopted empirical relationships.

Local phenomena induced by the topography and by the building itself was not considered in equation (2.4). The particular wind flow pattern around a building causes deflection of the wind and of the raindrop trajectories (Blocken, B., & Carmeliet, J., 2004). As a result, the amount of wind-driven rain on buildings can widely differ from the free wind-driven rain. Considering the local effects the equation becomes as following (Blocken, B., & Carmeliet, J., 2004):

$$R_{wdr} = \alpha * U * R_h^{0.88} * \cos\theta \quad (2.5)$$

Where α is the wind-driven rain coefficient and θ is the angle between the wind direction and the line normal to the wall. This equation is the wind-driven rain relationship for wind-driven rain on buildings. Researchers found wide variation wind-driven rain coefficient with the size of the building and across the building façade, which ranges from 0.02 s/m (9% of 0.222) to 0.26 s/m (120% of 0.222) (Blocken, B., & Carmeliet, J., 2010). Equation (2.5) is considered as the basic for all semi-empirical models.

There are several models for semi-empirical method. The ISO Standard 15927 (NBN EN ISO 15927-3 (2009)), the ASHRAE 160 model (ASHRAE 2009) and the Straube and Burnett model (Straube, J., & Burnett, E., 2000) are the three commonly referenced models.

2.3.1 ISO model

In the ISO standard 15927 (NBN EN ISO 15927-3 (2009)), a detailed procedure is provided to assess the actual wind-driven rain impinged on building surfaces. The airfield index (I_A), which refers to wind-driven rain in free-field conditions, i.e. without the presence of buildings, can be calculated by equation (2.6).

$$I_A = \frac{2}{9} \sum U * R_h^{8/9} * \cos(D - \theta) \quad (2.6)$$

Where, U is the hourly mean wind speed in m/s, R_h is the hourly rainfall total in mm, D is hourly mean wind direction from north and θ is the wall orientation relative to north where $\cos(D-\theta)$ is positive, i.e., all those occasions when the wind is blowing against the wall.

Some correction coefficients are introduced in the ISO standard 15927 to convert the airfield indices (I_A) to wall indices (I_{WA}). These correction coefficients include terrain roughness coefficient (C_R), topography coefficient (C_T), obstruction factor (O), and wall factor (W). Then the actual amounts of rain that would impact on a real wall (wall indices) can be quantified using Equation (2.7).

$$I_{WA} = I_A * C_R * C_T * O * W \quad (2.7)$$

Blocken, B., and Carmeliet, J. (2010) compared equation (2.5) with the combination of equation (2.6) and (2.7) and found that the ISO model is actually a form of the wind-driven rain relationship in which the ratio $2/9$ corresponds to Lacy's free-field wind-driven rain coefficient 0.222, and the exponent $8/9$ corresponds to Lacy's exponent 0.88. Thus the wind-driven rain coefficient according to the ISO standard is given by:

$$\alpha = \frac{2}{9} * C_R * C_T * O * W \quad (2.8)$$

The ISO standard 15927 (NBN EN ISO 15927-3 (2009)) provides detailed procedure and suggested values for these correction coefficients. Terrain roughness coefficient (C_R) is calculated by equations (2.9) and (2.10).

$$C_R(z) = K_R * \ln(z/z_0) \quad \text{for } z \geq z_{min} \quad (2.9)$$

$$C_R(z) = C_R(z_{min}) \quad \text{for } z < z_{min} \quad (2.10)$$

Where, z is the height above ground. Values of K_R , z_0 and z_{min} for different terrain category should be selected from Table 2.1.

Table 2.1: Terrain categories and related parameters suggested by the ISO standard (source: (NBN EN ISO 15927-3 (2009)).

| Terrain Category | Description | K_R | z_0 | z_{min} |
|-------------------------|---|-------------------------|-------------------------|-----------------------------|
| I | Rough open sea, lake shore with at least 5 km open water upwind and smooth flat country without obstacles | 0.17 | 0.01 | 2 |
| II | Farm land with boundary hedges, occasional small farm structures, houses or trees | 0.19 | 0.05 | 4 |
| III | Suburban or industrial areas and permanent forests | 0.22 | 0.3 | 8 |
| IV | Urban areas in which at least 15% of the surface is covered with buildings of average height exceeding 15 m | 0.24 | 1 | 16 |

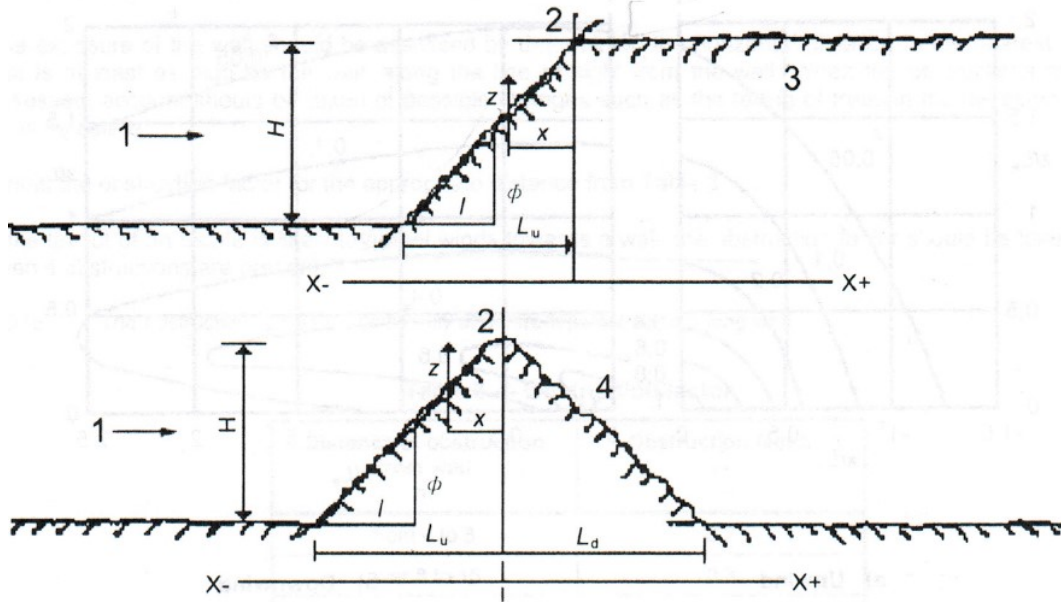
According to ISO standard 15927, the topography coefficient (C_T) accounts for the increase in mean wind speed over isolated hills and escarpments and is related to the wind velocity upwind of the hill or escarpment. The topography coefficient (C_T) should be considered for the locations which are more than half-way up the slope of a hill or which are within 1.5 times the height of the cliff from the base of a cliff. It can be calculated by equations (2.11) to (2.13).

$$C_T = 1 \quad \text{for } \phi < 0.05 \quad (2.11)$$

$$C_T = 1 + 2s\phi \quad \text{for } 0.05 \leq \phi \leq 0.03 \quad (2.12)$$

$$C_T = 1 + 0.6s \quad \text{for } \phi > 0.03 \quad (2.13)$$

Where, s is a factor obtained from Figure 2.5 and ϕ is the upwind slope in the wind direction.



Key

- 1 wind
- 2 crest
- 3 downwind slope < 0.05
- 4 downwind slope > 0.05
- L_u is the actual length of the upwind slope in the wind direction
- L_d is the actual length of the downwind slope
- L_e is the effective length of the upwind slope defined in Table 2.2
- H is the effective height of the feature
- x is the horizontal distance of the site from the top of the crest
- z is the vertical distance from the ground level of the site

Figure 2.4: Definition of factors determining the topography coefficient (C_T) (source: (NBN EN ISO 15927-3 (2009))

The effective length of the upwind slope (L_e) can be calculated according to Table 2.2 using the actual length of the upwind slope in the wind direction (L_u) and the effective height of the feature (H) for shallow and steep slope respectively.

Table 2.2 : Effective length, L_e

| Upwind slope ϕ ($=H/L_u$) | |
|---------------------------------------|------------------------|
| Shallow ($0.05 \leq \phi \leq 0.3$) | Steep ($\phi > 0.3$) |
| $L_e = L_u$ | $L_e = H/0.3$ |

Obstruction factor (O) depends on the horizontal distance to the nearest obstacle that is at least as high as the wall, along the sight from the wall. Table 2.3 shows the Obstruction factor (O) for different conditions.

Table 2.3 : Obstruction factor (source: (NBN EN ISO 15927-3 (2009)))

| Distance of obstruction from wall (m) | Obstruction factor, O |
|---------------------------------------|-------------------------|
| From 4 to 8 | 0.2 |
| Over 8 to 15 | 0.3 |
| Over 15 to 25 | 0.4 |
| Over 25 to 40 | 0.5 |
| Over 40 to 60 | 0.6 |
| Over 60 to 80 | 0.7 |
| Over 80 to 100 | 0.8 |
| Over 100 to 120 | 0.9 |
| Over 120 | 1.0 |

2.3.1.1 Wall factor

Among the correction factors used in the ISO standard 15927 (NBN EN ISO 15927-3 (2009)), terrain roughness coefficient (C_R), topography coefficient (C_T) and obstruction factor (O) are used to convert the meteorological wind speed for onsite condition. Wall factor (W), which takes into account the variation of wind-driven rain over the surface of the wall, is used to convert the airfield wind-driven rain amount for specific façade locations. The ISO standard 15927 provides wall factor values for different types of buildings as shown in Figure 2.6. It is observed that the ISO standard provides wall factor values that are limited to only a few locations on the building façade and same values for all four façades. For example for a multi-storey building with flat roof (pitch $<20^\circ$), the ISO standard gives only two values, i.e., 0.5 for top 2.5 m of the façade and 0.2 for the remainder (Figure 2.6). For two and three storey building with overhang it gives a constant value at different height of the building façade. The ISO standard has only been designed for some ordinary types of façade shapes and suggested wall factor values are very limited (Coutu et al., 2013). Ge and Krpan (H. Ge & Krpan, 2007) found that wall factor is not a constant and it varies with rain events.

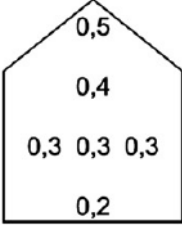
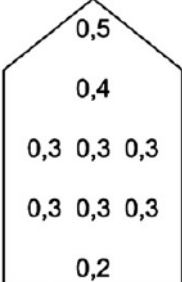
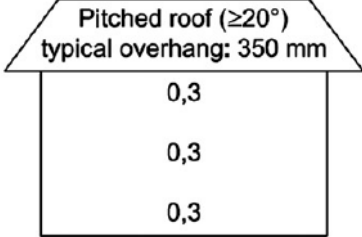
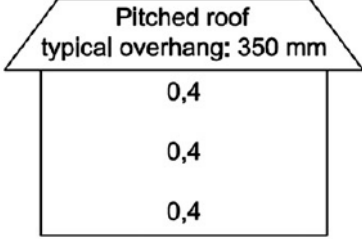
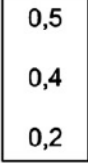
| Description of wall | Average value | Distribution |
|--|--|---|
| Two-storey gable | 0,4 |  |
| Three-storey gable | 0,3 |  |
| Multi-storey building with flat roof (pitch < 20°) | 0,2 for a ten-storey building, for example, but with a higher intensity at top | 0,5 for top 2,5 m 0,2 for remainder |
| Two-storey wall with eaves | 0,3 |  |
| Three-storey wall with eaves | 0,4 |  |
| Two-storey building with flat roof (pitch < 20°) | 0,4 |  |

Figure 2.6 : Wall factors in the ISO standard 15927 (NBN EN ISO 15927-3 (2009))

2.3.2 ASHRAE 160 model

In the ASHRAE 160 model, the amount of rain striking a vertical surface can be calculated using the following equation:

$$R_{wdr} = 0.2 * F_E * F_D * U_{10} * \cos\theta * R_h \quad (2.14)$$

Where, F_E is the rain exposure factor and F_D is the rain deposition factor. ASHRAE 160 model provides recommended values for these parameters. R_h is the horizontal rainfall intensity in mm/hr, U_{10} is the hourly average wind speed at 10 m in m/s and θ is the angle between wind direction and normal to the wall.

The rain exposure factor (F_E) is influenced by the surrounding topography and height of the building. The ASHRAE 160 standard recommended values for rain exposure factor (F_E) are given in Table 2.4. In the table severe exposure includes hilltops, coastal areas, and funneled wind. Sheltered exposure includes shelter from trees, nearby buildings or a valley.

Table 2.4: Exposure factor (source: ASHRAE 2009)

| Building Height, m (ft) | Type of Terrain | | |
|-------------------------|-----------------|--------|-----------|
| | Severe | Medium | Sheltered |
| <10 (<33) | 1.3 | 1.0 | 0.7 |
| 10-15 (33-49) | 1.3 | 1.1 | 0.8 |
| 15-20 (49-66) | 1.4 | 1.2 | 0.9 |
| 20-30 (66-98) | 1.5 | 1.3 | 1.1 |
| 30-40 (98-131) | 1.5 | 1.4 | 1.2 |
| 40-50 (131-164) | 1.5 | 1.5 | 1.3 |
| >50 (>164) | 1.5 | 1.5 | 1.5 |

The values of rain deposition factor (F_D) recommended by the ASHRAE 160 are given in Table 2.5.

Table 2.5 : Deposition factor (source: ASHRAE 2009)

| Wall Type | Deposition Factor (F_D) |
|--------------------------------|-----------------------------|
| Walls below a steep-slope roof | 0.35 |
| Walls below a low-slope roof | 0.5 |
| Walls subject to rain runoff | 1.0 |

2.3.3 Straube and Burnett model

Straube, J. and Burnett, E. (2000) introduce the “Driving Rain Factor (DRF)” which is the inverse of the raindrop terminal velocity of fall (V_t). Here the wind driven rain is given by:

$$R_{wdr} = \frac{1}{V_t} * U * R_h = DRF * U * R_h \quad (2.15)$$

According to Straube, J. (2000), DRF vary considerably for different rainfall intensities and rain storm types and can range from more than 0.5s/m for drizzle to as little as 0.15 s/m for intense cloudbursts. However, the value of DRF ranges from 0.20 to 0.25 s/m for average conditions. Straube, J. and Schumacher, C. (2006) provided a detail procedure to calculate the terminal velocity and hence the DRF.

The distribution of raindrop sizes as a function of rainfall intensity can be calculated as follows:

$$\phi = 1.1042 * R_h^{0.232} \quad (2.16)$$

Where,

ϕ is the equivalent spherical raindrop diameter (mm), and

R_h is the horizontal rainfall intensity (mm/m²/h).

The terminal velocity (V_t) can be determined in m/s by:

$$V_t(\phi) = -0.166033 + 4.9184\phi - 0.888016\phi^2 + 0.054888\phi^3 \leq 9.20 \quad (2.17)$$

Then the DRF can be calculated as the inverse of the terminal velocity:

$$DRF = \frac{1}{V_t} \quad (2.18)$$

The cosine of the angle between the building façades and the direction of the wind can be used to account for wind direction on a plane oriented in a specific direction.

$$R_{wdr} = DRF * U * R_h * \cos\theta \quad (2.19)$$

Where θ is the angle between a line drawn perpendicular to the wall of interest and the wind direction.

Straube, J. and Burnett, E. (2000) used rain deposition factor (RDF), to transform the rate of wind-driven rain in the free wind (i.e. outside of the region disturbed by a building) to the rate of rain deposition on a particular building. For a particular orientation and spot on the building face, the free wind-driven rain values can be modified as:

$$R_{wdr} = RDF * DRF * U * R_h * \cos\theta \quad (2.20)$$

RDF is the ratio of rain in the free wind to rain deposition on a building, which accounts for the effect of building shape and size on rain deposition. RDF values proposed by Straube and Burnett for different types of buildings are shown in Figure 2.7.

Straube, J. and Burnett, E. (2000) also introduced some correction factor which consider onsite conditions to calculate wind driven rain. These factors include Exposure and Height Factor (EHF) and Topography Factor (TOF). The recommended values for EHF for different height and topography is shown in Figure 2.8. TOF is obtained according to NBCC. The wind-driven rain is then given by:

$$R_{wdr} = RDF * DRF * U * R_h * \cos\theta * EHF * TOF \quad (2.21)$$

Comparing equation (2.5) with equation (2.20) and taking into account the power law relationship, the wind-driven rain coefficient (α) can be obtained by the following equation (Blocken, B. & Carmeliet, J., 2010):

$$\alpha = DRF * RAF * \left(\frac{z}{10}\right)^\beta * R_h^{0.12} \quad (2.22)$$

Where β is the power law exponent of the mean wind speed profile.

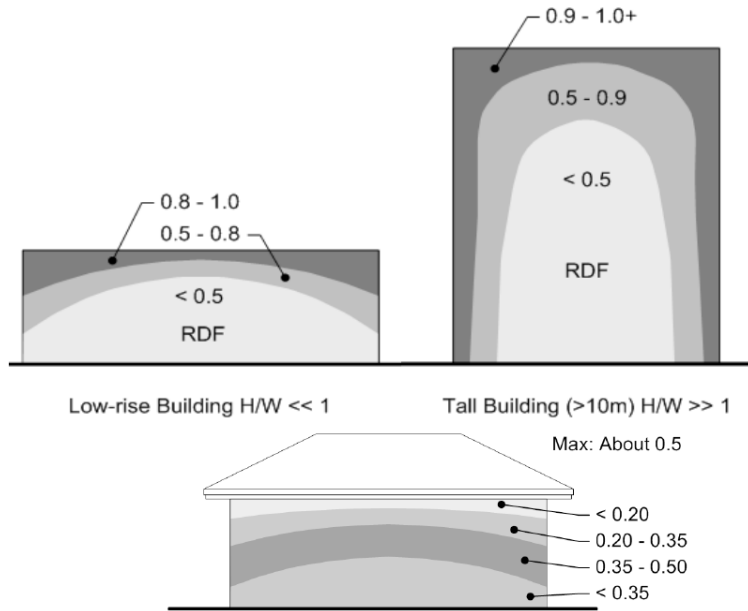
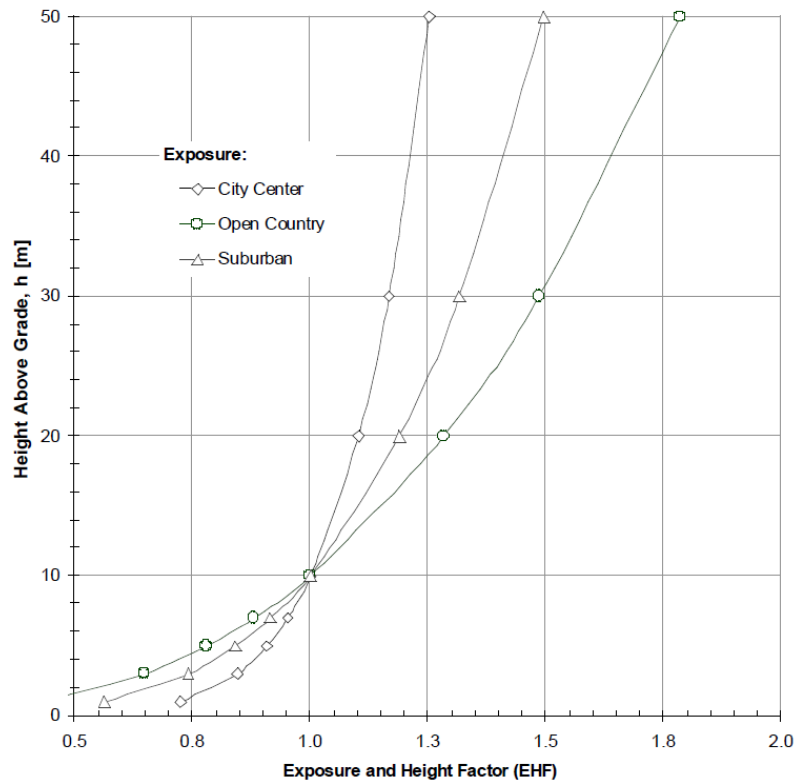


Figure 2.7: Values of RDF (Straube, J. & Burnett, E. 2000)



Recommended multiplication factors to apply to above:
 Sheltered: 0.5 if buildings or obstruction of building height are within a distance equal to twice the building height
 Hilltop or Cliff top: See speed-up correction factor in text

Figure 2.8 : Recommended values for EHF (Straube, J. & Burnett, E. 2000)

A number of studies based on semi-empirical models have been carried out in different countries in the past. There are two categories, one focuses on generating wind-driven rain maps based on airfield wind-driven rain. Airfield wind-driven rain is an indicator of the wetness of a location. The other is the prediction of wind-driven rain on actual façade using these semi-empirical models.

Generation of driving rain index maps using wind and rain data by semi-empirical models become a well-known practice throughout the world in the last few decades. P. (1987) calculated wind-driven rain using wind and rain data for 10 years collected from 108 meteorological stations and created driving rain index map for China in 1987, which categorizes cities and provinces as moderate and severe exposure. Zhu, D. et al. (1995) derived quantitative driving rain exposure for fifteen important Canadian cities using the climatological data recorded at local meteorological stations. Chand, I. and Bhargava, P. (2002) computed average annual driving rain indices using wind and rain data for 350 stations across India and generated driving rain exposure level map for India in 2002. In 2005, Rydock, J.P. et al. (2005) assessed driving rain exposure based on multi-year records of synoptic observations of present weather, wind speed and direction. Sahal, N. (2006) computed annual driving rain indices based on monthly rainfall amounts and monthly mean wind speed for 238 stations across Turkey and produced driving rain map of Turkey in 2006. Pérez-Bella, J.M. et al. (2012) estimated driving rain index based on ISO semi-empirical model and produced a map of driving rain in Spain. In another study by the same author (Pérez-Bella, J.M. et al., 2013), risk index has been calculated for 80 Spanish sites. According to the authors, compared with the usual wind-driven rain exposure maps, the inclusion of driving rain wind pressure in this index permits a more complete assessment of risk for rain penetration. In their recent study, Pérez-Bella, J.M. et al. (2014) has calculated risk index considering more Spanish locations.

As discussed earlier, to predict the actual wind-driven rain on the façade, correction factors are required. The study carried out during the years 2006 to 2008 in British Columbia, Canada (Ge, H. & Krpan, R. 2009), where 8 buildings were studied, shows the comparison of wall factors suggested by British standard (BS1804-1992), Straube (2006), Blocken (2004) with the values obtained from field experiments. Wall factor values recommended by the British Standard (BSI, 1992) and Straube, J. (2006) are based on long-term field measurements and do not account for

specific wind and rain conditions. On the other hand values recommended by Blocken, B. (2004) are generated through a validated CFD model and are specific to wind and rain conditions. In general, it is found that the wall factors obtained through field measurements are similar or smaller than reported. In the same study Ge, H. and Krpan, R. (2009) also calculated the airfield driving rain index and compared it with the measured wind-driven rain. It is found that building geometry and design details have a significant influence on a building's wind-driven rain exposure. So it is not the same for the buildings with different geometry and design. Also the semi-empirical method overestimated the amount of wind-driven rain.

Kubilay, A. et al. (2014) estimated catch ratios using both the ISO model and ASHRAE model and compared with measured values over façade. The values estimated by the semi-empirical models shows very large deviations. The ISO model tends to underestimate the average of measured values by about 59% on cube building without shielding effect and by about 87% on cube building shielded by the upstream cubes. The ASHRAE model overestimates the average of measured values by up to 88% on cube building without shielding effect and by up to 40% on cube building shielded by the upstream cubes. Kubilay, A. et al. (2014) found that both models lack the information on spatial distribution of wind-driven rain intensity on the façade. They concluded that the existing semi-empirical models give limited information on wind-driven rain distribution and they are more convenient for simpler geometries that involve less interaction from surrounding objects.

Wolf, J. and Griffith, M. (2008) conducted wind-driven rain analysis using semi-empirical method and found that wind-driven rain intensity varies considerably by location and by building elevation. Júnior, C.M.M. and Carasek, H. (2014) conducted a study in the city of Goiania, Brazil where they calculated the monthly directional driving rain index and driving rain amount in vertical wall using semi-empirical model and evaluated the influence of façades orientation on the amount of wind-driven rain.

Conclusions of the previous studies confirm that the semi-empirical models suffer from a number of drawbacks and are unable to provide good estimation of wind-driven rain. The reason behind

this is that these semi-empirical models are limited to simpler building geometries and suffers from lack of the information on spatial distribution of wind-driven rain intensity on the façade. Should the predictive performance of these semi-empirical models be improved, the semi-empirical methods could be the most suitable methods for wind-driven rain estimation because of their simplicity in use.

2.4 NUMERICAL METHOD

As discussed in the previous sections, though the experimental method provides the basic knowledge for understanding wind-driven rain, it is time consuming, expensive, and can suffer from large errors. Semi-empirical models are easy to use but they were developed based on measurements on a limited number of building geometries and façade locations. Regarding to these complexity of experimental and semi-empirical methods, researchers realized that further achievements to be gained through numerical simulation. Computational Fluid Dynamics (CFD) modelling procedure was firstly introduced by Choi who developed a numerical method where the raindrop trajectories were calculated based on a steady-state 3D wind flow pattern (Choi, E., 1993; Choi, E., 1994; Choi, E., 1999; Choi, E., 2000). Numerical simulation comprises the calculation of the wind flow pattern around the building by solving the complex three dimensional Reynolds-averaged Navier-Stokes equations (RANS) with a CFD code and the calculation of raindrop trajectories in this flow pattern. Blocken and Carmeliet advanced this simulation by including the temporal component using Euler-Lagrangian approach and by developing a new weighted data averaging technique, which allowed the determination of both the spatial and temporal distribution of wind-driven rain (Blocken, B. & Carmeliet, J., 2000a; Blocken, B. & Carmeliet, J., 2000b; Blocken, B. & Carmeliet, J., 2002; Blocken, B. & Carmeliet, J., 2004). Comparison with measurements demonstrated that accurate results can be obtained by numerical simulations (Blocken, B. & Carmeliet, J., 2007). Huang, S. and Li, Q. (2010) found that Eulerian Multiphase (EM) model with Reynolds-averaged Navier-Stokes equations is capable of providing accurate results for wind-driven rain on the windward façade of an isolated low-rise building. Kubilay, A. et al. (2013) performed a validation study with the EM model on a historical building with a monumental tower by comparing the results with measurement data and found that EM model can be an easier way to include the turbulent dispersion into wind-driven rain calculations with

substantially reduced calculation time. As a further advancement on wind-driven rain calculation, the turbulent dispersion of raindrops was implemented into the Eulerian Multiphase (EM) model by Kubilay, A. et al. (2014). From the study it is shown that taking turbulent dispersion into account reduces the deviation between CFD simulations and field measurements for a high-rise tower building.

The speed at which raindrops fall is a function of the size of the drop and as the drop size increases the rain drop terminal speed increases at a decreasing rate (Straube, J., & Burnett, E., 2000). Choi, E. (1993) found that close to a building, the local wind speed is very much affected by the building itself. So he concluded that obviously raindrop trajectories are affected by the local flow pattern. He also observed that raindrops, especially for the smaller radius, can move in an upward direction. This upward movement is stronger for a higher wind speed. For the larger raindrops, although no upward movements are observed, the horizontal longitudinal velocity component can be quite large. Rychtarikova, M. and Vargova, A. (2008) stated that generally, raindrop trajectories are more inclined and distorted for small raindrops and higher wind speeds. They found that trajectories are more rectilinear for larger drops and lower wind speeds. Heavy raindrops require a stronger winds to fall less vertically, e.g., to have more probability of hitting the whole façade. Foroushani, M. et al. (2014) found that wind-driven rain drops are mainly affected by two forces namely gravity force and drag force. Balance between these two forces determines the trajectory of a rain drop. Rain drops with smaller diameter is mainly affected by the drag force and follow the wind flow patterns and hence they have highly curved trajectories. But larger rain drops are mainly affected by gravity and they are less influenced by the local wind flow. As a result larger rain drops have straight trajectories.

Hangan, H. (1999a; 1999b) carried out a study to compare the results obtained from wind tunnel experiments with that of CFD simulations. For this study prevailing wind direction was assumed to be perpendicular to the main façade of the building with a speed of 10 m/s at a height of 10 m and rainfall intensity was assumed as 10 mm/hr. The results were compared in terms of Local Intensity Factor (LIF). LIF is the ratio of wind-driven rain intensity on building face to the unobstructed rainfall intensity. Simulation was carried out for both tall and low-rise buildings.

Even though some discrepancies between the measurements and CFD simulation are observed at upper zone of taller building and middle zone of lower building, the wetting pattern is similar.

The wind-driven rain striking the exterior façade of a short building and a tall building has been generated using a three-dimensional computer fluid dynamics (CFD) model by Karagiozis, A. et al. (1997). It has been observed that for both the buildings, the amount of wind-driven rain striking the façades increase from bottom to top. Influence of rainfall intensity has not been found significant on the wetting pattern but higher wind speed has been found to significantly increase the amount of wind-driven rain received on the façades.

A numerical study was carried out by Blocken, B. and Carmeliet, J. (2006) to examine the influence the wind-blocking effect by a building on its wind-driven rain exposure. It is found that wind-blocking effect is an important factor that govern the amount of wind-driven rain and its distribution pattern on the façades of isolated buildings. Results show that the larger wind-blocking effect by the building, the less wind-driven rain it receives at its lower part and that is why high-rise buildings do not necessarily receive more wind-driven rain than low-rise buildings.

Recently Kubilay, A. et al. (2014) has estimated wind-driven rain intensities on an array of 9 low-rise cubic building models using CFD simulations with Eulerian Multiphase (EM) modelling and validated the numerical results by comparing the calculated catch ratio values with data from field measurements. It has been found that the numerical model estimates the wind-driven rain amounts and gradients over the façades successfully. It is also found that the EM model has the advantage of predicting the wind-driven rain intensity on all surfaces of a complex geometry and can provide accurate spatial and temporal information on wind-driven rain.

Blocken, B. and Carmeliet, J. (2000; 2007) found that arithmetic averaging to obtain hourly data generally cause an important loss of information about the co-occurrence of wind and rain. They proposed a weighted averaging technique that takes into account the co-occurrence of wind speed and horizontal rainfall intensity to obtain hourly data and suggested to use hourly data obtained by this proposed technique for wind-driven rain calculation to avoid errors. The influence of the averaging techniques on the quantification of wind-driven rain amount on building facades using

semi-empirical and CFD models for Canadian climates was investigated by Ge, H. (2015). It is found that the arithmetic averaging gives a better estimation of the wind-driven rain amount than the weighted averaging when semi-empirical wind-driven models are used. But when CFD based catch ratio method is used, the weighted averaging technique provides a better estimation over the arithmetic averaging technique even though the difference between the arithmetic and weighted averaging is within 3–7% for the three investigated Canadian cities.

Numerical simulation has provided a new impulse in driving rain research. Significant advancement has been achieved in CFD simulation since its first use. Now a days, the CFD model is capable of providing accurate spatial distribution of wind-driven rain on building facades even for those of a complex geometries.

2.5 BUILDING GEOMETRY AND WIND-DRIVEN RAIN

In the past several studies have been done to find out the relation between the building characteristics (dimensions, presence of overhangs) and wind driven rain. Blocken, B. et al. (2013) concluded that as low-rise buildings are sheltered by surrounding buildings but high-rise buildings are not substantially sheltered, so high-rise buildings are more exposed to wind-driven rain. Karagiozis, A. et al. (2003) indicated wind-driven rain as a strong function of building orientation. According to them for many locations in North America a predominant wind-driven rain location exists. For this predominant orientation the building envelope may receive the majority of the moisture load.

2.5.1 Effect of overhang in reducing wind-driven rain

Some past studies found overhangs are effective to reduce the quantity of wind-driven rain on building façades as they found lower catch ratios for the building façades containing overhangs (Ge, H., & Krpan, R., 2007; Nore, K., 2006). Ge, H. and Krpan, R. (2007) found that the effectiveness of overhangs depends on the wind and rain characteristics. Hangan, H. (1999a; 1999b) conducted simulation to estimate the effectiveness of the cornice in reducing the rain impact on the upper part of a low-rise building façade. Two simulations were performed: one with

cornice and another without cornice. Results were analyzed for both cases (i.e., with and without cornice). It is found that cornice can reduce the rainfall for the building zones located immediate below the cornice. The upper wall zones, which are immediately below the cornice, are well protected from rain. Blocken, B. and Carmeliet, J. (2004) carried out a numerical study to develop a simplified approach to estimate catch ratio and driving rain coefficient. They did the analysis for VLIET building which is the test building of the Laboratory of Building Physics at the University of Leuven. From the catch ratio values, the driving rain coefficient is easily determined by dividing the catch ratio by the reference wind speed U .

$$\alpha = \frac{R_{wdr}}{U * R_h} = \frac{\eta}{U} \quad (2.23)$$

Form the results of this study (Blocken, B., & Carmeliet, J., 2004) it is found that for the positions on the façade that are sheltered by roof overhang, the driving rain coefficient suddenly drops to zero below a certain wind speed. It is also found that the driving rain coefficient steeply increases with increasing intensity for the lowest horizontal rainfall intensities. But for the higher intensities, it changes only slightly with intensity.

Rychtáriková, M. and Vargova, A. (2008) conducted a CFD study to predict the behavior of rain water on window surfaces and investigate the self-protecting effects of buildings. They used a reference model which is a family house with a small garage built in Belgium. The main building has a length of 10.9 m and width of 8.15 m wide. The sloped-roof overhang depth is 30 cm. From this CFD study they found that the effect of the roof overhang is very significant as the areas of the façades immediate beneath the overhang are sheltered from rain due to the effect of overhang.

Foroushani, M. et al. (2014) have investigated the effect of overhangs of various sizes on the wind-driven rain wetting for different wind and rain conditions for a low-rise cube building using CFD simulations. According to them overhang provides two types of protections. First one is that it provides shade which is the direct effect and the second one is that it creates disturbance to the incoming wind which is the indirect effect. As the wind speed increases the horizontal component of raindrop velocity increases and the direct effect decreases. As the small raindrops are drag driven and they follow the wind flow more strictly, the indirect effect is more significant on smaller

raindrops. So indirect effect is dominant under low rainfall intensities as small raindrops holds a greater shear for low rainfall intensities. In this study simulation results were validated by experimental and numerical data. It is seen that presence of an overhang can significantly change the amount of wind-driven rain as well as the wetting pattern of the façade, especially at the upper locations. From the results it has been seen that when overhang is introduced, a narrow strip of the façade beneath the overhang is fully protected from wind-driven rain. As the width of the overhang is increased the height of the dry strip is also increased. But the overhang has no effect on the lower part of the façade. According to the investigators, it is happened because as the width of the overhang increases, both the area shaded by overhang and the disturbance introduced by overhang increases. So both the effects (direct and indirect) increase with increased overhang width. Thus wider overhangs are more effective to reduce the effect of wind-driven rain. It was also found that wind direction have significant effect on indirect effect of overhangs than the direct effect. This is because as the wind angle increases, the blocking effect decreases and the wind can flow over the wind ward façade more easily. Foroushani, M. et al. (2014) concluded that compared to rainfall intensity, wind speed and wind direction have larger impacts on the performances of overhang and also on wind-driven rain load.

So, it was found that presence of overhang can significantly reduce the wind-driven rain on the upper part of the façade (immediate below the overhang) but it doesn't have any effect at bottom locations. Even though the wider overhang is more effective, but its performance is effected by wind and rain characteristics.

2.6. SUMMARY

Blocken, B. et al. (2010) conducted study to compare two semi-empirical models (the semi-empirical model in the ISO Standard and the semi-empirical model by Straube and Burnett (SB)) with the CFD model by Choi by applying them to four idealized buildings (a low-rise cubic building, a low-rise wide building, a high-rise wide building and a tower building) under steady-state conditions of wind and rain. The CFD results are considered as the reference case and the performance of the two semi-empirical models is evaluated by comparison with the CFD results. The comparison was based on the basis of the wind-driven rain coefficient (equation (2.8) and

(2.22)). The maximum values for wind-driven rain coefficient are found on the upper portion of the buildings and it gradually reduces to the lower portion. For low-rise building it is found that the ISO model provides a fairly good agreement, although it generally underestimates the values at the top of the façade. For rainfall intensity of 1 mm/hr, the values at the top and along the edge line of the façade are considerably overestimated by the SB model. However, for rainfall intensities of 10 and 30 mm/hr, the SB model provides quite good results. For tall building the ISO model provides a good agreement for some cases, although it provides underestimations for the upper part of the façade. The SB model strongly overestimates the values near the top of the middle line and along the entire edge line of the façade. Blocken, B. et al. (2010) also applied these three models to a high-rise tower building and compared with full-scale measurements. Results showed that the agreement between measurements and CFD is quite good at the upper part of the tower, however the discrepancies between the measurements and the ISO and SB model are large.

Despite new modelling advances, the experimental method is still most important in the field of wind-driven rain research (Blocken, B. & Carmeliet, J., 2005; Nore, K. et al., 2007). The other two methods of wind-driven rain measurements, i.e., semi-empirical method and numerical method are increasingly being used to calculate wind-driven rain on building façades. Semi-empirical models are easy to use but they were developed based on measurements on a limited number of building geometries and façade locations. As a result, these models suffers from lack of the information on spatial distribution of wind-driven rain intensity on the façade and wind-driven rain estimated by these semi-empirical models may have large deviations from field measurements (Ge, H., & Krpan, R., 2009; Kubilay, A. et al., 2014). Numerical simulation has provided a new impulse in wind-driven rain research. Significant advancement has been achieved in CFD simulation since its first use. Now a days, the CFD model is capable of providing accurate spatial distribution of wind-driven rain on building façades even for those of a complex geometries, however, it requires a large amount of preparation work and high computing cost (Blocken, B., & Carmeliet, J., 2004). In addition, high-quality measurements are needed to validate the CFD models. The development, verification and validation of semi-empirical and numerical models require accurate and complete wind-driven rain measurement datasets (Nore, K. et al., 2007).

However, there is very limited data on the amount of wind-driven rain. An adequate experimental wind-driven rain dataset should comprise and/or be accompanied by the following information: (1) a detailed description of the building site and the building geometry; (2) a detailed description of the measurement setup; (3) measurements of the reference wind speed, the reference wind direction and the horizontal rainfall intensity; (4) wind-driven rain measurements at the façade(s) with a sufficiently high resolution in space; and time and (5) error estimation for the wind-driven rain measurements (Blocken, B., & Carmeliet, J., 2005). To the knowledge of the author, some complete field data are: the wind-driven rain data by the Unit Building Physics and Systems, Technical University of Eindhoven (TUE), Netherland and the wind-driven rain data by the Laboratory of Building Physics, Katholieke Universiteit Leuven (K.U.Leuven), Belgium (Nore, K. et al., 2007). Recently Kubilay, A. et al. (2014) have conducted wind-driven rain measurements within a test setup and developed another dataset of wind-driven rain measurement. Baheru, T. et al. (2014) conducted a laboratory experimental study to investigate the distribution of wind-driven rain deposition on the external façade of low-rise buildings and developed test-based data on the rain admittance factors (RAFs) and surface runoff coefficients (SRCs) for three types of building shapes (glabe, flat and hip-roof buildings). In spite of the generation of new data sets through field experiments, but the quantity of such studies is not as per requirement. Considering the necessity of experimental data sets, Wolf, J., and Griffith, M. (2008) proposed to measure wind-driven rain experimentally at least at major airport locations.

Given the needs to further develop semi-empirical models and validate CFD models, measurements on buildings with various geometries and design details under different climatic conditions are essential for the advancement of research in wind-driven rain. With the aims to generate a unique set of measurements to characterize the wind-driven rain distribution on mid- and high-rise buildings and to evaluate the existing semi-empirical models used for quantifying wind-driven rain loads, field measurements of wind-driven rain on mid - and high - rise buildings in three Canadian regions have been conducted in this study.

Chapter 3

METHODOLOGY

3.1 INTRODUCTION

In this chapter, the experimental part of the study is presented. Three buildings located in two regions of Canada (i.e., Fredericton, New Brunswick and Montreal, Quebec) have been instrumented with equipment to record simultaneously on-site weather data including wind speed, wind direction, temperature, relative humidity, and horizontal rainfall; and wind-driven rain on building façade. These buildings are (1) McLeod House, Fredericton, NB, Canada, (2) HB Building, Montreal, QC, Canada, and (3) FB Building, Montreal, QC, Canada. These buildings represent a variety of building geometry, topography and construction type.

3.2 BUILDING LOCATION AND DESCRIPTION




Figure 3.1 shows the locations of the test buildings.



Figure 3.1: Locations of test buildings (Google maps.2015a)

Details of these test buildings including their construction type, geometry and obstruction are shown in Table 3.1. This table also represents the number of driving rain gauges that has been installed on different façades of these buildings.

Table 3.1: Details of test buildings

| Buildings | Construction type | Geometry | Obstruction | No. of rain gauges | Picture |
|---|-----------------------------------|----------------------------|--------------------|---|---|
| McLeod House, Fredericton, NB | Seven-storey residential building | Flat roof without overhang | Moderate | 7 (south-west) 6 (south-east) 2 (north-east) 1 (north-west) |  |
| Hingston Hall B (HB) Building, Montreal, QC | Four-storey residential building | Flat roof without overhang | Moderate | 10 (south-west) 4 (south-east) 2 (north-west) |  |
| Faubourg Tower (FB), Montreal, QC | Thirteen-storey office building | Flat roof without overhang | Moderate | 7 (south-west) 6 (south-east) 10 (north-east) 1 (north-west) |  |

3.2.1 McLeod House

Opened in 1974, McLeod House is the tallest residence at University of New Brunswick. It is located at the top of College Hill on the south end of campus. This is a seven storey building with flat roof and without any overhang. The height of the building is 22 m (72'-2"). The satellite image of the building and its surrounding is presented in Figure 3.2. A 22 m high neighbouring building is located about 20 m away from McLeod House on the north-west side. On the west to south-west side is a parking lot with a long field of trees. These trees are about 40 m away from the building. There are a couple of low-rise houses on the south-east side, located over 100 m away from the

building. On the north-east side is an open grass field with some low-rise constructions across the road, over 100 m away from the building.



Figure 3.2: Satellite image of the surroundings of McLeod House (Google maps.2015b)

On-site weather data is measured by a weather station placed on top of the roof (Figure 3.3) and wind-driven rain on façade is measured by customized driving rain gauges. Analysis of historical data for Fredericton shows that normally the prevailing wind direction is the north, south-south-west, and west-north-west but during rain hours the wind mainly comes from the north, south and north-east directions (Figure 3.4).



Figure 3.3: Photo of wind monitor, temperature and relative humidity probe and the horizontal rain gauge installed on the roof top of McLeod House

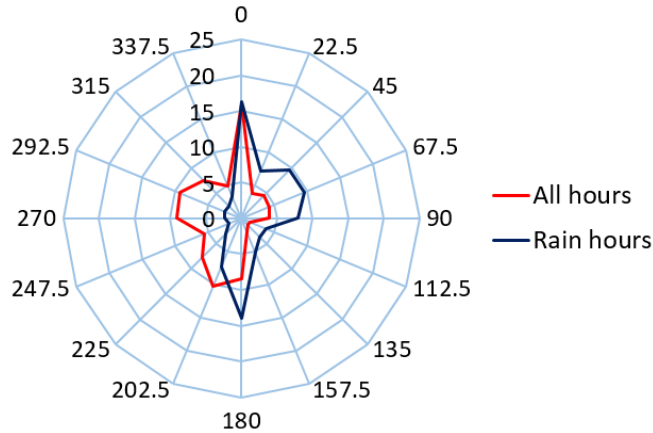


Figure 3.4: Prevailing wind direction at Fredericton obtained from Fredericton airport station data

Based on the prevailing wind direction and the actual building geometry and surrounding details sixteen locations on the building façades were selected to install driving rain gauges. Seven driving rain gauges were installed on the south-west façade (SW1, SW2, SW3, SW4, SW5, SW6 and SE1), six on the south-east façade (E1, E2, E3, E4, E5, and E6), two on the north-east façade (N1, N2), and one on the north-west façade (W1). The driving rain gauges were installed at the heights of 0.61 m (2'), 4.88 m (16') and 9.14 m (30') from the roofline of the building. To capture the typical spatial distribution of wind-driven rain, more driving rain gauges were placed on façade facing the prevailing wind-driven rain direction and at top and corners where higher wind-driven rain amount and greater variation of wind-driven rain are expected. Figure 3.5 shows the driving rain gauges location on the plan view of McLeod House. Figure 3.6 to Figure 3.13 show the driving rain gauges location on the elevations of McLeod House and photos corresponding to each façade with installed driving rain gauges.

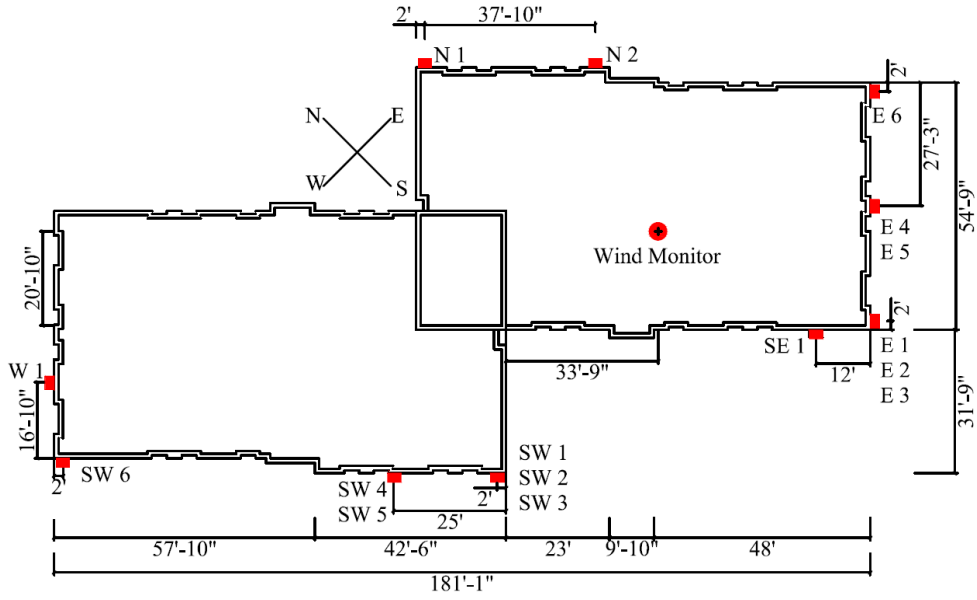


Figure 3.5: Plan view of McLeod House with driving rain gauge locations

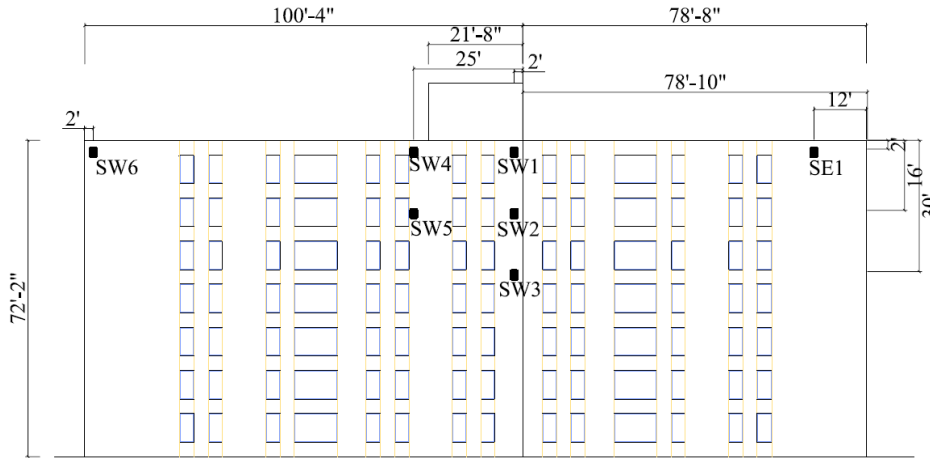


Figure 3.6 : South-west elevation of McLeod House with the driving rain gauge locations



Figure 3.7 : Photo of the south-west façade of McLeod House with driving rain gauges

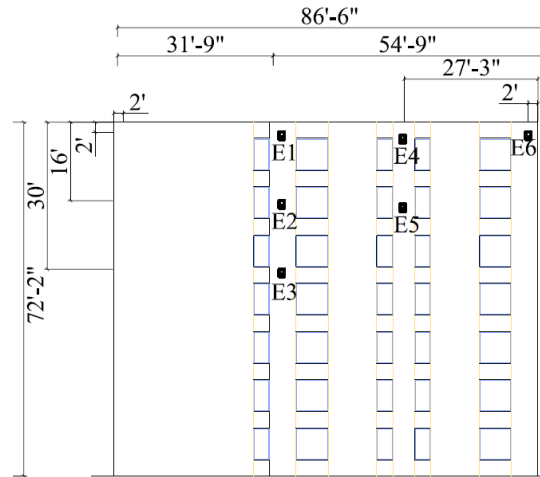


Figure 3.8: South-east elevation of McLeod House with driving rain gauge locations



Figure 3.9 : Photo of the south-east façade of McLeod House with driving rain gauges

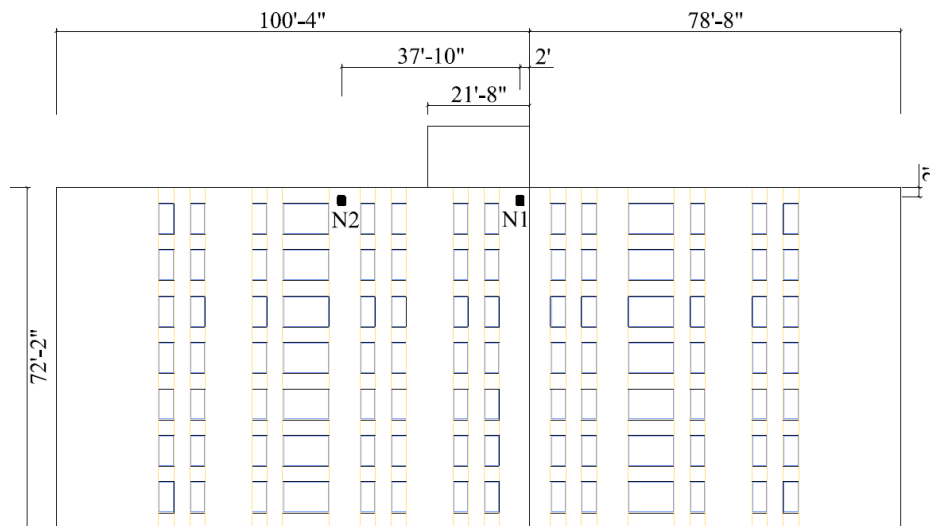


Figure 3.10 : North-east elevation of McLeod House with driving rain gauge locations



Figure 3.11 : Photo of the north-east façade of McLeod House with driving rain gauges

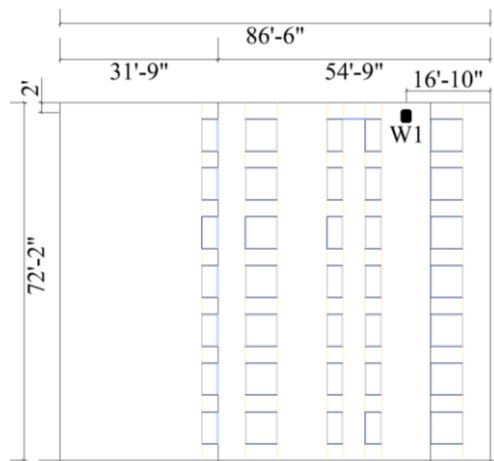


Figure 3.12 : North-west elevation of McLeod House with driving rain gauge locations



Figure 3.13 : Photo of the north-west façade of McLeod House with driving rain gauges

3.2.2 Hingston Hall B (HB) Building

Hingston Hall B Building (HB Building) is a four story hostel building located on Loyola campus of Concordia University, Montreal, Quebec. It is a flat roof building without overhang. The height of the building is 15.06 m (49'-5"). Figure 3.14 shows the satellite image of the building and its surrounding. In the south-west direction of HB Building there is a long open area and further upstream there exists a parking area. On the north-west side the nearby two storey building is about 50 m away from HB Building. At the right corner of the north-east side is another a four- storey building located about 20 m away from HB Building. On the south-east side there exists long filed containing trees.

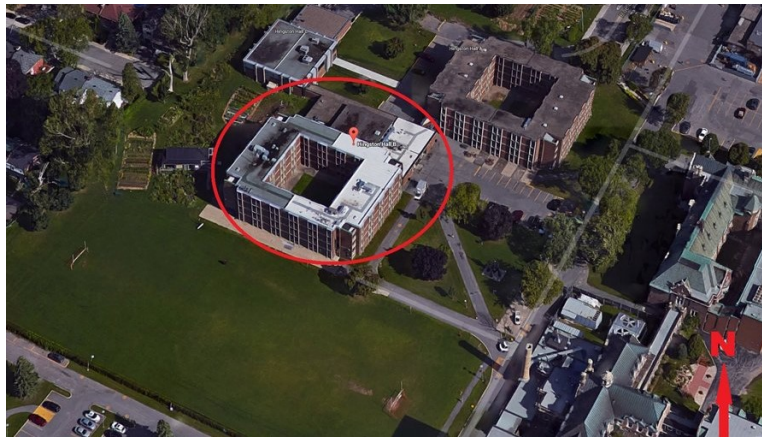


Figure 3.14 : Satellite image of the surroundings of HB Building (Google maps.2015c)

The analysis of historical data shows that the prevailing wind direction for Montreal is west, south-west, and north during all hours and north-east, south-south-east and south-west during rain hours (Figure 3.15). Based on the prevailing wind direction and the actual building geometry and surrounding details sixteen locations on the building façades were selected to install driving rain gauges. Ten driving gauges were installed on the south-west façade (SW1, SW2, SW3, SW4, SW5, SW6, SW7, SW8, SW9 and SW10), four on the south-east façade (SE1, SE2, SE3 and SE4), and two in the north-west façades (NW1 and NW2). No rain gauge was installed on the north-east façade. The gauges were installed at the heights of 0.61 m (2') and 4.88 m (16') from the roofline of the building. Locations of the driving rain gauges on the building plan view elevations is shown in the Figure 3.16. Driving rain gauges location on the elevations of HB Building and photos

corresponding to each façade with installed rain gauges are shown in the Figure 3.17 to Figure 3.22. Figure 3.23 show the photo of wind monitor, temperature and relative humidity probe, and the horizontal rain gauge installed on the roof top of HB Building.

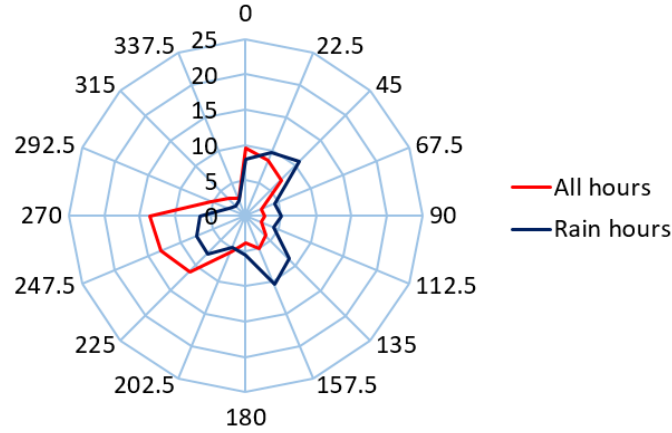


Figure 3.15: Prevailing wind direction at Montreal obtained from Montreal international airport station data

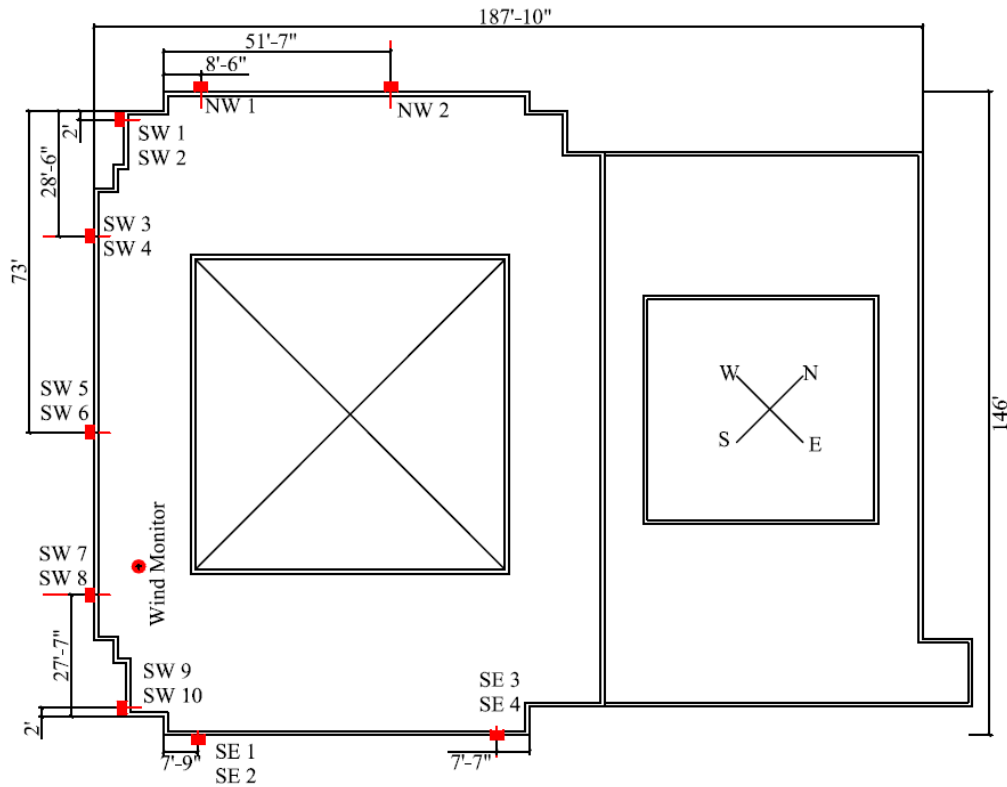


Figure 3.16 : Plan view of HB Building with driving rain gauge locations

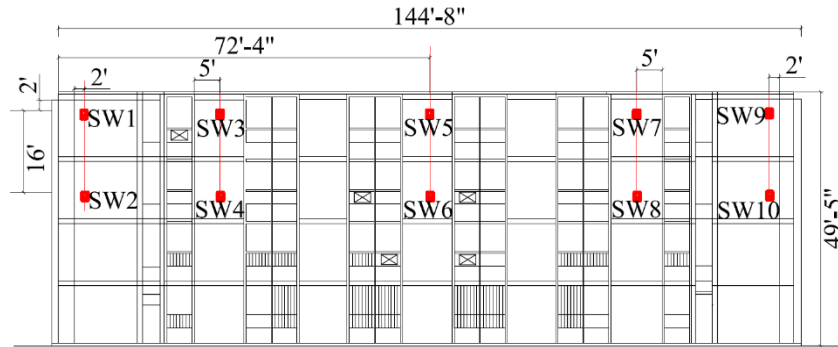


Figure 3.17 : South-west elevation of HB Building with driving rain gauge locations



Figure 3.18 : Photo of the south-west façade of HB Building with driving rain gauges

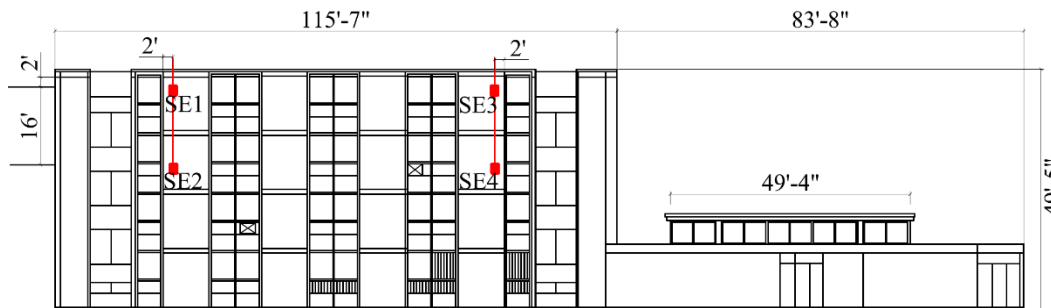


Figure 3.19 : South-east elevation of HB Building with driving rain gauge locations



Figure 3.20 : Photo of the south-east façade of HB Building with driving rain gauges

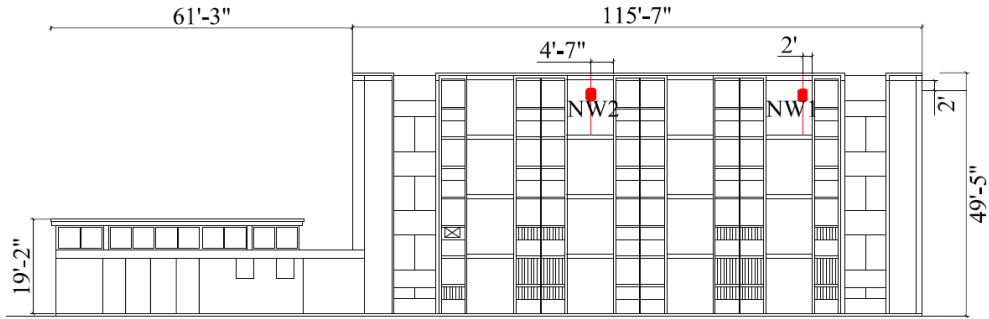


Figure 3.21 : North-west elevation of HB Building with driving rain gauge locations



Figure 3.22 : Photo of the north-west façade of HB Building with driving rain gauges



(a)



(b)

Figure 3.23: Photo of: (a) wind monitor, temperature and relative humidity probe; and (b) horizontal rain gauge installed on the roof top of HB Building

3.2.3 Faubourg Tower (FB Building)

The FB Building is a thirteen story office building located on SGW campus of Concordia University in downtown Montreal, Quebec. It is a flat roof building without overhang. The height of the building is 45.6 m (149'-7"). Satellite image of the building and its surrounding is presented in Figure 3.24. On the south-west direction is a five-storey wing attached to FB Building. On the north-west side there is a five-storey building is about 25 m away from FB Building. Further away there exists a fifteen-storey building located about 60 m away from FB Building. On the south-east side is a four-story building located about 22m away from FB Building. On the north-east side the nearby building is three storeys high and located about 23m away from FB Building.

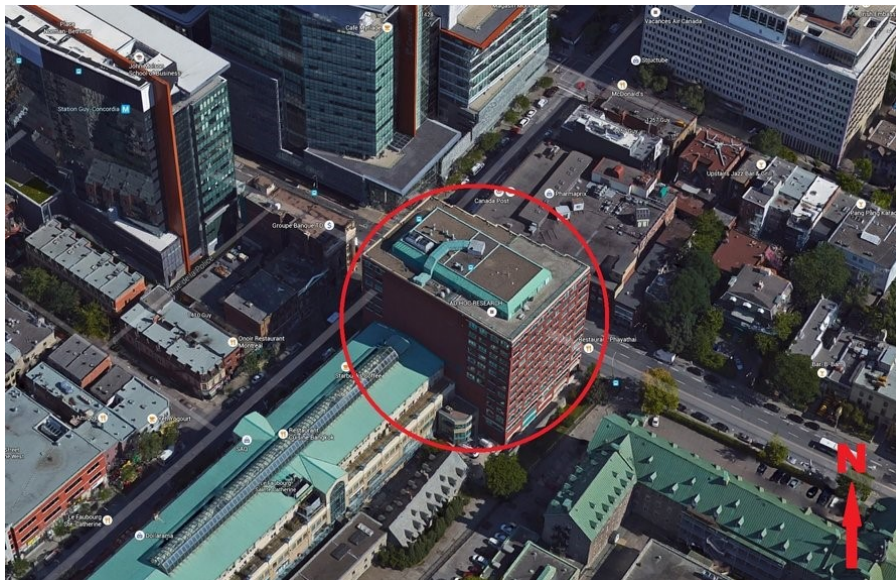


Figure 3.24 : Satellite image of the surroundings of FB Building (Google maps.2015d)

Based on the prevailing wind direction (shown in Figure 3.15) and the actual building geometry and surrounding details twenty four locations on the building façades were selected to install driving rain gauges. Seven driving rain gauges were installed on the south-west façade (SW1, SW2, SW3, SW4, SW5, SW6, and SW7), six on the south-east façade (SE1, SE2, SE3, SE4, SE5 and SE6), one on the north-west façade (NW1) and ten on the north-east façade (NE1, NE2, NE3, NE4, NE5, NE6, NE7, NE8, NE9, NE10). The driving rain gauges were installed at the heights of 0.61 m (2'), 4.88 m (16'), 10.67 m (35') and 21.34 m (70') from the roofline of the building. The

locations of driving rain gauges are all above the height of the nearby buildings on each façade. Figure 3.25 shows the driving rain gauges location on the plan view of FB Building. Figure 3.26 to Figure 3.33 show the driving rain gauges location on the elevations of FB Building and photos corresponding to each façade with installed driving rain gauges. Similar set up is installed on the roof top to measure on-site weather data.

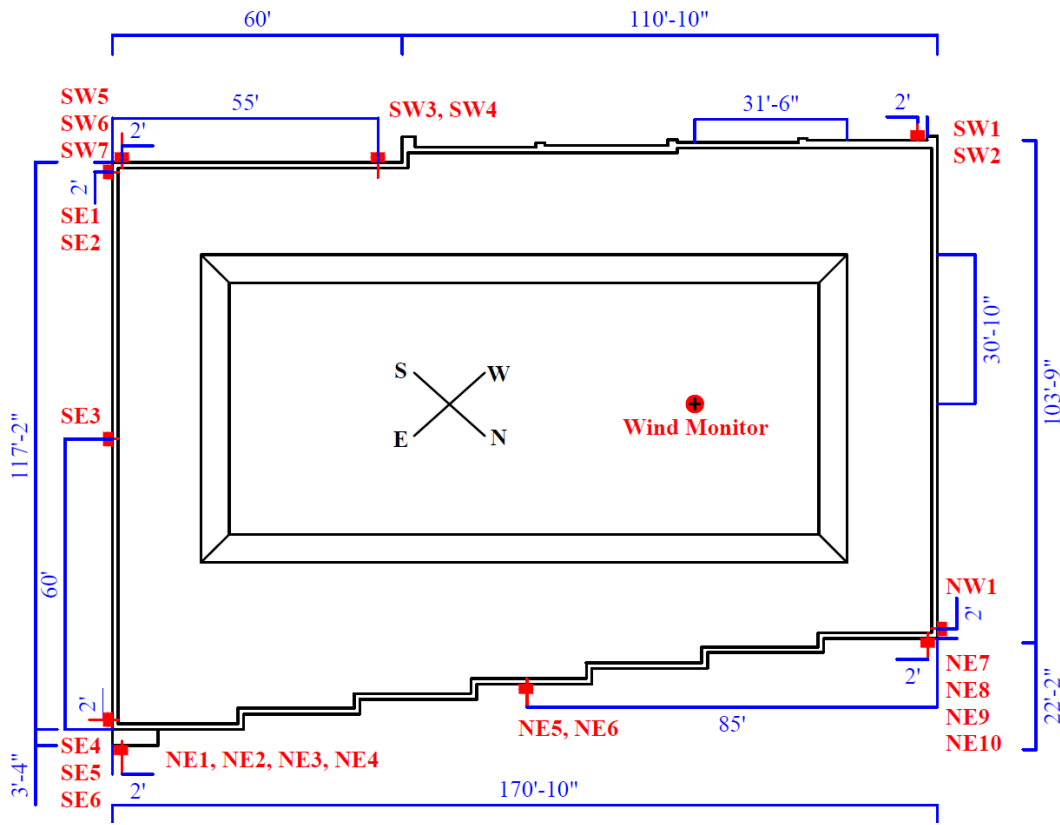


Figure 3.25 : Plan view of FB Building with driving rain gauge locations

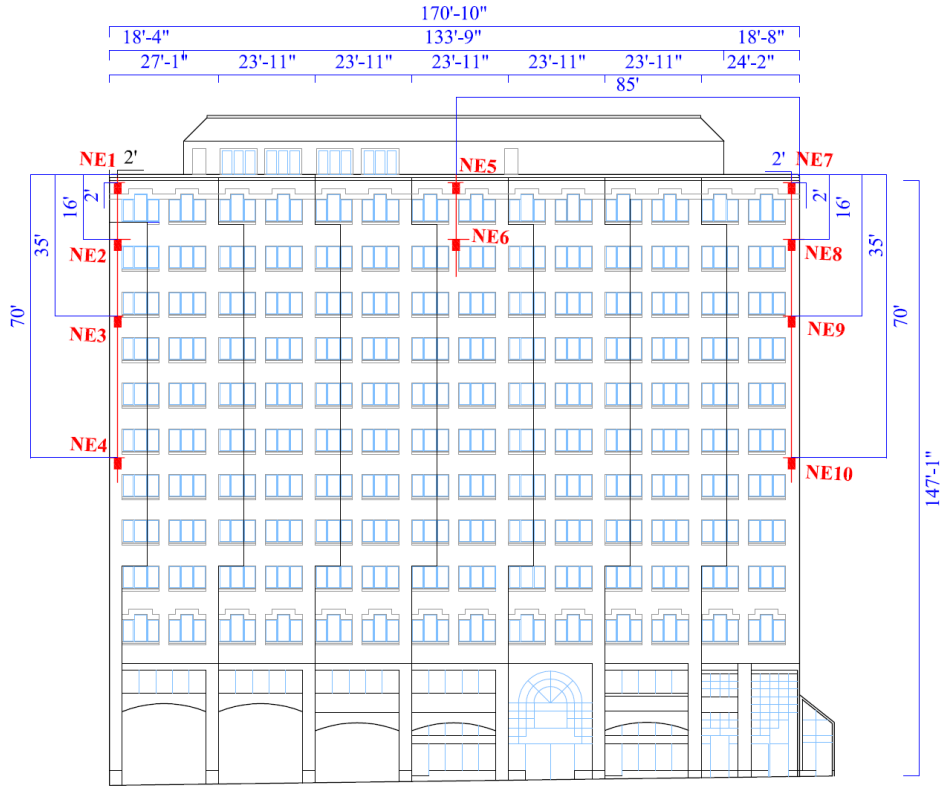


Figure 3.26 : North-east elevation of FB Building with driving rain gauge locations



Figure 3.27 : Photo of the north-east façade of FB Building with driving rain gauges

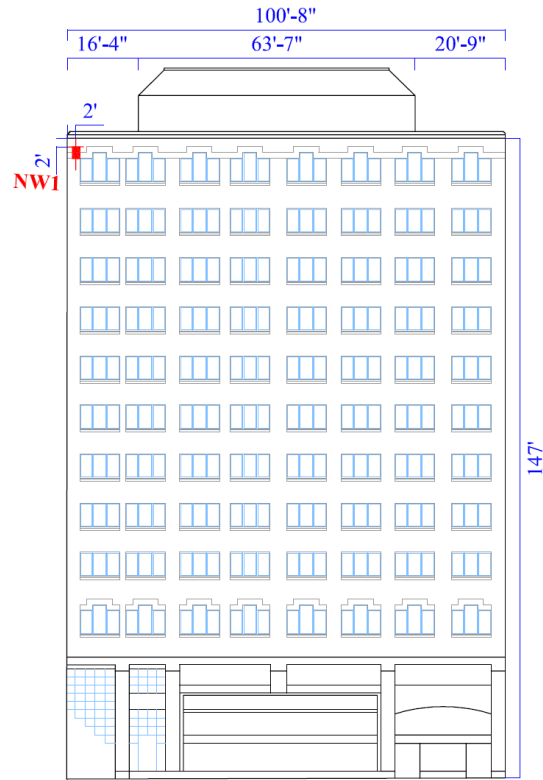


Figure 3.28 : North-west elevation of FB Building with driving rain gauge locations

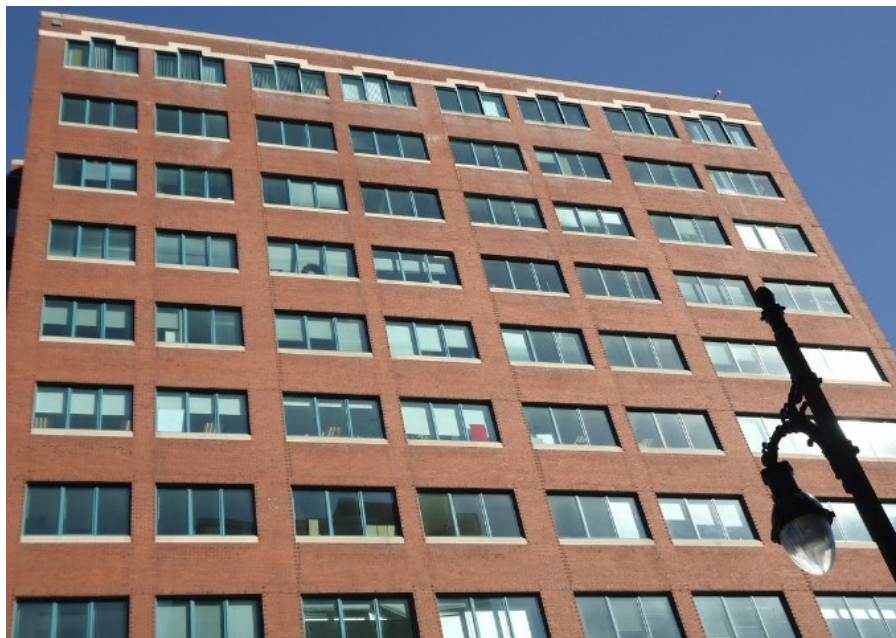


Figure 3.29: Photo of the north-west façade of FB Building with driving rain gauge

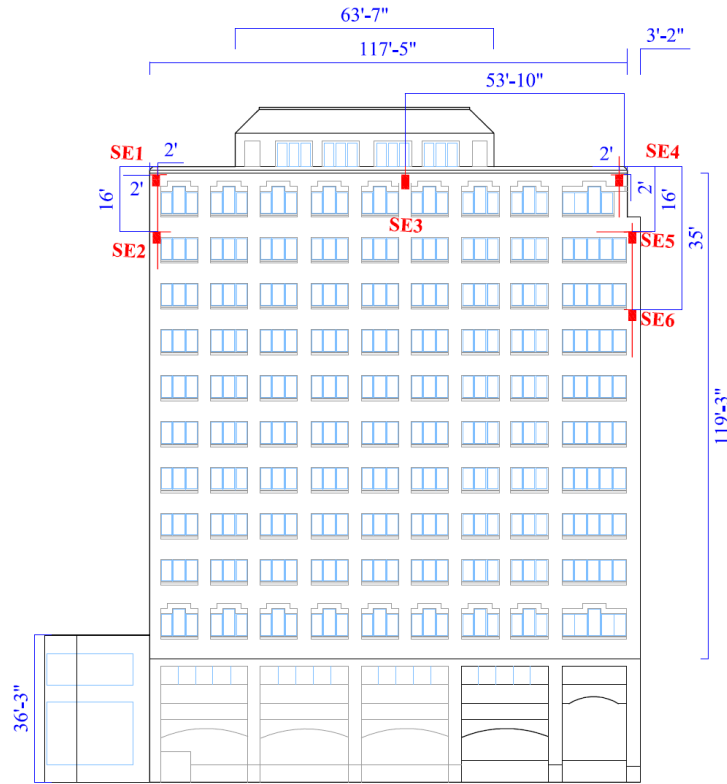


Figure 3.30 : South-east elevation of FB Building with driving rain gauge locations



Figure 3.31 : Photo of the south-east façade of FB Building with driving rain gauges

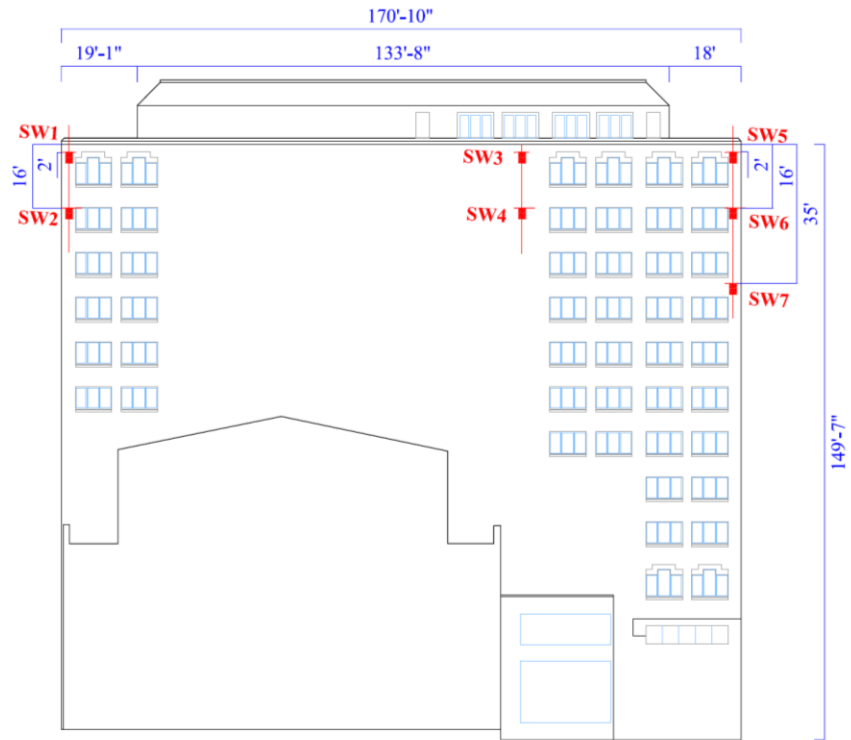


Figure 3.32 : South-west elevation of FB Building with driving rain gauge locations



Figure 3.33: Photo of the south-west façade of FB Building with driving rain gauges (Source: Google maps)

3.3 EQUIPMENT USED

The different equipment installed for field measurements includes:

- i) A wind monitor sensor,
- ii) A temperature and relative humidity probe,
- iii) A tipping bucket horizontal rain gauge, and
- iv) A number of customized driving rain gauges.

Among these equipment the first three has been installed on the roof top of the test buildings and the rest on the building façades.

3.3.1 Wind monitor

The wind monitor sensor can measure horizontal wind speed and direction. It has been supplied by Campbell Scientific (Canada) Corp. The Wind monitor is placed on a tripod at a height of 4.572 m (15') above the roof top for McLeod House and HB Building but for FB Building the monitor is placed 4.572 m (15') above the roof of the mechanical room. It can measure wind speed with a range of 0 – 50 ms⁻¹ (0 – 112 mph) with an accuracy of ±0.2 ms⁻¹ (±0.4 mph) or 1% of reading. It can measure wind direction with a range of 0 – 360° with an accuracy of ±0.3° (Campbell Scientific (Canada) Corp., June 2013a).

3.3.2 Temperature and relative humidity probe

The temperature and relative humidity probe is housed inside a multi-plate radiation shield and placed on the tripod (Campbell Scientific (Canada) Corp., 2003). The temperature measurement range is -50°C to +50°C with an accuracy of ±0.1° C. The measurement range of relative humidity sensor is 0 to 100% non-condensing with an accuracy of 0.8% (Campbell Scientific (Canada) Corp., June 2013b)

3.3.3 Tipping bucket horizontal rain gauge

A tipping bucket horizontal rain gauge is used to measure the amount of horizontal rainfall. It is placed on the roof top of McLeod House and HB Building and on the roof of mechanical room of

FB Building. The rain gauge was supplied by Campbell Scientific (Canada) Corp. The height of the tipping bucket horizontal rain gauge is 29.2 cm and weight is 1.1 kg. Its resolution 0.1 mm/hr with an accuracy of 1% up to 50 mm/hr (Campbell Scientific (Canada) Corp., 2013).

3.3.4 Driving rain gauge

Customized driving rain gauges that can measure wind driven rain were installed on the building façades. These driving rain gauges are made of aluminum plate. The collector's rim height of the driving rain gauge is 25.4 mm; and it has tipping-bucket mechanism. The collection area has a square shape with a dimension of 30.5 cm by 30.5 cm (12" by 12"). It has a resolution of 5.5 g/tip, which is equivalent to 0.060 mm per tip for the driving rain gauge with a collection area of 930.3 cm² (Osorio, M., Ge, H., April 2013).

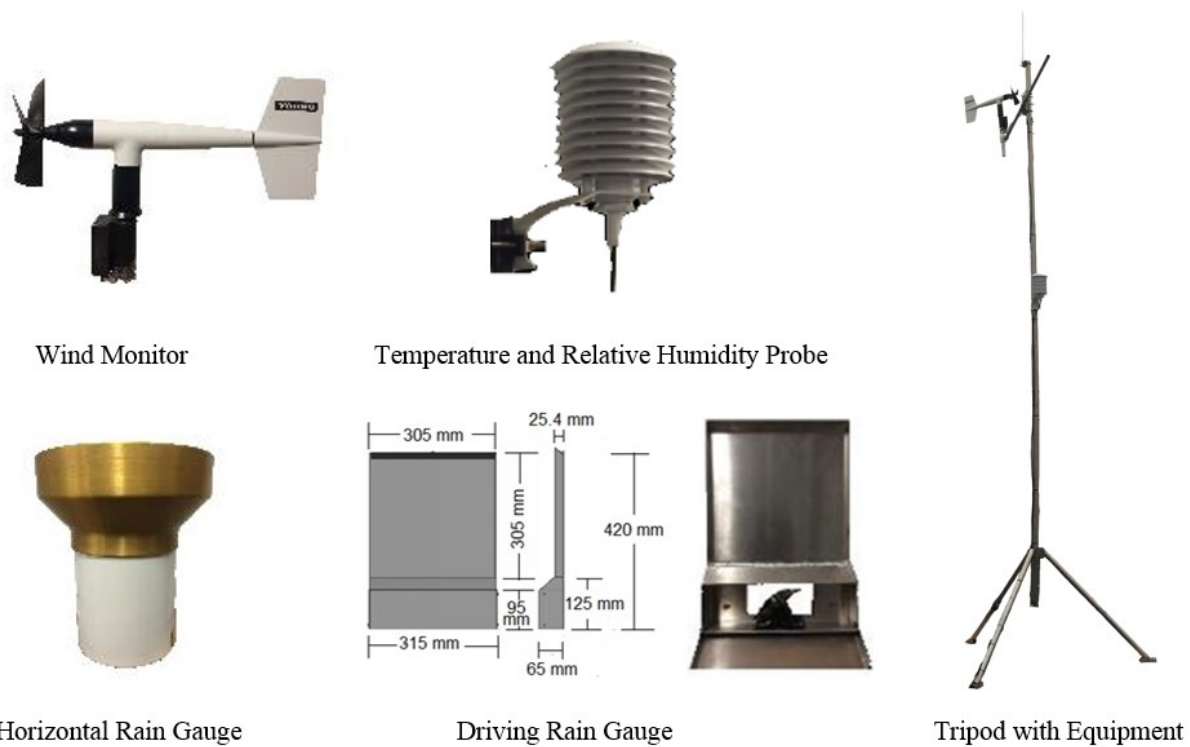


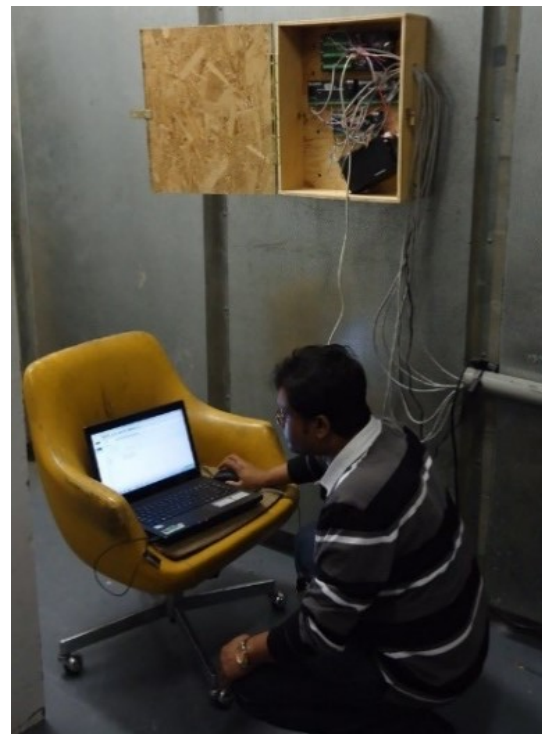
Figure 3.34 : Equipment used for measurements

3.4 DATA COLLECTION AND PROCESSING

All the equipment are connected to a data logger that collects and save the raw data in every 5 minutes. The data is then collected from the data logger using computer in every month. Wind speed and wind direction is sampled at 1 Hz frequency but averaged over 5-minute. The wind monitor gives 5-minute data of wind speed in m/s and 5-minute data of wind direction in degree. The temperature and relative humidity probe provides 5-minute data of temperature in °C and 5-minute data of relative humidity in %. The horizontal and driving rain gauge counts the number of tips in every 5 minutes. To get the 5 min data for horizontal rain and driving rain in mm, the number of tips recorded by the horizontal and driving rain gauges in every 5 minutes is multiplied by 0.1 and 0.06, respectively. This data has been averaged for every hour to obtain hourly data. Arithmetic-averaging technique is used to obtain hourly data. Table 3.2 shows a list of different types of data analyses carried out in this study and their purposes:



(a)



(b)

Figure 3.35 : Photos of: (a) data logger; and (b) data Collection

Table 3.2: List of different types of data analysis conducted in this study with their purpose

| Types of analysis | | Purpose | | |
|--|---|--|---|--|
| Historical wind and rain data analysis | 1. Prevailing wind direction | The purposes of these analyses are to understand the characteristic wind and rain conditions in these two regions, to compare short-term on-site measurement with long-term historical data, and to guide the selection of locations to install driving rain gauges. Analyses are conducted for 42 and 12 years data for Montreal and Fredericton, respectively. | | |
| | 2. Frequency analysis of wind speed | | | |
| | 3. Rainfall analysis including total annual rainfall, frequency distribution of rainfall intensity and average total rainfall per month | | | |
| Onsite data analysis | 1. Comparison of onsite weather data with data from nearby weather stations | | To check the quality of onsite data collected by the installed equipment on test buildings, onsite wind speed; wind direction; temperature and relative humidity data collected for the first couple of months of the monitoring period is compared with the data obtained from nearby meteorological stations for all test building sites. | |
| | 2. Wind and rain data analysis | I. Prevailing wind direction | To understand onsite wind and rain conditions. | |
| | | II. Frequency analysis of wind speed | | |
| | | III. Frequency analysis of rainfall intensity | | |
| | 3. Wind-driven rain analysis | I. Error analysis | | To estimate the errors occurred during wind-driven rain measurements from different types of errors sources, like evaporation, splashing, condensation etc., so that these losses can be taken into account in different wind-driven rain analysis. |
| | | II. Spatial distribution of wind-driven rain | i. Catch ratio analysis | To understand the spatial distribution of wind-driven rain on building façades including variations of catch ratio and wall factor with wind and rain parameters, and to compare the wall factors suggested in the ISO standard with those calculated based on measurements. |
| ii. Wall factor analysis | | | | |
| III. Comparison between measurements and predictions using semi-empirical models | | To evaluate the accuracy of existing semi-empirical methods used for quantifying wind-driven rain loads on building façades | | |

Chapter 4

DATA ANALYSIS AND RESULTS

4.1 INTRODUCTION

Results of historical weather data and experimental data analyses will be presented in this chapter. Historical data of wind speed, wind direction and rainfall intensity for these two locations (i.e., Fredericton and Montreal) were obtained from Environment Canada's National Climate Services. Analysis of historical data has been conducted with the objectives to understand the characteristic wind and rain conditions in these two regions, to compare short-term on-site measurement with long-term historical data, and to guide the selection of locations to install driving rain gauges on façade based on the prevailing wind directions and surrounding conditions of the test buildings.

4.2 ANALYSIS OF HISTORICAL DATA

Hourly data from Fredericton International Airport and Montreal International Airport has been analyzed to obtain wind speed, wind direction and rainfall condition of these three cities. Data for the years 1984 to 1995 for Fredericton and for the years 1953 to 1994 for Montreal has been analyzed.

4.2.1 Prevailing wind direction

As shown in Figure 4.1, there is slight difference in the prevailing wind direction during rain hours and all hours. Here rain hours correspond to the hours during which rainfall occurred (i.e., only rainy periods). All hours correspond the entire time for which data is analyzed. All hours include both rainy and dry periods. For Fredericton, usually the prevailing wind directions are the north, south-south-west, and west-north-west, whereas during rain hours the wind mainly comes from the north, south and north-east directions. In Montreal usually the prevailing wind directions are the west, west-south-west, south-west and north, whereas during rain hours the wind mainly comes from the north-east, south-south-east and south-west directions.

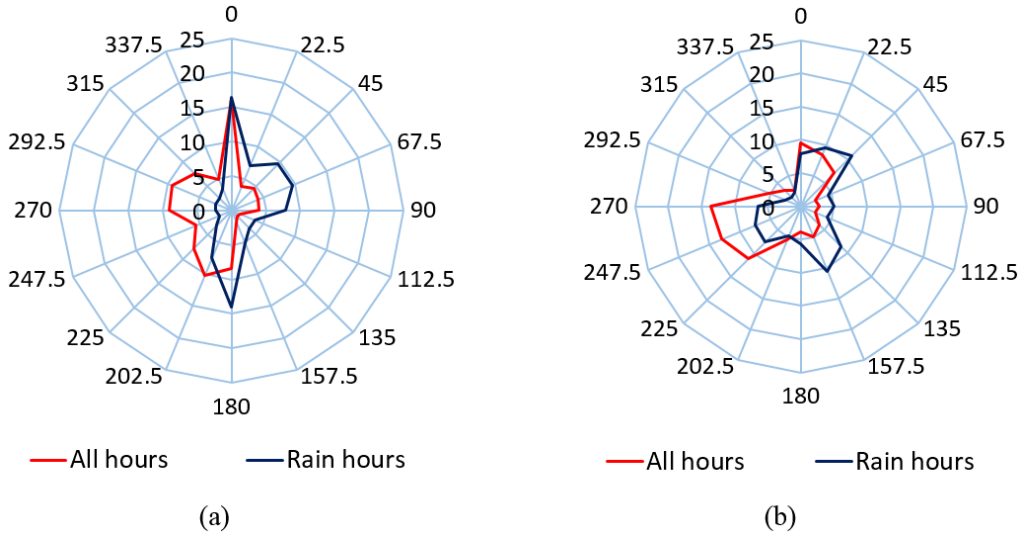


Figure 4.1 : Prevailing wind direction in: (a) Fredericton; and (b) Montreal

4.2.2 Wind speed

Figure 4.2 presents the comparison of wind speed frequency between these two cities. Generally wind speed is higher during rain hours. The difference of wind speed during all hours and rain hours is found to be very small in Fredericton. In general the wind speed is higher in Montreal compared to Fredericton. In Fredericton, more than 80% of the time the wind speed is less than 6 m/s and less than 5% of the time it exceeds 8 m/s. In Montreal, during all hours about 77% of the time the wind speed is less than 6 m/s but during rain hours about 74% of the time the wind speed is less than 6 m/s. Here about 10% of the time the wind speed exceeds 8 m/s.

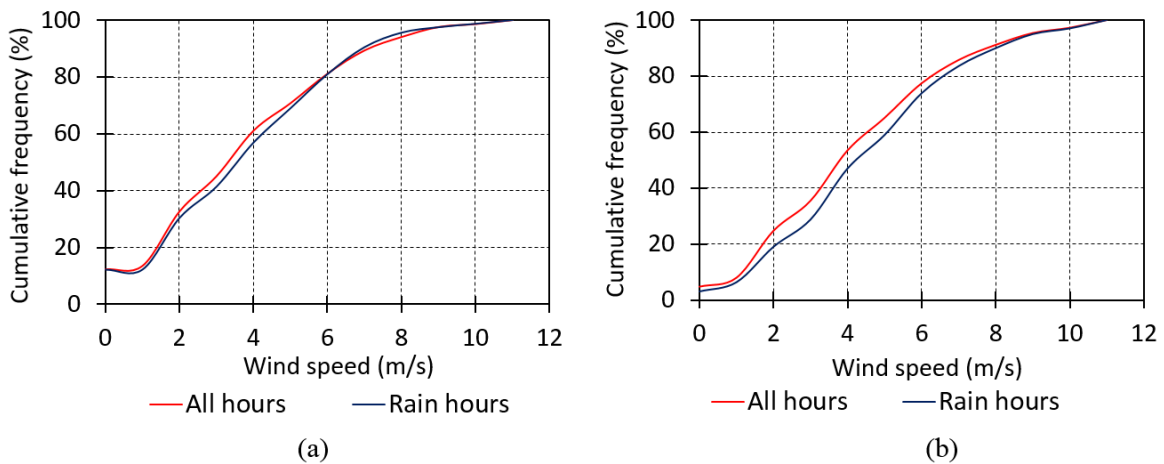


Figure 4.2 : Comparison of wind speed frequency in: (a) Fredericton; and (b) Montreal

4.2.3 Rainfall

Figure 4.3 shows the average total annual rainfall in Fredericton and Montreal. The annual rainfall amount for Fredericton and Montreal is 730 mm and 690 mm, respectively. Frequency analysis of rainfall intensity for these two cities is shown in Figure 4.4. The frequency distribution of rainfall intensity is almost similar for Fredericton and Montreal. In both cities the rainfall intensity is less than 2 mm/hr for about 80% of time and less than 10% of time it exceeds 4 mm/hr. As shown in these figures, although the rainfall intensity is similar in Fredericton and Montreal, the total annual amount of rainfall is slightly higher in Fredericton. This is mainly due to relatively higher rainy periods in Fredericton compared to that in Montreal. The average rain hours for Fredericton and Montreal is 532 hours and 514 hours, respectively.

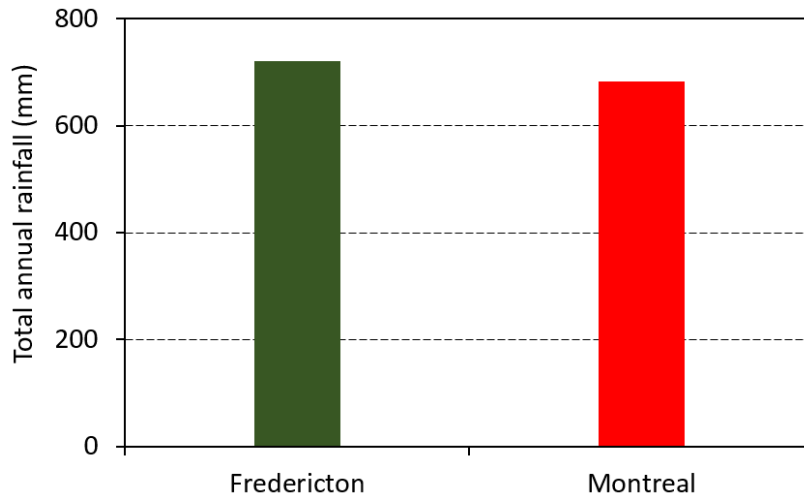


Figure 4.3 : Comparison of total annual rainfall in Fredericton and Montreal

Figure 4.5 shows the average monthly rainfall amount for these two cities. In Fredericton the maximum rainfall happens in the month of May and August with a rainfall amount of 95 mm and minimum rain occurs in the month of February with an amount of about 10 mm. In Montreal maximum rainfall happens in the months of June to September, which can be as high as 85 mm, whereas the minimum rainfall occurs in the month of February with an amount of about 15 mm. For these two cities most of the rainfall occurs during summer and fall season, whereas minimum rainfall occurs during winter.

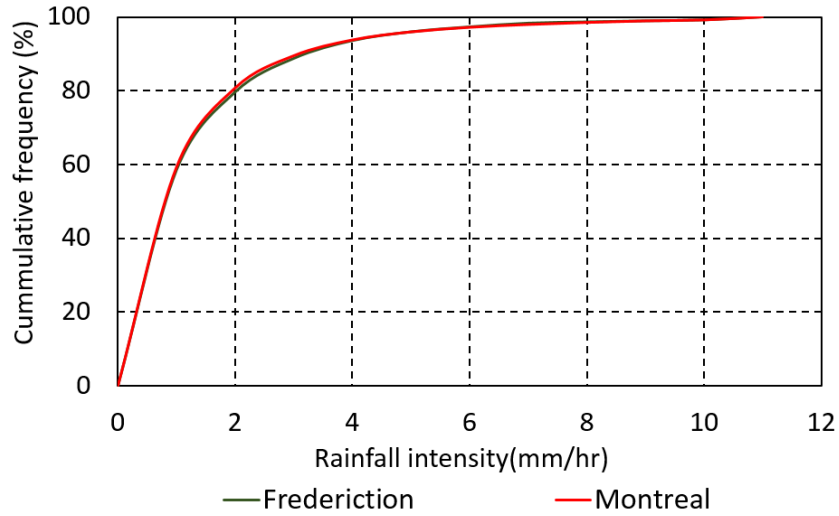


Figure 4.4 : Comparison of frequency distribution of rainfall intensity in Fredericton and Montreal

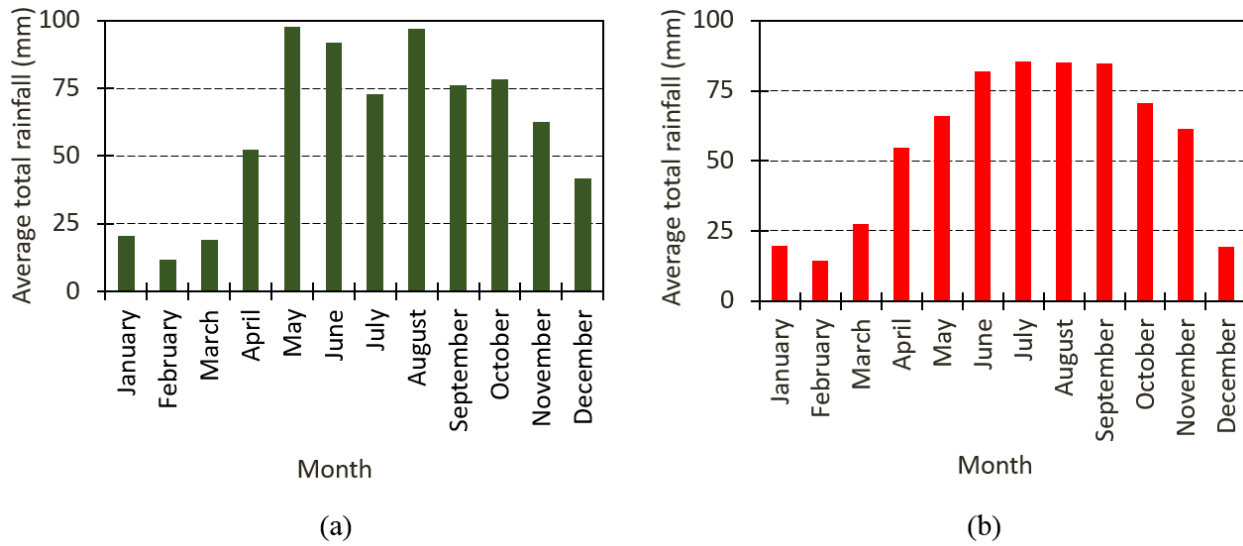


Figure 4.5 : Average total rainfall per month in (a) Fredericton; and (b) Montreal

4.3 COMPARISON OF ONSITE WEATHER DATA WITH DATA FROM NEARBY WEATHER STATIONS

To check the quality of onsite data collected by the installed equipment on test buildings, onsite wind speed; wind direction; temperature and relative humidity data collected for the first couple of months of the monitoring period is compared with the data obtained from nearby meteorological

stations for all test building sites. It is found that onsite data is close enough to the meteorological station data, which ensures that the data collected by onsite equipment is of good quality. Comparison of wind direction and wind speed is presented below. Comparison for temperature and relative humidity is included in Appendix A.

4.3.1 McLeod House, Fredericton

Three meteorological stations close to the Fredericton building site have been selected for the comparison. These meteorological stations are Fredericton (Fredericton airport), Fredericton CDA CS and Fredericton Aquatic Centre. The locations of these stations as well as the location of the test building is shown in Figure 4.6. All the comparisons are carried out for the period from August 2013 to March 2014.

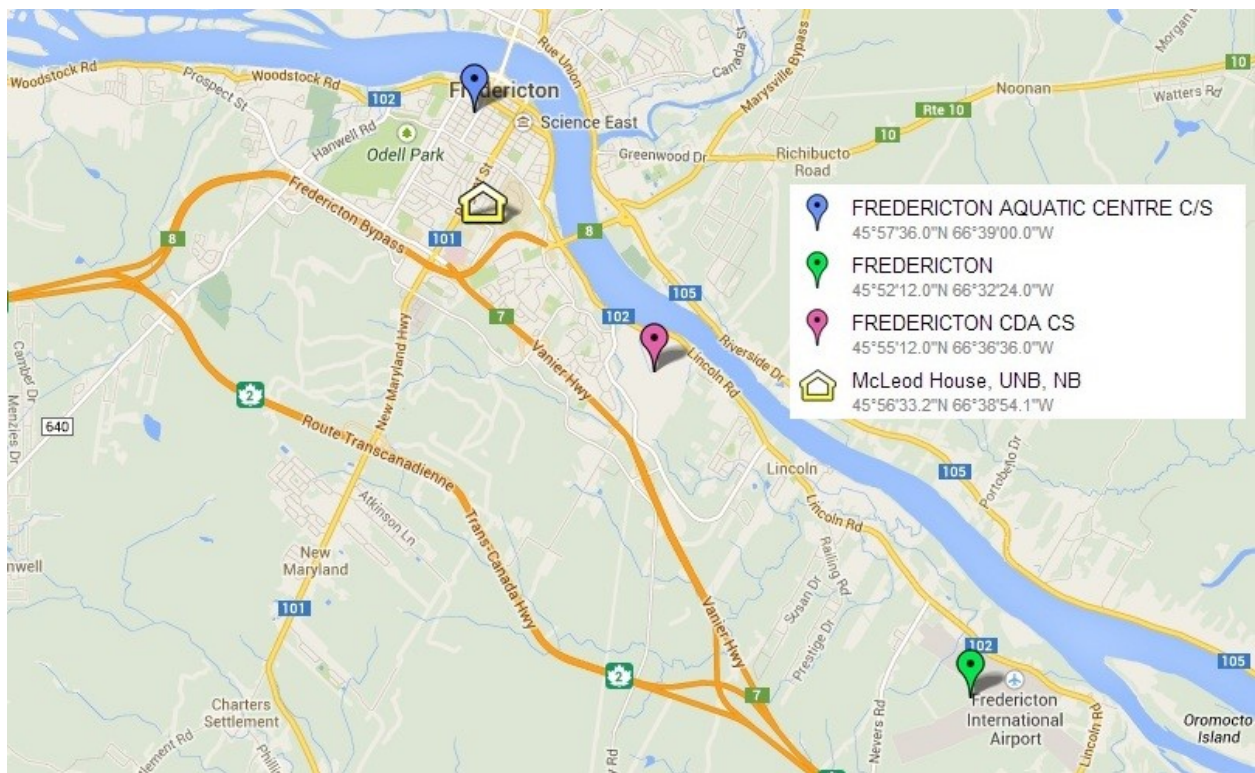


Figure 4.6: Locations of the test building at Fredericton and nearby meteorological stations

4.3.1.1 Prevailing wind direction

Figure 4.7 presents the comparison of prevailing wind direction for all hours. It can be seen that prevailing wind direction slightly varies from station to station, which may be attributed to the variation of local surroundings. The prevailing wind direction is from the west for Fredericton aquatic centre and Fredericton CDA CS stations, which is similar to the on-site prevailing wind direction, i.e. west-north-west, while the prevailing wind direction for the Fredericton station is from the south.

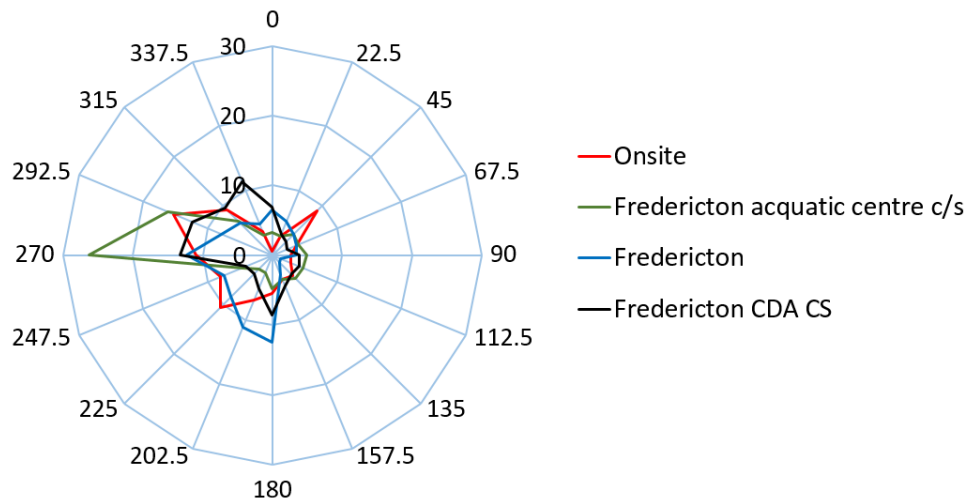


Figure 4.7: Comparison of prevailing wind direction for all hours obtained from onsite measurements and nearby meteorological stations for the period from August 2013 to March 2014

4.3.1.2 Wind speed

Onsite measured wind speeds are compared with wind speeds obtained from the Fredericton airport. The hourly wind speed data obtained from the Fredericton airport station is converted for the onsite conditions using the power law correlation, the procedure of which is outlined below:

The power law is generally used to represent variation of wind speed with height. It is an empirical equation and expressed as:

$$\frac{U_z}{U_g} = \left[\frac{Z}{Z_g} \right]^\alpha \quad (4.1)$$

Where, U_z and U_g are the wind speeds at height Z and at gradient height Z_g , respectively and α is the mean speed exponent. The values of Z_g and α for different types of terrain category can be obtained from Table 4.1.

*Table 4.1: values of gradient height and power law exponents for different terrain categories
[Source: (Hutcheon, N. B., & Handergord G.O.P, 1995)]*

| Terrain Category | Terrain description | Gradient height, Z_g (m) | Mean speed exponent, α |
|-------------------------|--|--|---|
| 1 | Open sea, ice, tundra, desert | 250 | 0.11 |
| 2 | Open country with low scrub or scattered trees | 300 | 0.15 |
| 3 | Suburban areas, small towns, well wooded areas | 400 | 0.25 |
| 4 | Numerous tall buildings, city centers, well developed industrial areas | 500 | 0.36 |

Note that the airport station and the McLeod House fall in terrain category 2 and 3 respectively. The values of Z_g and α for these two terrain categories have been obtained for Table 4.1, and airport wind speed has been converted for onsite condition using equation (4.1). The comparison of wind speed is presented in the Figure 4.8. It shows the comparison of maximum, minimum, average wind speed as well as standard deviation. It is found that the average wind speed obtained from onsite measurement and from converted airport data is very close (i.e., 2.80 m/s and 2.81 m/s respectively). The occurrence time of maximum wind speed is exactly the same, even though the values are not same (12.72 m/s and 9.70 m/s reported by Fredericton airport station and onsite measurements, respectively). The minimum wind speed reported by onsite measurements is 0.18 m/s, whereas the airport station found few completely windless moments. The standard deviation obtained from onsite measurement and from converted airport data is 1.53 m/s and 1.74 m/s respectively and the root mean square deviation (RMSD) between onsite data and airport data is 1.15 m/s.

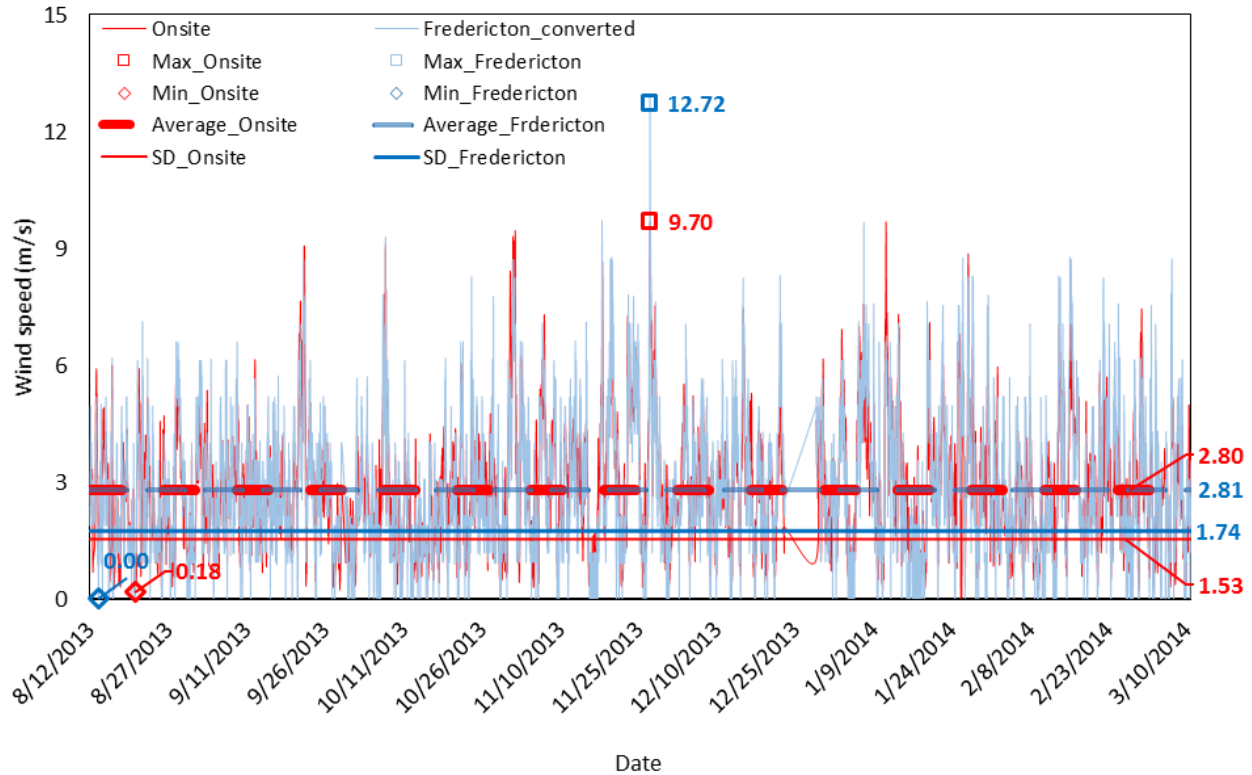
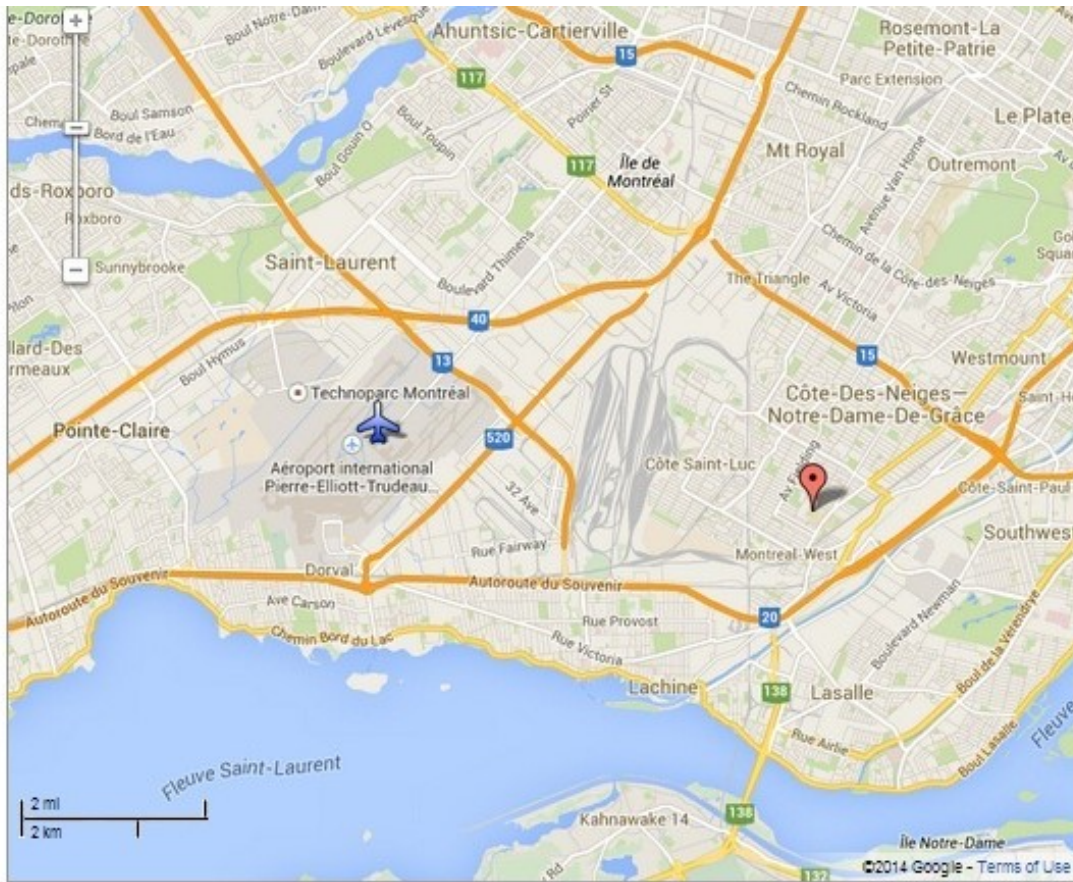




Figure 4.8 : Comparison of wind speed obtained from the onsite measurements and Fredericton airport station for the period from August 2013 to March 2014

4.3.2 HB Building, Montreal

Hourly wind direction, wind speed, temperature and relative humidity data obtained from HB Building, Montreal site has been compared with the data obtained from Montreal international airport station. The locations of Montreal international airport station and HB Building is shown in Figure 4.9.



- 

Montreal Intl Airport
 45°28'12.0"N 73°44'24.0"W
- 

Hingston Hall B
 Concordia University - Loyola Campus, Montreal, QC H4B, Canada

Figure 4.9: Locations of HB Building and Montreal international airport station

4.3.2.1 Prevailing wind direction

Figure 4.10 shows the comparison of prevailing wind direction for all hours for the period from April 2014 to June 2014. Montreal international airport station shows the prevailing wind direction is mainly from the south-west and north, whereas onsite data shows it from the west-south-west.

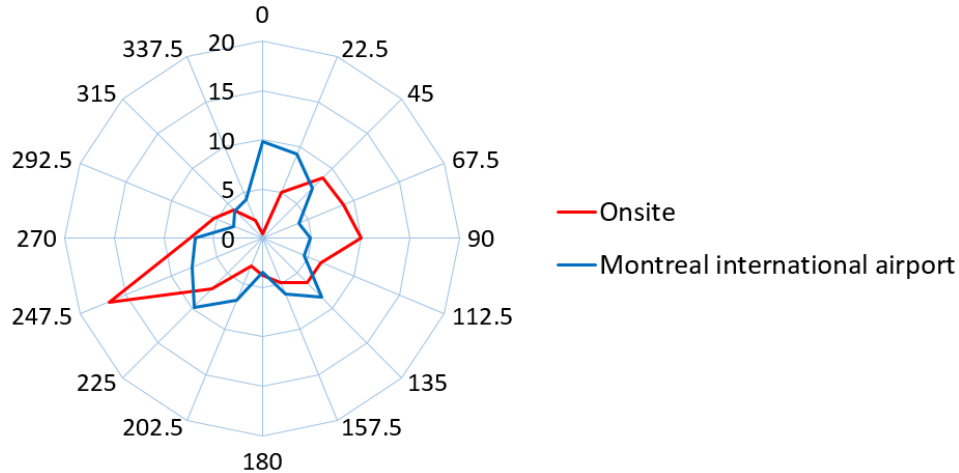


Figure 4.10: Comparison of prevailing wind direction for all hours obtained from the onsite measurements and Montreal international airport station for the period from April 2014 to June 2014

4.3.2.2 Wind speed

The comparison of hourly wind speed for the period from May 2014 to September 2014 is presented in the Figure 4.11. Power law conversion has been used to convert the airport data for the onsite condition. Average wind speed obtained from Montreal international airport and onsite is 2.22 m/s and 2.18 m/s, respectively. The maximum and minimum wind speed are found at the same time for both dataset. The maximum and minimum wind speed reported by airport station are 7.93 m/s and 0.14 m/s, respectively, whereas those reported by onsite measurements are 7.93 m/s and 0.04 m/s. The standard deviation obtained from onsite measurement and from converted airport data is 1.04 m/s and 1.11 m/s, respectively and the root mean square deviation (RMSD) between onsite data and airport data is 0.7 m/s.

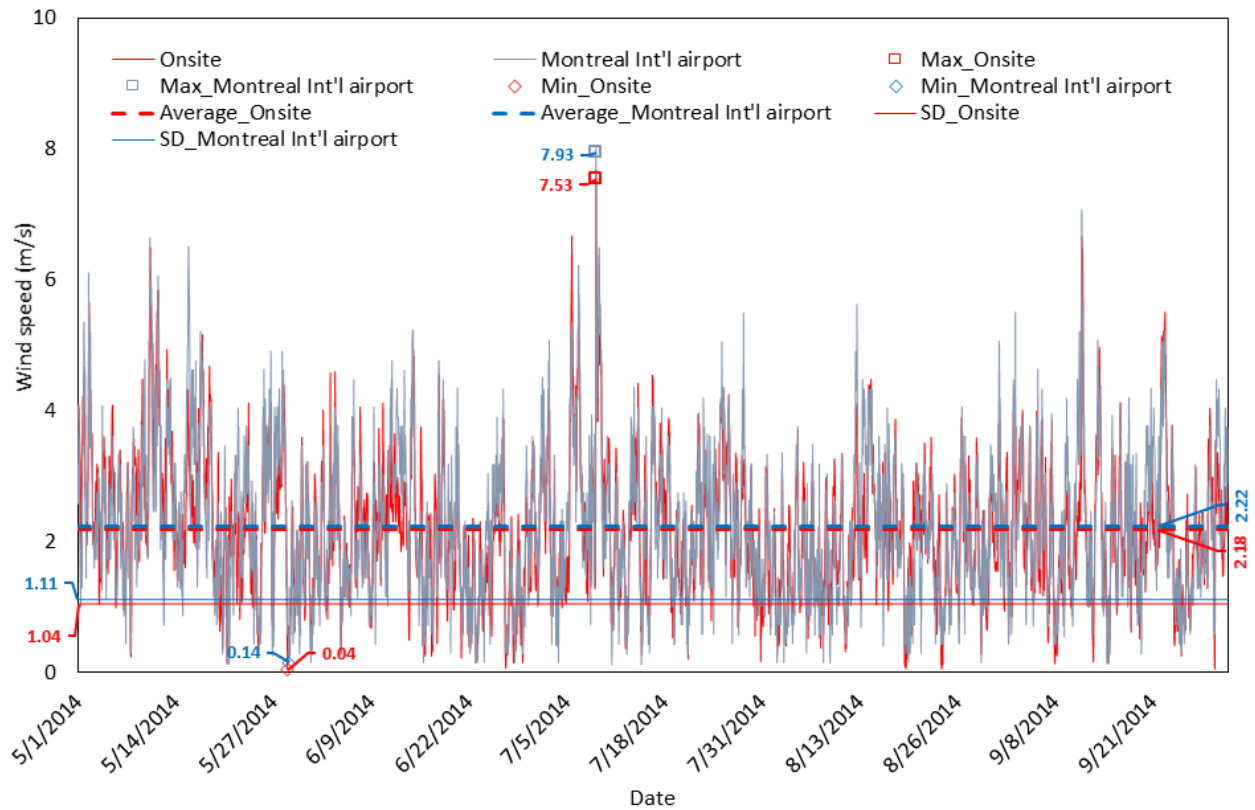
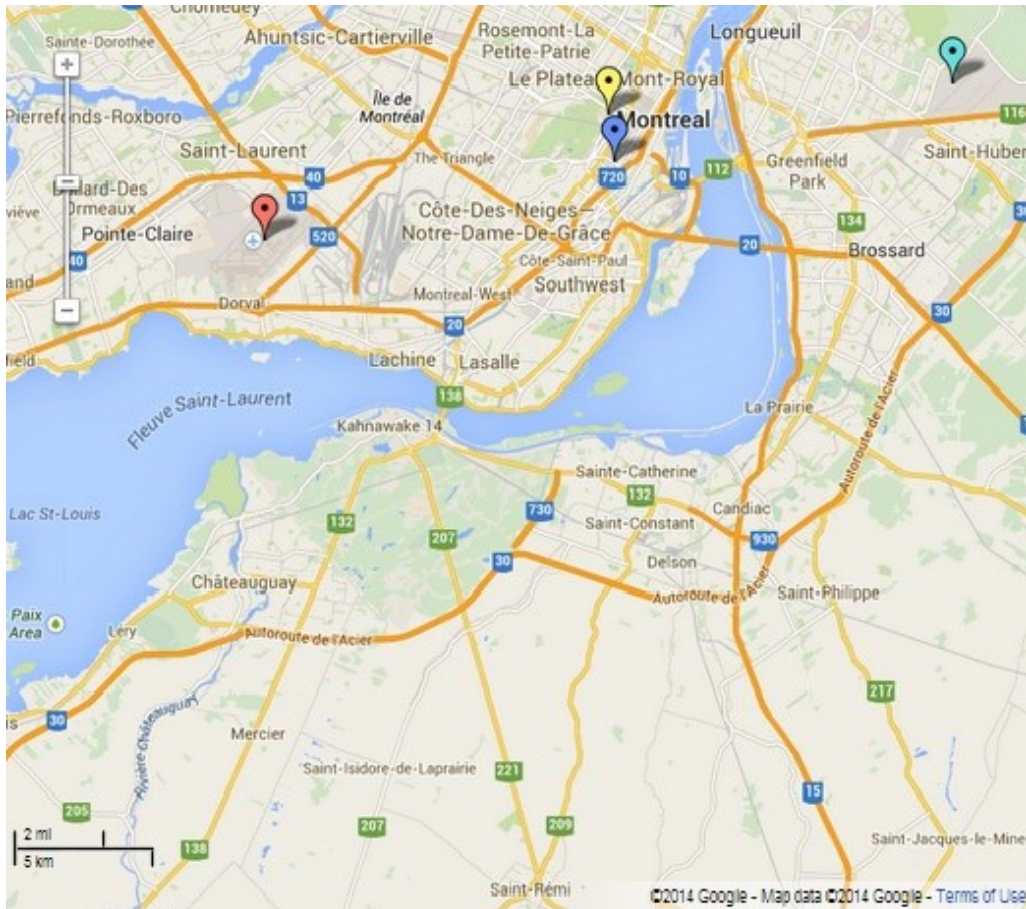


Figure 4.11: Comparison of hourly wind speed obtained from the onsite measurements and Montreal international airport station for the period from May 2014 to September 2014

4.3.3. FB Building, Montreal

Data obtained from FB Building site, Montreal has been compared with the data obtained from Montreal international airport, Mctavish and Montreal/St-Hubert station for the period from July 2014 to August 2014. The locations of these meteorological stations and FB Building is shown in Figure 4.12.



- | | | | |
|---|---|---|--|
|  | FB Building Montreal, QC H3H, Canada |  | Montreal Intl Airport 45°28'12.0"N 73°44'24.0"W |
|  | MCTAVISH 45°30'36.0"N 73°34'48.0"W |  | Montreal/St-Hubert 45°31'12.0"N 73°25'12.0"W |

Figure 4.12: Locations of FB Building and nearby meteorological stations

4.3.3.1 Prevailing wind direction

Comparison of prevailing wind direction for all hours for the period from July 2014 to August 2014 is shown in Figure 4.13. The prevailing wind direction is from the south-west for Montreal international airport and Montreal/St-Hubert stations, which is similar to the on-site prevailing wind direction, i.e. west-south-west, while the prevailing wind direction for the Mctavish station is from the south.

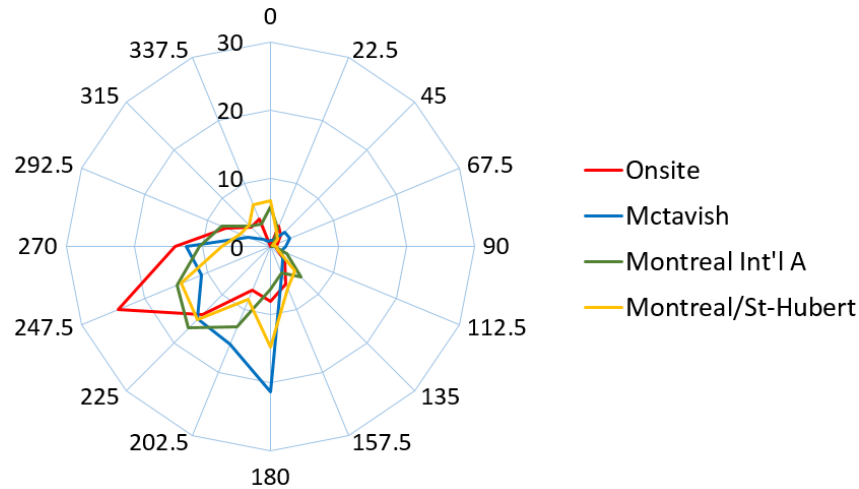


Figure 4.13 : Comparison of prevailing wind direction for all hours obtained from the onsite measurements and nearby meteorological stations for the period from July 2014 to August 2014

4.3.3.2 Wind speed

Onsite hourly wind speed data has been compared with Montreal international airport and Montreal/St-Hubert for the period from July 2014 to August 2014. Terrain category 4 is used for FB Building to convert the airport station data for onsite condition using the Power law. The comparison is presented in the Figure 4.14. Figure shows equal average wind speed (2.76 m/s) for measurement and for Montreal/St-Hubert station, whereas Montreal international airport shows slightly higher wind speed (2.95 m/s). The maximum wind speed recorded by Montreal/St-Hubert station is also close to the onsite measurements (7.32 m/s and 7.0 m/s respectively), whereas Montreal international airport shows comparatively higher value (8.31 m/s). The standard deviation for Montreal/St-Hubert, Montreal international airport and onsite measurements is 1.53 m/s, 1.50 m/s and 1.28 m/s respectively. The root mean square deviation (RMSD) between onsite data and Montreal/St-Hubert station data is 1.06 m/s, whereas that between onsite data and Montreal international airport station data is 1.12 m/s.

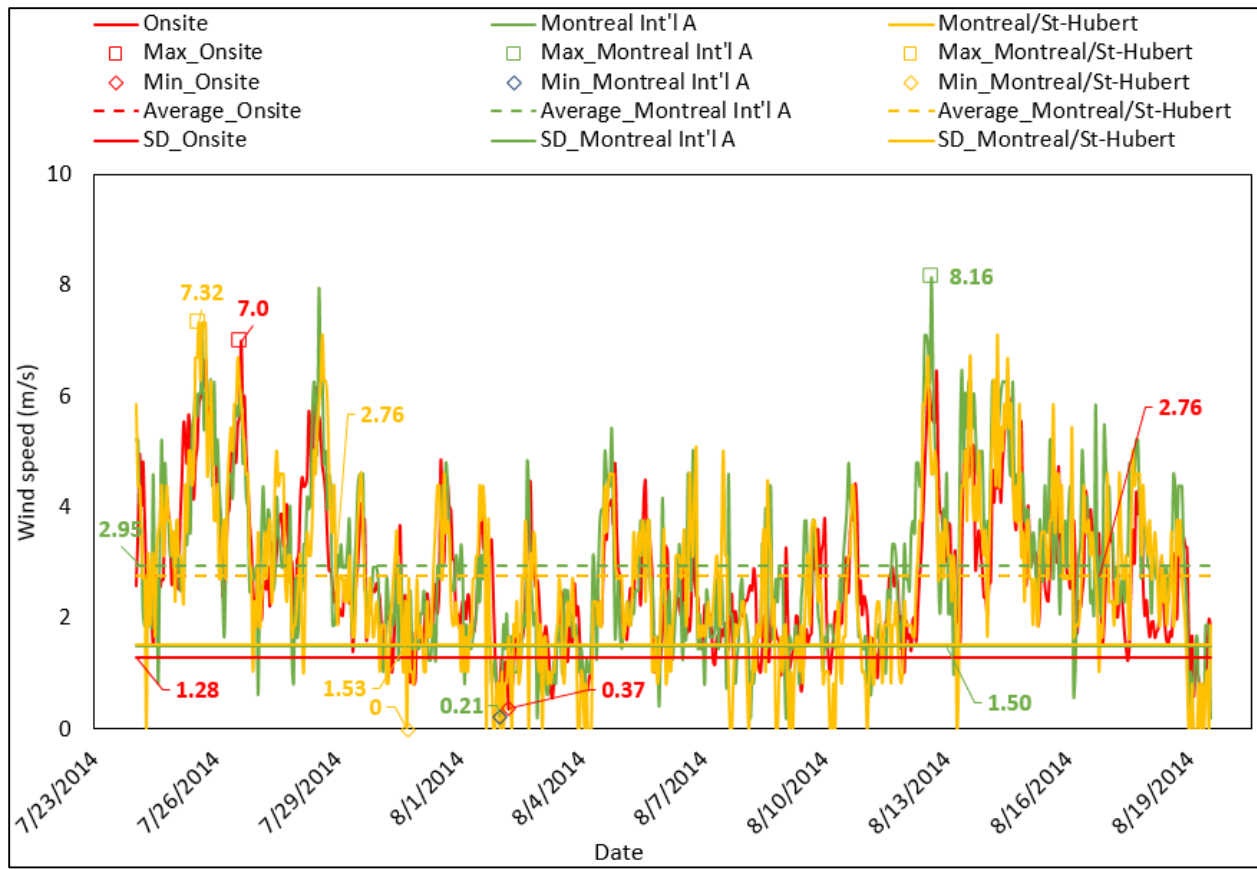


Figure 4.14 : Comparison of hourly wind speed obtained from FB Building site and nearby meteorological stations for the period from July 2014 to August 2014

The following sections present the results of onsite data analyses which include onsite wind and rain characteristics, error associated with experimental method, spatial distribution of wind-driven rain in terms of catch ratio and wall factor, and comparison between measured and predicted wind-driven rain using the semi-empirical models. Data collected for the following periods is used for analyses: 1) from August 2013 to June 2014 and from April 2015 to June 2015 for McLeod House, Fredericton, 2) from April 2014 to June 2015 for HB Building, Montreal, and 3) from July 2014 to June 2015 for FB Building, Montreal. Note that the horizontal rain gauge installed on McLeod House was defective from July 2014 to March 2015 and data for this period obtained from McLeod House are not analyzed.

4.4 ONSITE WEATHER DATA ANALYSIS

This section presents the analysis of weather conditions at test building sites including prevailing wind direction, wind speed and rainfall intensity.

4.4.1 Prevailing wind direction

Figure 4.15 shows the prevailing wind direction at the test building sites during the monitoring periods. For comparison purpose, the prevailing wind direction for the same period obtained from nearby airport data for both all hours and rain hours are also presented. At Fredericton site, the prevailing wind direction is from the west-north-west for all hours, while during rain hours wind blows from the south-west direction. Data from Fredericton airport station shows that wind comes mainly from the south direction during both all hours and rain hours for this period. At HB Building site in Montreal normally the wind comes from the west-south-west and the west direction, whereas during rain hours the prevailing wind directions are from the west-south-west and the east. Montreal international airport data shows that during the same period the prevailing wind directions are mainly from the south-west and the south-east during all hours and rain hours, respectively. At FB Building site in Montreal, during the monitoring period the prevailing wind directions for all hours are from the west and west-south-west direction, whereas during rain hours the prevailing wind directions are from the west-south-west, south-west and north-north-east. The prevailing on-site wind direction at FB Building is similar to that at the Montreal international airport.

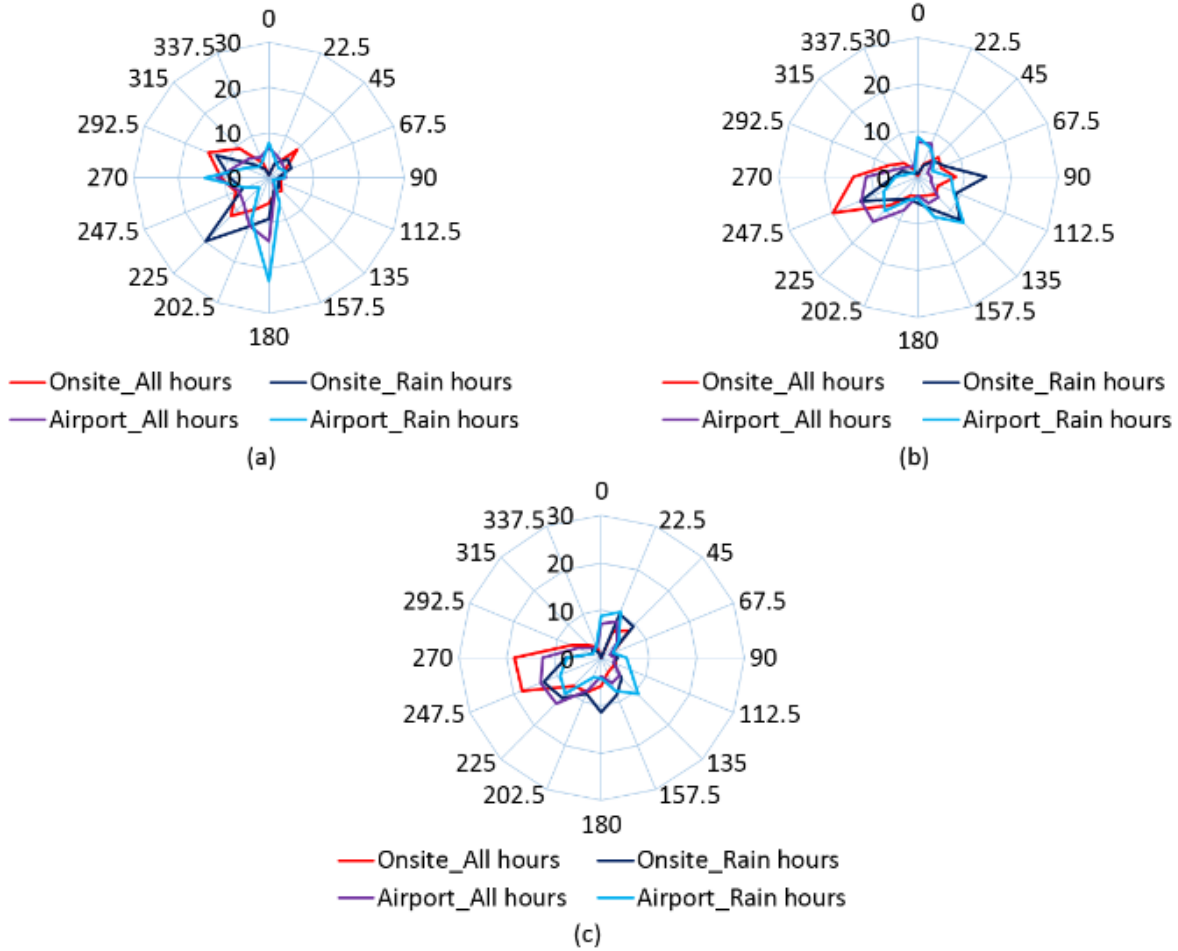


Figure 4.15 : Prevailing wind direction at test building sites: (a) McLeod House, Fredericton; (b) HB Building, Montreal; (c) FB Building, Montreal

4.4.2 Wind speed

Frequency distributions of wind speed obtained from onsite data and airport data during rain hours and all hours for the monitoring period are presented in Figure 4.16. As stated earlier, the wind monitor is placed on a tripod at a height of 4.572 m (15') above the roof top of McLeod House and HB Building, and 4.572 m (15') above the roof of mechanical room of FB Building. So the wind speed is measured at a height of 26.57 m (87'-2"), 19.63 m (64'-5") and 55.09 m (180'-9") from the ground level for McLeod House, HB Building and FB Building, respectively. Note that the airport wind speed data, which is measured at a height of 10 m above the ground, is converted for onsite condition and at wind monitor height using the power law (equation (4.1), section 4.3.1.2) for this

analysis. At McLeod House location, wind speed obtained from airport is exactly the same as that obtained from onsite data for both all hours and rain hours. For Montreal locations, wind speed obtained from airport and onsite is almost similar during all hours, whereas, during rain hours airport shows slightly higher wind speed. This is usual as airport is located in open area and hence wind can blow more freely without the interference from surrounding obstructions. At Fredericton both of the onsite data and airport data shows that the wind speed is higher during rain hours than that of all hours. At Fredericton, the wind speed exceeds 4 m/s for about 25% and 50% of time during all hours and rain hours, respectively. At Montreal sites wind speed distribution obtained from onsite data is similar for both all hours and rain hours. Wind speed is relatively higher at FB Building site than that at HB Building site. At HB Building site about 15% of time the wind speed exceeds 4 m/s, but at FB Building site about 35% of time the wind speed is higher than 4 m/s.

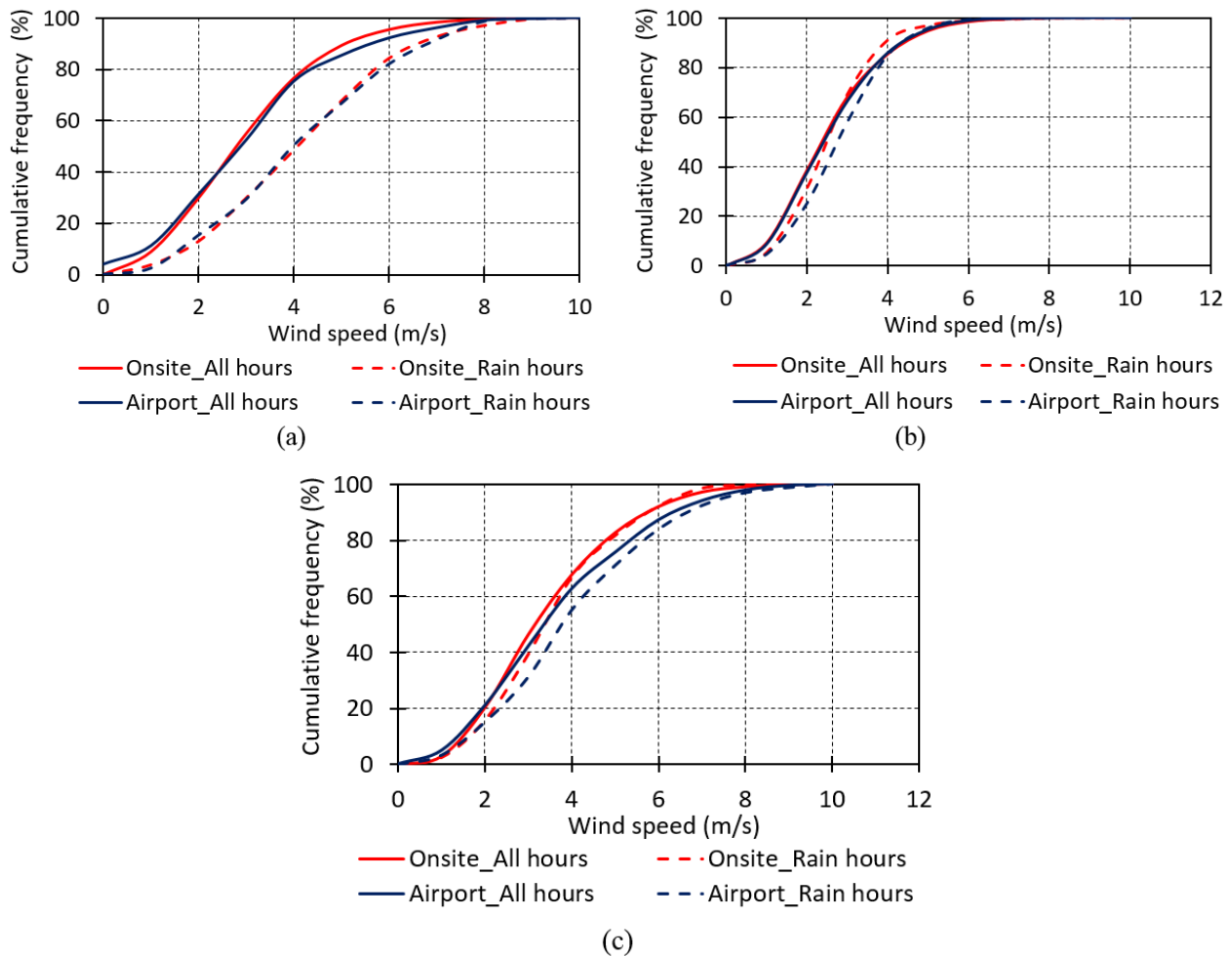


Figure 4.16 : Frequency distribution of wind speed at test building sites: (a) McLeod House, Fredericton; (b) HB Building, Montreal; (c) FB Building, Montreal

4.4.3 Rainfall intensity

Frequency distribution of rainfall intensity at three test building sites during the monitoring period is presented in Figure 4.17. The rainfall intensity at FB Building site is slightly lower as compared to other two sites, which indicates that the intensity of rain in suburban area is higher than that of city center. As shown in figure, rainfall intensity is less than 4 mm/hr for about 91%, 92% and 95% of the time at McLeod House site, HB Building site and FB Building site, respectively.

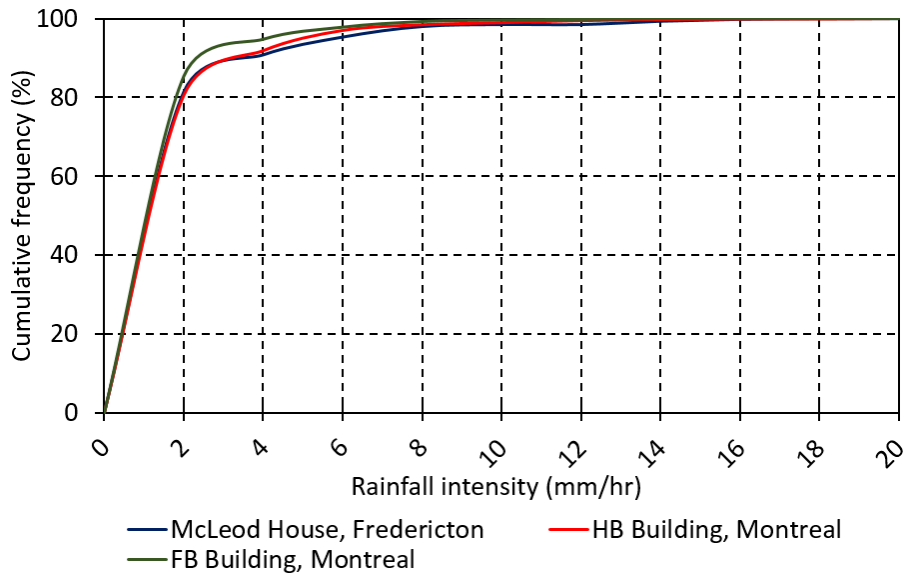
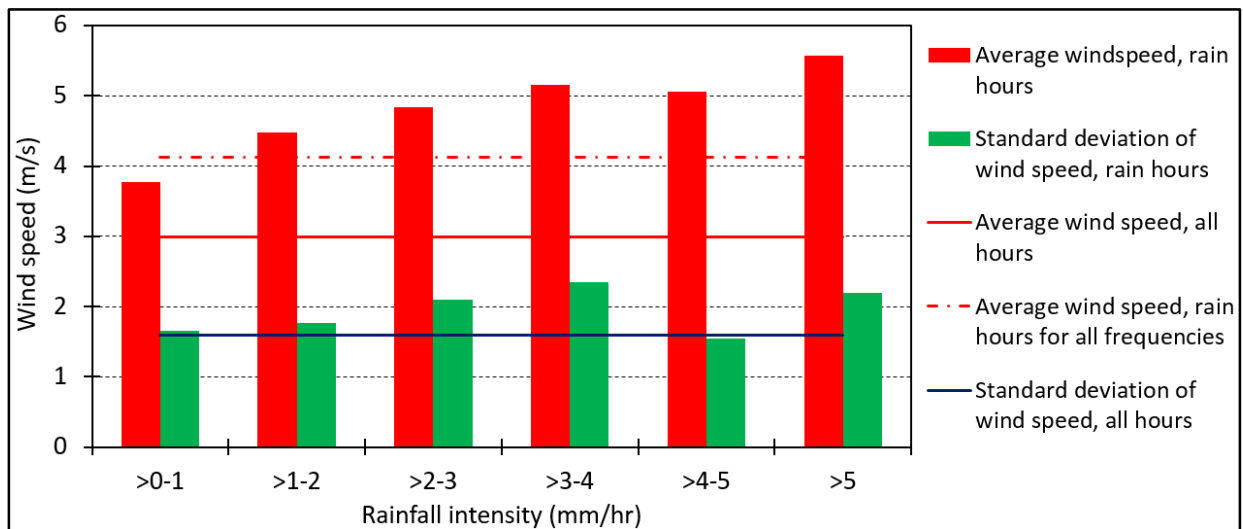


Figure 4.17 : Frequency distribution of rainfall intensity at test building site: (a) McLeod House, Fredericton; (b) HB Building, Montreal; (c) FB Building, Montreal

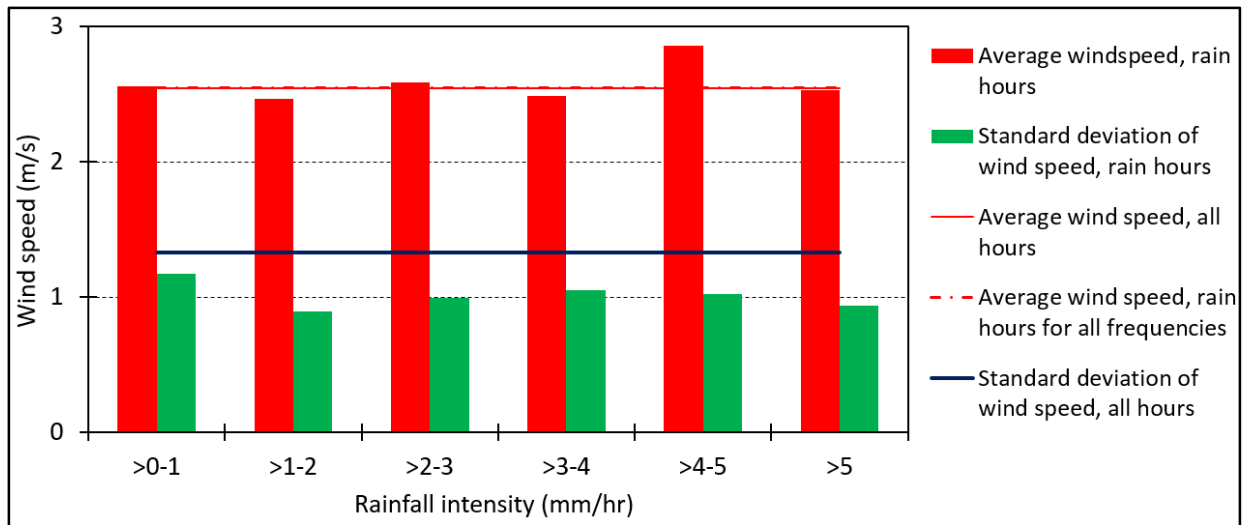
4.4.4 Wind speed variation with rainfall intensity

The analysis is carried out to find correlations between wind speed and rainfall intensity. Figure 4.18 shows the average wind speed in relation to rainfall intensity categories for the monitoring periods. It can be seen that at Fredericton site the average wind speed during rain hours (4.12 m/s) is higher than that of during all hours (2.98 m/s). However, at Montreal sites the average wind speeds during all hours are close to that during rain hours. At HB Building site the average wind speed is 2.55 m/s during rain hours and 2.54 m/s during all hours, whereas at FB Building site the average wind speed is 3.53 m/s and 3.42 m/s during rain hours and all hours, respectively. Note that the average wind speed is higher at FB Building site as compared to HB Building site because

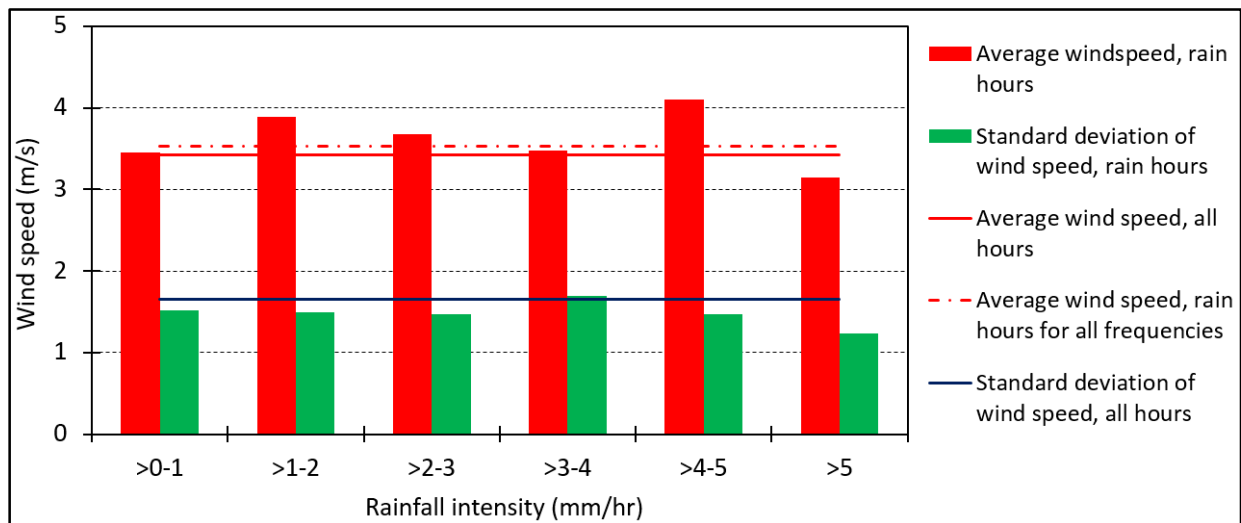
of the difference in measurement height and surroundings. As mentioned earlier the wind speed measurement height at FB Building site (55.09 m) is higher than that of HB Building site (19.63 m), so it is usual that the wind monitor at FB Building site will get higher wind speed values compared to the one at HB Building site. At Fredericton site the average wind speed increases with the increase of rainfall intensity and reaches to the peak when the rainfall intensity is greater than 5 mm/hr, which indicates that stronger wind associates with heavier rain. However, no such a correlation is observed for test building sites in Montreal. For both HB and FB Building sites, the maximum wind speed is found for rainfall intensity of 4~5 mm/hr. At Fredericton the average standard deviation for rain hours is higher than that for all hours, which indicates that wind speeds show greater variation during rain hours. However, at Montreal sites, the average standard deviation for all hours is higher than the standard deviation for rain hours, which indicates that wind speeds show less variation during rain hours.



(a)



(b)



(c)

Figure 4.18 : Rainfall intensity versus wind speed at test building site: (a) McLeod House, Fredericton; (b) HB Building, Montreal; (c) FB Building, Montreal

4.5 WIND-DRIVEN RAIN ANALYSIS

4.5.1 Error analysis

Experimental method of wind-driven rain measurements can suffer from different types of errors resulting from evaporation, splashing, condensation etc. In wind-driven rain measurements, errors

or loss represents the amount of wind-driven rain that has not been registered by the driving rain gauges. The total error in the wind-driven rain measurement at the end of each rain event is estimated by the following equation (M. Osorio & Ge, April 2013):

$$E_{TOT} = E_{AW} + \sum E_{EVAP} + \sum E_{UC} + S_{WDR} \left(\frac{E_{RW} + nE_{TIP}}{nV_{BOWL}} \right) \quad (4.2)$$

Where,

E_{AW} is the adhesion-water-evaporation error during the rain event and assuming worst-case scenario (i.e.: complete evaporation of AW after every break or dry period in the rain event) and no evaporation during rain. E_{AW} is determined by multiplying the adhesion-water error for a single occurrence of adhesion-water evaporation with the number of interruptions of the rainfall by dry periods (equation (4.3)).

$$E_{AW} = \text{Number of interruptions} \times AW \quad (4.3)$$

E_{EVAP} is the hourly evaporation error from the tipping bucket and collection plate at every hour in the rain event (in mm). Then, the total evaporation is determined by summation of hourly evaporation errors for the number of hours in the rain event from the start to the end of the horizontal rainfall registration.

E_{UC} is the hourly condensation error at every hour in the rain event (in mm). Then, the total condensation error is determined in a similar matter as the total evaporation error.

E_{RW} is the rest-water error (in grams of water).

E_{TIP} is the collection loss during every tip (in grams of water).

n is the amount of tips during the rain event.

V_{BOWL} is the content of the bowls (in grams of water).

S_{WDR} is the total accumulated wind-driven rain for the rain event (in mm).

Then, the relative error associated with the wind-driven rain measurement with a wall-mounted driving rain gauge is given by:

$$e_{TOT} = \frac{E_{TOT}}{S_{WDR}} \quad (4.4)$$

A lab experiment was carried out by Mariana Osorio (Osorio, M., Ge, H., 2013) to determine adhesion-water loss at the collection area and the maximum amount of rest water in the bucket for the driving rain gauge. An average value of adhesion-water of about 4.7 g was found on the collection area, which is equal to 0.050 mm for a collection area of 930.3 cm² and an average value of rest water at the tipping bucket of 5.5g, which is equivalent to 0.060 mm per tip for the driving rain gauge with a collection area of 930.3 cm².

Hourly evaporation error (E_{EVAP}) can be calculated using equation (4.5) (Hens, H., 2007):

$$g_v = \beta (p_s - p) \quad (4.5)$$

Where, g_v is the vapour flow rate in kg/m²s, p_s and p are the partial vapour pressure (Pa) at the surface and in the air, respectively. β is the moisture transfer coefficient in m/s, which can be calculated by the following equation (Hagentoft, C., 2001):

$$\beta = \frac{\alpha_c}{\rho_a c_{pa}} \quad (4.6)$$

Where ρ_a is the air density (kg/m³), c_{pa} is the specific heat at constant pressure (J/kgK) and α_c is the convective heat transfer coefficient (W/m²K), which depends on the air velocity close to the surface and can be estimated by the following equations (Hagentoft, C., 2001):

$$\alpha_c = 6 + 4 * u \quad u \geq 5m/s \quad (4.7)$$

$$\alpha_c = 7.41 * u^{0.78} \quad u \geq 5m/s \quad (4.8)$$

Given that the wind speed close to the wall surface is very small and the relative humidity is typically high, over 90% rh during rain, the evaporation loss (E_{EVAP}) is estimated very small and

can be neglected. According to B. Blocken & Carmeliet, 2006, the condensation error (E_{UC}) is very small and can also be neglected. Since two-bucket tipping bucket is used in the driving rain gauge and laboratory testing did not show any loss of water during the tips, so collection loss (E_{TIP}) can be neglected. Therefore, only adhesion-water-evaporation error and rest water error are considered. As a result equation (4.2) can be written as follows:

$$E_{TOT} = E_{AW} + S_{WDR} \left(\frac{E_{RW}}{nV_{BOWL}} \right) \quad (4.9)$$

Where,

$$E_{AW} = \text{Number of interruptions} \times AW = \text{Number of interruptions} \times 0.050 \text{ mm}$$

$$E_{RW} = 5.5 \text{ grams, and,}$$

$$V_{BOWL} = 5.5 \text{ grams}$$

Number of interruptions refers to the number of dry periods that are long enough for the adhesion water to completely evaporate.

Equation (4.9) is used for estimating the total error that may occur in wind-driven rain measurements for each rain event over the monitoring periods. Rain events are identified according to the ISO standard 15927. According to the ISO 15927-3:2009 (NBN EN ISO 15927-3 (2009)), a spell is a period of wind-driven rain during which the risk of penetration through masonry increases, i.e., a period in which amount of water due to wind-driven rain exceeds the loss due to evaporation (Figure 4.19). A gap between two spells is defined by a period of at least 96 hours. Hence rain events have been separated in such a way so that there exists at least 96 hours dry period between two rain events.

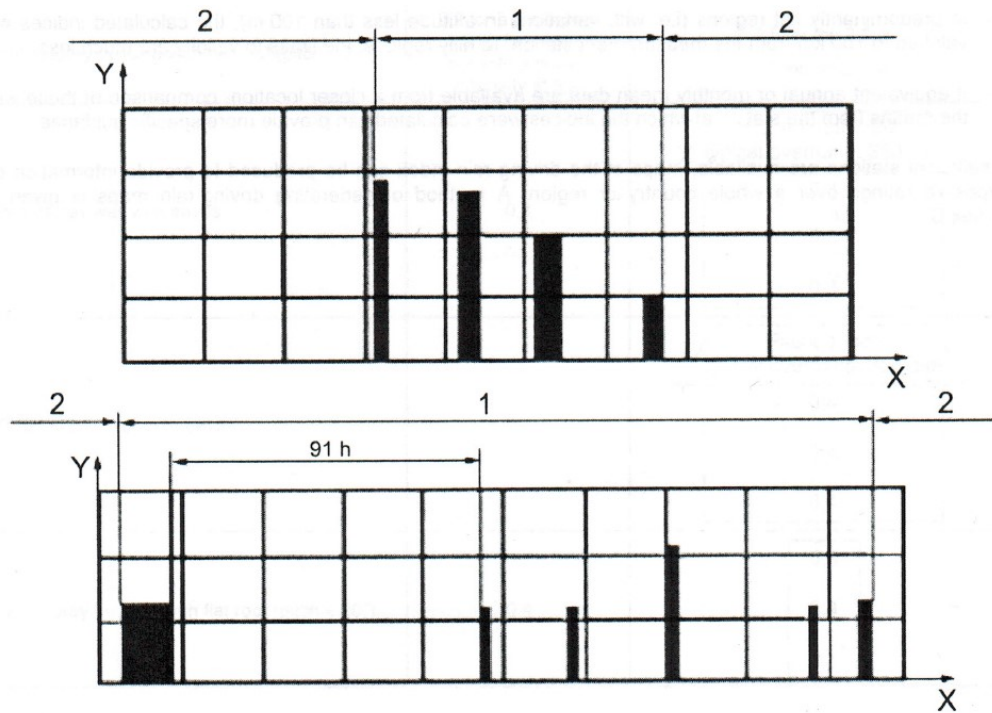


Figure 4.19 : Typical spells (NBN EN ISO 15927-3 (2009))

Total errors are calculated for all the rain events identified over the monitoring periods. Table 4.2 shows the results of error analysis for one rain event for the three buildings as an example. Results for other rain events for all three buildings are presented in Appendix B.

For McLeod House, Fredericton, the rain event used as an example is from October 26, 2013 to November 28, 2013. The total amount of rainfall for this rain event is 218.7 mm, which is the highest observed over the entire monitoring period. The average rainfall intensity of this rain event is 1.4 mm/hr. During this rain event the average air temperature is 3⁰C and the mean relative humidity is 69%. The wind speed is converted at 10 m height using the power law (section 4.3.1.2). The average wind speed at 10 m height is 4.8 m/s and the prevailing wind direction is from the west-north-west and the south-west.

In case of HB Building, Montreal, the results has been presented for the rain event from May 9, 2014 to May 17, 2014. The total amount of rainfall for this rain event is 59.2 mm with an average intensity of 2.04 mm/hr. The average air temperature during this period is 17⁰C and the mean

relative humidity is 63%. The average wind speed at 10 m height is 2.5 m/s and the prevailing wind direction is the west-south-west and the south-south-east.

For FB Building, Montreal, the rain event used as an example is from August 12, 2014 to August 17, 2014. The total amount of rainfall for this rain event is 76.8 mm with an intensity of 1.75 mm/hr. The average air temperature during this period is 17°C and the mean relative humidity is 85%. The average wind speed at 10 m height is 1.97 m/s and the prevailing wind direction is the west-south-west and the south-west.

From the results it is found that the amount of error varies with rain events and the main portion of error is due to adhesion-water-evaporation error (E_{AW}). The largest relative error during each rain event is found at rain gauges where the smallest amount of wind-driven rain is registered. That is why the gauges located on the façades that face the prevailing wind-driven rain shows lower errors compared to other façades. For McLeod House, the error is less than 10% varying from 3-10% for most of the gauges, except for N1, N2 and E5 where small amount of wind-driven rain is registered. For HB Building, the majority of the gauges have small error, except for SE2 and SE4, and 50% of the rain gauges (8 out of 16) show error less than 5%. For FB Building, gauges on the south-east and south-west façade, the façades facing prevailing wind-driven rain, typically have smaller error as compared to gauges on the north-east and north-west façade. On the south-east and south-west façade the error is less than 12% varying from 1-11%.

Table 4.2: Error estimation for the accumulated wind-driven rain: (a) McLeod House - for the rain event from October 26 to November 28, 2013; (b) HB Building - for the rain event from May 9 to May 17, 2014; (c) FB Building - for the rain event from August 12 to August 17, 2014

(a)

| WDR gauge | SW1 | SW2 | SW3 | SW4 | SW5 | SW6 | W1 | N1 | N2 | E1 | E2 | E3 | E4 | E5 | E6 | SE1 |
|-------------------------|------------|------------|------------|------------|------------|------------|------------|-------------|-------------|------------|------------|------------|------------|-------------|------------|------------|
| Number of tips | 369 | 190 | 71 | 372 | 160 | 375 | 73 | 4 | 23 | 202 | 214 | 124 | 379 | 69 | 225 | 105 |
| Number of interruptions | 12 | 10 | 7 | 11 | 12 | 12 | 5 | 3 | 9 | 8 | 6 | 5 | 11 | 11 | 7 | 11 |
| Vbowl (g) | 5.5 | 5.5 | 5.5 | 5.5 | 5.5 | 5.5 | 5.5 | 5.5 | 5.5 | 5.5 | 5.5 | 5.5 | 5.5 | 5.5 | 5.5 | 5.5 |
| Swdr (mm) | 22.1 | 11.4 | 4.3 | 22.3 | 9.6 | 22.5 | 4.4 | 0.2 | 1.4 | 12.1 | 12.8 | 7.4 | 22.7 | 4.1 | 13.5 | 6.3 |
| EAW (mm) | 0.6 | 0.5 | 0.4 | 0.6 | 0.6 | 0.6 | 0.3 | 0.2 | 0.5 | 0.4 | 0.3 | 0.3 | 0.6 | 0.6 | 0.4 | 0.6 |
| EEVAP (mm) | 0 | 0 | 0 | 0 | 0 | 0 | 0 | 0 | 0 | 0 | 0 | 0 | 0 | 0 | 0 | 0 |
| EUC (mm) | 0 | 0 | 0 | 0 | 0 | 0 | 0 | 0 | 0 | 0 | 0 | 0 | 0 | 0 | 0 | 0 |
| ERW (g) | 5.5 | 5.5 | 5.5 | 5.5 | 5.5 | 5.5 | 5.5 | 5.5 | 5.5 | 5.5 | 5.5 | 5.5 | 5.5 | 5.5 | 5.5 | 5.5 |
| ETIP (g/tip) | 0 | 0 | 0 | 0 | 0 | 0 | 0 | 0 | 0 | 0 | 0 | 0 | 0 | 0 | 0 | 0 |
| ETOT (mm) | 0.7 | 0.6 | 0.4 | 0.6 | 0.7 | 0.7 | 0.3 | 0.2 | 0.5 | 0.5 | 0.4 | 0.3 | 0.6 | 0.6 | 0.4 | 0.6 |
| eTOT (%) | 3.0 | 4.9 | 9.6 | 2.7 | 6.9 | 2.9 | 7.1 | 87.5 | 37.0 | 3.8 | 2.8 | 4.2 | 2.7 | 14.7 | 3.0 | 9.7 |

(b)

| WDR gauge | NW1 | NW2 | SW1 | SW2 | SW3 | SW4 | SW5 | SW6 | SW7 | SW8 | SW10 | SE1 | SE2 | SE3 | SE4 |
|-------------------------|------------|------------|------------|------------|------------|------------|------------|------------|------------|------------|------------|-------------|-------------|-------------|-------------|
| Number of tips | 114 | 113 | 244 | 85 | 159 | 63 | 148 | 66 | 169 | 69 | 101 | 38 | 16 | 50 | 19 |
| Number of interruptions | 0 | 0 | 4 | 3 | 2 | 4 | 3 | 4 | 3 | 4 | 5 | 5 | 5 | 6 | 4 |
| Vbowl (g) | 5.5 | 5.5 | 5.5 | 5.5 | 5.5 | 5.5 | 5.5 | 5.5 | 5.5 | 5.5 | 5.5 | 5.5 | 5.5 | 5.5 | 5.5 |
| Swdr (mm) | 6.8 | 6.8 | 14.6 | 5.1 | 9.5 | 3.8 | 8.9 | 4.0 | 10.1 | 4.1 | 6.1 | 2.3 | 1.0 | 3.0 | 1.1 |
| EAW (mm) | 0.0 | 0.0 | 0.2 | 0.2 | 0.1 | 0.2 | 0.2 | 0.2 | 0.2 | 0.2 | 0.3 | 0.3 | 0.3 | 0.3 | 0.2 |
| EEVAP (mm) | 0 | 0 | 0 | 0 | 0 | 0 | 0 | 0 | 0 | 0 | 0 | 0 | 0 | 0 | 0 |
| EUC (mm) | 0 | 0 | 0 | 0 | 0 | 0 | 0 | 0 | 0 | 0 | 0 | 0 | 0 | 0 | 0 |
| ERW (g) | 5.5 | 5.5 | 5.5 | 5.5 | 5.5 | 5.5 | 5.5 | 5.5 | 5.5 | 5.5 | 5.5 | 5.5 | 5.5 | 5.5 | 5.5 |
| ETIP (g/tip) | 0 | 0 | 0 | 0 | 0 | 0 | 0 | 0 | 0 | 0 | 0 | 0 | 0 | 0 | 0 |
| ETOT (mm) | 0.1 | 0.1 | 0.3 | 0.2 | 0.2 | 0.3 | 0.2 | 0.3 | 0.2 | 0.3 | 0.3 | 0.3 | 0.3 | 0.4 | 0.3 |
| eTOT (%) | 0.9 | 0.9 | 1.8 | 4.1 | 1.7 | 6.9 | 2.4 | 6.6 | 2.1 | 6.3 | 5.1 | 13.6 | 32.3 | 12.0 | 22.8 |

(c)

| WDR gauge | NE1 | NE2 | NE5 | NE7 | NE8 | NW1 | SW1 | SW2 | SW3 | SW4 | SW5 | SW6 | SW7 | SE1 | SE2 | SE3 | SE4 | SE5 | SE6 |
|-------------------------|-------------|-------------|-------------|-------------|-------------|-------------|------------|-------------|------------|-------------|------------|------------|------------|------------|------------|------------|------------|------------|------------|
| Number of tips | 17 | 7 | 26 | 24 | 14 | 9 | 174 | 58 | 155 | 53 | 203 | 95 | 110 | 345 | 153 | 240 | 321 | 113 | 49 |
| Number of interruptions | 1 | 4 | 5 | 4 | 6 | 2 | 8 | 6 | 8 | 6 | 10 | 2 | 4 | 5 | 4 | 5 | 5 | 3 | 3 |
| Vbowl (g) | 5.5 | 5.5 | 5.5 | 5.5 | 5.5 | 5.5 | 5.5 | 5.5 | 5.5 | 5.5 | 5.5 | 5.5 | 5.5 | 5.5 | 5.5 | 5.5 | 5.5 | 5.5 | 5.5 |
| Swdr (mm) | 1.0 | 0.4 | 1.6 | 1.4 | 0.8 | 0.5 | 10.4 | 3.5 | 9.3 | 3.2 | 12.2 | 5.7 | 6.6 | 20.7 | 9.2 | 14.4 | 19.3 | 6.8 | 2.9 |
| EAW (mm) | 0.1 | 0.2 | 0.3 | 0.2 | 0.3 | 0.1 | 0.4 | 0.3 | 0.4 | 0.3 | 0.5 | 0.1 | 0.2 | 0.3 | 0.2 | 0.3 | 0.3 | 0.2 | 0.2 |
| EEVAP (mm) | 0 | 0 | 0 | 0 | 0 | 0 | 0 | 0 | 0 | 0 | 0 | 0 | 0 | 0 | 0 | 0 | 0 | 0 | 0 |
| EUC (mm) | 0 | 0 | 0 | 0 | 0 | 0 | 0 | 0 | 0 | 0 | 0 | 0 | 0 | 0 | 0 | 0 | 0 | 0 | 0 |
| ERW (g) | 5.5 | 5.5 | 5.5 | 5.5 | 5.5 | 5.5 | 5.5 | 5.5 | 5.5 | 5.5 | 5.5 | 5.5 | 5.5 | 5.5 | 5.5 | 5.5 | 5.5 | 5.5 | 5.5 |
| ETIP (g/tip) | 0 | 0 | 0 | 0 | 0 | 0 | 0 | 0 | 0 | 0 | 0 | 0 | 0 | 0 | 0 | 0 | 0 | 0 | 0 |
| ETOT (mm) | 0.1 | 0.3 | 0.3 | 0.3 | 0.4 | 0.2 | 0.5 | 0.4 | 0.5 | 0.4 | 0.6 | 0.2 | 0.3 | 0.3 | 0.3 | 0.3 | 0.3 | 0.2 | 0.2 |
| eTOT (%) | 10.8 | 61.9 | 19.9 | 18.1 | 42.9 | 29.6 | 4.4 | 10.3 | 4.9 | 11.3 | 4.6 | 2.8 | 3.9 | 1.5 | 2.8 | 2.2 | 1.6 | 3.1 | 7.1 |

Figure 4.20 shows percentage of error as a function of wind-driven rain amount (mm) for three test buildings. These graphs have been plotted for all the rain gauge locations and for all rain events over the entire monitoring period. This figure confirms that the lower the amount of wind-driven rain, the higher the error.

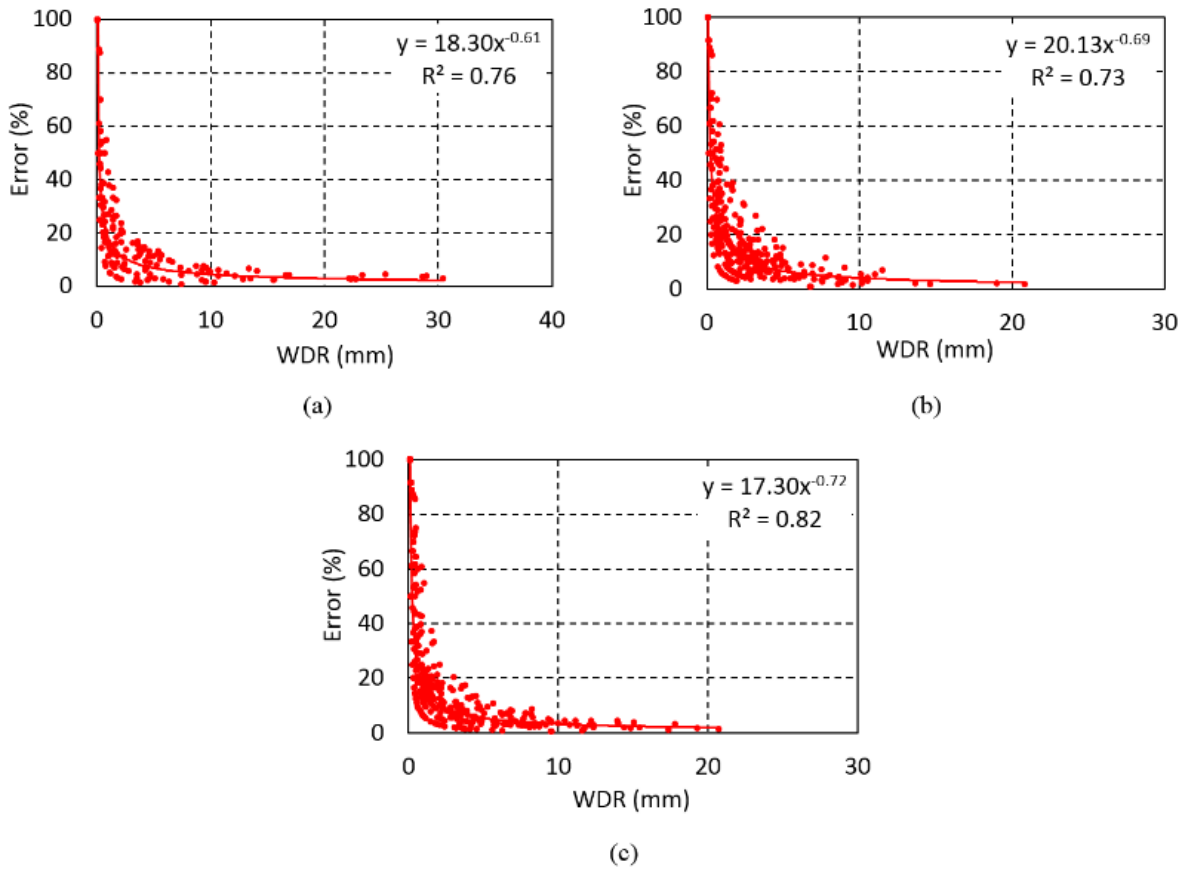


Figure 4.20 : Error as a function of wind-driven rain amount for: (a) McLeod House, Fredericton; (b) HB Building, Montreal; (c) FB Building, Montreal

Errors associated with each rain event during the entire monitoring period have been summed up to obtain total amount of losses that happened with wind-driven rain measurement during this period. Table 4.3 shows the total amount of wind-driven rain registered by each driving rain gauge and the total amount of losses along with the percentage of losses during the entire monitoring period for all three test buildings. It is found that usually the amount of loss is not significant. The error is less than 15%, for 82% (13 out of 16 locations) and 87% (14 out of 16 locations) of the locations at McLeod House and HB Building, respectively. At FB Building, for 71% of the locations error is less than 15%. Here error is less than 15% for 100% locations on the north-west,

south-east and south-west façade but significant error is found at locations about 10.67 m (35') and 21.34 m (70') below the roofline (the 3rd and 4th row; NE3, NE4, NE9, NE10) of the north-east façade. The errors have been taken into account and all the following analyses have been conducted with corrected measurements (i.e., including losses).

Table 4.3 : Total amount of wind-driven rain registered by each driving rain gauge and total amount of losses during the entire monitoring period for all three test buildings

| McLeod house, Fredericton | | | | HB building, Montreal | | | | FB building, Montreal | | | |
|---------------------------|----------------|-----------------------|------------------------|-----------------------|----------------|-----------------------|------------------------|-----------------------|----------------|-----------------------|------------------------|
| Driving rain gauges | Total WDR (mm) | Total loss/error (mm) | Percentage of Loss (%) | Driving rain gauges | Total WDR (mm) | Total loss/error (mm) | Percentage of Loss (%) | Driving rain gauges | Total WDR (mm) | Total loss/error (mm) | Percentage of Loss (%) |
| SW1 | 69.8 | 4.28 | 6 | NW1 | 52.95 | 5.61 | 11 | NE1 | 52.37 | 3.71 | 7 |
| SW2 | 38.97 | 3.63 | 9 | NW2 | 38.24 | 4.46 | 12 | NE2 | 28.36 | 4.96 | 17 |
| SW3 | 24.27 | 3.03 | 12 | SW1 | 49.36 | 4.06 | 8 | NE3 | 9.50 | 2.66 | 28 |
| SW4 | 73.33 | 4.63 | 6 | SW2 | 50.08 | 6.46 | 13 | NE4 | 8.16 | 3.06 | 38 |
| SW5 | 36.36 | 3.78 | 10 | SW3 | 75.64 | 7.66 | 10 | NE5 | 43.31 | 4.91 | 11 |
| SW6 | 78.65 | 4.43 | 6 | SW4 | 36.22 | 6.76 | 19 | NE6 | 12.42 | 2.46 | 20 |
| W1 | 53.45 | 3.23 | 6 | SW5 | 66.14 | 6.26 | 9 | NE7 | 43.58 | 4.16 | 10 |
| N1 | 6.72 | 1.98 | 29 | SW6 | 37.6 | 5.26 | 14 | NE8 | 22.26 | 3.66 | 16 |
| N2 | 24.13 | 3.13 | 13 | SW7 | 79.03 | 7.51 | 10 | NE9 | 8.06 | 2.06 | 26 |
| E1 | 40.33 | 3.13 | 8 | SW8 | 46.09 | 7.51 | 16 | NE10 | 1.60 | 1.36 | 85 |
| E2 | 23.62 | 3.28 | 14 | SW9 | 26.52 | 3.66 | 14 | NW1 | 31.41 | 4.71 | 15 |
| E3 | 14.92 | 2.98 | 20 | SW10 | 46.07 | 7.01 | 15 | SW1 | 107.52 | 6.66 | 6 |
| E4 | 50.47 | 4.33 | 9 | SE1 | 108.2 | 5.96 | 6 | SW2 | 40.86 | 4.86 | 12 |
| E5 | 24.1 | 4.18 | 17 | SE2 | 51.38 | 5.36 | 10 | SW3 | 93.64 | 5.26 | 6 |
| E6 | 30.09 | 3.63 | 12 | SE3 | 126.3 | 6.96 | 6 | SW4 | 35.47 | 4.81 | 14 |
| SE1 | 58.86 | 4.08 | 7 | SE4 | 51.88 | 6.46 | 12 | SW5 | 143.51 | 7.01 | 5 |
| | | | | | | | | SW6 | 48.11 | 4.31 | 9 |
| | | | | | | | | SW7 | 40.44 | 3.96 | 10 |
| | | | | | | | | SE1 | 102.18 | 3.96 | 4 |
| | | | | | | | | SE2 | 48.97 | 3.31 | 7 |
| | | | | | | | | SE3 | 77.97 | 4.41 | 6 |
| | | | | | | | | SE4 | 104.68 | 4.66 | 4 |
| | | | | | | | | SE5 | 45.88 | 3.16 | 7 |
| | | | | | | | | SE6 | 19.79 | 2.81 | 14 |

4.5.2 Spatial distribution of wind-driven rain

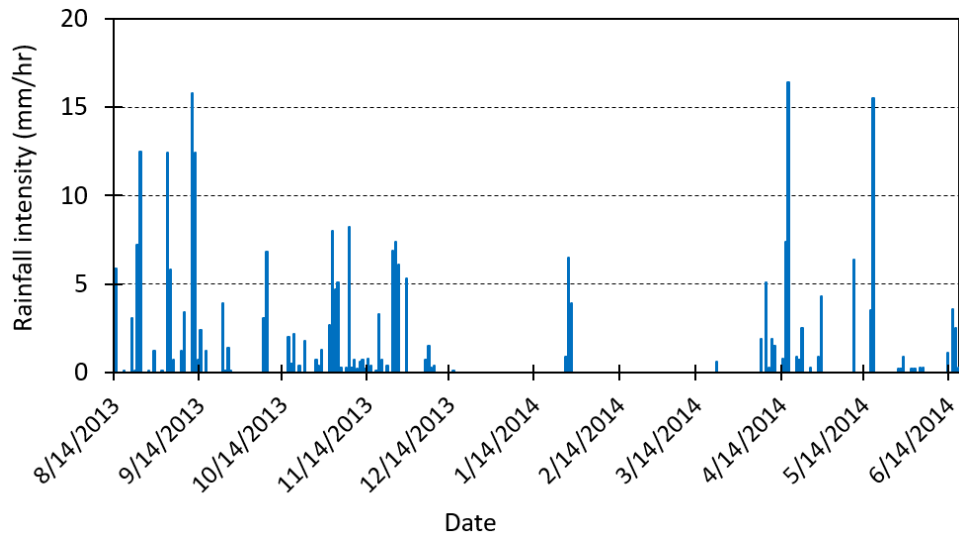
The following sections present the spatial distribution of wind-driven rain on façades in terms of catch ratios and wall factors.

4.5.2.1 Catch ratio analysis

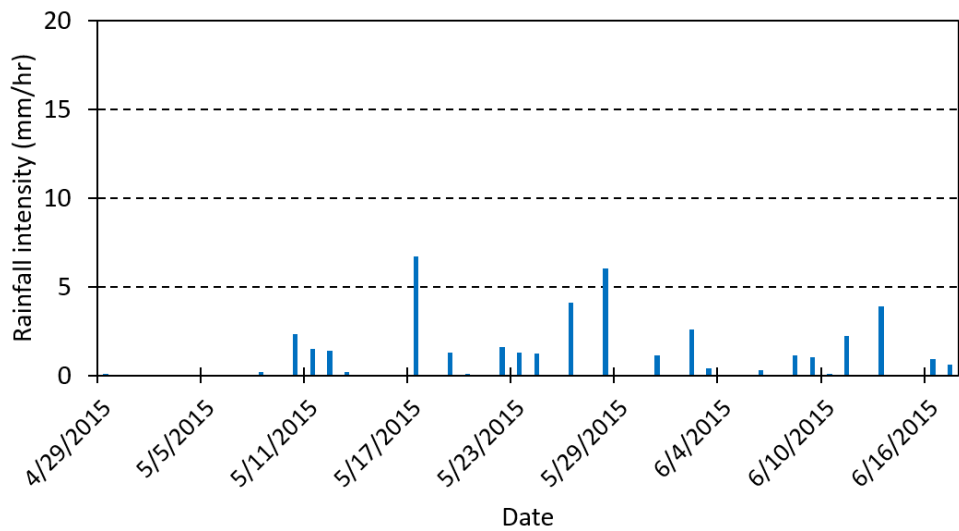
Catch ratios provide the basics to understand the spatial distribution of wind-driven rain on the building façades. Definition and significance of catch ratio have been discussed in section 2.3.1. In the current section the catch ratios are calculated for the entire monitoring period with all approaching wind angles using equation (2.1).

The plots of rainfall distribution over time during monitoring period at McLeod House, HB Building and FB Building site are shown in Figure 4.21, Figure 4.25 and Figure 4.29, respectively. The prevailing wind direction during rain hours at these sites for the entire monitoring period and plan view with rain gauge locations are presented in Figure 4.22, Figure 4.26 and Figure 4.30. A combined graph showing the total horizontal rainfall, wind-driven rain received by each rain gauge and catch ratios at gauge locations during the monitoring period for all three sites are presented in the Figure 4.23, Figure 4.27 and Figure 4.31. The catch ratio value at each rain gauge location on different façades of the McLeod House, HB Building and FB Building is presented in Figure 4.24, Figure 4.28 and Figure 4.32, respectively.

At McLeod House site the total rainfall recorded during the monitoring period is 811.7 mm and the prevailing wind direction for this period is from the south-west. As shown in Figure 4.23 and Figure 4.24, the catch ratio values are typically higher on the south-west façade, the façade facing the prevailing wind-driven rain, compared to the values for the locations at the same height of other façades. The catch ratio varies from 0.07 to 0.1, and 0.01 to 0.03, at the top locations (0.61 m below the roofline) of the windward façade (south-west) and leeward façade (north-east), respectively, whereas value ranges from 0.04 to 0.07 at the same height on other façades (south-east and north-west). At bottom locations (4.88 m and 9.14 m below the roofline) catch ratio ranges from 0.03 to 0.05 and 0.02 to 0.03 for windward façade and other façades respectively. The catch ratio values and hence the amount of rain deposited on the building surface varies with locations (Figure 4.24) and typically catch ratios are higher at the top of the facades and decrease towards the bottom. The corners and edges have higher catch ratio values, which indicates that the corners and edges receive the higher amount of rain. This supports the classical wetting pattern of building façades.



(a)



(b)

Figure 4.21 : Horizontal rainfall intensity recorded at test building site in Fredericton: (a) from August 2013 to June 2014 and (b) from April 2015 to June 2015

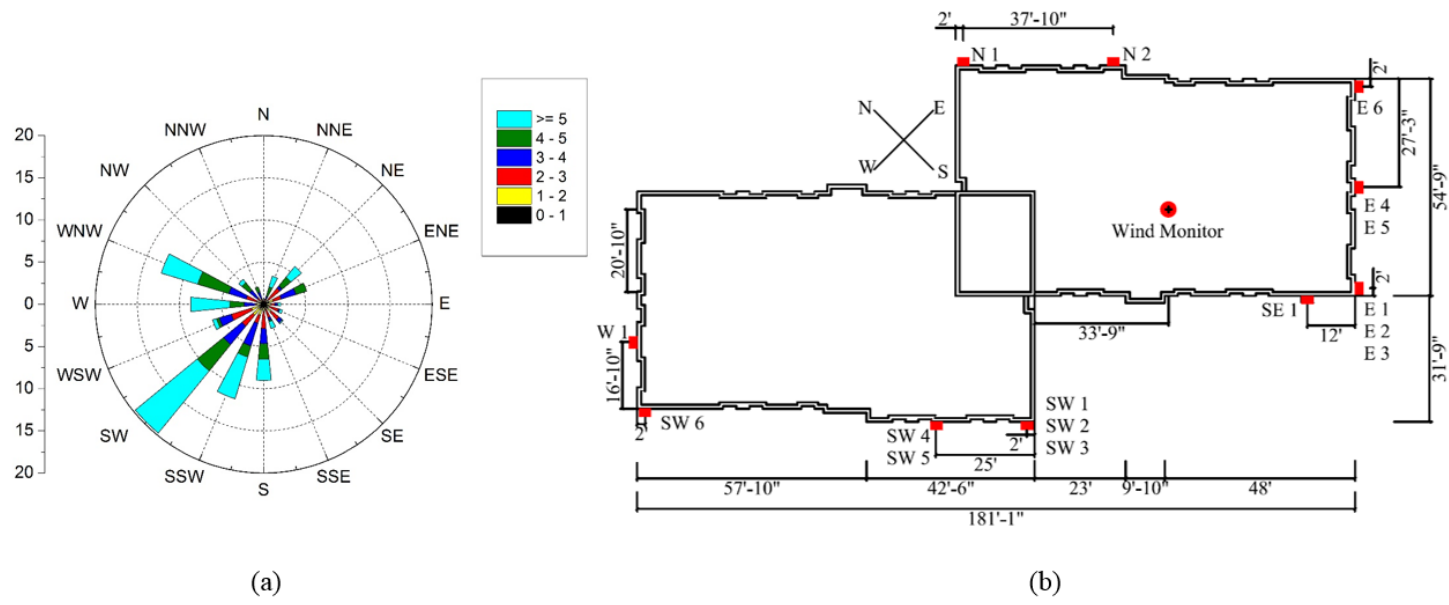


Figure 4.22 : (a) Prevailing wind direction during rain hours for the entire monitoring period; (b) Plan view with rain gauge locations of McLeod House in Fredericton

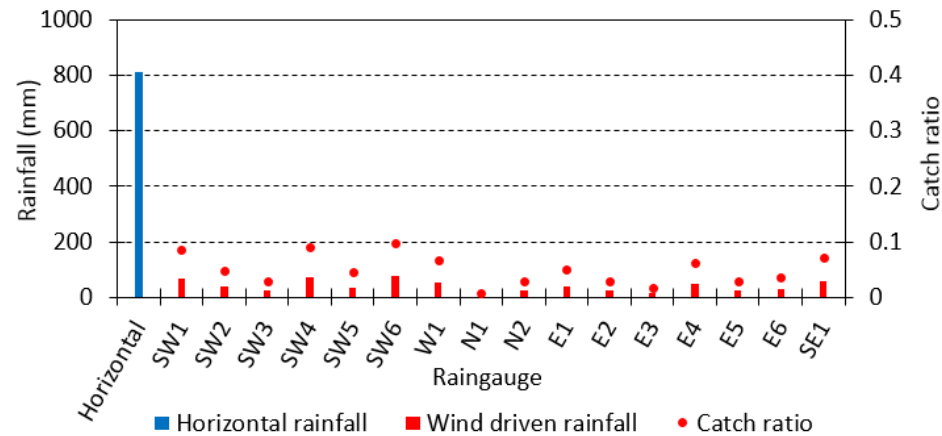
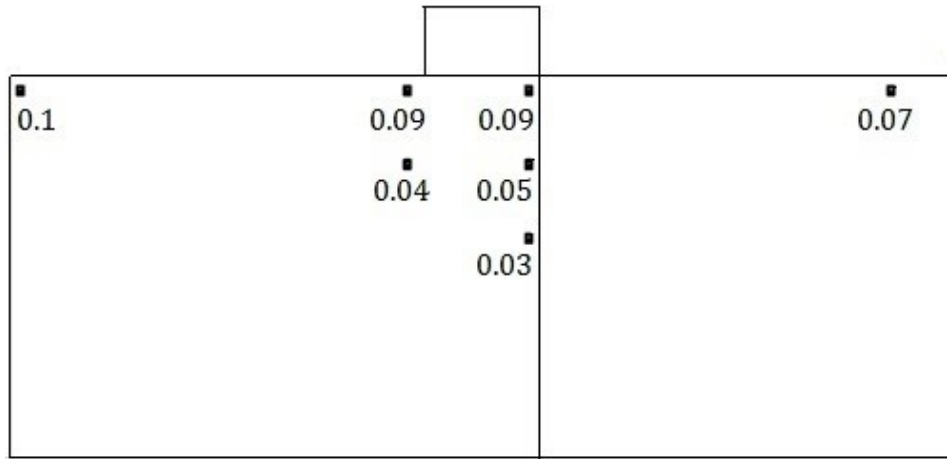
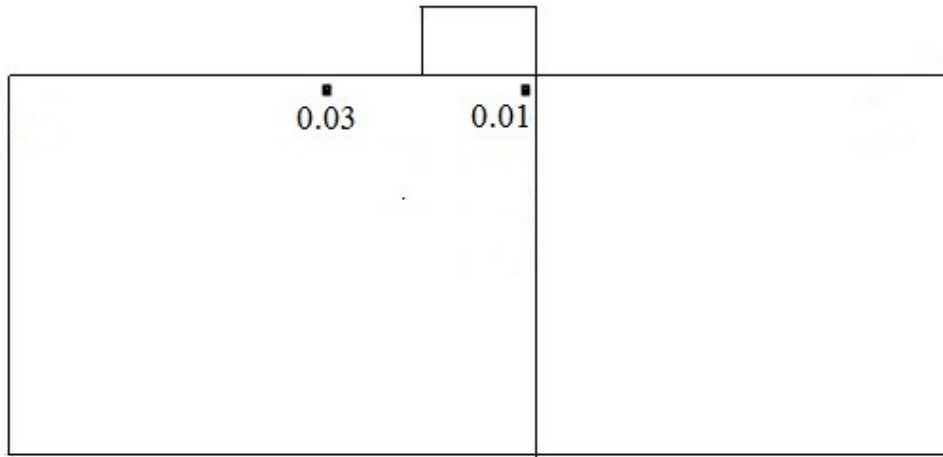


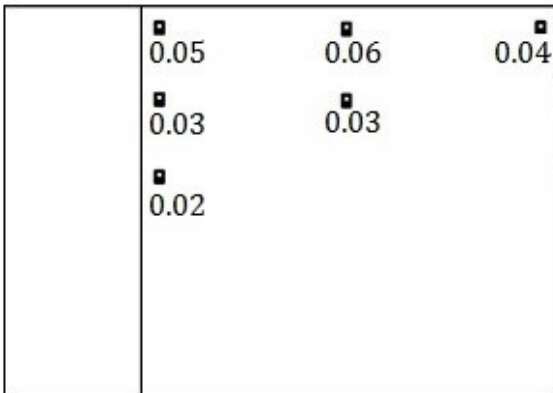
Figure 4.23 : Total rainfall, wind-driven rain and catch ratio values at driving rain gauge locations for the entire monitoring period at McLeod House in Fredericton



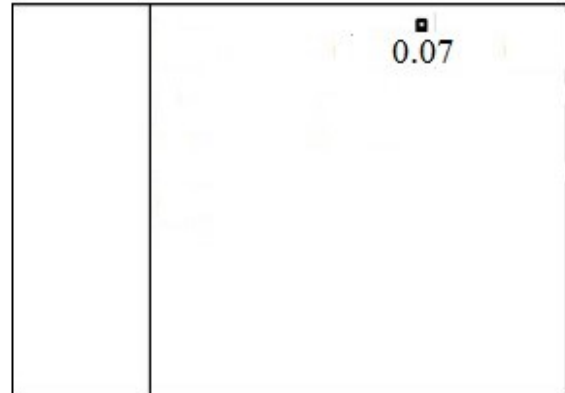
(a)



(b)



(c)



(d)

Figure 4.24 : Catch ratio values on rain gauge locations on the: (a) south-west; (b) north-east; (c) south-east; (d) north-west façade of McLeod House in Fredericton

Total rainfall recorded during the monitoring period at HB Building site is 989.4 mm. Figure 4.27 and Figure 4.28 show that the catch ratio values are typically higher on the south-west and the south-east façade, the façades facing prevailing wind-driven rain, compared to the values for the locations at the same heights of north-west façade. Here also catch ratio values are higher at the top of the façades and at corners and edges. The catch ratio varies from 0.07 to 0.13 at the top locations (0.61 m below the roofline) of the windward façades (south-west and south-east), whereas value ranges from 0.04 to 0.05 at the bottom locations (4.88 m below the roofline) of windward façades and top locations on the other façade.

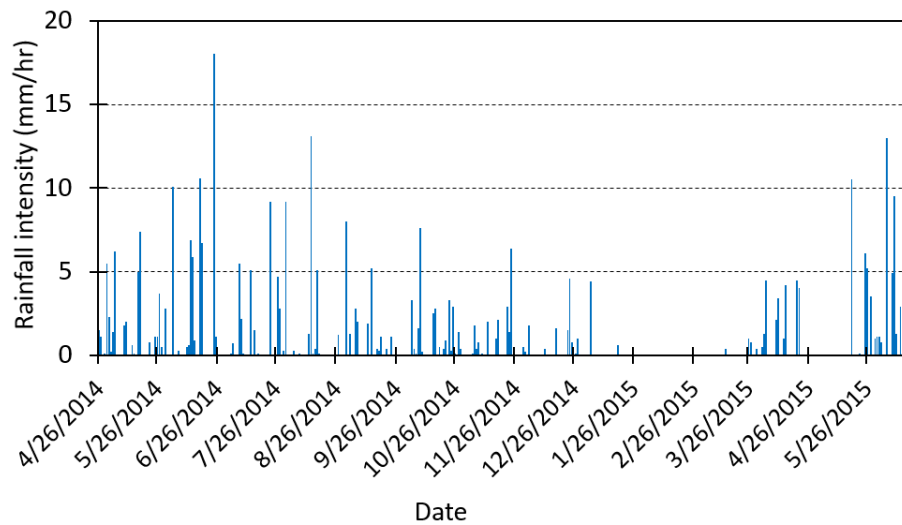


Figure 4.25 : Horizontal rainfall intensity recorded at HB Building site in Montreal from April 2014 to June 2015

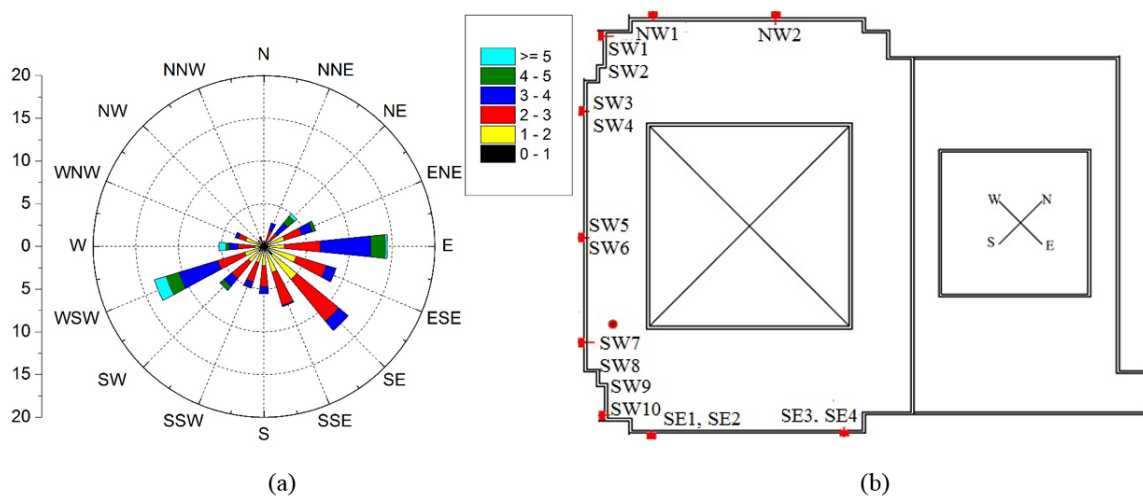


Figure 4.26 : (a) Prevailing wind direction during rain hours for the entire monitoring period; (b) Plan view with rain gauge locations of HB Building in Montreal

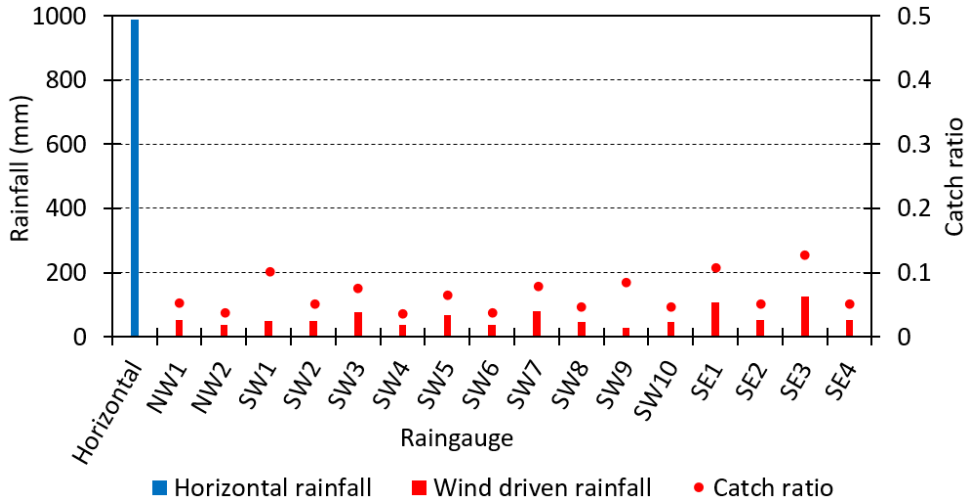


Figure 4.27 : Total rainfall, wind-driven rain and catch ratio values at driving rain gauge locations for the entire monitoring period at HB Building in Montreal

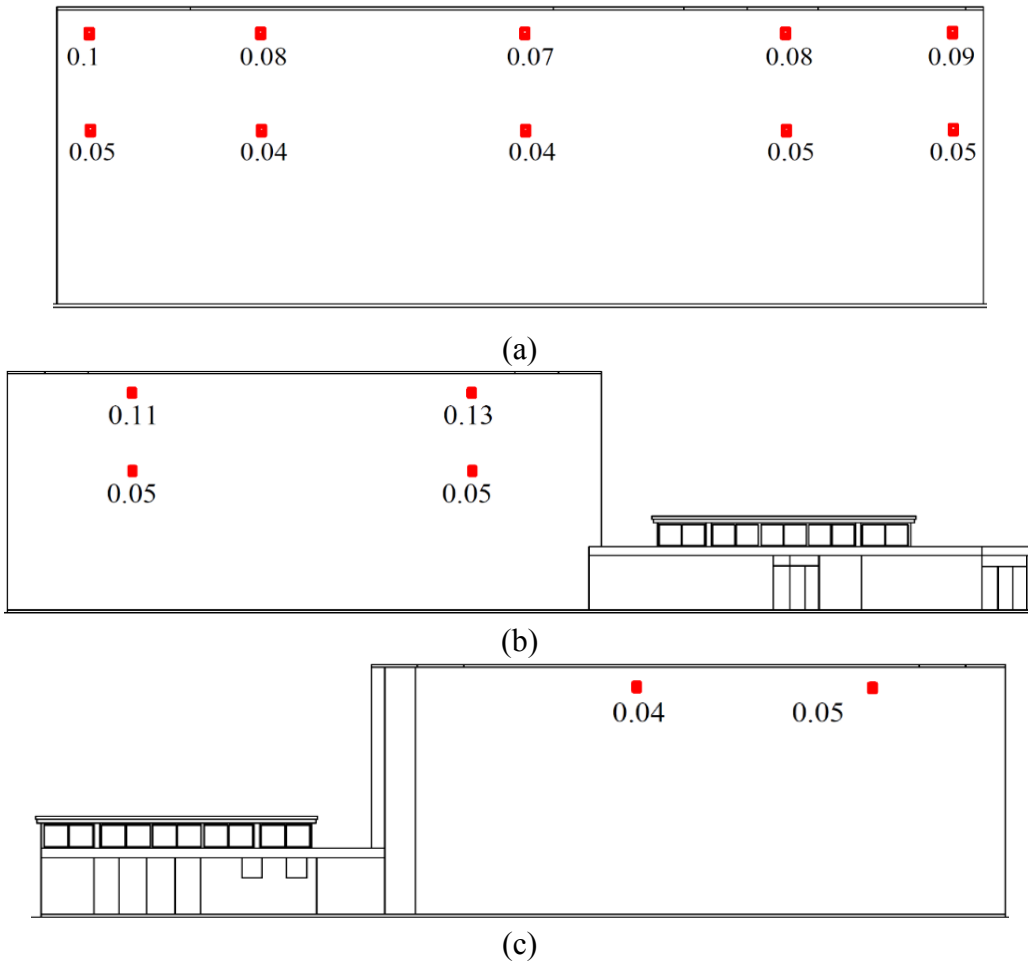


Figure 4.28 : Catch ratio values on rain gauge locations on the: (a) south-west; (b) south-east; (c) north-west façade of HB Building in Montreal

At FB Building site the total rainfall recorded during the monitoring period is 573.1 mm. As shown in Figure 4.31 and Figure 4.32, the catch ratio values are typically higher on the façades facing the prevailing wind-driven rain (south-west and south-east façades), compared to the values for the locations at the same height of other façades. At the top locations (0.61 m below the roofline) and bottom locations (4.88 m and 10.67 m below the roofline) of the windward façades the catch ratio ranges from 0.14 to 0.25 and 0.05 to 0.08, respectively. For other façades value ranges from 0.05 to 0.09 at top locations, whereas at bottom locations (4.88 m and 9.14 m below the roofline) value ranges from 0.003 to 0.05 with the lowest value (0.003) at location 21.34 m below the roofline. Similar to other two buildings, catch ratio values are higher at the top of the façades which decrease towards the bottom and the corners and edges face higher amount of rain deposition.

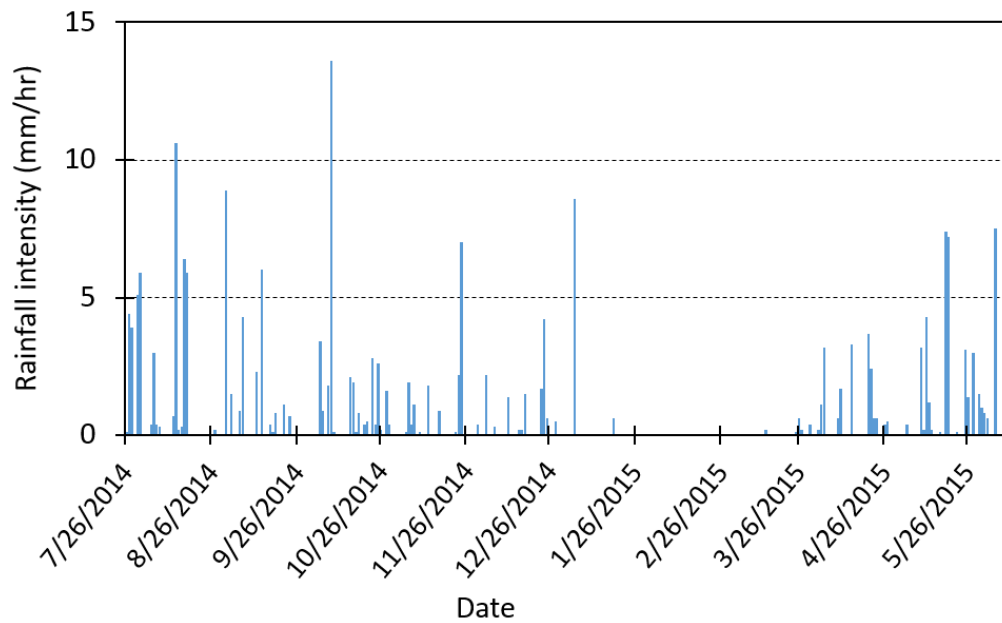


Figure 4.29 : Horizontal rainfall intensity recorded at HB Building site in Montreal from July 2014 to June 2015

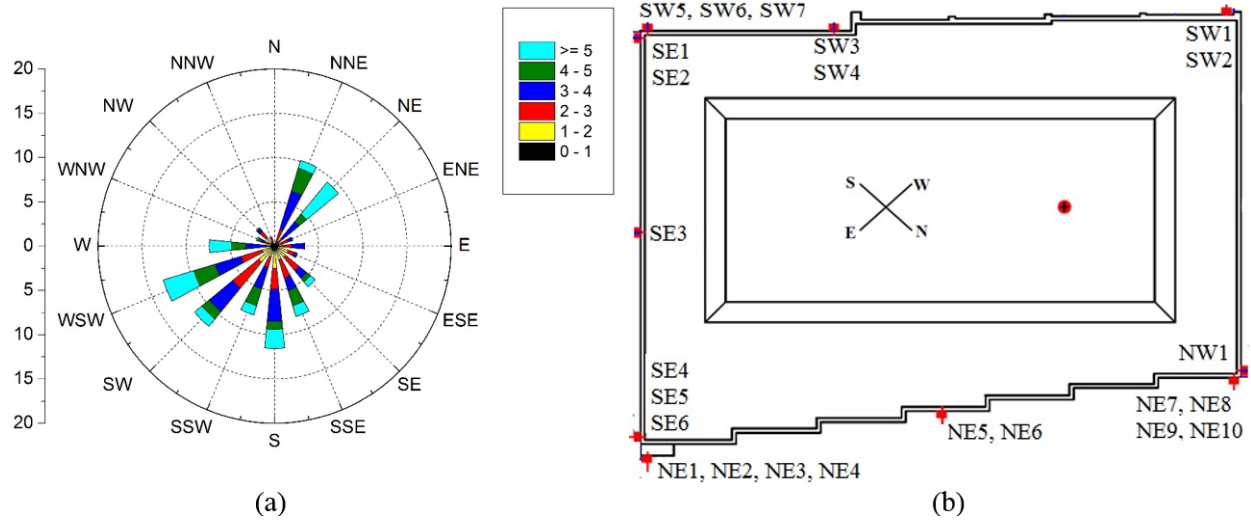


Figure 4.30 : (a) Prevailing wind direction during rain hours for the entire monitoring period; (b) Plan view with rain gauge locations of FB Building in Montreal

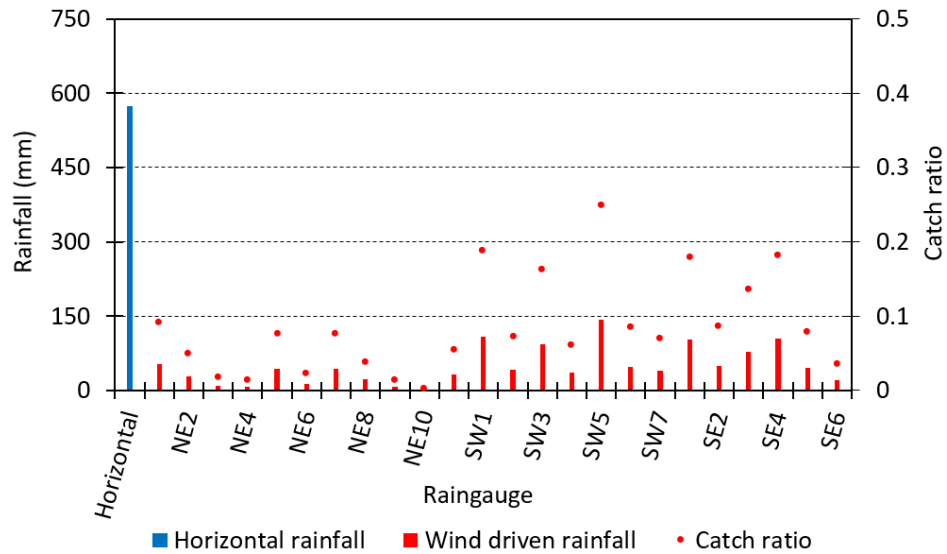
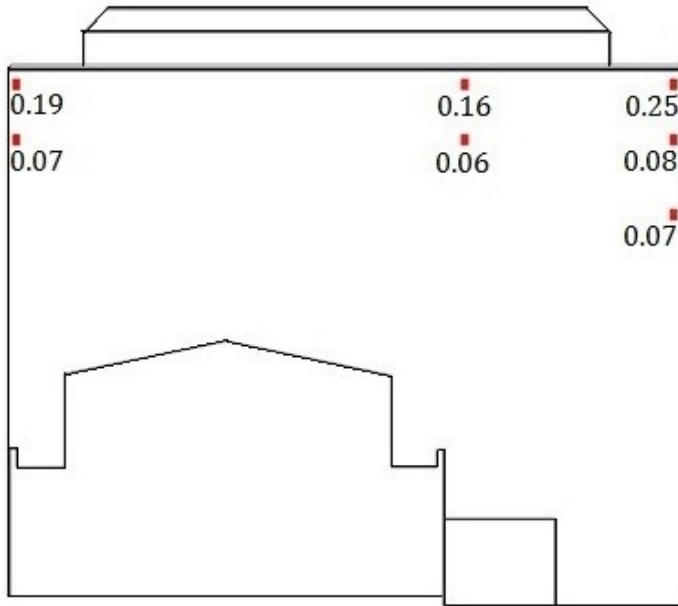
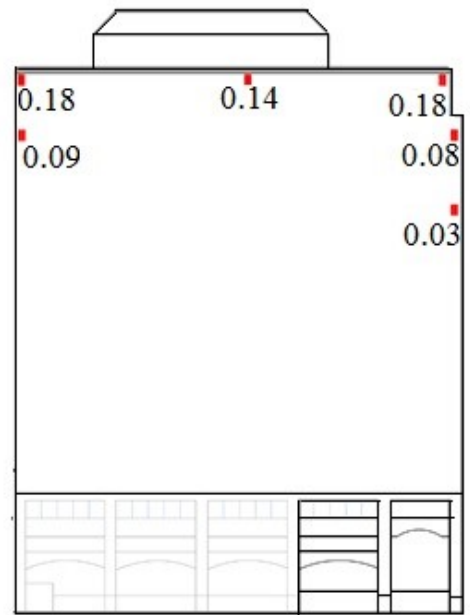


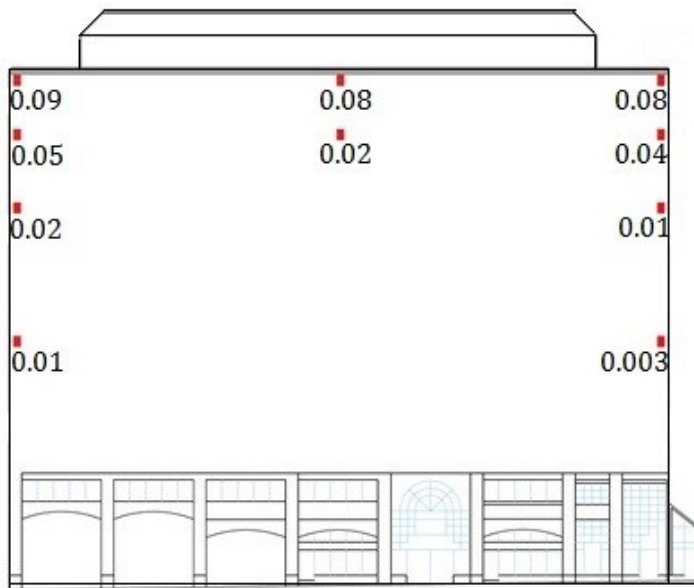
Figure 4.31 : Total rainfall, wind-driven rain and catch ratio values at driving rain gauge locations for the entire monitoring period at FB Building in Montreal



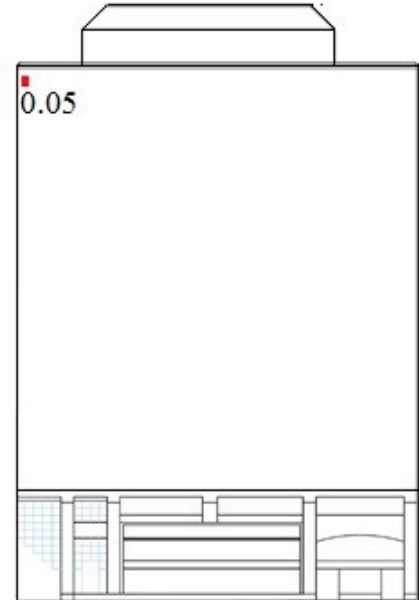
(a)



(b)



(c)



(d)

Figure 4.32 : Catch ratio values at rain gauge locations on the: (a) south-west; (b) south-east; (c) north-east; (d) north-west façade of FB Building in Montreal

4.5.2.2 Frequency analysis of catch ratios

Frequency distribution of catch ratios has been conducted for the entire monitoring periods for all three sites in relation to incidence angles. Incidence angle (θ) is the angle between the approaching wind direction and the line normal to the building façade on the both side of the normal line (Figure 4.33). Analysis has been done for all incidence angle as well as for incidence angles ranging from 0° to 15° .

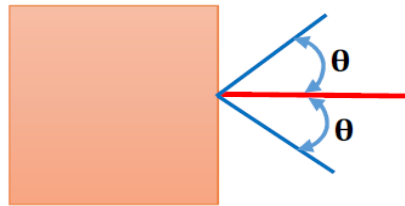


Figure 4.33 : Incidence angle (θ)

Figure 4.34 to Figure 4.36 show the results for different locations on the south-west façade of three test buildings as an example. Results at locations 0.61 m (SW1), 4.88 m (SW2) and 9.14 m (SW3) below the roofline for McLeod House; 0.61 m (SW5) and 4.88 m (SW6) below the roofline for HB Building; and 0.61 m (SW5), 4.88 m (SW6) and 10.67m (SW7) below the roofline for FB Building is shown in the figures. As shown in figures, catch ratio values are relatively higher when calculated for incidence angles ranging form 0° to 15° compared to that calculated for all incidence angles, which indicates higher catch ratio values for normal approaching wind. It can be found that the catch ratios are higher for FB Building compared to those for McLeod House and HB Building at the same heights below the roofline. For example, at locations 0.61 m below the roofline of FB Building (SW5), 80% of the time catch ratio (calculated for all incidence angles) varies from 0 to 0.55, whereas values range from 0 to 0.35 and 0 to 0.25 for 80% of the time at the same heights below the roofline For McLeod House and HB Building, respectively. Values range from 0 to 0.25 for 80% of the time at all bottom locations of FB Building and at locations 4.88 m below the roof line of McLeod House. At locations 9.14 m below the roof line of McLeod House and 4.88 m below the roof line of HB Building, catch ratio varies from 0 to 0.15 for 80% of the time.

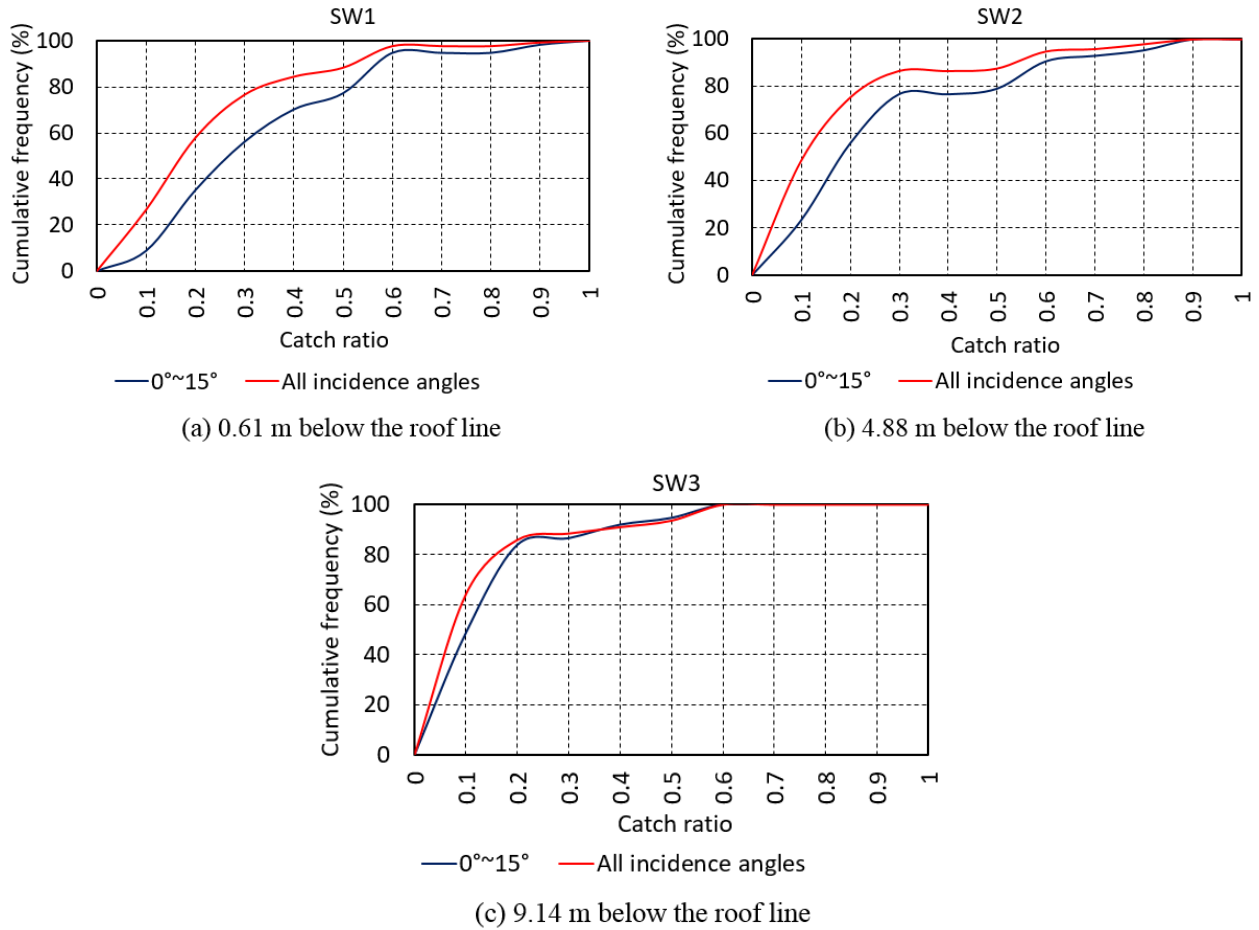


Figure 4.34 : Frequency distribution of catch ratio at different locations on the south-west façade of McLeod House

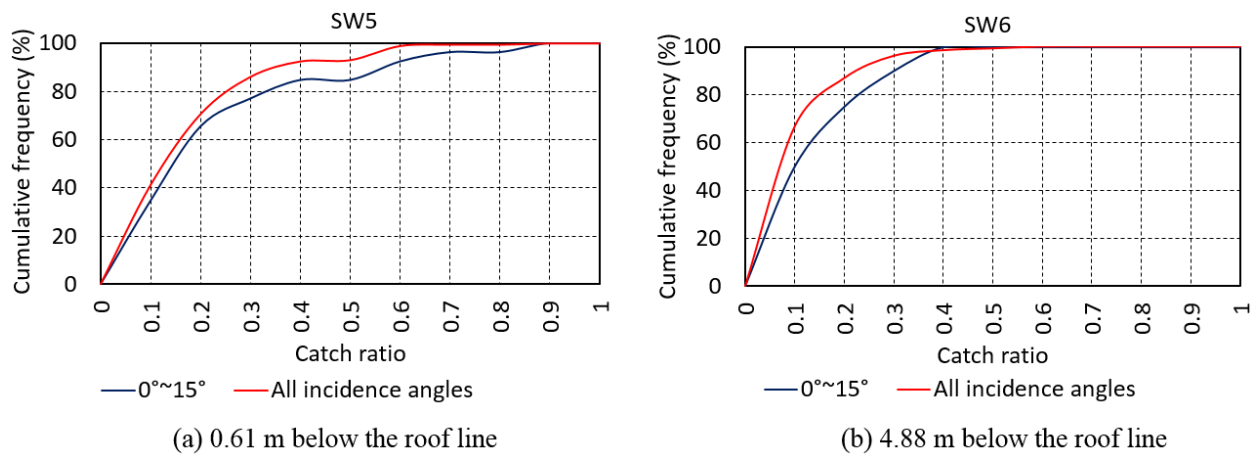


Figure 4.35 : Frequency distribution of catch ratio at different locations on the south-west façade of HB Building

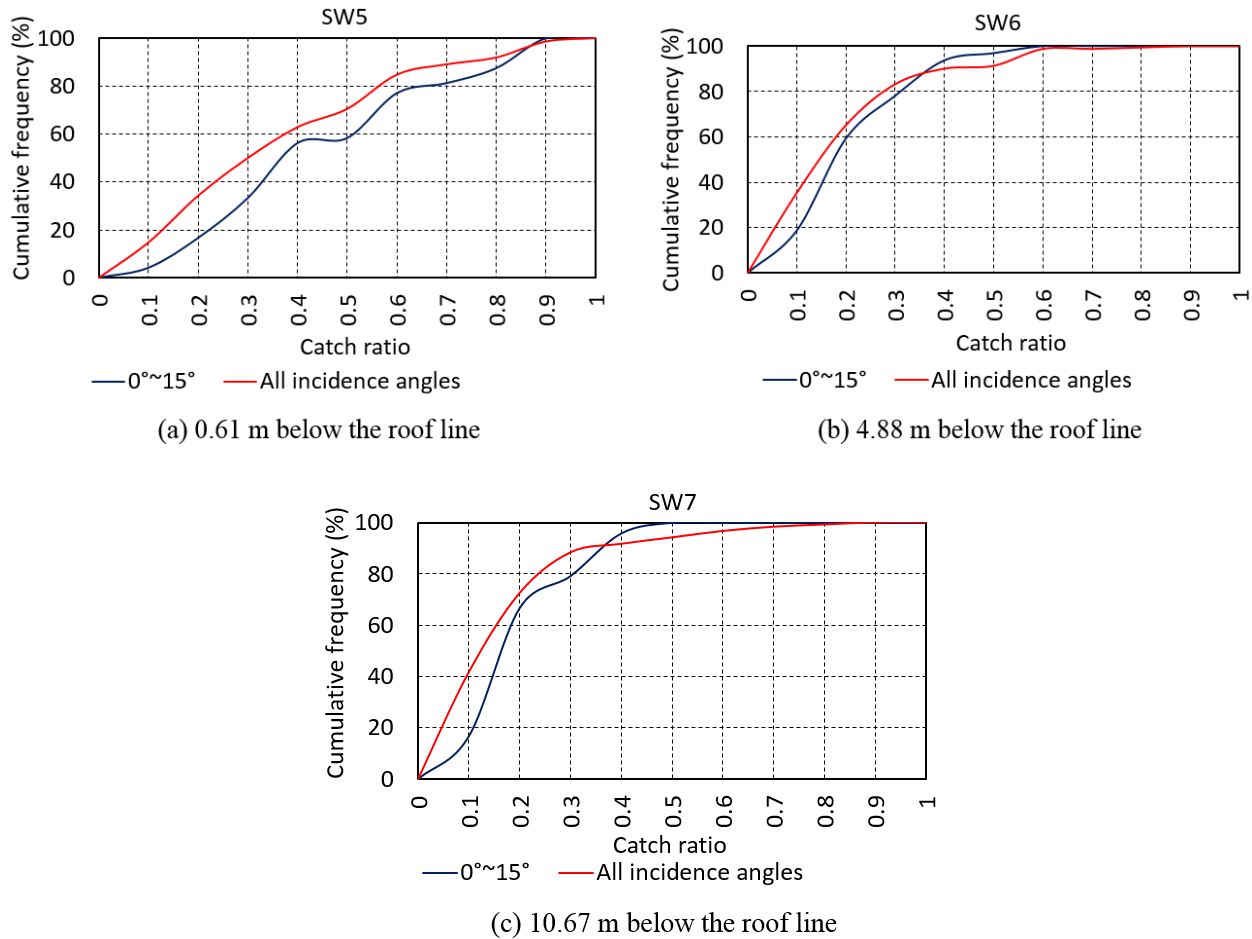


Figure 4.36 : Frequency distribution of catch ratio at different locations on the south-west façade of FB Building

4.5.2.3 Catch ratio as a function of incidence angle

Analysis has been conducted to observe how the catch ratio varies with incidence angle. To do so, hourly data for the entire monitoring period is used to plot catch ratios versus incidence angle. Better correlations, for which R-squared (R^2) value is greater than 0.5, are found at top locations on the façade (0.61 m below the roof line) of the buildings. Result for one top location on the south-west façade of all three buildings is shown in Figure 4.37 as an example. As shown in figure, catch ratio is maximum when approaching wind is normal to the façade (incidence angle 0°).

Values decrease with the increase of incidence angle and become minimum for parallel approaching wind.

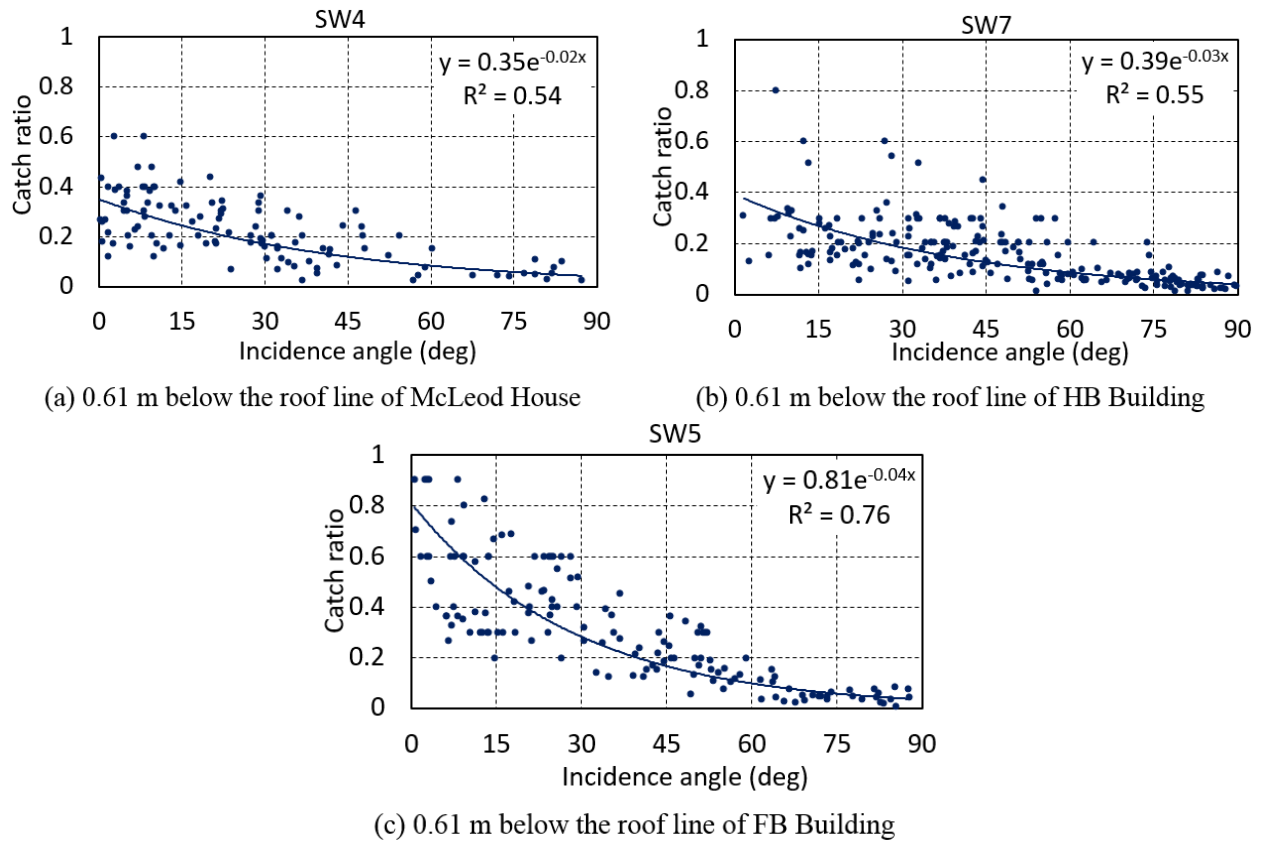
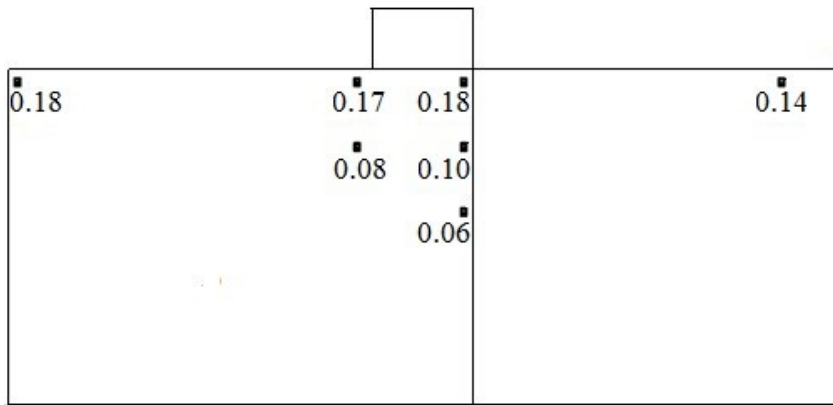
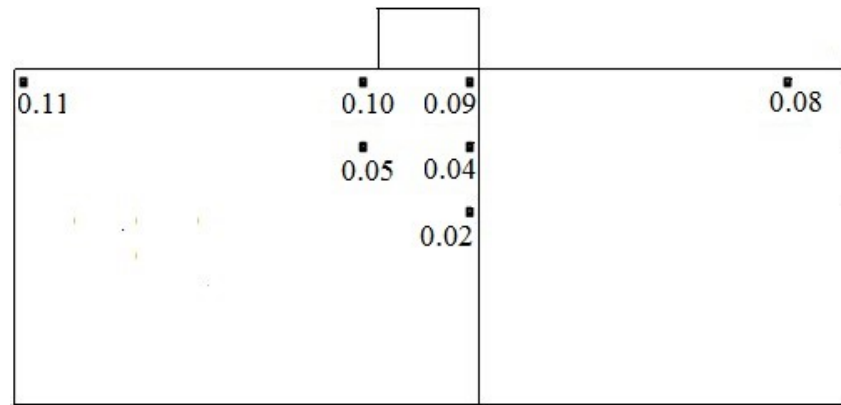


Figure 4.37: Catch ratio variation with incidence angle at locations 0.61 m below the roofline of the south-west façade of: (a) McLeod House; (b) HB Building; (c) FB Building

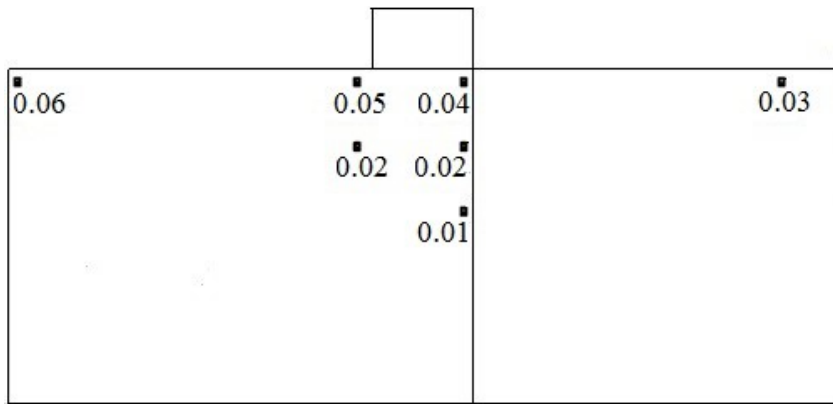
Average catch ratio values over the entire monitoring period for different ranges of incidence angles have also been calculated. Results for various locations on the south-west façade of three test buildings are shown in Figure 4.38 to Figure 4.40. Average catch ratio values are found to be the highest when incidence angle ranging from 0 to 15° (approaching wind is normal to the façade); values decrease with the increase of incidence angles; and become the lowest when incidence angle ranging from 75 to 90° (approaching wind is parallel to the façade) at all the monitored locations on the south-west façade of McLeod House. Similar result is found for most of the locations of HB and FB Building except for the top locations of HB Building and left locations of FB Building, where catch ratio values are higher for incidence angle range of 15 to 45° than those for incidence angle range of 0 to 15°.



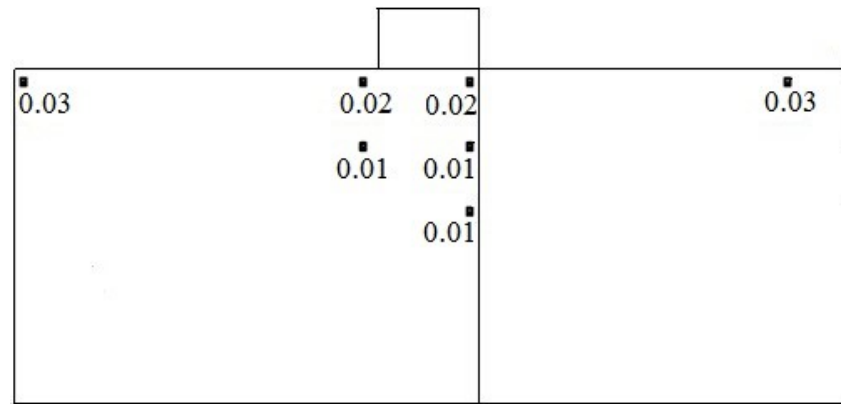
(a) 0°~15°



(b) 15°~45°

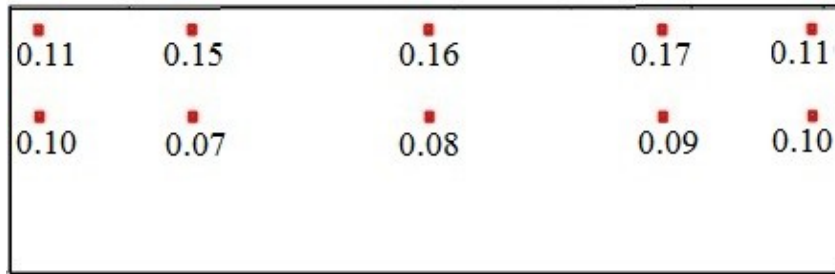


(c) 45°~75°

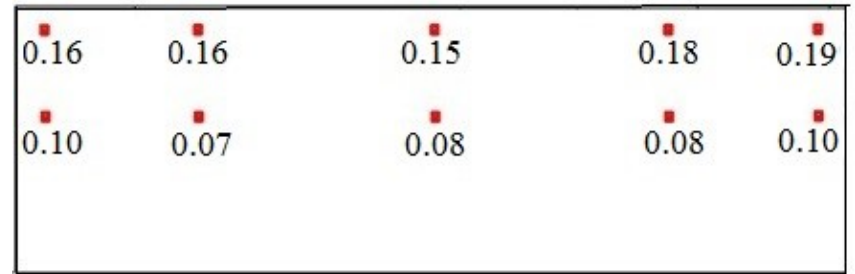


(d) 75°~95°

Figure 4.38: Average catch ratio values over the entire monitoring period at different locations on the south-west façade of McLeod House for different ranges of incidence angles



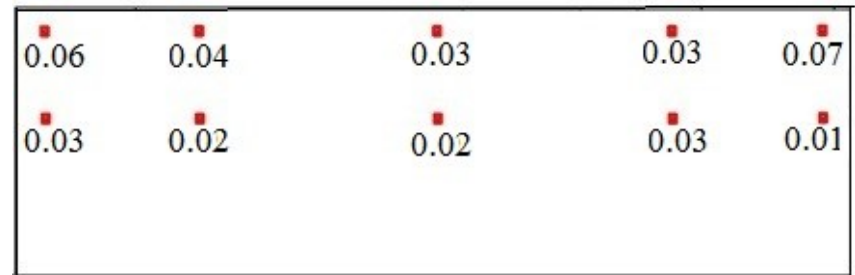
(a) 0°~15°



(b) 15°~45°

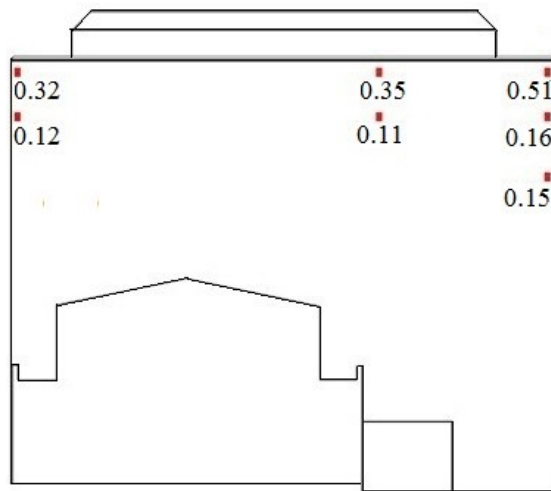


(c) 45°~75°

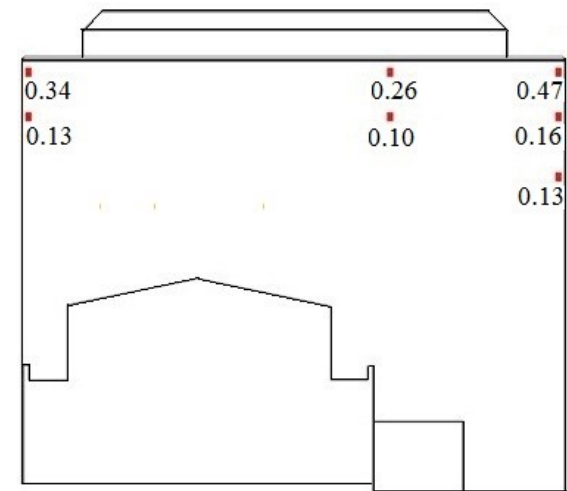


(d) 75°~95°

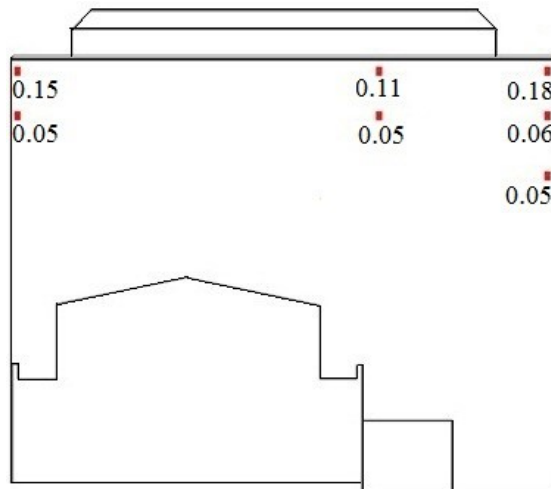
Figure 4.39: Average catch ratio values over the entire monitoring period at different locations on the south-west façade of HB Building for different ranges of incidence angles



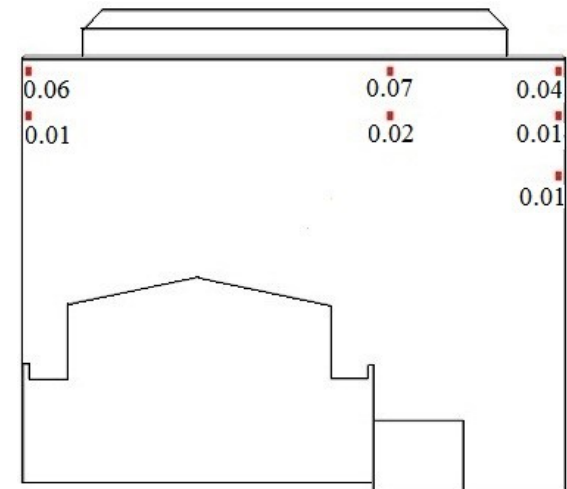
(a) $0^{\circ}\sim 15^{\circ}$



(b) $15^{\circ}\sim 45^{\circ}$



(c) $45^{\circ}\sim 75^{\circ}$



(d) $75^{\circ}\sim 95^{\circ}$

Figure 4.40: Average catch ratio values over the entire monitoring period at different locations on the south-west façade of FB Building for different ranges of incidence angles

4.5.2.4 Catch ratio as a function of wind speed

Wind speed has been found to have an important effect on catch ratio values. Analysis has been done for all incidence angles with hourly data for the entire monitoring periods. Correlations are found better (higher R^2 values) at the top locations on the façade (0.61 m below the roof line) compared to the bottom locations. Variation of catch ratios with increasing wind speed for one top location on the south-west façade of each building is shown in Figure 4.41 as an example. As shown in the figure, lower wind speed results in lower catch ratio and values increases with the increase of wind speed.

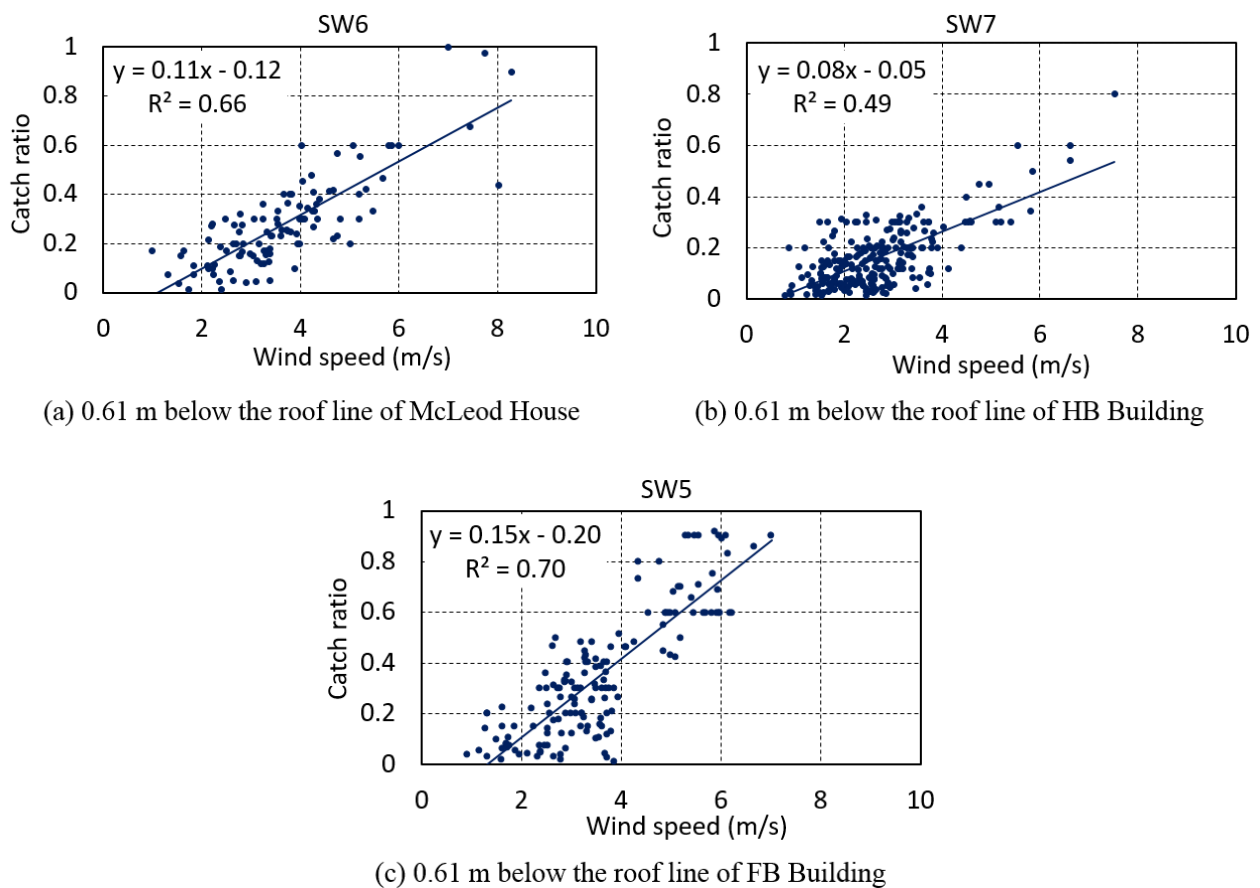


Figure 4.41 : Catch ratio variation with wind speed at different locations on the south-west façade of: (a) McLeod House; (b) HB Building; (c) FB Building

4.5.2.5 Catch ratio as a function of horizontal rainfall intensity

Attempt has been made to see how catch ratios vary with horizontal rainfall intensities. Analysis has been conducted with hourly data for the entire monitoring period which includes all incidence angles and all wind speeds. Figure 4.42 presents the variation of catch ratio with rainfall intensity at top locations (0.61 m below the roofline) on the south-west façade of three test buildings as an example. Similar results are found for all other locations on the façades. Power correlation have been tried but low correlation coefficient less than 0.4 was found. Even though, figure shows that catch ratio is influenced by rainfall intensity up to a limit of 4 mm/hr, within which catch ratio decreases with increasing rainfall intensity.

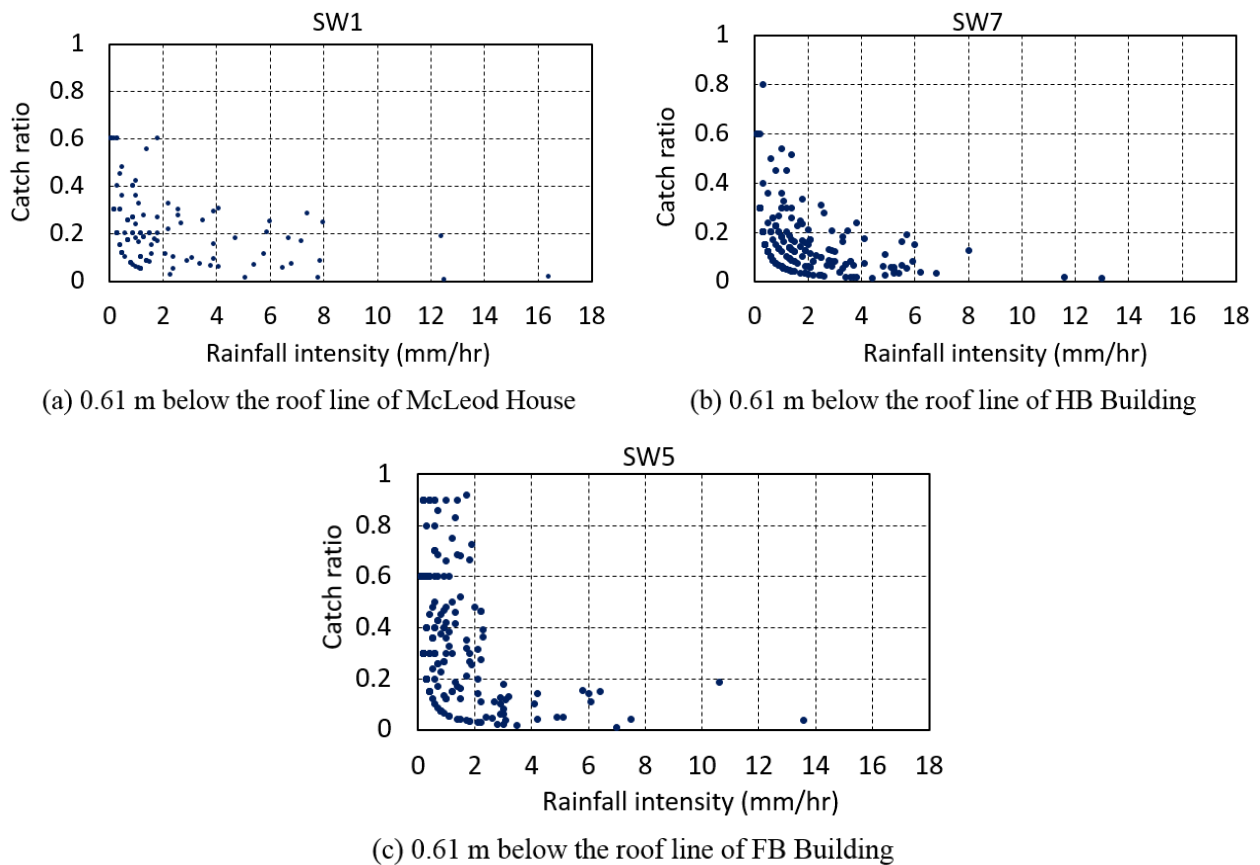


Figure 4.42: Catch ratio variation with rainfall intensity at locations 0.61 m below the roofline on the south-west façade of: (a) McLeod House; (b) HB Building; and (c) FB Building

Frequency analyses of rainfall intensity (section 4.4.3) show that more than 90% of the time the rain fall intensity is less than 4 mm/hr at these test building sites, which means that variations of

wind speed and wind direction occurs within this rainfall intensity range. Therefore large variation of catch ratio with rainfall is found within 0 to 4 mm/hr intensity range. Theoretically with the increase of rainfall intensity, terminal drop velocity increases, and driving rain factor (DRF) and hence amount of wind-driven rain decreases, which justifies the decreasing trend of catch ratio with increasing rainfall intensity. Driving rain factor (DRF) is the ratio of rain on a vertical plane (wind-driven rain) to rain on a horizontal plane and equal to the inverse of the terminal drop velocity (V_t) (Straube, J., & Burnett, E., 2000). Using the relationships mentioned in section 2.3.2 (equation 2.16 to 2.18) and the hourly data for the entire monitoring period, hourly DRF has been calculated. The distribution of raindrop sizes as a function of rainfall intensity (ϕ) is calculated by equation 2.16 and then the terminal velocity (V_t) is determined in m/s by equation 2.17. Using this terminal velocity the DRF has been calculated by equation 2.18. Figure 4.43 shows the plots of calculated DRF versus rainfall intensity for all three test sites. As shown in figure, DRF decreases with the increase of rainfall intensity.

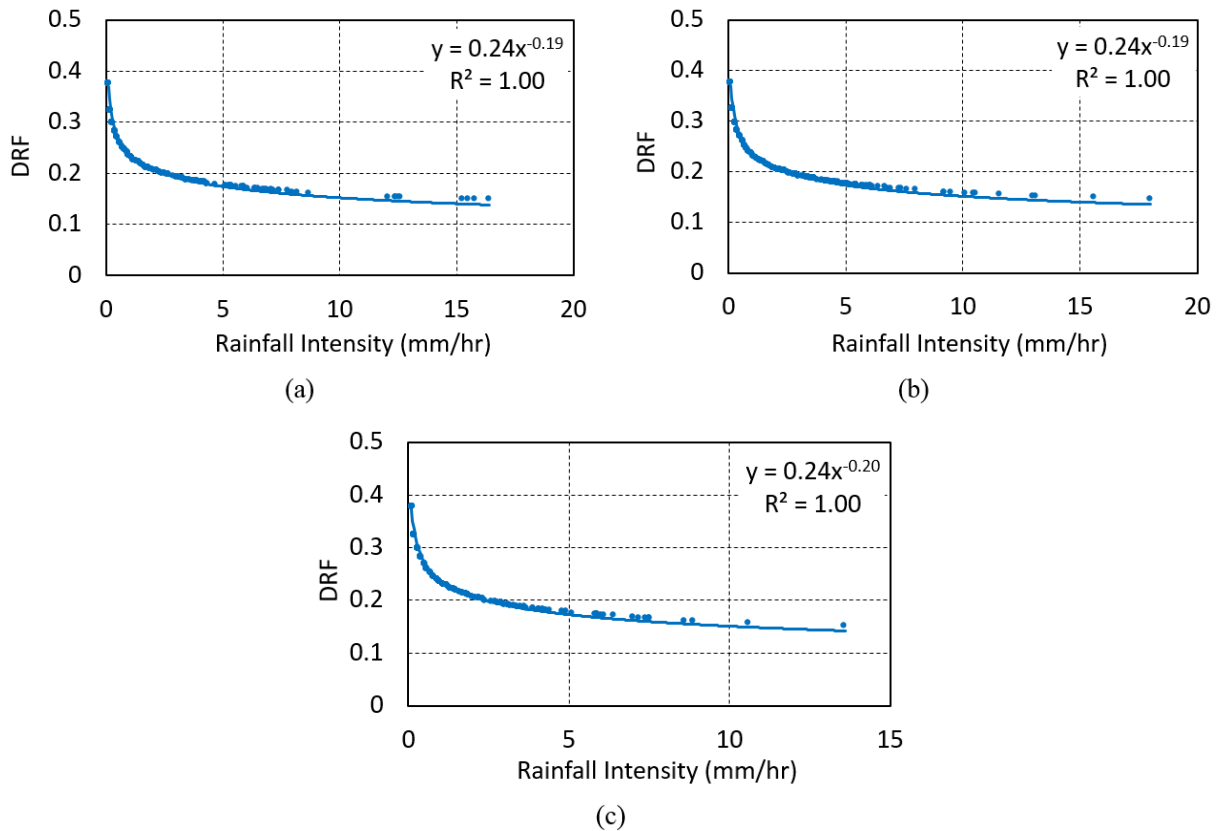


Figure 4.43: Calculated DRF versus rainfall intensity for: (a) McLeod House; (b) HB Building; (c) FB Building

4.5.2.7 Summary of weather data and catch ratios for different rain events

Table 4.4 to Table 4.6 present the average wind speed, wind direction, total horizontal rainfall, total rain hours, rainfall intensity and catch ratio values at different locations on the south-west façade of three test buildings during different rain events. Total number of rain events observed during the monitoring periods at McLeod House site, HB Building site and FB Building site is 13, 25 and 21 with intensity ranging from 0.38 to 2.46 mm/hr, 0.38 to 5.5 mm/hr and 0.37 to 5.2 mm/hr, respectively. Note that as the rain gauge at location SW9 was defective for first few months of the monitoring period, catch ratio values are not available for the first 14 rain events at location SW9 of HB Building. From these tables it is found that catch ratio varies with rain events and in general catch ratio values are maximum for the rain events which satisfy the condition of maximum wind speed and minimum incidence angle simultaneously. For example, at McLeod House site, during the rain event occurring from 10/07/2013 to 10/08/2013, the average wind speed is as high as 4.47 m/s and average wind direction is 202.41° , which creates an incidence angle of 10.59° (as the line normal to the south-west façade of McLeod House makes an angle of 213° with the north, so incidence angle for a wind direction of 202.41° is $213^\circ - 202.41^\circ = 10.59^\circ$). As a result the catch ratio values are relatively higher for this rain event. Note that the line normal to the south-west façade of HB Building and FB Building make 210° and 222° angles with the north.

Table 4.4: Summary of weather data and catch ratios at different locations on the south-west façade of McLeod House for different rain events

| Rain event | Horizontal rainfall (mm) | No. of rainhours (hr) | Rainfall intensity (mm/hr) | Avg wind speed (m/s) | Avg wind direction (deg) | Catch ratio | | | | | | |
|-------------------------|--------------------------|-----------------------|----------------------------|----------------------|--------------------------|-------------|-------|-------|------|------|------|-------|
| | | | | | | SW1 | SW2 | SW3 | SW4 | SW5 | SW6 | SE1 |
| 8/14/2013 - 9/16/2013 | 205.2 | 104 | 1.97 | 2.46 | 216.3 | 0.12 | 0.07 | 0.05 | 0.13 | 0.07 | 0.15 | 0.15 |
| 9/22/2013 - 9/25/2013 | 20.1 | 23 | 0.87 | 2.08 | 219.5 | 0.23 | 0.09 | 0.05 | 0.18 | 0.08 | 0.24 | 0.07 |
| 10/7/2013 - 10/8/2013 | 24.1 | 13 | 1.85 | 4.47 | 202.41 | 0.39 | 0.25 | 0.16 | 0.40 | 0.22 | 0.43 | 0.40 |
| 10/16/2013 - 10/22/2013 | 17.1 | 34 | 0.5 | 2.02 | 159.4 | 0.05 | 0.02 | 0.01 | 0.07 | 0.03 | 0.06 | 0.02 |
| 10/26/2013 - 11/28/2013 | 218.7 | 158 | 1.38 | 4.77 | 251.6 | 0.10 | 0.05 | 0.02 | 0.10 | 0.05 | 0.11 | 0.03 |
| 12/5/2013 - 12/8/2013 | 4.6 | 12 | 0.38 | 3.67 | 239.8 | 0.15 | 0.08 | 0.03 | 0.20 | 0.08 | 0.20 | 0.08 |
| 1/25/2014 - 1/27/2014 | 17.2 | 7 | 2.46 | 5.7 | 208.1 | 0.16 | 0.10 | 0.03 | 0.14 | 0.08 | 0.15 | 0.05 |
| 4/6/2014 - 4/28/2014 | 85.1 | 69 | 1.23 | 4.94 | 155.3 | 0.05 | 0.03 | 0.02 | 0.06 | 0.03 | 0.05 | 0.02 |
| 5/10/2014 - 5/10/2014 | 8.8 | 4 | 2.2 | 6.82 | 218.3 | 0.14 | 0.25 | 0.14 | 0.39 | 0.20 | 0.41 | 0.10 |
| 6/13/2014 - 6/17/2014 | 18 | 14 | 1.29 | 4.52 | 98.06 | 0.01 | 0.003 | 0.003 | 0.01 | 0.01 | 0.01 | 0.003 |
| 5/10/2015 - 5/13/2015 | 12.3 | 24 | 0.51 | 2 | 222.2 | 0.14 | 0.06 | 0.03 | 0.14 | 0.05 | 0.16 | 0.05 |
| 5/17/2015 - 6/3/2015 | 62 | 69 | 0.9 | 2.67 | 201.4 | 0.13 | 0.06 | 0.04 | 0.16 | 0.07 | 0.15 | 0.07 |
| 6/8/2015 - 6/17/2015 | 20.4 | 26 | 0.78 | 2.77 | 221.7 | 0.20 | 0.11 | 0.07 | 0.21 | 0.09 | 0.20 | 0.27 |

Table 4.5: Summary of weather data and catch ratios at different locations on the south-west façade of HB Building for different rain events

| Rain event | Horizontal rainfall (mm) | No. of rainhours (hr) | Rainfall intensity (mm/hr) | Avg wind speed (m/s) | Avg wind direction (deg) | Catch ratio | | | | | | | | | |
|-------------------------|--------------------------|-----------------------|----------------------------|----------------------|--------------------------|-------------|------|------|------|-------|-------|------|------|-------|------|
| | | | | | | SW1 | SW2 | SW3 | SW4 | SW5 | SW6 | SW7 | SW8 | SW9 | SW10 |
| 4/26/2014 - 5/4/2014 | 79.4 | 71 | 1.12 | 2.60 | 150.8 | 0.09 | 0.03 | 0.04 | 0.02 | 0.04 | 0.02 | 0.05 | 0.03 | | 0.03 |
| 5/9/2014 - 5/17/2014 | 59.2 | 29 | 2.04 | 2.46 | 223.5 | 0.25 | 0.09 | 0.16 | 0.07 | 0.15 | 0.07 | 0.17 | 0.07 | | 0.11 |
| 5/22/2014 - 6/6/2014 | 37.7 | 30 | 1.26 | 2.15 | 199 | 0.18 | 0.07 | 0.12 | 0.06 | 0.11 | 0.07 | 0.15 | 0.08 | | 0.09 |
| 6/11/2014 - 6/18/2014 | 97.8 | 49 | 2 | 2.47 | 107.1 | 0.11 | 0.03 | 0.03 | 0.01 | 0.03 | 0.02 | 0.03 | 0.02 | | 0.01 |
| 6/24/2014 - 6/25/2014 | 51.1 | 14 | 3.65 | 1.32 | 100.8 | 0.12 | 0.02 | 0.02 | 0.01 | 0.01 | 0.02 | 0.02 | 0.02 | | 0.01 |
| 7/3/2014 - 7/9/2014 | 17.3 | 15 | 1.15 | 1.77 | 190.4 | 0.003 | 0.10 | 0.15 | 0.06 | 0.11 | 0.07 | 0.16 | 0.08 | | 0.07 |
| 7/13/2014 - 7/17/2014 | 15.3 | 12 | 1.28 | 2.11 | 201.9 | 0.004 | 0.14 | 0.19 | 0.09 | 0.17 | 0.09 | 0.20 | 0.11 | | 0.11 |
| 7/23/2014 - 8/4/2014 | 61 | 38 | 1.61 | 2.15 | 214.3 | 0.002 | 0.10 | 0.15 | 0.08 | 0.15 | 0.14 | 0.18 | 0.09 | | 0.11 |
| 8/12/2014 - 8/17/2014 | 68.7 | 45 | 1.53 | 1.72 | 143.2 | 0.01 | 0.06 | 0.08 | 0.04 | 0.07 | 0.06 | 0.08 | 0.05 | | 0.04 |
| 8/31/2014 - 9/6/2014 | 24.4 | 21 | 1.16 | 1.99 | 224.9 | 0.03 | 0.10 | 0.17 | 0.08 | 0.18 | 0.02 | 0.21 | 0.11 | | 0.13 |
| 9/11/2014 - 9/23/2014 | 26.8 | 30 | 0.89 | 2.44 | 205.8 | 0.02 | 0.09 | 0.13 | 0.05 | 0.23 | 0.08 | 0.12 | 0.07 | | 0.07 |
| 10/4/2014 - 10/9/2014 | 52.8 | 40 | 1.32 | 2.17 | 155.6 | 0.02 | 0.06 | 0.10 | 0.04 | 0.001 | 0.08 | 0.09 | 0.05 | | 0.05 |
| 10/15/2014 - 10/29/2014 | 39 | 65 | 0.6 | 2.13 | 115.1 | 0.01 | 0.02 | 0.04 | 0.01 | 0.002 | 0.01 | 0.04 | 0.02 | | 0.02 |
| 11/4/2014 - 11/12/2014 | 14 | 28 | 0.5 | 2.2 | 172.5 | 0.01 | 0.07 | 0.11 | 0.05 | 0.004 | 0.08 | 0.13 | 0.06 | | 0.07 |
| 11/16/2014 - 11/17/2014 | 6.7 | 7 | 0.96 | 1.87 | 106.6 | 0.01 | 0.08 | 0.02 | 0.07 | 0.01 | 0.08 | 0.02 | 0.07 | 0.01 | 0.06 |
| 11/22/2014 - 11/24/2014 | 22 | 13 | 1.69 | 2.88 | 145.6 | 0.003 | 0.06 | 0.07 | 0.05 | 0.06 | 0.06 | 0.07 | 0.06 | 0.003 | 0.05 |
| 11/30/2014 - 12/3/2014 | 11.8 | 17 | 0.69 | 2.21 | 212.6 | 0.01 | 0.03 | 0.08 | 0.03 | 0.11 | 0.04 | 0.07 | 0.04 | 0.09 | 0.04 |
| 12/17/2014 - 12/17/2014 | 2.3 | 3 | 0.77 | 0.88 | 69.43 | 0.03 | 0.03 | 0.03 | 0.03 | 0.03 | 0.03 | 0.03 | 0.03 | 0.03 | 0.03 |
| 12/23/2014 - 12/28/2014 | 41.3 | 36 | 1.15 | 2.45 | 110.2 | 0.001 | 0.03 | 0.04 | 0.02 | 0.05 | 0.001 | 0.03 | 0.03 | 0.07 | 0.02 |
| 1/18/2015 - 1/18/2015 | 1.9 | 5 | 0.38 | 1.35 | 139 | 0.03 | 0.06 | 0.03 | 0.03 | 0.06 | 0.03 | 0.03 | 0.03 | 0.03 | 0.06 |
| 3/25/2015 - 4/4/2015 | 23.8 | 36 | 0.66 | 2.14 | 181.8 | 0.003 | 0.04 | 0.06 | 0.03 | 0.06 | 0.003 | 0.06 | 0.05 | 0.10 | 0.05 |
| 4/9/2015 - 4/14/2015 | 26.7 | 29 | 0.92 | 3.08 | 152.9 | 0.002 | 0.09 | 0.13 | 0.06 | 0.14 | 0.002 | 0.13 | 0.07 | 0.17 | 0.07 |
| 4/20/2015 - 4/21/2015 | 30.1 | 19 | 1.58 | 2.61 | 110.9 | 0.002 | 0.02 | 0.03 | 0.02 | 0.03 | 0.002 | 0.03 | 0.02 | 0.06 | 0.02 |
| 5/18/2015 - 5/18/2015 | 22 | 4 | 5.5 | 1.62 | 145.2 | 0.003 | 0.08 | 0.11 | 0.07 | 0.10 | 0.003 | 0.11 | 0.06 | 0.13 | 0.07 |
| 5/25/2015 - 6/16/2015 | 140.8 | 84 | 1.68 | 1.53 | 173.8 | 0.0004 | 0.03 | 0.04 | 0.02 | 0.03 | 0.000 | 0.04 | 0.03 | 0.06 | 0.02 |

Table 4.6 : Summary of weather data and catch ratios at different locations on the south-west façade of FB Building for different rain events

| Rain event | Horizontal rainfall (mm) | No. of rainhours (hr) | Rainfall intensity (mm/hr) | Avg wind speed (m/s) | Avg wind direction (deg) | Catch ratio | | | | | | |
|-------------------------|--------------------------|-----------------------|----------------------------|----------------------|--------------------------|-------------|------|-------|------|------|------|-------|
| | | | | | | SW1 | SW2 | SW3 | SW4 | SW5 | SW6 | SW7 |
| 7/26/2014 - 8/7/2014 | 53.4 | 35 | 1.53 | 1.80 | 216 | 0.19 | 0.09 | 0.16 | 0.07 | 0.19 | 0.08 | 0.05 |
| 8/12/2014 - 8/17/2014 | 76.8 | 44 | 1.75 | 1.97 | 211.1 | 0.14 | 0.05 | 0.13 | 0.05 | 0.17 | 0.08 | 0.09 |
| 8/31/2014 - 9/6/2014 | 27.9 | 22 | 1.27 | 1.64 | 242.9 | 0.24 | 0.09 | 0.29 | 0.08 | 0.26 | 0.12 | 0.08 |
| 9/11/2014 - 9/23/2014 | 26.4 | 28 | 0.94 | 2.62 | 216.8 | 0.32 | 0.02 | 0.00 | 0.07 | 0.33 | 0.14 | 0.15 |
| 10/4/2014 - 10/9/2014 | 65.1 | 41 | 1.59 | 2.19 | 214.6 | 0.22 | 0.08 | 0.01 | 0.06 | 0.24 | 0.11 | 0.07 |
| 10/15/2014 - 10/29/2014 | 35 | 64 | 0.55 | 1.97 | 125 | 0.12 | 0.02 | 0.17 | 0.03 | 0.14 | 0.03 | 0.02 |
| 11/4/2014 - 11/12/2014 | 16 | 27 | 0.59 | 2.06 | 175.6 | 0.21 | 0.07 | 0.45 | 0.06 | 0.49 | 0.09 | 0.05 |
| 11/16/2014 - 11/16/2014 | 1.2 | 3 | 0.4 | 1.83 | 228.35 | 0.1 | 0.05 | 0.05 | 0.05 | 0.35 | 0.1 | 0.1 |
| 11/22/2014 - 11/24/2014 | 20.8 | 10 | 2.08 | 2.34 | 211.3 | 0.14 | 0.07 | 0.17 | 0.08 | 0.24 | 0.07 | 0.06 |
| 11/30/2014 - 12/6/2014 | 10.8 | 16 | 0.68 | 1.81 | 238.4 | 0.24 | 0.08 | 0.01 | 0.10 | 0.47 | 0.08 | 0.05 |
| 12/11/2014 - 12/17/2014 | 17.1 | 35 | 0.49 | 1.5 | 129.5 | 0.03 | 0.01 | 0.004 | 0.01 | 0.03 | 0.01 | 0.004 |
| 12/23/2014 - 12/28/2014 | 35.3 | 31 | 1.14 | 2.12 | 201.4 | 0.15 | 0.04 | 0.002 | 0.04 | 0.28 | 0.05 | 0.03 |
| 1/4/2015 - 1/4/2015 | 13.2 | 4 | 3.3 | 1.56 | 135.7 | 0.09 | 0.01 | 0.005 | 0.01 | 0.04 | 0.01 | 0.01 |
| 1/18/2015 - 1/18/2015 | 4.4 | 12 | 0.37 | 1.23 | 154.2 | 0.01 | 0.03 | 0.01 | 0.03 | 0.01 | 0.01 | 0.01 |
| 3/25/2015 - 4/4/2015 | 16 | 28 | 0.57 | 1.81 | 211.4 | 0.14 | 0.05 | 0.004 | 0.05 | 0.23 | 0.06 | 0.04 |
| 4/9/2015 - 4/14/2015 | 16 | 22 | 0.73 | 2.99 | 213.8 | 0.47 | 0.19 | 1.10 | 0.15 | 0.94 | 0.25 | 0.22 |
| 4/20/2015 - 4/27/2015 | 25.2 | 31 | 0.81 | 2 | 235.4 | 0.18 | 0.06 | 0.21 | 0.05 | 0.16 | 0.04 | 0.02 |
| 5/9/2015 - 5/13/2015 | 25.7 | 21 | 1.22 | 2.9 | 81.58 | 0.10 | 0.06 | 0.15 | 0.05 | 0.14 | 0.04 | 0.04 |
| 5/18/2015 - 5/19/2015 | 20.8 | 4 | 5.2 | 1.54 | 188.6 | 0.30 | 0.17 | 0.27 | 0.16 | 0.46 | 0.20 | 0.18 |
| 5/25/2015 - 5/26/2015 | 14.9 | 14 | 1.06 | 0.81 | 177 | 0.17 | 0.06 | 0.20 | 0.05 | 0.20 | 0.05 | 0.03 |
| 5/30/2015 - 6/10/2015 | 45.2 | 50 | 0.9 | 1.72 | 218.8 | 0.26 | 0.11 | 0.32 | 0.10 | 0.41 | 0.15 | 0.15 |

4.5.2.8 Wall factor analysis

In the ISO standard 15927 (NBN EN ISO 15927-3 (2009)) wall factor is defined as the ratio of the quantity of water hitting a wall to the quantity passing through an equivalent unobstructed space. It is one of the correction factors used in the ISO standard to calculate wall index from airfield index. Equations (2.6) and (2.7) are used for calculating the airfield indices (I_A) and wall indices (I_{WA}) according to the ISO standard. When the on-site wind and rain data are available, the factors C_R , C_T and O can be taken as 1.0. As a result, the wall factor is calculated as the ratio of measured wind-driven rain (I_{WA}) to air field index (I_A) at a specific location (equation (4.10)).

$$W = \frac{I_{WA}}{I_A} = \frac{I_{WA}}{\frac{2}{9} \sum U * R_h^{8/9} * \cos(D - \theta)} \quad (4.10)$$

As mentioned earlier the wind speed was measured at a height of 26.57 m (87'-2"), 19.63 m (64'-5") and 55.09 m (180'-9") from the ground level for McLeod House, HB Building and FB Building respectively. The wind speed obtained at these measured height has been converted to each driving rain gauge locations using the power law (equation (4.1) and Table 4.1). For meteorological station (airport station) terrain category is 2. For FB Building terrain category is 4 and for the other two buildings terrain category is 3. The wall orientation relative to north (θ) for each façade has been determined. The following table (Table 4.7) shows the value of θ for each façade of all three test buildings:

Table 4.7: Wall orientation relative to north (θ) for building façades

| Test Building | Wall orientation relative to north, θ° | | | |
|---------------|--|------------|------------|------------|
| | North-East | North-West | South-East | South-West |
| McLeod House | 33 | 303 | 123 | 213 |
| HB Building | 30 | 300 | 120 | 210 |
| FB Building | 42 | 312 | 132 | 222 |

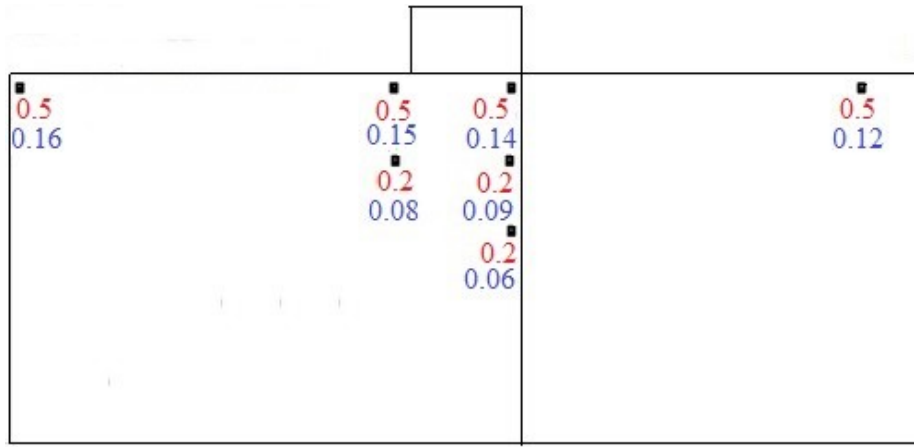
Then the hourly data of wind speed at rain gauge locations (U) in m/s, rainfall total (R_h) in mm, wind direction (D) and wall orientation relative to north (θ) has been put in Equation 2.6 to calculate airfield index (I_A). Now, the airfield index (I_A) for the hours where $\cos(D-\theta)$ is positive have been summed up to get total airfield index (ΣI_A). Then wall factor (W) is calculated using equation (4.11).

$$W = \frac{\Sigma R_{wdr}}{\Sigma I_A} \quad (4.11)$$

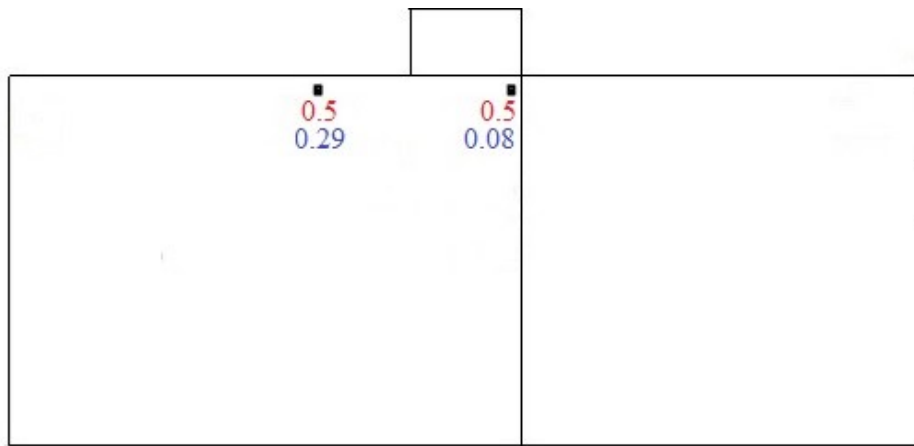
Where, ΣR_{wdr} is the total amount of wind-driven rain registered by the driving rain gauge.

Wall factors at different rain gauge locations on the building façades are calculated for the entire monitoring period with all approaching wind angles. Figure 4.44 to Figure 4.46 show the wall factors calculated based on measurements (blue colour) on different façades of McLeod House, HB Building and FB Building, respectively. For comparison, the wall factors suggested by the ISO standard 15927 are also shown (red colour) in these figures.

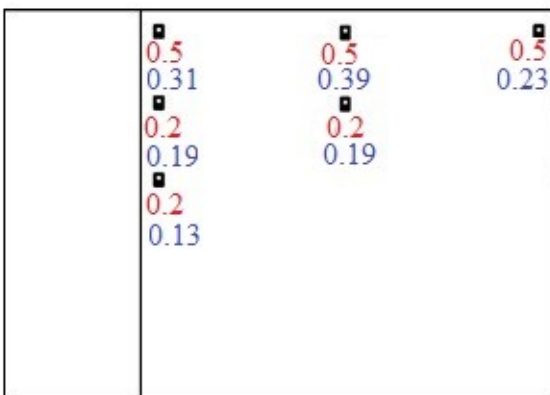
For the building in Fredericton (McLeod House), more than 25% discrepancies between the ISO standard suggested wall factors and wall factors based on measurements are observed for 82% of the monitored locations (13 out of 16). Wall factors based on measurements are significantly smaller than what the ISO standard suggests for all the locations on the façades (Figure 4.44) except for the south-east façade. Wall factors based on measurements are very close to the ISO suggested values at the second row (4.88 m below the roof line) on south-east façade. Value at the top-middle location (0.61 m below the roofline) of this facade is also closer to the ISO suggested values.



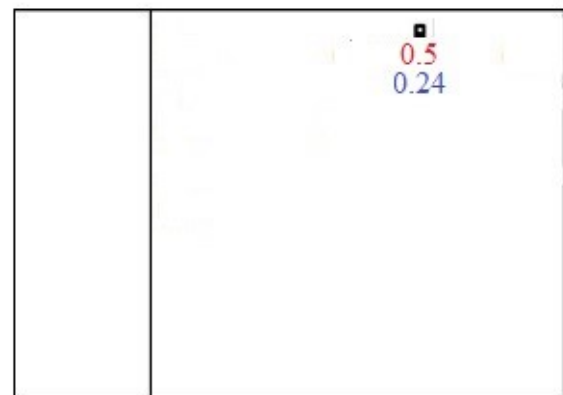
(a)



(b)



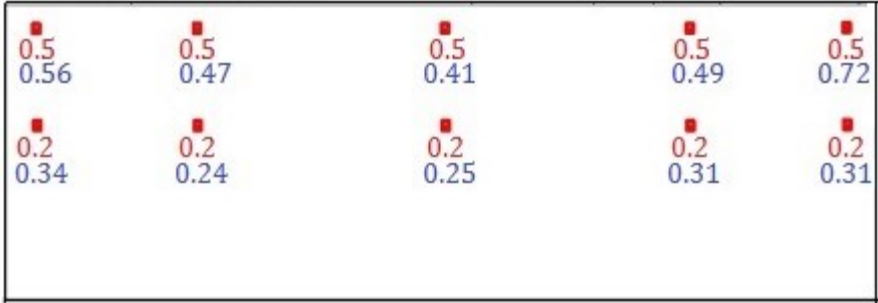
(a)



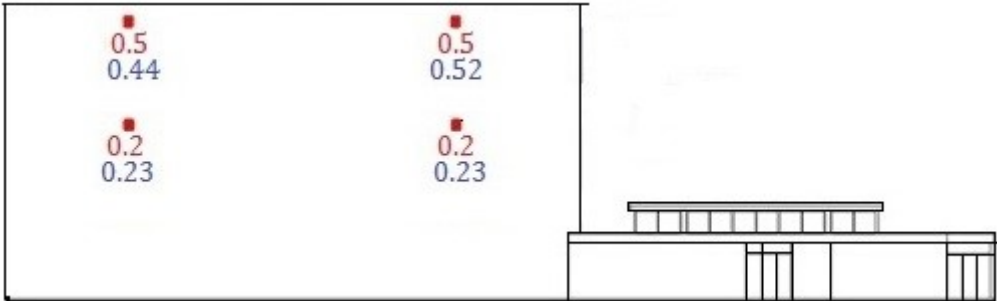
(b)

Figure 4.44 : Wall factors (red-ISO, blue-measurements) at driving rain gauge locations on the (a) south-west façade; (b) north-east façade; (c) south-east façade; (d) north-west façade of McLeod House, Fredericton

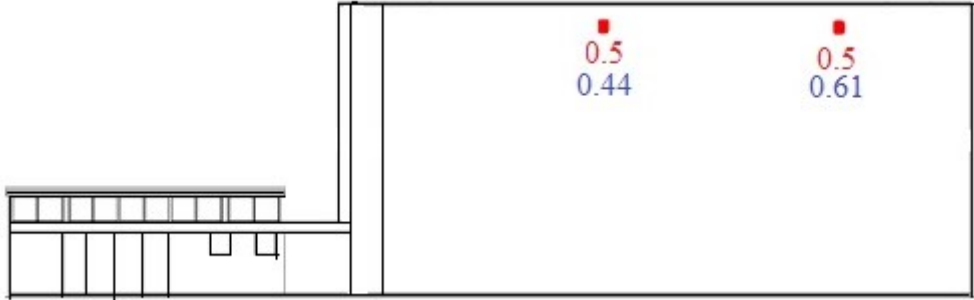
For HB Building, Montreal (Figure 4.45), the measured wall factors are close to the ISO standard suggested values for most of the monitored locations. Only 25% of the monitored locations (4 out of 16) shows discrepancies more than 25%. Wall factors based on measurements are close to the ISO suggested values for most of the top locations (0.61 m below the roofline) except for the one at right top corner of the south-west and north-west façade. At locations 4.88 m (16') below the roofline (2nd row) of the south-east façade the measured and the ISO suggested wall factor values are close, whereas for 60% locations (3 out of 5) at the same height of the south-west façade the measured values are higher than the ISO suggested values.



(a)



(b)



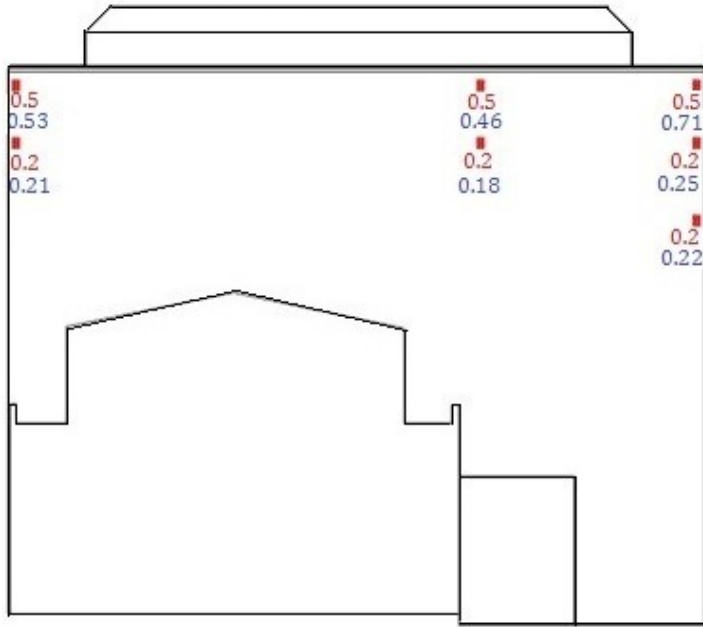
(c)

Figure 4.45 : Wall factors (red-ISO, blue-measurements) at driving rain gauge locations on the (a) south-west façade; (b) south-east façade; (c) north-west façade of HB Building, Montreal

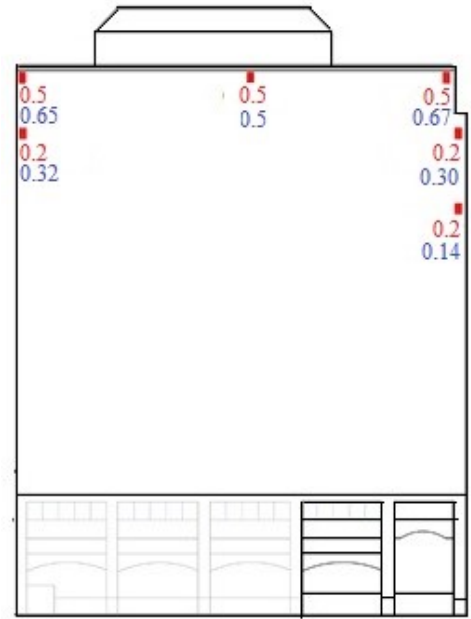
Figure 4.46 shows the results for FB Building, Montreal. More than 25% discrepancies between the ISO standard suggested wall factors and wall factors based on measurements are observed for 55% of the monitored locations (13 out of 24) of FB Building. As shown in figure, for the south-west façade, the façade facing the prevailing wind-driven rain, measured wall factor values are close to the ISO suggested values for most of the locations except for the one at right top corner. The measured values are higher than what the ISO standard suggests for the edge locations at 0.61 m and 4.88 m below the roof line (1st and 2nd row) of the south-east façade, whereas values are close for other locations on this façade. For the north-east façade the measured wall factor values are lower than the ISO suggested values at 3rd and 4th row (10.67 m and 21.34 m below the roofline), but close at the middle locations across the façade width. Measured values at 1st and 2nd row on left edge are so high compared to those at right edge of the north-east façade. The only top location on the north-west façade shows comparable wall factor value with the ISO standard.

It is found that the wall factor values are not symmetrical throughout the façades. For example the wall factor value at right top corner of south-west façade is higher than that of left top corner of the same façade. The reason behind this is the approaching wind angle. From the analysis it is found that 67% of the time during rain hours the wind is blowing towards the right corner of the south-west façade, resulting higher wind-driven rain amount as well as higher wall factor value at the right top corner compared to the left top corner. Similarly 82% of the time during rain hours the wind is blowing towards the left corner of the north-east façade, resulting higher wall factor values at left side.

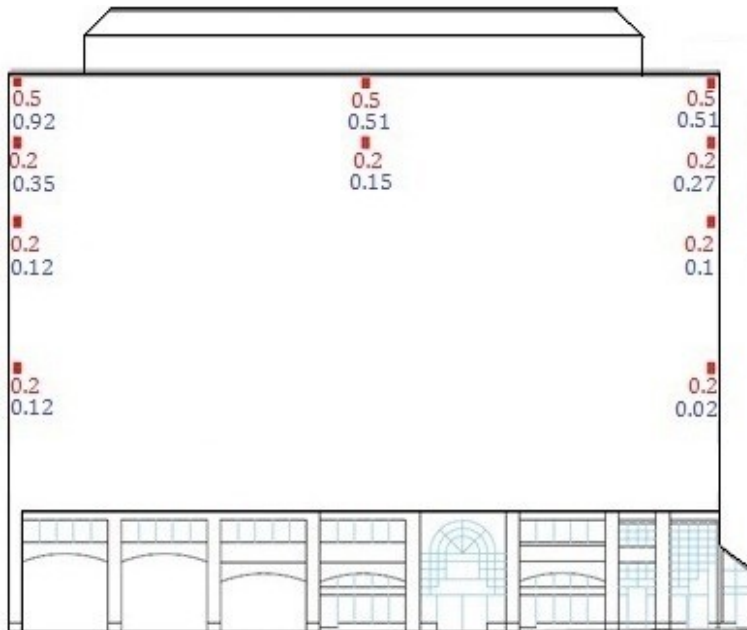
It should be noted that for all three test buildings, there is a large variation of wall factors across the width of the building façade although the ISO standard suggests constant values across the building width.



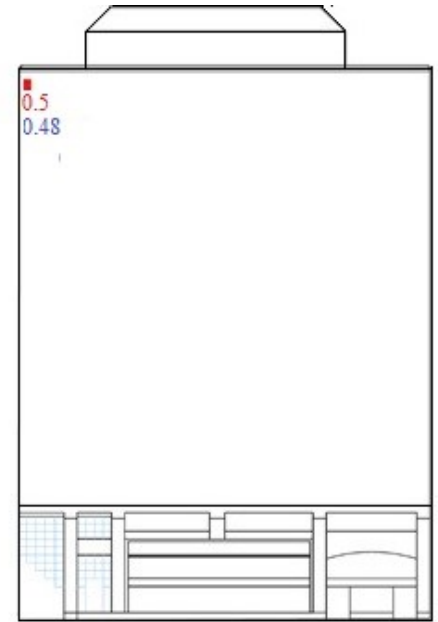
(a)



(b)



(c)



(d)

Figure 4.46 : Wall factors (red-ISO, blue-measurements) at wind-driven rain gauge locations on the (a) south-west façade; (b) south-east façade; (c) north-east façade; (d) north-west façade of FB Building, Montreal

4.5.2.9 Wall factor as a function of wind speed

Wall factor has been plotted as a function of wind speed. Analysis has been done for all incidence angles with hourly data for the entire monitoring periods. Figure 4.47 shows the results for location at 0.61 m below the roofline on the south-west façade of three test buildings. Several types of correlations (i.e., linear, exponential, power) have been tried but for all cases, the correlation coefficients (R^2 value) were very poor (less than 0.3). Note that the wind speed used for this analysis is the wind speed at wind monitor locations.

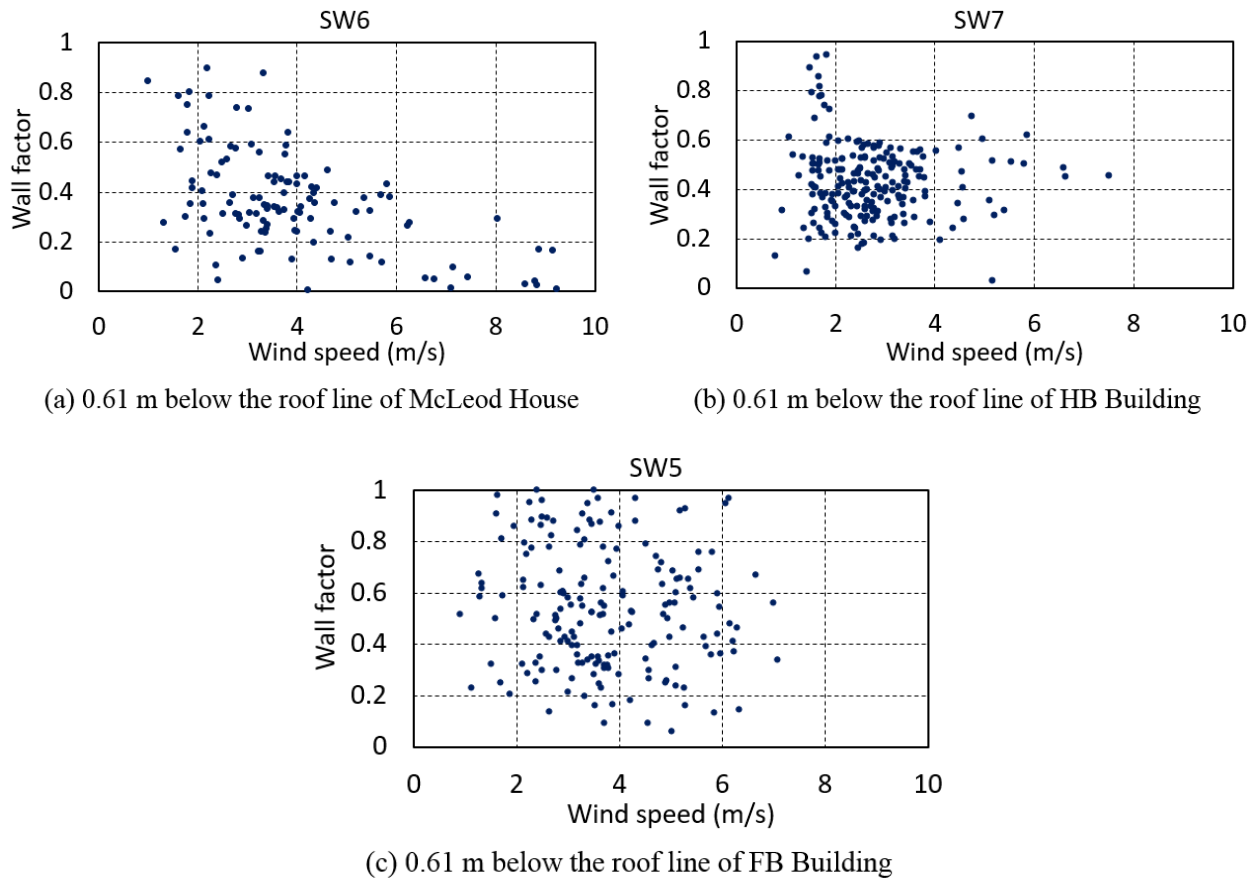


Figure 4.47 : Wall factor variation with wind speed at locations 0.61 m below the roofline on the south-west façade of: (a) McLeod House; (b) HB Building; and (c) FB Building

4.5.2.10 Wall factor as a function of rainfall intensity

Wall factor is found to vary a bit with rainfall intensity at all façade locations of all the buildings. Analysis has been done for all incidence angles with hourly data for the entire monitoring periods. Figure 4.48 shows the results for the top locations (0.61 m below the roofline) on the south-west façade of three test buildings as an example. Similar to previous analysis, poor correlation has been found with a very poor correlation factor (R^2 value less than 0.25).

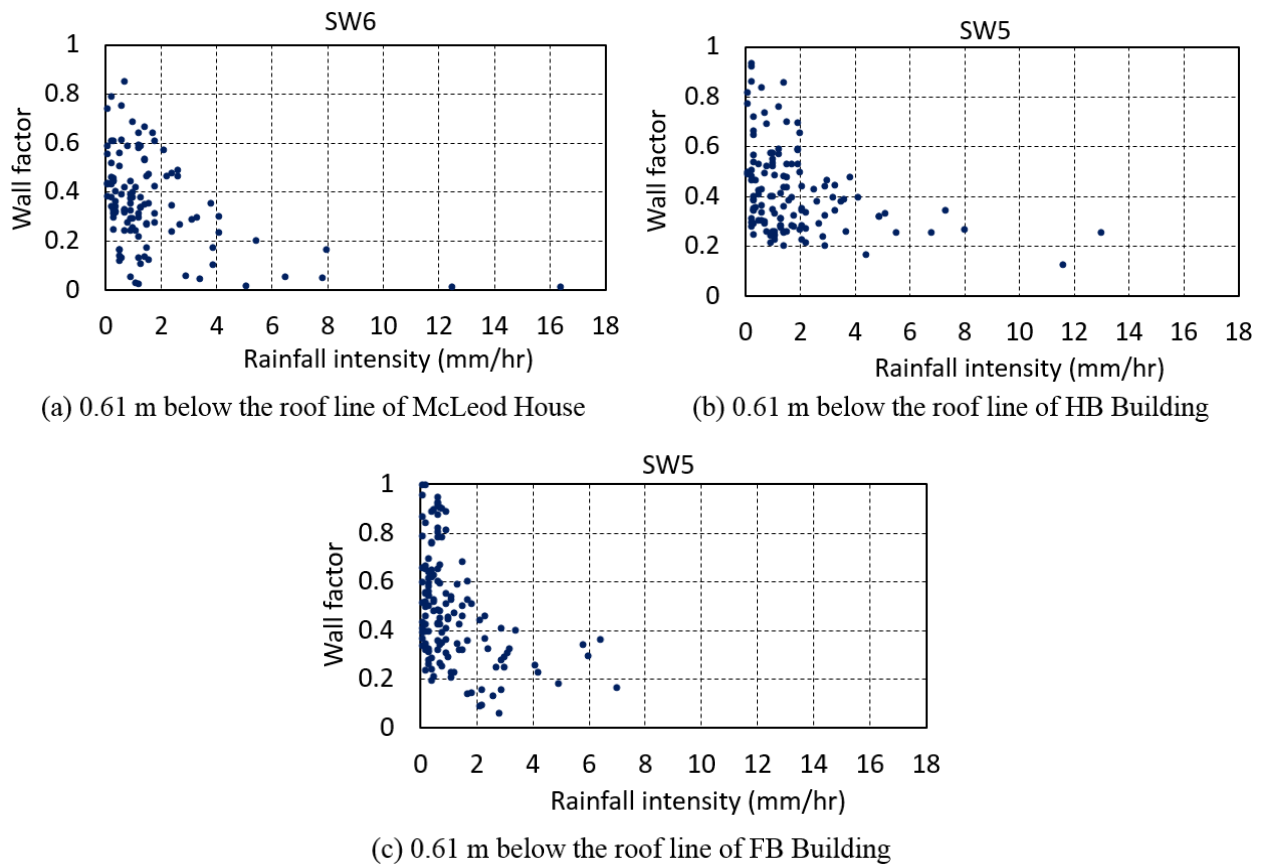
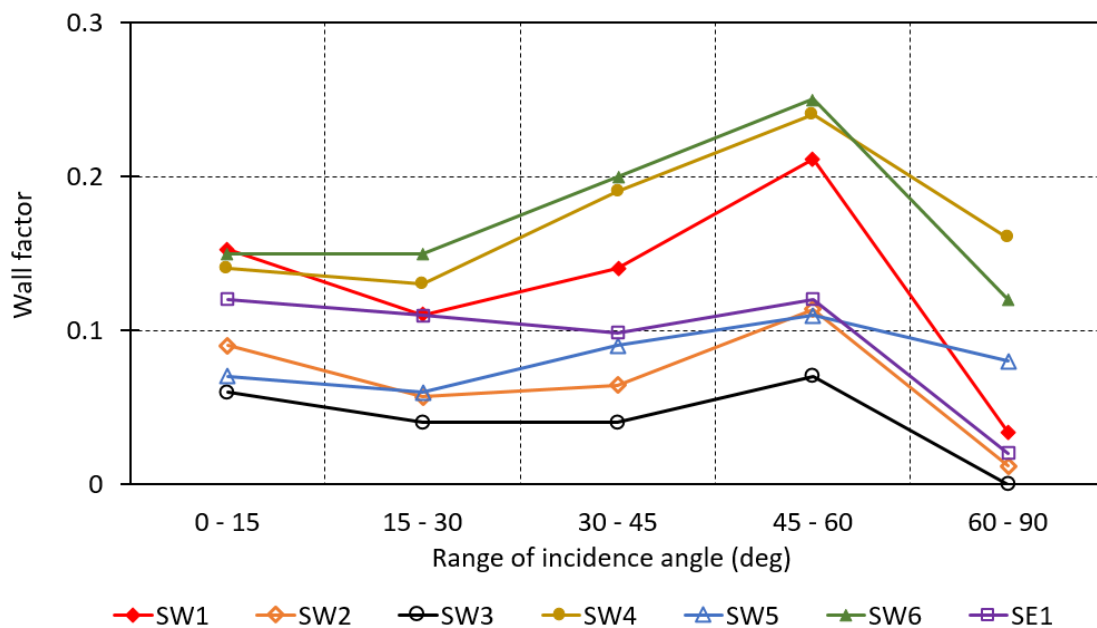


Figure 4.48 : Wall factor variation with rainfall intensity at locations 0.61 m below the roofline on the south-west façade of: (a) McLeod House; (b) HB Building; and (c) FB Building

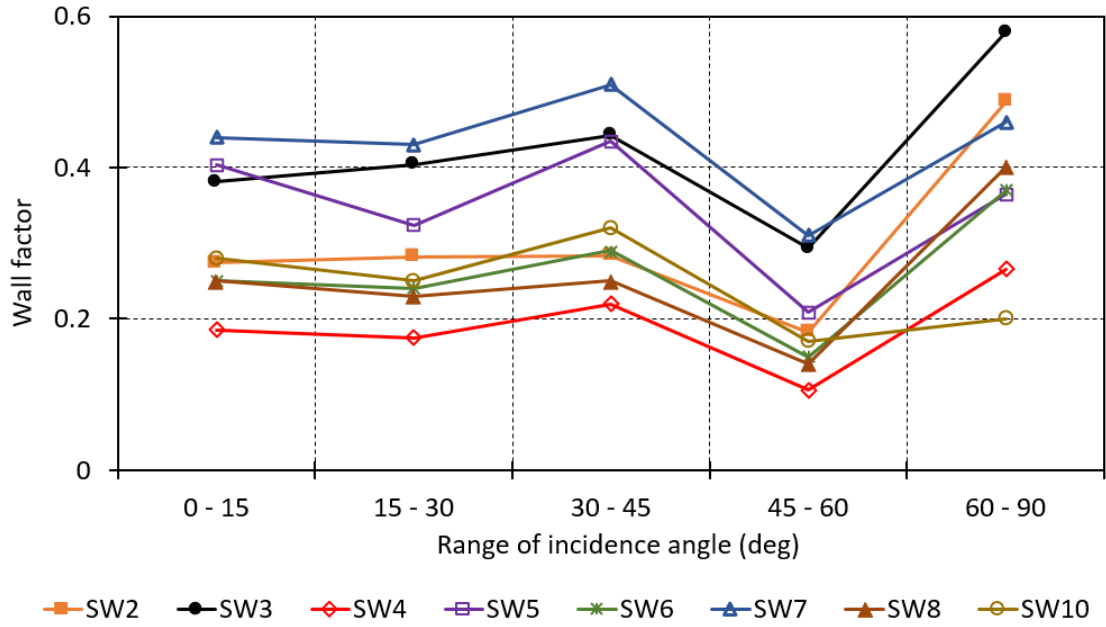
4.5.2.11 Wall factor as a function of incidence angle

An attempt has been made to see the variation of wall factor with incidence angle. Plots of wall factor as a function of incidence angle for different locations on the south-west facades of all three buildings is shown in Figure 4.49. In these analysis average wall factor has been calculated for

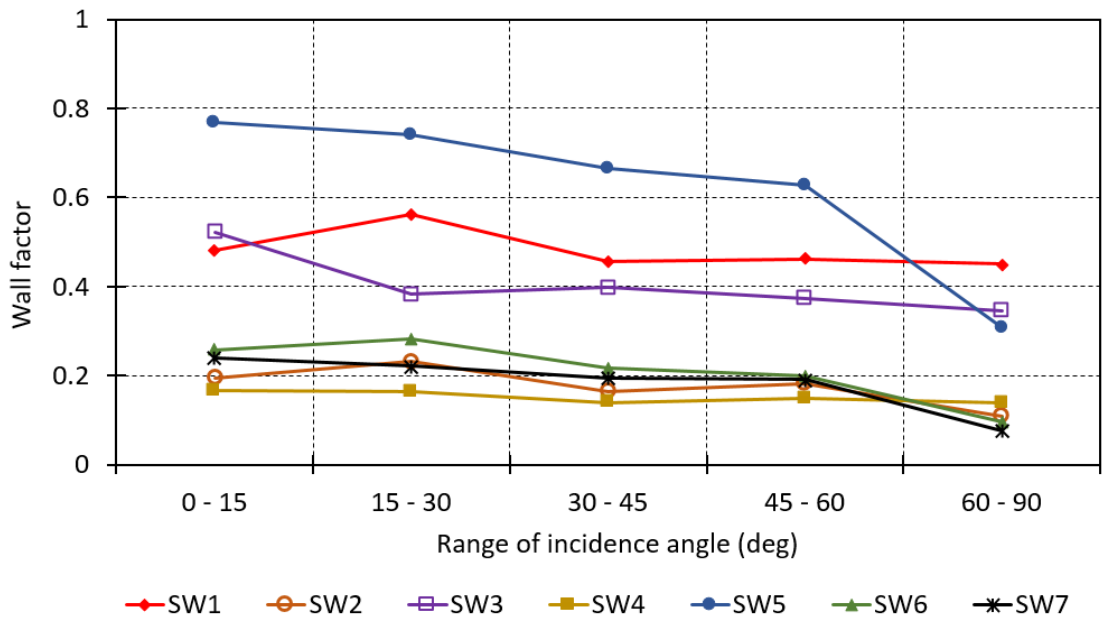
different strip of incidence angles (i.e., 0° to 15° , 15° to 30° , 30° to 45° , 45° to 60° , 60° to 90°). As shown in figure, there is no consistent trend in terms of wall factor versus incidence angle. As stated earlier, wall factors should not be influenced by wind speed, rainfall intensity and incident angles. However, the wall factor is a single value to reflect the complex interaction between wind, rain and the building. The wind flow around the building changes with the change of wind direction and wind speed, so does the trajectory of rain drops. Therefore, the spatial distribution of wind-driven rain will change with changing wind and rain conditions, so are the wall factors although we try to minimize the influence of wind speed, rainfall intensity, and incidence angle by applying a simplified linear correlation. The variation of wall factors is a proof that this linear correlation cannot fully account for the complex interaction among wind, rain and the building. A constant single value used in equation (2.7) can only be used as a simplified approach to account for the long-term effect of wind-driven rain on the moisture condition on façade. For situations such as evaluating the rain penetration risks, extreme values over short period may be used.



(a)



(b)



(c)

Figure 4.49 : Wall factor variation with incidence angle at different locations on the south-west façade of: (a) McLeod House; (b) HB Building; (c) FB Building

4.5.3 Comparison between WDR measured and WDR estimated by semi-empirical models

In this study, amount of wind-driven rain on building façades has been estimated using the ISO standard 15927 (NBN EN ISO 15927-3 (2009)) and ASHRAE 160 model (ASHRAE 2009) and compared it with the measured amount to evaluate the predictive performance of these two models. Hourly wind speed and wind direction data obtained from the nearby meteorological station for the monitoring period are used for the calculation. Data has been collected from Environment Canada website (Environment canada.2015). As hourly rainfall data for the monitoring period is not available at the meteorological station, hourly rainfall measured onsite is used for calculating the wind-driven rain.

4.5.3.1 Calculation procedure for the ISO standard

Procedure and formulas suggested by the ISO standard 15927 (NBN EN ISO 15927-3 (2009)) to estimate wind-driven rain are described in sections 2.3.1 and 4.5.2.8. Equation (2.6) to (2.13) are used to calculate the wind-driven rain amount by the ISO standard. All the correction factors (i.e., terrain roughness coefficient (C_R), topography coefficient (C_T), obstruction factor (O), and wall factor (W) are calculated according to the ISO standard. Terrain roughness coefficient (C_R) has been calculated by ISO suggested equations (2.9) and (2.10) and using Table 2.1. Terrain category and corresponding values of K_R , z_0 and z_{min} used for calculation for three test buildings are as follows:

Table 4.8: Terrain categories and values of related parameters for three test buildings

| Test Building | Terrain Category | K_R | z_0 | z_{min} |
|---------------------------|------------------|-------|-------|-----------|
| McLeod House, Fredericton | III | 0.22 | 0.3 | 8 |
| HB Building, Montreal | III | 0.22 | 0.3 | 8 |
| FB Building, Montreal | IV | 0.24 | 1 | 16 |

C_T has been taken as 1.0 because all the test buildings are located on flat area. For calculation of wind-driven rain, obstruction factor (O) has been selected from the ISO suggested table (Table 2.3) based on the distance and height of the nearest obstacle corresponding to each façade. Distance

and height of the nearest obstacle corresponding to each façade for all three test buildings has been described in Chapter 3 (section 3.2).

The ISO standard 15927 suggests wall factor (W) values for different types of buildings. All the test buildings in this thesis are multi storey with flat roof and according to the ISO standard 15927, for a multi-storey building with flat roof, wall factor (W) is 0.5 for top 2.5 m and 0.2 for the remainder.

Table 4.9 : Wall factor, W (source: (NBN EN ISO 15927-3 (2009)).

| Description of wall | Average value | Distribution |
|--|--|--|
| Multi-storey building with flat roof (pitch < 20 ⁰) | 0.2 for a ten-storey building, for example, but with a higher intensity at top | 0.5 for top 2.5 m 0.2 for remainder |

Values of all the correction factors, obtained according to the above described procedure, at each rain gauge locations of three test buildings are shown in Table 4.10 to Table 4.12. These values are used for estimating wind-driven rain amount at different rain gauge locations using the ISO standard.

Table 4.10 : Values of the correction factors used for estimating wind-driven rain amount at different rain gauge locations of McLeod House using the ISO standard

| Test Building | Facade | Rain gauge location | Correction factors | | | |
|-------------------------------|------------|---------------------|---|---------------------|----------------------------|----------------------------------|
| | | | Terrain roughness coefficient (C_R) | Wall factor (W) | Obstruction factor (O) | Topography coefficient (C_T) |
| McLeod House, Fredericton, NB | South-west | SW1, SW4, SW6, SE1 | 0.94 | 0.5 | 1 | 1 |
| | | SW2, SW5 | 0.89 | 0.2 | | |
| | | SW3 | 0.83 | 0.2 | | |
| | South-east | E1, E4, E6 | 0.94 | 0.5 | 1 | 1 |
| | | E2, E5 | 0.89 | 0.2 | | |
| | | E3 | 0.83 | 0.2 | | |
| | North-east | N1, N2 | 0.94 | 0.5 | 1 | 1 |
| North-west | W1 | 0.94 | 0.5 | 0.4 | 1 | |

Table 4.11 : Values of the correction factors used for estimating wind-driven rain amount at different rain gauge locations of HB Building using the ISO standard

| Test Building | Facade | Rain gauge location | Correction factors | | | |
|---------------------------|------------|--------------------------|---|---------------------|----------------------------|----------------------------------|
| | | | Terrain roughness coefficient (C_R) | Wall factor (W) | Obstruction factor (O) | Topography coefficient (C_T) |
| HB Building, Montreal, QC | South-west | SW1, SW3, SW5, SW7, SW9 | 0.85 | 0.5 | 1 | 1 |
| | | SW2, SW4, SW6, SW8, SW10 | 0.77 | 0.2 | | |
| | South-east | SE1, SE3 | 0.85 | 0.5 | 0.8 | 1 |
| | | SE2, SE4 | 0.77 | 0.2 | | |
| | North-west | N1, N2 | 0.85 | 0.5 | 1 | 1 |

Table 4.12 : Values of the correction factors used for estimating wind-driven rain amount at different rain gauge locations of FB Building using the ISO standard

| Test Building | Facade | Rain gauge location | Correction factors | | | |
|---------------------------|------------|---------------------|---|---------------------|----------------------------|----------------------------------|
| | | | Terrain roughness coefficient (C_R) | Wall factor (W) | Obstruction factor (O) | Topography coefficient (C_T) |
| FB Building, Montreal, QC | South-west | SW1, SW3, SW5 | 0.92 | 0.5 | 1 | 1 |
| | | SW2, SW4, SW6 | 0.89 | 0.2 | | |
| | | SW7 | 0.85 | 0.2 | | |
| | South-east | SE1, SE3, SE4 | 0.92 | 0.5 | 0.9 | 1 |
| | | SE2, SE5 | 0.89 | 0.2 | | |
| | | SE6 | 0.85 | 0.2 | | |
| | North-east | NE1, NE5, NE7 | 0.92 | 0.5 | 0.9 | 1 |
| | | NE2, NE6, NE8 | 0.89 | 0.2 | | |
| | | NE3, NE9 | 0.85 | 0.2 | | |
| | | NE4, NE10 | 0.76 | 0.2 | | |
| North-west | NW1 | 0.92 | 0.5 | 0.7 | 1 | |

4.5.3.2 Calculation procedure for the ASHRAE 160 model

A brief description of the ASHRAE 160 (ASHRAE 2009) model used for estimating wind-driven rain on building façades is provided in Chapter 2 (section 2.3.2) of this thesis. Equation (2.14) (section 2.3.2) has been used to calculate the wind-driven rain by the ASHRAE 160 model. The wind speed data obtained from meteorological station has been converted at 10 m height of the test buildings site using the power law (equation (4.1)) for estimation of wind-driven rain using the ASHRAE 160 method. The rain exposure factor (F_E) and the rain deposition factor (F_D) are selected according to the ASHRAE 160 guidelines. The rain exposure factor (F_E) is selected from the ASHRAE recommended values (Table 2.4). Different façades of the current test buildings fall in the category of medium and sheltered depending on their surroundings. The values of rain deposition factor (F_D) have been taken as recommended by the ASHRAE model (Table 2.5). In the table no value has been suggested for flat roof building. So for these flat roof test buildings F_D factor of 0.5 is chosen. Values of exposure factor (F_E) and the rain deposition factor (F_D), obtained from the procedure described above, for each façade of three test buildings are shown in Table 4.13. These values are used for estimating wind-driven rain amount at different rain gauge locations using the ASHRAE 160 model.

Table 4.13: Values of exposure factor (F_E) and the rain deposition factor (F_D) for each façade of three test buildings

| Test Building | Façade | Exposure factor (F_E) | Deposition factor (F_D) |
|--------------------------------------|---------------|---|---|
| McLeod House, Fredericton, NB | South-west | 1.3 | 0.5 |
| | South-east | 1.1 | |
| | North-east | 1.3 | |
| | North-west | 1.1 | |
| HB Building, Montreal, QC | South-west | 1.2 | 0.5 |
| | South-east | 1.2 | |
| | North-west | 1.2 | |
| FB Building, Montreal, QC | South-west | 1.5 | 0.5 |
| | South-east | 1.5 | |
| | North-east | 1.5 | |
| | North-west | 1.3 | |

4.5.3.3 Comparison between measured and predicted wind-driven rain

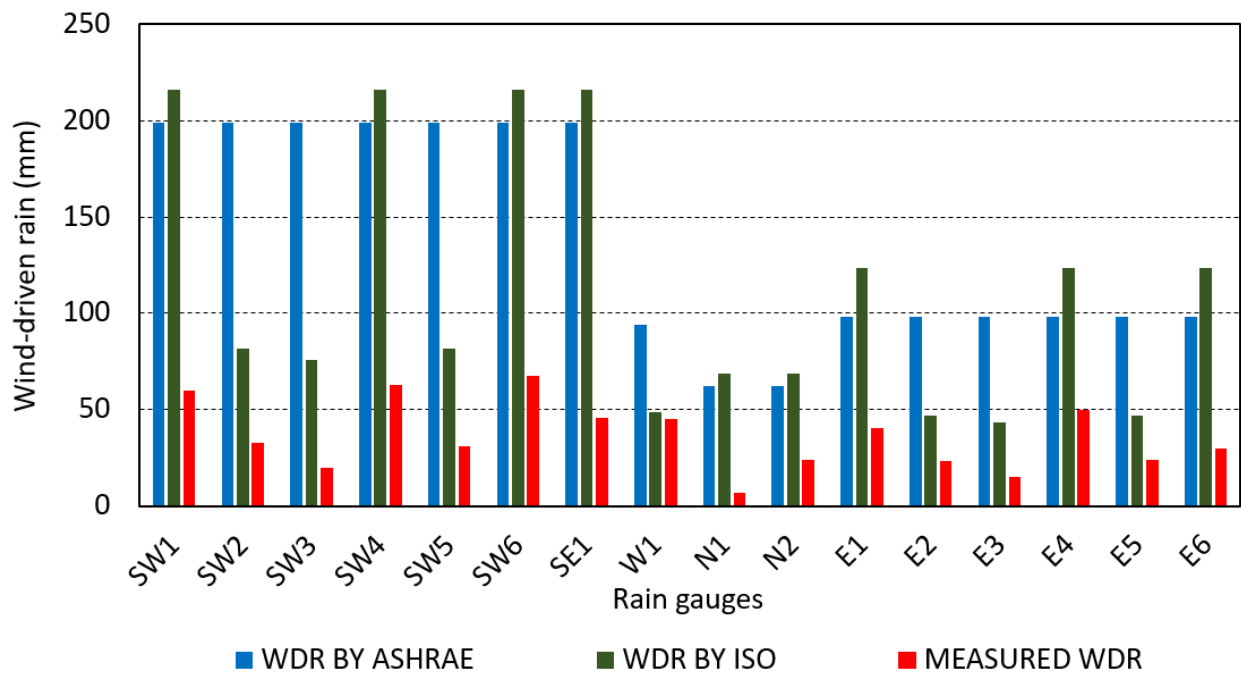
Figure 4.50 shows the comparison between the measured wind-driven rain and the wind-driven rain calculated using semi-empirical models (i.e., the ISO model and the ASHRAE model). Note that the wind-driven rain amount has been calculated for the entire monitoring period with all approaching wind angles.

Generally the ASHRAE 160 model overestimates the wind-driven rain amount for most of the monitored façade locations of the test buildings. As shown in Figure 4.50, the ASHRAE model overestimates the WDR amount largely (discrepancies are higher than 100%) for all the monitored locations of McLeod House and 81% of monitored locations of HB Building. For FB Building, even though the ASHRAE model provides better estimations (discrepancies are less than 20%) for 70% of the monitored top locations (7 out of 10), but for rest of the locations discrepancies are higher than 50%. The discrepancies between the measurements and the predictions by the ASHRAE model are very high for the bottom locations of the façades (2nd, 3rd, and 4th rows). This is happened because the ASHRAE 160 model suggests a constant value of the rain deposition factor ($F_D = 0.5$) for all façade heights, which is seemed to be higher for bottom locations.

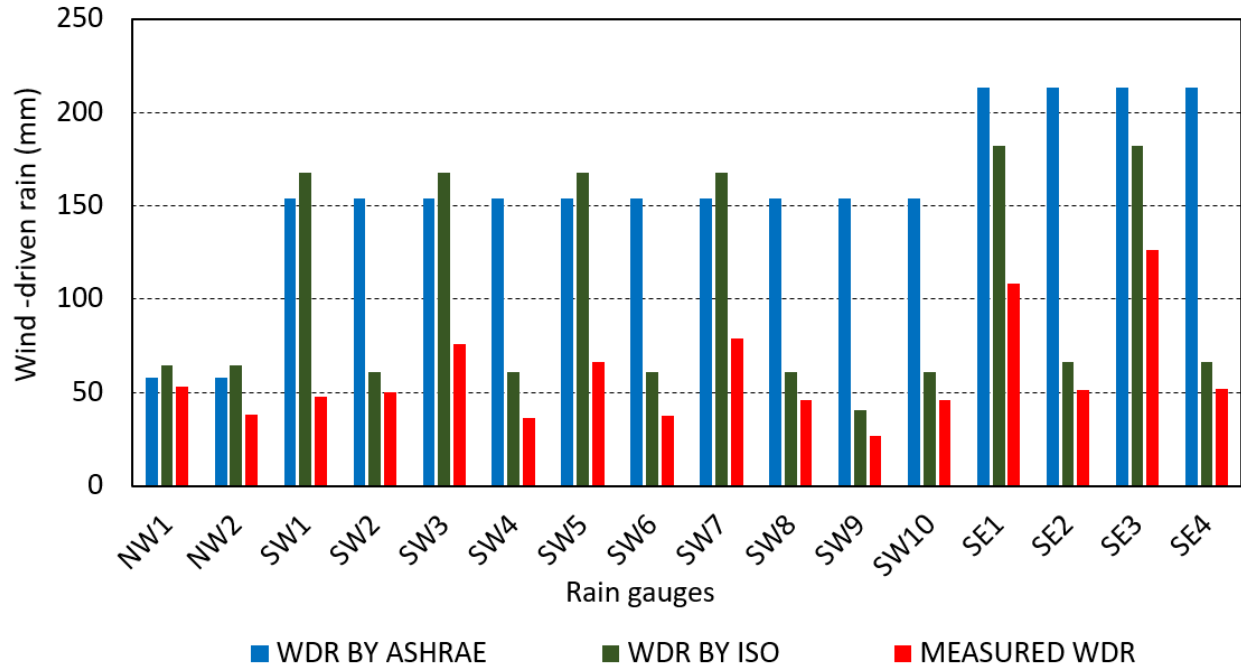
The ISO model overestimates the WDR amount for all the monitored façade locations of McLeod House except for the location on the north-west façade (W1) for which the discrepancy between the measurement and the prediction is 15%. For the remaining 95% (15 out of 16) of the monitored locations the discrepancies are higher than 100%.

In case of HB Building, the discrepancies between the measurements and the predictions by the ISO model are found to be higher than 50% for 50% of the locations (8 out of 16). Only 3 locations (NW1, SW2 and SE4) show discrepancies less than 25%. It has been found that the ISO model estimates better for most of the bottom locations (4.88 m (16') below the roofline; 2nd row) on the south-west (SW2, SW8 and SW10) and the south-east (SE2, SE4) façades and one top location (0.61 m (2') below the roofline) on the north-west façade (NW1). But the ISO standard overestimates for all other top locations on the south-west, south-east and north-west façade of HB Building.

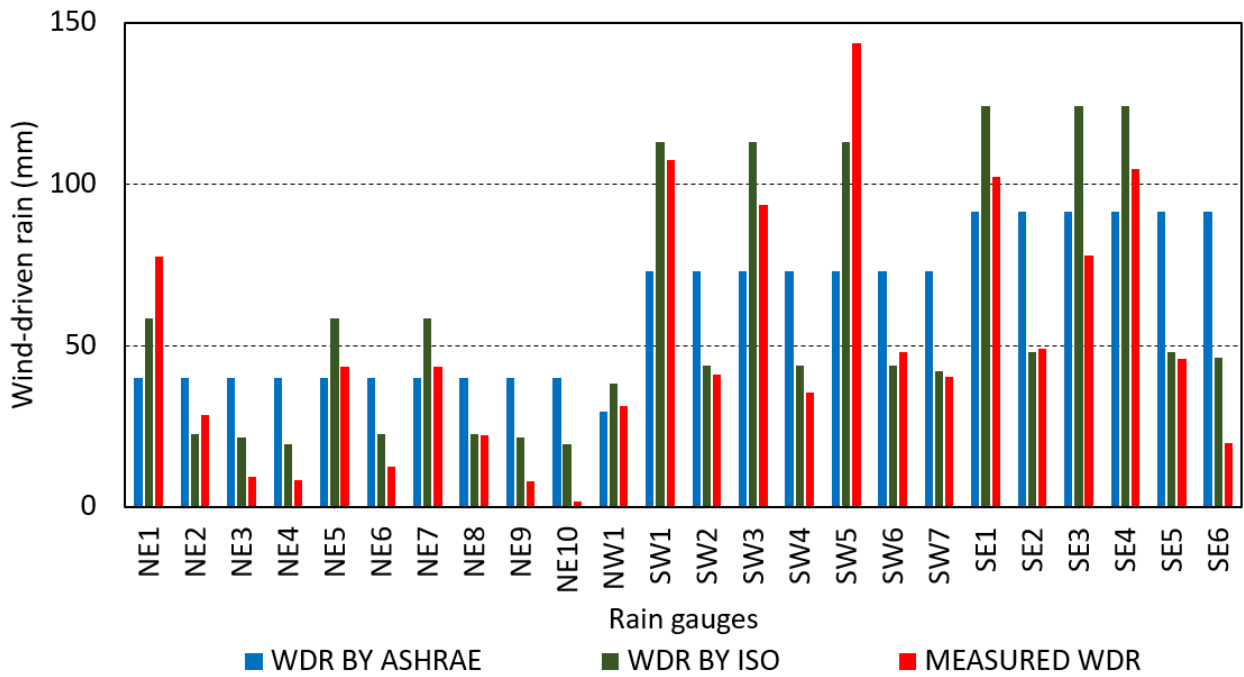
The ISO standard has been found to overestimate the WDR amount at 83% of the monitored locations (20 out of 24) and underestimate for the remaining 17% (4 out of 24) locations of FB Building. Better estimation of WDR by the ISO standard is found at 29% of the locations (7 out of 24) where the discrepancies are less than 10%. For 58% (14 out of 24) of the locations the discrepancies are higher than 25% and 25% (6 out of 24) of the locations shows discrepancies more than 100%. The highest discrepancies are found at bottom locations on the north-east façade which are located at 10.67 m (35') and 21.34 m (70') below the roofline. This is happened because the wall factor values at these lower locations should be smaller but the ISO standard suggests only a constant wall factor, 0.2 from locations 2.5 m below the top to the reminder part of the façade. So use of a higher wall factor value leads to higher estimated WDR. The discrepancy between measurements and predictions is probably attributed to the difference in building geometry, the lack of variation of wall factors across building façade suggested by the standard, and the determination of correction factors.



(a)



(b)



(c)

Figure 4.50 : Comparison between measured wind-driven rain and the estimated wind-driven rain using semi-empirical models for: (a) McLeod House; (b) HB Building; (c) FB Building

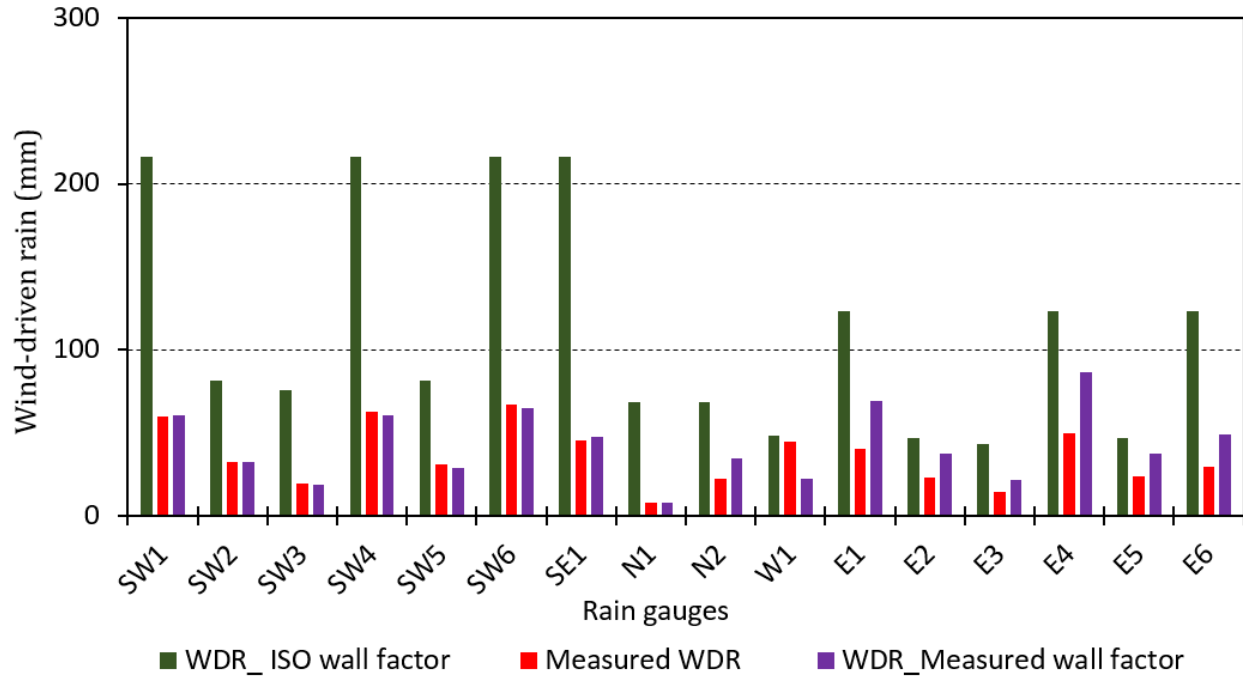
4.5.3.4 Validity of the ISO suggested wall factor

The overestimation by the ISO standard is mainly due to the wall factors suggested by the model, which are in general greater than what have been measured and lack of variation over the façade surface. Calculations are carried out using the ISO standard with measured wall factors instead. Note that these measured wall factors are averaged over the entire monitoring period over all incidence angles. Figure 4.51 shows the comparison for all three test buildings. As shown in the figure, generally use of measured wall factors provide better estimation of wind-driven rain amount compared to that obtained by using model suggested values.

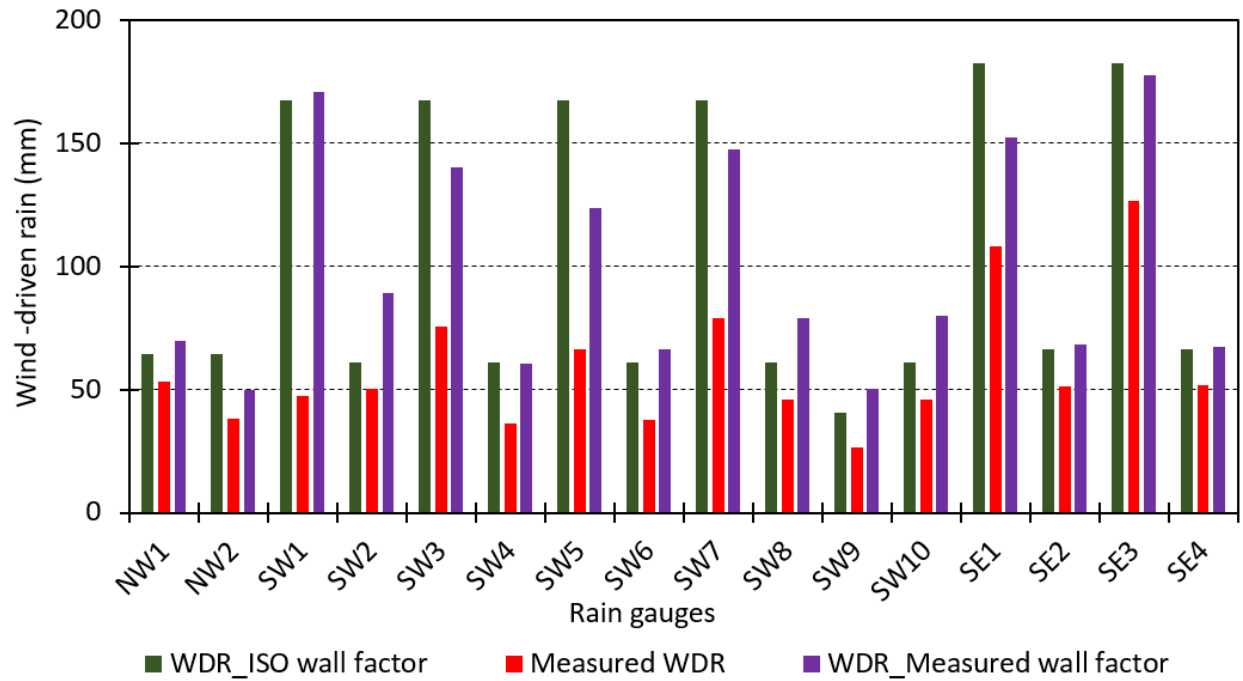
For McLeod House, discrepancies between the measured and the predictions become less than 8% for 50% of the monitored locations after using the measured wall factors. For the remaining locations percentage of discrepancies become smaller as a result of using measured wall factor values.

Significant improvement has not been found for HB Building because as shown in section 4.5.2.8, the measured wall factor values are close the ISO suggested values for most of the monitored locations of the HB Building.

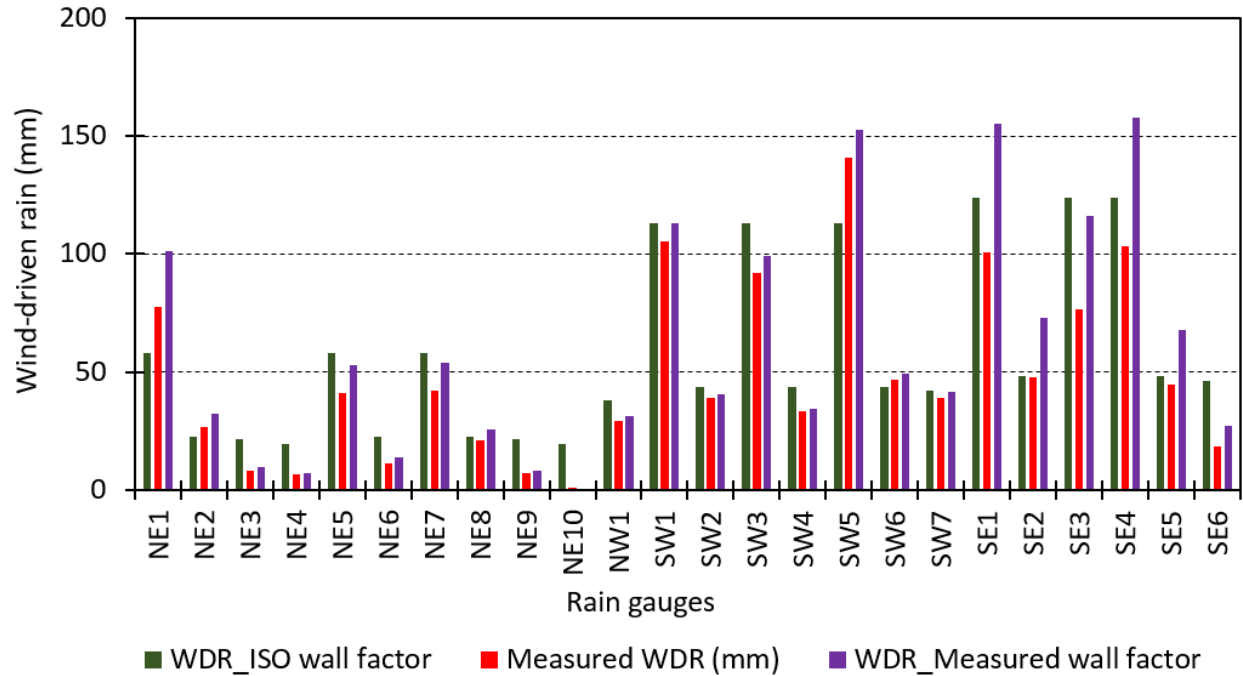
Results of FB Building also show better estimation after using measured wall factors. Now the discrepancies between the measured and predictions are less than 25% for 63% of the locations. 96% of the locations (23 out of 24) shows discrepancy less than 50% after using measured wall factors. Discrepancy higher than 50% is found for 25 % and 4% locations while using the ISO suggested wall factors and measured wall factors respectively. In general, it can be said that the overall predictive performance of the ISO standard is improved after using the measured wall factors. It is also found that use of measured wall factors results in better predictive performance for the FB Building (height 45.6 m) and the McLeod House (height 22 m) than the low-rise HB Building (height 15.06 m). This indicates that only two wall factor values for multi-storey building may be sufficient for a low-rise building like HB Building, but more wall factor values along the façade height should be suggested for high-rise buildings to improve the predictive performance of the ISO model.



(a)



(b)



(c)

Figure 4.51 : Comparison of estimated wind-driven rain by the ISO standard suggested equation using the ISO suggested wall factors and the measured wall factors with the measured wind-driven rain amount for: (a) McLeod House; (b) HB Building; (c) FB Building

Chapter 5

CONCLUSIONS

5.1 SUMMARY OF FINDINGS

Three buildings (i.e., McLeod House, Fredericton; HB Building, Montreal and FB Building, Montreal) in two provinces of Canada (i.e., Quebec and New Brunswick) have been instrumented with equipment to characterize wind-driven rain loads on façades. The simultaneous recordings of onsite weather data of wind speed, wind direction, temperature, relative humidity, horizontal rainfall, and wind-driven rain on the façade have been collected for fourteen months (from August 2013 to June 2014 and from April 2015 to June 2015) for McLeod House, fifteen months (from April 2014 to June 2015) for HB Building and twelve months (from July 2014 to June 2015) for FB building, respectively. Onsite data collected during these periods have been used for analysis. Historical wind and rain data have also been analyzed with the objectives to understand the characteristic wind and rain conditions in these regions and to guide the selection of locations to install driving rain gauges on façade. The historical and onsite wind and rain conditions, spatial distribution of wind-driven rain on façades in terms of catch ratios and wall factors, and comparisons between measured and predicted wind-driven rain using the semi-empirical models are reported for the monitoring periods.

The main findings include:

5.1.1 Wind and rain conditions at test sites

5.1.1.1 Prevailing wind directions

- Historical data shows that in Fredericton usually the wind comes from the north and south-south-west directions, whereas during rain hours the prevailing wind directions are from the north and south. Onsite data for the monitoring period shows that the prevailing wind direction is from the west-north-west during all hours, while from the south-west during

rain hours. However, airport data for the same period shows that wind mainly comes from the south direction during both all and rain hours.

- The prevailing wind directions for all hours in Montreal obtained from historical data are from the west and west-south-west, which are similar to those obtained from onsite and airport data for the monitoring period. Historical data shows that the prevailing wind directions during rain hours are from the north-east and south-south-east, whereas the onsite and airport data for the monitoring period show that wind mainly comes from the west-south-west and south-west direction during rain hours.

5.1.1.2 Wind speed

- Historical data shows similar wind speed distribution for all hours and rain hours in Fredericton, but onsite and airport data for the monitoring period show higher wind speed during rain hours. Historical data (measured at 10 m height) shows that in Fredericton about 40% of time the wind speed is higher than 4 m/s at airport station, whereas onsite data, measured at roof top of test building, for the monitoring period shows that the wind speed exceeds 4 m/s for about 25% and 50% of the time during all hours and rain hours, respectively. The airport data for the monitoring period, converted for wind monitor location at test building site, shows similar wind speed distribution as the onsite data.
- Historical data shows that in general the wind speed is higher in Montreal than that in Fredericton and wind speed is higher during rain hours compared to all hours. Onsite data shows almost similar wind speed distribution for all hours and rain hours at Montreal sites. Historical data shows that at Montreal airport the wind speed (measured at 10 m height) is higher than 4 m/s for about 50% of time during both all hours and rain hours. Onsite data for the monitoring period (measured at roof top of test building) shows that the wind speed exceeds 4 m/s for 15% and 35% of the time at HB and FB Building site, respectively. The airport data for the monitoring period, converted for wind monitor locations at test building sites, shows almost similar wind speed distribution as the onsite data.

5.1.1.3 Rainfall intensity

- Historical analysis of rainfall data shows that the frequency distribution of rainfall intensity and the annual rainfall amount for Fredericton and Montreal is close (730 mm and 690 mm in Fredericton and Montreal, respectively). In both cities the rainfall intensity is less than 2 mm/hr for about 80% of time, and most of the rainfall occurs during summer and fall season, whereas minimum rainfall occurs during winter.
- ✓ In Fredericton the maximum rainfall happens in May and August with a rainfall amount of 95 mm and the minimum rain occurs in February with an amount of about 10 mm.
- ✓ In Montreal the maximum rainfall occurs from June to September, which can be as high as 85 mm per month, whereas the minimum rainfall occurs in February with an amount of about 15 mm.
- Onsite data for the monitoring periods shows that the rainfall intensity at FB Building site is slightly lower than that of other two sites. Rainfall intensity is less than 4 mm/hr for about 91%, 92% and 95 % of the time at McLeod House, HB Building and FB Building site, respectively.

5.1.2 Error associated with wind-driven rain measurements

- The errors associated with wind-driven rain measurements vary with rain events with the maximum error contributed by adhesion-water-evaporation, however, the total amount of error is small as compared to wind-driven rain amount.
- The lower the wind-driven rain amount, the higher the error. The largest error during each rain event is found at gauges where the smallest amount of wind-driven rain is registered, and hence the error is relatively low for the gauges which are located on the façade facing the prevailing wind-driven rain and at top and edges.

- ✓ For McLeod House, the error is less than 10% varying from 3-10% for most of the gauges (81% of the gauges).
- ✓ For HB Building, 73% of the gauges have error less than 10% varying from 0.5-7%.
- ✓ For FB Building, the error is less than 15% varying from 4-15% for 71% of the gauges.

5.1.3 Spatial distribution of wind-driven rain

5.1.3.1 In terms of catch ratios

- Generally catch ratio values are higher on the façades facing the prevailing wind-driven rain compared to other façades. Values are relatively higher at the corners and edges of the façades. Typically catch ratio is the maximum at the top of the façades and decreases towards the bottom. It is also found that the catch ratios are higher for the thirteen story high-rise building compared to the four and seven story mid-rise buildings at the same height below the roofline.
- ✓ For McLeod House the average catch ratios vary from 0.07 to 0.1 at the top locations (0.61 m below the roofline) of the windward façade (south-west) and 0.01 to 0.03 at the top locations at leeward façade (north-east), respectively, whereas values range from 0.04 to 0.07 at the same height on other façades (south-east and north-west). At bottom locations (4.88 m and 9.14 m below the roofline) catch ratio ranges from 0.03 to 0.05 on windward façade and 0.02 to 0.03 on other façades, respectively.
- ✓ For HB building, the average catch ratios at top locations of the windward façades (south-west and south-east) vary from 0.07 to 0.13, whereas value ranges from 0.04 to 0.05 at bottom locations of wind ward façades and top locations of the other façade.
- ✓ For FB building, the catch ratio ranges from 0.14 to 0.25 at top locations, and 0.05 to 0.08 at bottom locations (4.88 m and 10.67 m below the roof line) on the windward

façade. On other façades value ranges from 0.05 to 0.09 at top locations, whereas from 0.003 to 0.05 at bottom locations (4.88 m and 9.14 m below the roofline).

- Catch ratio varies with rain events and values are generally higher at higher wind speed and smaller incidence angle. Catch ratios increase with the increase of wind speed and decrease with the increase of incidence angle.
- Catch ratio is influenced by rainfall intensity up to a limit of 4 mm/hr. The general trend is that catch ratio decreases with the increase of rainfall intensity although the correlation is not very strong.

5.1.3.2 In terms of wall factors

- More than 25% discrepancies between the ISO standard suggested wall factors and wall factors based on measurements are observed for 82% (13 out of 16) of locations at McLeod House, 25% (4 out of 16) of the locations at HB building, and 55% (13 out of 24) of the locations of FB Building, respectively. Wall factors vary along both building heights and across building width while the ISO standard suggests only two values along building height with no change across the building width.
- According to the definition, wall factors should not be influenced by wind speed, rainfall intensity and incident angles. However, given that wall factor is a lump sum value to account for the complex interaction between wind, rain and the building, wall factors are found varying with rain and wind conditions, however, no correlations were found between wall factors with wind speed, incidence angle, or rainfall intensity.

5.1.4. Comparison between measured and predicted WDR using the semi-empirical models

- Comparison between measurements and predictions using semi-empirical models shows that these models suffer from limitations and unable to predict wind-driven rain amount accurately at all façade locations.

- ✓ The ASHRAE 160 model has been found to overestimate the wind-driven rain amount largely for most of the monitored façade locations of the test buildings. The discrepancies between the measurements and the predictions by the ASHRAE model are very high for the bottom locations of the façades. This is happened because the ASHRAE 160 model suggests a constant value of the rain deposition factor ($F_D = 0.5$) for all façade heights, which is seemed to be higher for bottom locations.

- ✓ The ISO model overestimates the wind-driven rain amount for most of the façade locations of all three test buildings.
 - For McLeod House and HB Building the ISO model overestimates the wind-driven rain amount for all the monitored locations. Larger discrepancies (higher than 100%) are found for 95% of the locations (15 out of 16) of McLeod House, whereas, the discrepancies are relatively low for HB Building. In case of HB Building, the discrepancies are higher than 50% for 50% of the locations (8 out of 16).

 - Overestimation of wind-driven rain by the ISO standard is found for 83% of the monitored locations (20 out of 24) of FB Building, whereas underestimation is found for the rest 17% locations (4 out of 24). For 58% (14 out of 24) of the locations the discrepancies are higher than 25% and 25% (6 out of 24) of the locations show discrepancies more than 100%. The highest discrepancies are found at bottom locations which. This is happened because the wall factor values at bottom locations should be smaller but the ISO standard suggests only a constant wall factor, 0.2 for locations 2.5 m below the top to the reminder part of the façade.

- ✓ The discrepancies between measurements and predictions using semi-empirical models are due to the lack of variation of wall factors across building façade suggested in the standards and limited number of building geometries. Analysis shows that only two wall factor values for multi-storey building (as suggested in the ISO standard) may be sufficient for a low-rise building like HB Building, but more wall factor values along the façade height and

across the façade width should be suggested for high-rise buildings to improve the predictive performance of the ISO model. It is observed that use of wall factors based on measurements provide better estimation of wind-driven rain at different façade locations. The discrepancies between the measured and the prediction become less than 25% for 50% and 63% of the locations on McLeod House and FB Building respectively, after using measured wall factor values. Therefore, to improve the semi-empirical models for estimating wind-driven rain on façade, wall factors based on field measurements on buildings with a wider range of building geometries and at more façade locations need to be provided.

5.2 CONTRIBUTIONS

The main contributions of this research project include:

- This is the first field experiment carried out to characterize wind-driven rain loads on mid-rise and high-rise building in Quebec and New Brunswick province in Canada.
- This study has generated a unique set of wind-driven rain data collected on real buildings with high spatial and temporal resolutions, which will be very valuable for the improvement of semi-empirical models and validation of CFD models.
- This research presents a comprehensive study of the spatial distribution of wind-driven rain on building façade based on field measured data, i.e., the influence of wind speed, incidence angles and rainfall intensity on catch ratios and wall factors.
- This study compares the estimated wind-driven rain amount by semi-empirical models (the ASHRAE 160 and the ISO model) with the wind-driven rain measured on real buildings, which confirm the necessity of revised wall factors based on field measurements on buildings with a wider range of building geometries and at more façade locations to improve the semi-empirical models for estimating wind-driven rain on façade.

5.3 RECOMMENDATIONS FOR FUTURE WORKS

- To better characterize wind-driven rain loads on building façade, more full scale field measurements are needed on buildings with various geometries and surrounding conditions including multi-story and tower buildings in various climatic regions with different wind and rain characteristics. In the current study the three buildings are located in two provinces which have similar wind and rain characteristics.
- CFD analysis can be done for the buildings that has been tested in the current study. This will help to evaluate the performance of CFD model in predicting wind-driven rain amount and spatial distribution of wind-driven rain on building façades.

REFERENCES

- Abuku, M., Blocken, B., Carmeliet, J., & Roels, S. (2006). A status report of wind-driven rain research at the laboratory of building physics, KU Leuven. *Proceedings of the Fourth International Symposium on Computational Wind Engineering*,
- Abuku, M., Blocken, B., Nore, K., Thue, J. V., Carmeliet, J., & Roels, S. (2009). On the validity of numerical wind-driven rain simulation on a rectangular low-rise building under various oblique winds. *Building and Environment*, 44(3), 621-632.
- Abuku, M., Janssen, H., Blocken, B., Carmeliet, J., & Roels, S. (2006). Wind-driven rain load on building enclosures—towards the reliable prediction of absorption and evaporation. *IEA Annex 41 Whole Building Heat, Air and Moisture Response, Subtask 3-Boundary Condition*,
- Abuku, M., Janssen, H., & Roels, S. (2009). An onset to whole building hygrothermal modelling under wind-driven rain loads. *Building Simulation 2009: 11th International Building Performance Simulation Association Conference and Exhibition*,
- Abuku, M., Blocken, B., & Roels, S. (2009). Field measurement and numerical analysis of wind-driven rain absorption and evaporation on building facades.
- ASHRAE 2009. ASHRAE standard 160-criteria for moisture control design analysis in buildings. AHSRAE, Atlanta, USA.
- Baheru, T., Chowdhury, A. G., Bitsuamlak, G., & Tokay, A. (2013). A parametric representation of wind-driven rain in experimental setups. *Advances in Hurricane Engineering@ sLearning from our Past*, 270-282.
- Baheru, T., Chowdhury, A. G., Pinelli, J., & Bitsuamlak, G. (2014). Distribution of wind-driven rain deposition on low-rise buildings: Direct impinging raindrops versus surface runoff. *Journal of Wind Engineering and Industrial Aerodynamics*, 133, 27-38.

- Blocken, B.J.E. & Carmeliet, J.E. (2005). Guidelines for wind, rain and wind-driven rain measurements at test-building sites. *Proceedings of the 7th Symposium on Building Physics in the Nordic Countries: Reykjavik*, pp 530-537.
- Blocken, B., Abuku, M., Roels, S., & Carmeliet, J. (2009). Wind-driven rain on building facades: Some perspectives. *EACWE*, 5, 19-23.
- Blocken, B., Briggen, P., Schellena, H., & Carmeliet, J. (2010). Intercomparison of wind-driven rain models based on a case study with full-scale measurements.
- Blocken, B., & Carmeliet, J. (2000a). Driving rain on building envelopes—I. numerical estimation and full-scale experimental verification. *Journal of Building Physics*, 24(1), 61-85.
- Blocken, B., & Carmeliet, J. (2000b). Driving rain on building envelopes—II. representative experimental data for driving rain estimation. *Journal of Building Physics*, 24(2), 89-110.
- Blocken, B., & Carmeliet, J. (2002). Spatial and temporal distribution of driving rain on a low-rise building. *Wind and Structures*, 5(5), 441-462.
- Blocken, B., & Carmeliet, J. (2004). A simplified approach for quantifying driving rain on buildings. *Proc. of Performance of Exterior Envelopes of Whole Buildings IX, Clearwater*,
- Blocken, B., & Carmeliet, J. (2005). High-resolution wind-driven rain measurements on a low-rise building—experimental data for model development and model validation. *Journal of Wind Engineering and Industrial Aerodynamics*, 93(12), 905-928.
- Blocken, B., & Carmeliet, J. (2006). The influence of the wind-blocking effect by a building on its wind-driven rain exposure. *Journal of Wind Engineering and Industrial Aerodynamics*, 94(2), 101-127.
- Blocken, B., & Carmeliet, J. (2007). On the errors associated with the use of hourly data in wind-driven rain calculations on building facades. *Atmospheric Environment*, 41(11), 2335-2343.

Blocken, B., & Carmeliet, J. (2010). Overview of three state-of-the-art wind-driven rain assessment models and comparison based on model theory. *Building and Environment*, 45(3), 691-703.

Blocken, B., & Carmeliet, J. (2008). Guidelines for the required time resolution of meteorological input data for wind-driven rain calculations on buildings. *Journal of Wind Engineering and Industrial Aerodynamics*, 96(5), 621.

Blocken, B., & Carmeliet, J. (2012). A simplified numerical model for rainwater runoff on building facades: Possibilities and limitations. *Building and Environment*, 53, 59.

Blocken, B., Derome, D., & Carmeliet, J. (2013). Rainwater runoff from building facades: A review. *Building and Environment*, 60, 339.

Blocken, B., Dezso, G., van Beeck, J., & Carmeliet, J. (2010). Comparison of calculation models for wind-driven rain deposition on building facades. *Atmospheric Environment*, 44(14), 1714.

Blocken, B., & Carmeliet, J. (2004). A review of wind-driven rain research in building science. *Journal of Wind Engineering and Industrial Aerodynamics*, 92(13), 1079.

Blocken, B., & Carmeliet, J. (2006). On the accuracy of wind-driven rain measurements on buildings. *Building and Environment*, 41(12), 1798.

Blocken, B., & Carmeliet, J. (2007). Validation of CFD simulations of wind-driven rain on a low-rise building facade. *Building and Environment*, 42(7), 2530.

Campbell Scientific (Canada) Corp. (2003). Instruction manual: Meteorological instruments-multi-plate radiation shield. In Campbell Scientific (Canada) corp. (Ed.), (pp. 1-8)

Campbell Scientific (Canada) Corp. (2013). Instruction manual: TE525 tipping bucket rain gage. In Campbell Scientific (Canada) Corp. (Ed.), (pp. 1-14)

Campbell Scientific (Canada) Corp. (June 2013a). Instruction manual: 05103, 05103-45, 05106, and 05305 R.M. young wind monitors. In Campbell Scientific (Canada) Corp. (Ed.), (pp. 1-16)

Campbell Scientific (Canada) Corp. (June 2013b). Instruction manual: HC2-S3-L temperature and relative humidity probes. In Campbell Scientific (Canada) Corp. (Ed.), (pp. 4-18)

Chand, I., & Bhargava, P. (2002). Estimation of driving rain index for India. *Building and Environment*, 37(5), 549-554.

Choi, E. (1993). Velocity and impact direction of WDR on building facade. (). Singapore 2263: School of Civil and Structural Engineering, Nanyang Technological University.

Choi, E. C. (1994). Parameters affecting the intensity of wind-driven rain on the front face of a building. *Journal of Wind Engineering and Industrial Aerodynamics*, 53(1), 1-17.

Choi, E. C. (1999). Wind-driven rain on building faces and the driving-rain index. *Journal of Wind Engineering and Industrial Aerodynamics*, 79(1), 105-122.

Choi, E. C. (2000). Variation of wind-driven rain intensity with building orientation. *Journal of Architectural Engineering*, 6(4), 122-128.

Choi, E. C. C. (1994). Determination of wind-driven-rain intensity on building faces. *Journal of Wind Engineering and Industrial Aerodynamics*, 51(1), 55.

Coutu, S., Wyrsh, V., Rossi, L., Emery, P., Golay, F., & Carneiro, C. (2013). Modelling wind-driven rain on buildings in urbanized area using 3-D GIS and LiDAR datasets. *Building and Environment*, 59, 528-535.

Environment canada. (2015). Retrieved from

http://www.climate.weather.gc.ca/advanceSearch/searchHistoricData_e.html#stnNameTab

Erkal, A., D' Ayala, D., & Sequeira, L. (2012). Assessment of wind-driven rain impact, related surface erosion and surface strength reduction of historic building materials. *Building and Environment*, 57, 336-348.

Ge, H. (2015). Influence of time resolution and averaging techniques of meteorological data on the estimation of wind-driven rain load on building facades for canadian climates. *Journal of*

Wind Engineering and Industrial Aerodynamics, 143, 50-61.

doi:<http://dx.doi.org/10.1016/j.jweia.2015.04.019>

Ge, H., & Krpan, R. (2009). Wind-driven rain study in the coastal climate of British Columbia. (No. Final Report). BC, Canada: Submitted to: Canada Mortgage and Housing Corporation.

Ge, H., & Krpan, R. (2007). Field measurement of wind-driven rain on a low-rise building in the coastal climate of British Columbia. *Proceedings of the 11 Th Canadian Conference on Building Science and Technology, March, Banff*,

Giarma, C., & Aravantinos, D. (2014). On building components' exposure to driving rain in Greece. *Journal of Wind Engineering and Industrial Aerodynamics*, 125, 133-145.

Google maps. (2015a). Retrieved from

<https://www.google.com/maps/d/edit?mid=z9TtLVWPjIY.kGZjZ2WKAPc4&hl=en>

Google maps. (2015b). Retrieved from

<https://www.google.com/maps/d/edit?mid=z9TtLVWPjIY.kAMjYGV4N9jY&hl=en>

Google maps. (2015c). Retrieved from

https://www.google.com/maps/d/edit?mid=z9TtLVWPjIY.k3_3bUt05Lq4&hl=en

Google maps. (2015d). Retrieved from

<https://www.google.com/maps/d/edit?mid=z9TtLVWPjIY.kyUiOgdIjjsM&hl=en>

Hagentoft, C. (2001). Introduction to building physics. Lund: Studentlitteratur.

Hangan, H. (1999a). Wind-driven rain simulations. *Journal of Visualization*, 1(4), 337-343.

Hangan, H. (1999b). Wind-driven rain studies. A C-FD-E approach. *Journal of Wind Engineering and Industrial Aerodynamics*, 81(1-4), 323.

Hens, H. (2010). Wind-driven rain: From theory to reality, in proceedings thermal performance of the exterior envelopes of whole buildings XI. Clearwater, FL.

- Hens, H. S. L. C. (2007). *Building physics - heat, air and moisture: Fundamentals and engineering methods with examples and exercises*. Berlin: Ernst & Sohn.
- Högberg, A. B., Kragh, M. K., & van Mook, F. J. (1999). A comparison of driving rain measurements with different gauges. *Proceedings of the 5th Symposium of Building Physics in the Nordic Countries, Gothenburg*, 361-368.
- Hoppestad, S. (1955). Slagregni norge (in Norwegian). Norwegian building research institute, rapport nr. 13, Oslo.
- Huang, S., & Li, Q. (2010). Numerical simulations of wind-driven rain on building envelopes based on eulerian multiphase model. *Journal of Wind Engineering and Industrial Aerodynamics*, 98(12), 843-857.
- Hutcheon, N. B., & Handergord G.O.P. (1995). *Building science for a cold climate*. Canada: IRC.
- Júnior, C. M. M., & Carasek, H. (2014). Relationship between the deterioration of multi story buildings facades and the driving rain. *Revista De La Construcción*, 13(1), 64-73.
- Juras, P., Durica, P., & Korenkova, R. (2014). Comparison of different wind-driven rain gauges. *Advanced Materials Research*, 1057 97-104.
- Karagiozis, A. N., Salonvaara, M., Holm, A., & Kuenzel, H. (2003). Influence of wind-driven rain data on hygrothermal performance. *Proceedings of the Eighth International IBPSA Conference, Eindhoven, the Netherlands*, 627-634.
- Karagiozis, A., Hadjisophocleous, G., & Cao, S. (1997). Wind-driven rain distributions on two buildings. *Journal of Wind Engineering and Industrial Aerodynamics*, 67, 559-572.
- Kubilay, A., Derome, D., Blocken, B., & Carmeliet, J. (2014a). High-resolution field measurements of wind-driven rain on an array of low-rise cubic buildings. *Building and Environment*, 78, 1-13.

- Kubilay, A., Derome, D., Blocken, B., & Carmeliet, J. (2014b). High-resolution field measurements of wind-driven rain on an array of low-rise cubic buildings. *Building and Environment*, 78, 1-13.
- Kubilay, A., Derome, D., Blocken, B., & Carmeliet, J. (2014c). Numerical modeling of turbulent dispersion for wind-driven rain on building facades. *Environmental Fluid Mechanics*, 15(1), 109-133.
- Kubilay, A., Derome, D., Blocken, B., & Carmeliet, J. (2013). CFD simulation and validation of wind-driven rain on a building facade with an eulerian multiphase model. *Building and Environment*, 61, 69-81.
- Lacy, R. E. (1965). Driving-rain maps and the onslaught of rain on buildings. RILEM/CIB symp. on moisture problems in buildings, rain penetration, Helsinki, Vol. 3(August 16-19), paper 3-4.
- Mohaddes Foroushani, S. S., Ge, H., & Naylor, D. (2014). Effects of roof overhangs on wind-driven rain wetting of a low-rise cubic building: A numerical study. *Journal of Wind Engineering and Industrial Aerodynamics*, 125, 38-51.
- Mook, F. (1998). Measurements of driving rain by a new gauge with wiper. (No. FAGO 98.62.K).article submitted to Building and Environment.
- NBN EN ISO 15927-3 (2009), Hygrothermal performance of buildings-Calculation and presentation of climatic data-Part3: Calculation of a driving rain index for vertical surfaces from hourly wind and rain data.
- Nore, K. (May 2006). Measurements of driving rain dispersion on a low-rise test building in Norway. ().Submitted to EIA-Annex 41 meeting, Montreal.
- Nore, K., Blocken, B., Petter Jelle, B., Thue, J. V., & Carmeliet, J. (2007). A dataset of wind-driven rain measurements on a low-rise test building in Norway. *Building and Environment*, 42(5), 2150.

Osorio, M., Ge, H. (April 2013). Report on the errors associated with a wind-driven rain gauge. Concordia University, Montreal, QC, Canada:

Osorio, M., & Ge, H. (April 2013). Error analysis of the wind-driven rain measurements taken on a six-storey building in lower mainland, British Columbia. Unpublished Concordia University,

Pérez-Bella, J. M., Domínguez-Hernández, J., Cano-Suñén, E., Del Coz-Díaz, J. J., & Martín-Rodríguez, Á. (2014). Procedure for a detailed territorial assessment of wind-driven rain and driving-rain wind pressure and its implementation to three Spanish regions. *Journal of Wind Engineering and Industrial Aerodynamics*, 128, 76-89.

Pérez-Bella, J. M., Domínguez-Hernández, J., Rodríguez-Soria, B., Del Coz-Díaz, J. J., & Cano-Suñén, E. (2012). Estimation of the exposure of buildings to driving rain in Spain from daily wind and rain data. *Building and Environment*, 57, 259-270.

Pérez-Bella, J. M., Domínguez-Hernández, J., Rodríguez-Soria, B., Del Coz-Díaz, J. J., & Cano-Suñén, E. (2013). Combined use of wind-driven rain and wind pressure to define water penetration risk into building façades: The Spanish case. *Building and Environment*,

Pérez-Bella, J. M., Domínguez-Hernández, J., Rodríguez-Soria, B., Del Coz-Díaz, J. J., & Cano-Suñén, E. (2013). Optimised method for estimating directional driving rain from synoptic observation data. *Journal of Wind Engineering and Industrial Aerodynamics*, 113, 1-11.

Rychtáriková, M., & Vargová, A. (2008). Bionics and wind-driven rain on building facades, Slovak journal of civil engineering. *Vol. 4*, pages 35-40.

Rydock, J. P., Lisø, K. R., Førland, E. J., Nore, K., & Thue, J. V. (2005). A driving rain exposure index for Norway. *Building and Environment*, 40(11), 1450-1458.

Sahal, N. (2006). Proposed approach for defining climate regions for turkey based on annual driving rain index and heating degree-days for building envelope design. *Building and Environment*, 41(4), 520-526.

Sauer, P. (1987). An annual driven rain index for china. *Building and Environment*, 22(4), 239-240.

Straube, J., & Burnett, E. (2000). Simplified prediction of driving rain on buildings. *Proceedings of the International Building Physics Conference*, 375-382.

Straube, J., & Schumacher, C. (2006). Driving rain loads for Canadian building design.

Tang, W., Davidson, C. I., Finger, S., & Vance, K. (2004). Erosion of limestone building surfaces caused by wind-driven rain: 1. field measurements. *Atmospheric Environment*, 38(33), 5589-5599.

Van den Brande, T., Blocken, B., & Roels, S. (2013). Rain water runoff from porous building facades: Implementation and application of a first-order runoff model coupled to a HAM model. *Building and Environment*,

Van Mook, F. J. (1999). Measurements and simulations of driving rain on the main building of the TUE. *Proceedings 5th Symposium on Building Physics in the Nordic Countries*, 377-384.

Wolf, J., & Griffith, M. (2008). Wind-driven rain as a design parameter. *Structures Congress 2008@sCrossing Borders*, 1-7.

Zhu, D. & Fazio, P. (1994). Quantitative studies of driving rain exposure on a vertical building facade in an urban area (M.A.Sc.).

Zhu, D., Mallidi, S. R., & Fazio, P. (1995). Quantitative driving rain exposure on a vertical wall at various Canadian cities. *Building and Environment*, 30(4), 533-544.

APPENDIX A

Comparison of weather data obtained from onsite and nearby meteorological stations

As mentioned in Chapter 4 (section 4.3.1), onsite wind speed; wind direction; temperature and relative humidity data collected for the first couple of months of the monitoring period was compared with the data obtained from nearby meteorological stations for all test buildings site to check the quality of onsite data. Comparison for wind speed and wind direction has been presented in section 4.3.1. Here results for temperature and relative humidity comparison are presented for all three test sites.

McLeod House, Fredericton, NB

For McLeod House site, the comparisons are done for the period from August 2013 to March 2014.

Comparison of temperature

Comparison of hourly temperature is shown in Figure A.1. It shows the comparison of maximum, minimum and average values as well as standard deviation. Maximum temperature recorded by onsite weather station is 30.07°C whereas recorded by Fredericton, Fredericton CDA CS and Fredericton aquatic centre are 30.8°C, 29.7°C and 31.4°C respectively. Minimum temperatures are also close as -27.19°C from onsite station and -28.8°C, -28.3°C and -29.4°C from Fredericton, Fredericton CDA CS and Fredericton aquatic centre c/s respectively. Average temperature obtained from onsite experiment is 2.19°C, whereas from Fredericton, Fredericton CDA CS, and Fredericton aquatic centre are 1.23°C, 1.28°C, and 2.51°C respectively.

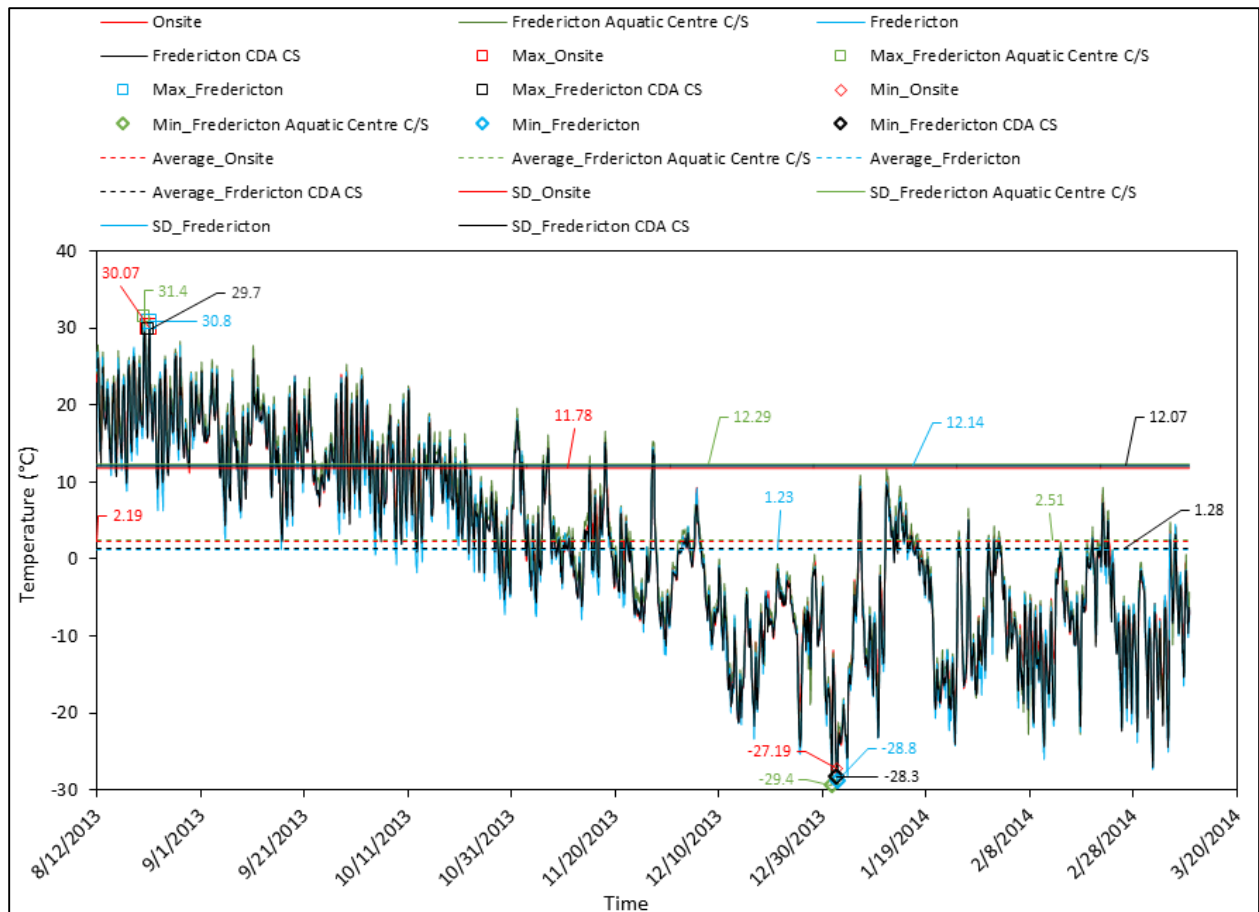


Figure A.1: Comparison of hourly temperature obtained from onsite and nearby meteorological stations for the period from August 2013 to March 2014

Comparison of relative humidity

Comparison of hourly relative humidity is shown in Figure A.2. The average relative humidity obtained from data logger is 70.7% whereas that obtained from Fredericton, Fredericton CDA CS and Fredericton aquatic centre c/s are 76.7%, 74.4% and 77.3% respectively.

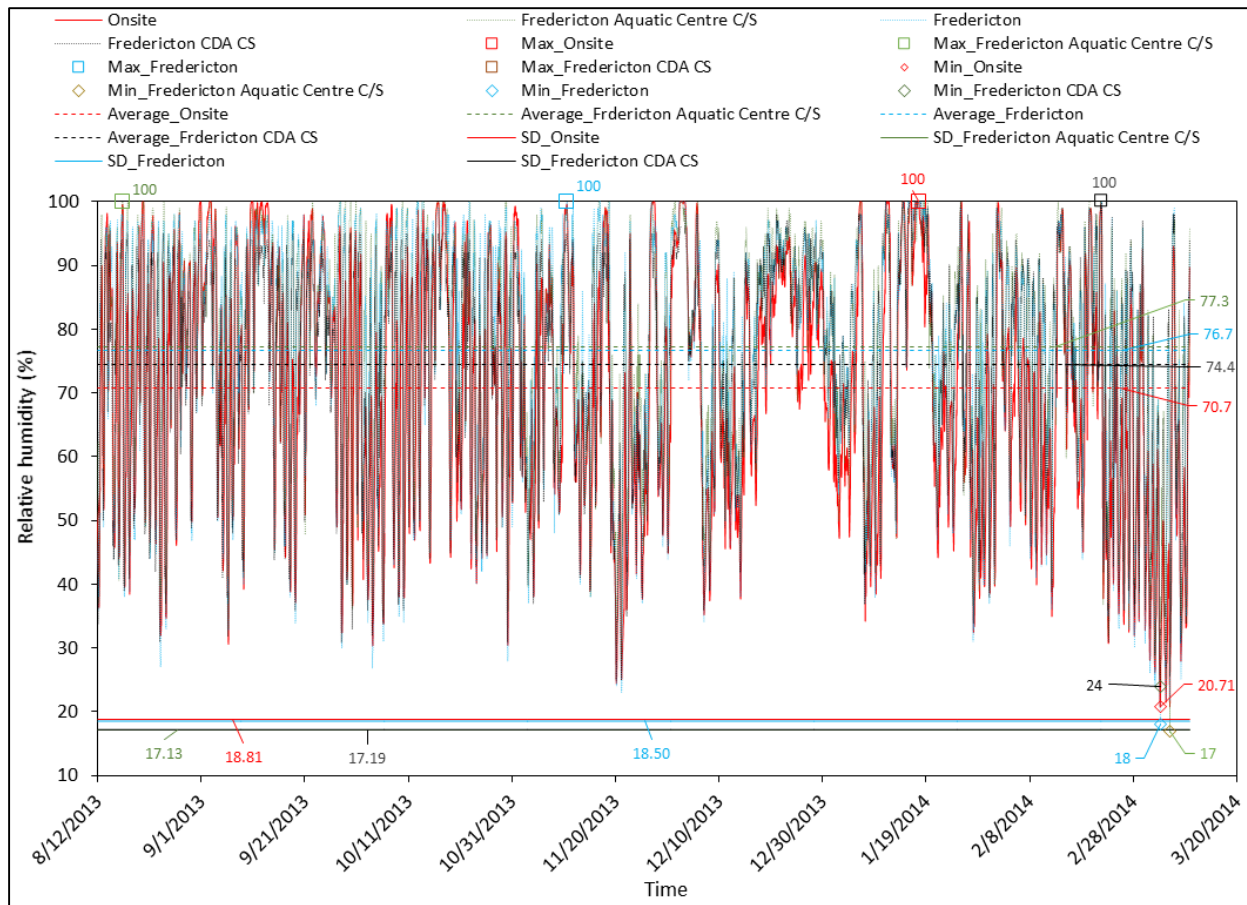


Figure A.2: Comparison of hourly relative humidity obtained from onsite and nearby meteorological stations for the period from August 2013 to March 2014

HB Building, Montreal, QC

For HB Building site, the comparisons are done for the period from April 2014 to June 2014.

Comparison of temperature

Comparison of hourly temperature for the period from May 2014 to June 2014 is shown in Figure A.3. Maximum temperature recorded onsite was 29.61°C, whereas the maximum temperatures recorded by Montreal international airport was 29.80°C for this period. Minimum temperatures

were 5.39°C from onsite station and 3.80°C from Montreal International Airport station. Average temperature obtained from onsite experiment was 17.04°C, from Montreal International Airport was 16.63°C.

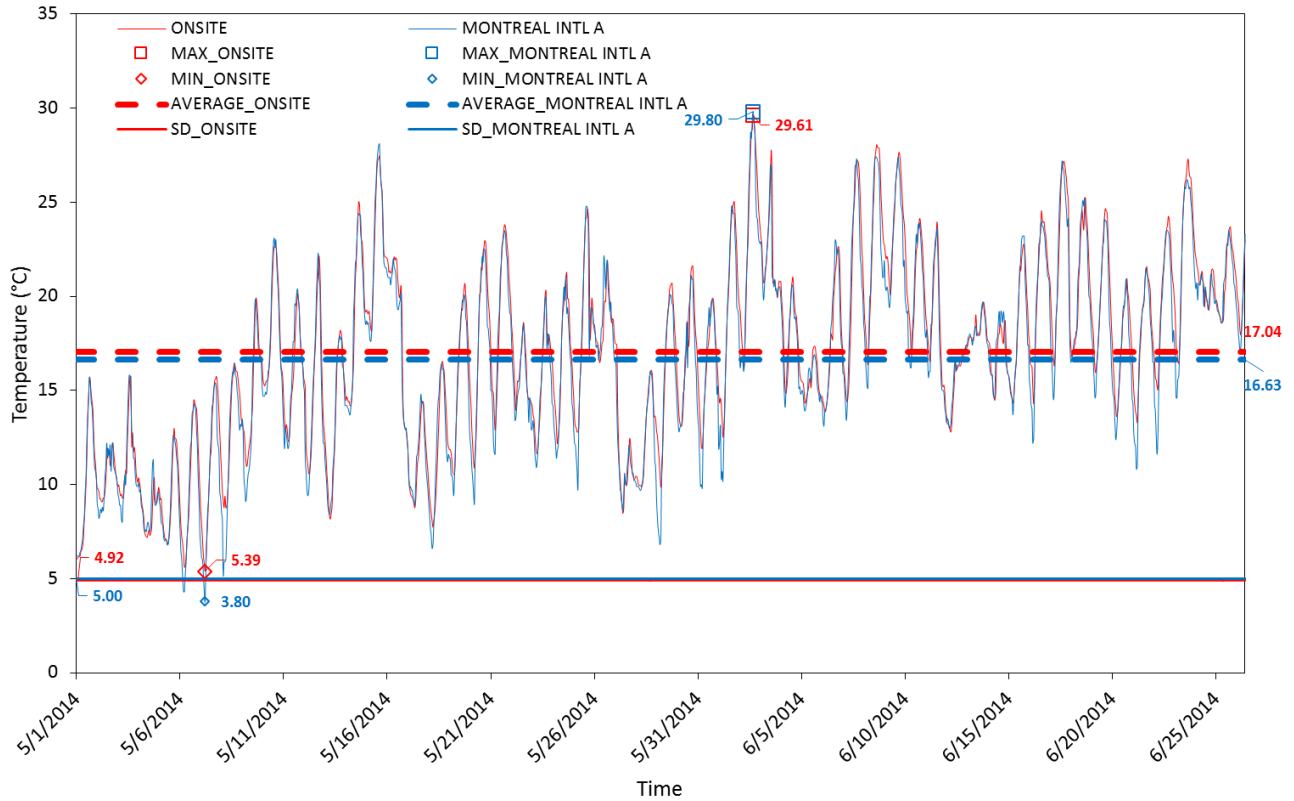


Figure A.3: Comparison of hourly temperature obtained from onsite and Montreal international airport station for the period from April 2014 to June 2014

Comparison of relative humidity

Figure A.4 shows the comparison of hourly temperature for the period from May 2014 to June 2014. The average relative humidity obtained onsite was 64.26% for this period, whereas it was obtained as 65.76% from Montreal international airport station data. Maximum and minimum values are also very close.

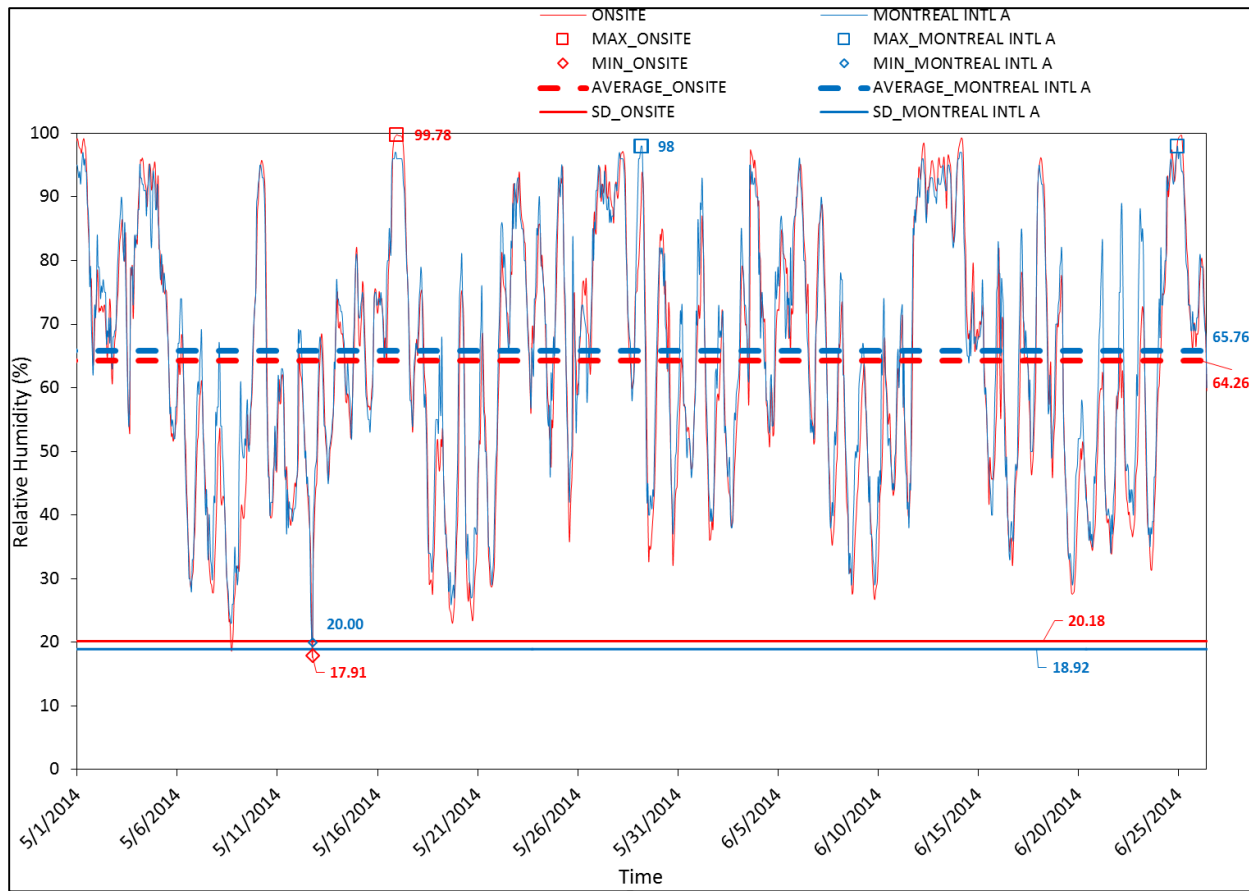


Figure A.4 : Comparison of hourly relative humidity obtained from onsite and Montreal international airport station for the period from April 2014 to June 2014

FB Building, Montreal, QC

For FB Building site, the comparisons are done for the period from July 2014 to August 2014.

Comparison of temperature

Comparison of hourly temperature for the period from July 2014 to August 2014 is shown in Figure A.5. Maximum temperature recorded by onsite weather station is 29.62°C whereas the maximum

temperatures recorded by Montreal international airport, Montreal/St-Hubert and Mctavish stations are 29.60°C, 28.9°C and 30.1°C respectively, which are very close. Minimum temperatures are 12.78°C from onsite station and 11.1°C, 9.4°C and 12.3°C from Montreal international airport, Montreal/St-Hubert and Mctavish respectively. Average temperature obtained from onsite experiment is 20.71°C, and 19.71°C, 19.35°C and 20.20°C from Montreal International Airport, Montreal/St-Hubert and Mctavish respectively.

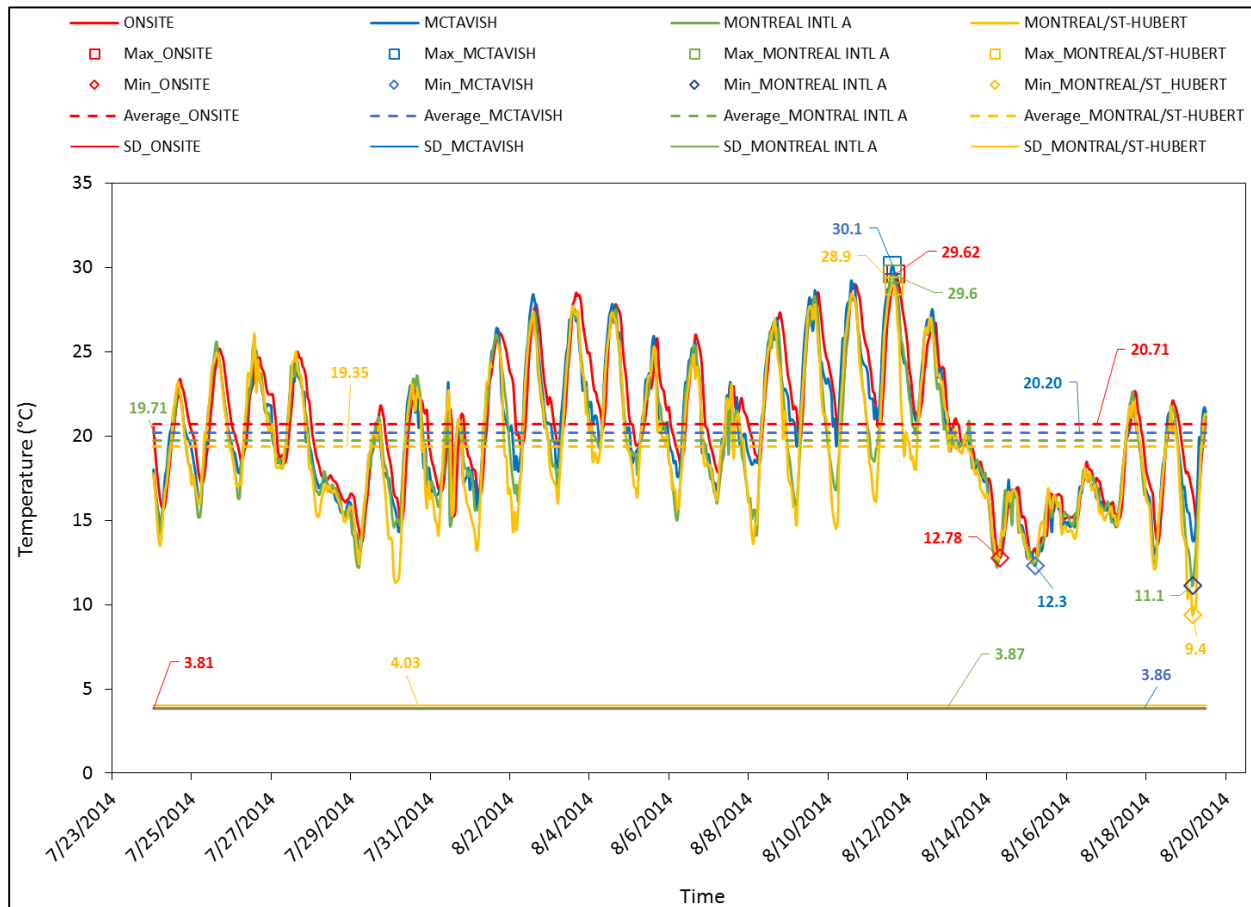


Figure A.5 : Comparison of hourly temperature obtained from FB Building site and nearby meteorological stations for the period from July 2014 to August 2014

Comparison of relative humidity

Comparison of hourly relative humidity is shown in Figure A.6. The average relative humidity obtained from onsite measurement is 68.25% whereas it is obtained as 70.86%, 69.13% and

67.51% from Montreal International Airport, Montreal/St-Hubert and Mctavish respectively for this period. Maximum and minimum values are also very close.

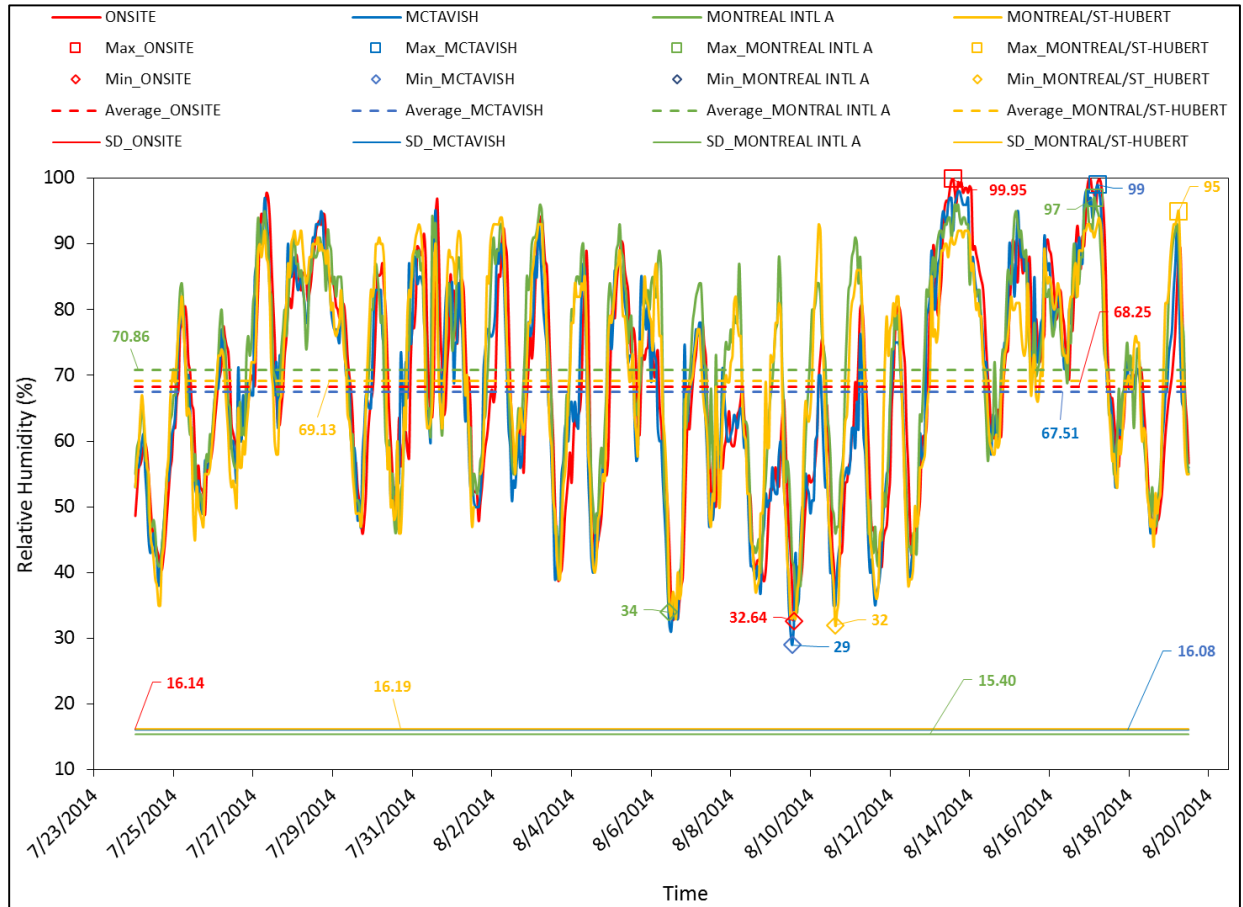


Figure A.6 : Comparison of hourly relative humidity obtained from FB Building site and nearby meteorological stations for the period from July 2014 to August 2014

APPENDIX B

Error analysis for major rain events

McLeod House, Fredericton, NB

Event: From August 14, 2013 to September 16, 2013

| | |
|-----------------------------------|--------------|
| Total horizontal rainfall | : 205.20 mm |
| Average rainfall intensity | : 1.97 mm/hr |
| Average air temperature | : 17.93°C |
| Average relative humidity | : 76.91% |
| Average wind speed at 10 m height | : 2.46 m/s |
| Prevailing wind direction | : South-west |

| WDR gauge | SW1 | SW2 | SW3 | SW4 | SW5 | SW6 | W1 | N1 | N2 | E1 | E2 | E3 | E4 | E5 | E6 | SE1 |
|-------------------------|-------|-------|------|-------|-------|-------|-------|-------|-------|-------|------|-------|-------|------|-------|-------|
| Number of tips | 389 | 235 | 156 | 422 | 222 | 482 | 476 | 23 | 276 | 260 | 134 | 75 | 281 | 145 | 93 | 507 |
| Number of interruptions | 18 | 15 | 13 | 22 | 17 | 22 | 20 | 8 | 13 | 7 | 8 | 9 | 13 | 12 | 12 | 18 |
| Vbowl (g) | 5.5 | 5.5 | 5.5 | 5.5 | 5.5 | 5.5 | 5.5 | 5.5 | 5.5 | 5.5 | 5.5 | 5.5 | 5.5 | 5.5 | 5.5 | 5.5 |
| Swdr (mm) | 23.34 | 14.10 | 9.36 | 25.32 | 13.32 | 28.92 | 28.56 | 1.38 | 16.56 | 15.60 | 8.04 | 4.50 | 16.86 | 8.70 | 5.58 | 30.42 |
| EAW (mm) | 0.9 | 0.75 | 0.65 | 1.1 | 0.85 | 1.1 | 1 | 0.4 | 0.65 | 0.35 | 0.4 | 0.45 | 0.65 | 0.6 | 0.6 | 0.9 |
| EEVAP (mm) | 0 | 0 | 0 | 0 | 0 | 0 | 0 | 0 | 0 | 0 | 0 | 0 | 0 | 0 | 0 | 0 |
| EUC (mm) | 0 | 0 | 0 | 0 | 0 | 0 | 0 | 0 | 0 | 0 | 0 | 0 | 0 | 0 | 0 | 0 |
| ERW (g) | 5.5 | 5.5 | 5.5 | 5.5 | 5.5 | 5.5 | 5.5 | 5.5 | 5.5 | 5.5 | 5.5 | 5.5 | 5.5 | 5.5 | 5.5 | 5.5 |
| ETIP (g/tip) | 0 | 0 | 0 | 0 | 0 | 0 | 0 | 0 | 0 | 0 | 0 | 0 | 0 | 0 | 0 | 0 |
| ETOT (mm) | 0.96 | 0.81 | 0.71 | 1.16 | 0.91 | 1.16 | 1.06 | 0.46 | 0.71 | 0.41 | 0.46 | 0.51 | 0.71 | 0.66 | 0.66 | 0.96 |
| eTOT (%) | 4.11 | 5.74 | 7.59 | 4.58 | 6.83 | 4.01 | 3.71 | 33.33 | 4.29 | 2.63 | 5.72 | 11.33 | 4.21 | 7.59 | 11.83 | 3.16 |

Event: From September 22, 2013 to September 25, 2013

| | |
|-----------------------------------|--------------|
| Total horizontal rainfall | : 20.10 mm |
| Average rainfall intensity | : 0.87 mm/hr |
| Average air temperature | : 10.96°C |
| Average relative humidity | : 88.70% |
| Average wind speed at 10 m height | : 2.08 m/s |
| Prevailing wind direction | : North-west |

| WDR gauge | SW1 | SW2 | SW3 | SW4 | SW5 | SW6 | W1 | N1 | N2 | E1 | E2 | E3 | E4 | E5 | E6 | SE1 |
|-------------------------|------|------|------|------|------|------|------|------|------|------|------|------|------|------|------|------|
| Number of tips | 74 | 30 | 16 | 58 | 24 | 78 | 30 | 0 | 3 | 3 | 1 | 1 | 16 | 7 | 6 | 20 |
| Number of interruptions | 1 | 0 | 1 | 2 | 1 | 3 | 3 | 0 | 2 | 1 | 0 | 0 | 1 | 2 | 2 | 2 |
| Vbowl (g) | 5.5 | 5.5 | 5.5 | 5.5 | 5.5 | 5.5 | 5.5 | 5.5 | 5.5 | 5.5 | 5.5 | 5.5 | 5.5 | 5.5 | 5.5 | 5.5 |
| Swdr (mm) | 4.44 | 1.80 | 0.96 | 3.48 | 1.44 | 4.68 | 1.80 | 0.00 | 0.18 | 0.18 | 0.06 | 0.06 | 0.96 | 0.42 | 0.36 | 1.20 |
| EAW (mm) | 0.05 | 0 | 0.05 | 0.1 | 0.05 | 0.15 | 0.15 | 0 | 0.1 | 0.1 | 0 | 0 | 0.05 | 0.1 | 0.1 | 0.1 |
| EEVAP (mm) | 0 | 0 | 0 | 0 | 0 | 0 | 0 | 0 | 0 | 0 | 0 | 0 | 0 | 0 | 0 | 0 |
| EUC (mm) | 0 | 0 | 0 | 0 | 0 | 0 | 0 | 0 | 0 | 0 | 0 | 0 | 0 | 0 | 0 | 0 |
| ERW (g) | 5.5 | 5.5 | 5.5 | 5.5 | 5.5 | 5.5 | 5.5 | 5.5 | 5.5 | 5.5 | 5.5 | 5.5 | 5.5 | 5.5 | 5.5 | 5.5 |
| ETIP (g/tip) | 0 | 0 | 0 | 0 | 0 | 0 | 0 | 0 | 0 | 0 | 0 | 0 | 0 | 0 | 0 | 0 |
| ETOT (mm) | 0.11 | 0.06 | 0.11 | 0.16 | 0.11 | 0.21 | 0.21 | 0.06 | 0.16 | 0.11 | 0.06 | 0.06 | 0.11 | 0.16 | 0.16 | 0.16 |
| eTOT (%) | 2.5 | 3.3 | 11.5 | 4.6 | 7.6 | 4.5 | 11.7 | | 88.9 | 61.1 | 100 | 100 | 11.5 | 38.1 | 44.4 | 13.3 |

Event: From October 07, 2013 to October 08, 2013

Total horizontal rainfall : 24.10 mm
Average rainfall intensity : 1.85 mm/hr
Average air temperature : 12.96°C
Average relative humidity : 93.91%
Average wind speed at 10 m height : 4.47 m/s
Prevailing wind direction : South

| WDR gauge | SW1 | SW2 | SW3 | SW4 | SW5 | SW6 | W1 | N1 | N2 | E1 | E2 | E3 | E4 | E5 | E6 | SE1 |
|-------------------------|------|------|------|------|------|-------|------|------|------|------|------|------|------|------|------|------|
| Number of tips | 154 | 97 | 63 | 158 | 85 | 172 | 123 | 0 | 3 | 37 | 16 | 9 | 46 | 9 | 22 | 160 |
| Number of interruptions | 3 | 2 | 0 | 2 | 2 | 2 | 0 | 0 | 0 | 2 | 2 | 3 | 2 | 3 | 2 | 2 |
| Vbowl (g) | 5.5 | 5.5 | 5.5 | 5.5 | 5.5 | 5.5 | 5.5 | 5.5 | 5.5 | 5.5 | 5.5 | 5.5 | 5.5 | 5.5 | 5.5 | 5.5 |
| Swdr (mm) | 9.24 | 5.82 | 3.78 | 9.48 | 5.10 | 10.32 | 7.38 | 0.00 | 0.18 | 2.22 | 0.96 | 0.54 | 2.76 | 0.54 | 1.32 | 9.60 |
| EAW (mm) | 0.15 | 0.1 | 0 | 0.1 | 0.1 | 0.1 | 0 | 0 | 0 | 0.1 | 0.1 | 0.15 | 0.1 | 0.15 | 0.1 | 0.1 |
| EEVAP (mm) | 0 | 0 | 0 | 0 | 0 | 0 | 0 | 0 | 0 | 0 | 0 | 0 | 0 | 0 | 0 | 0 |
| EUC (mm) | 0 | 0 | 0 | 0 | 0 | 0 | 0 | 0 | 0 | 0 | 0 | 0 | 0 | 0 | 0 | 0 |
| ERW (g) | 5.5 | 5.5 | 5.5 | 5.5 | 5.5 | 5.5 | 5.5 | 5.5 | 5.5 | 5.5 | 5.5 | 5.5 | 5.5 | 5.5 | 5.5 | 5.5 |
| ETIP (g/tip) | 0 | 0 | 0 | 0 | 0 | 0 | 0 | 0 | 0 | 0 | 0 | 0 | 0 | 0 | 0 | 0 |
| ETOT (mm) | 0.21 | 0.16 | 0.06 | 0.16 | 0.16 | 0.16 | 0.06 | 0.06 | 0.06 | 0.16 | 0.16 | 0.21 | 0.16 | 0.21 | 0.16 | 0.16 |
| eTOT (%) | 2.3 | 2.7 | 1.6 | 1.7 | 3.1 | 1.6 | 0.8 | | 33.3 | 7.2 | 16.7 | 38.9 | 5.8 | 38.9 | 12.1 | 1.7 |

Event: From January 25, 2014 to January 27, 2014

Total horizontal rainfall : 17.20 mm
Average rainfall intensity : 2.46 mm/hr
Average air temperature : -8.35°C
Average relative humidity : 78.61%

Average wind speed at 10 m height : 5.70 m/s

Prevailing wind direction : West

| WDR gauge | SW1 | SW2 | SW3 | SW4 | SW5 | SW6 | W1 | N1 | N2 | E1 | E2 | E3 | E4 | E5 | E6 | SE1 |
|-------------------------|------|-------|-------|------|------|------|------|------|------|-------|-------|-------|-------|-------|-------|-------|
| Number of tips | 41 | 26 | 7 | 38 | 21 | 41 | 1 | 1 | 1 | 9 | 11 | 7 | 28 | 5 | 11 | 11 |
| Number of interruptions | 3 | 3 | 2 | 2 | 1 | 2 | 0 | 0 | 0 | 1 | 3 | 3 | 3 | 2 | 2 | 2 |
| Vbowl (g) | 5.5 | 5.5 | 5.5 | 5.5 | 5.5 | 5.5 | 5.5 | 5.5 | 5.5 | 5.5 | 5.5 | 5.5 | 5.5 | 5.5 | 5.5 | 5.5 |
| Swdr (mm) | 2.46 | 1.56 | 0.42 | 2.28 | 1.26 | 2.46 | 0.06 | 0.06 | 0.06 | 0.54 | 0.66 | 0.42 | 1.68 | 0.30 | 0.66 | 0.66 |
| EAW (mm) | 0.15 | 0.15 | 0.1 | 0.1 | 0.1 | 0.1 | 0 | 0 | 0 | 0.05 | 0.15 | 0.15 | 0.15 | 0.1 | 0.1 | 0.1 |
| EEVAP (mm) | 0 | 0 | 0 | 0 | 0 | 0 | 0 | 0 | 0 | 0 | 0 | 0 | 0 | 0 | 0 | 0 |
| EUC (mm) | 0 | 0 | 0 | 0 | 0 | 0 | 0 | 0 | 0 | 0 | 0 | 0 | 0 | 0 | 0 | 0 |
| ERW (g) | 5.5 | 5.5 | 5.5 | 5.5 | 5.5 | 5.5 | 5.5 | 5.5 | 5.5 | 5.5 | 5.5 | 5.5 | 5.5 | 5.5 | 5.5 | 5.5 |
| ETIP (g/tip) | 0 | 0 | 0 | 0 | 0 | 0 | 0 | 0 | 0 | 0 | 0 | 0 | 0 | 0 | 0 | 0 |
| ETOT (mm) | 0.21 | 0.21 | 0.16 | 0.16 | 0.11 | 0.16 | 0.06 | 0.06 | 0.06 | 0.11 | 0.21 | 0.21 | 0.21 | 0.16 | 0.16 | 0.16 |
| eTOT (%) | 8.54 | 13.46 | 38.10 | 7.02 | 8.73 | 6.50 | 100 | 100 | 100 | 20.37 | 31.82 | 50.00 | 12.50 | 53.33 | 24.24 | 24.24 |

Event: From April 06, 2014 to April 28, 2014

Total horizontal rainfall : 85.10 mm

Average rainfall intensity : 1.23 mm/hr

Average air temperature : -5.54°C

Average relative humidity : 65.71%

Average wind speed at 10 m height : 4.94 m/s

Prevailing wind direction : South-west

| WDR gauge | SW1 | SW2 | SW3 | SW4 | SW5 | SW6 | W1 | N1 | N2 | E1 | E2 | E3 | E4 | E5 | E6 | SE1 |
|-------------------------|------|-------|-------|-------|-------|------|-------|-------|------|-------|-------|-------|-------|-------|------|-------|
| Number of tips | 70 | 36 | 27 | 77 | 36 | 71 | 258 | 14 | 110 | 92 | 95 | 61 | 178 | 89 | 87 | 21 |
| Number of interruptions | 4 | 6 | 4 | 11 | 9 | 5 | 6 | 8 | 11 | 10 | 12 | 10 | 12 | 12 | 7 | 6 |
| Vbowl (g) | 5.5 | 5.5 | 5.5 | 5.5 | 5.5 | 5.5 | 5.5 | 5.5 | 5.5 | 5.5 | 5.5 | 5.5 | 5.5 | 5.5 | 5.5 | 5.5 |
| Swdr (mm) | 4.20 | 2.16 | 1.62 | 4.62 | 2.16 | 4.26 | 15.48 | 0.84 | 6.60 | 5.52 | 5.70 | 3.66 | 10.68 | 5.34 | 5.22 | 1.26 |
| EAW (mm) | 0.2 | 0.3 | 0.2 | 0.55 | 0.45 | 0.25 | 0.3 | 0.4 | 0.55 | 0.5 | 0.6 | 0.5 | 0.6 | 0.6 | 0.35 | 0.3 |
| EEVAP (mm) | 0 | 0 | 0 | 0 | 0 | 0 | 0 | 0 | 0 | 0 | 0 | 0 | 0 | 0 | 0 | 0 |
| EUC (mm) | 0 | 0 | 0 | 0 | 0 | 0 | 0 | 0 | 0 | 0 | 0 | 0 | 0 | 0 | 0 | 0 |
| ERW (g) | 5.5 | 5.5 | 5.5 | 5.5 | 5.5 | 5.5 | 5.5 | 5.5 | 5.5 | 5.5 | 5.5 | 5.5 | 5.5 | 5.5 | 5.5 | 5.5 |
| ETIP (g/tip) | 0 | 0 | 0 | 0 | 0 | 0 | 0 | 0 | 0 | 0 | 0 | 0 | 0 | 0 | 0 | 0 |
| ETOT (mm) | 0.26 | 0.36 | 0.26 | 0.61 | 0.51 | 0.31 | 0.36 | 0.46 | 0.61 | 0.56 | 0.66 | 0.56 | 0.66 | 0.66 | 0.41 | 0.36 |
| eTOT (%) | 6.19 | 16.67 | 16.05 | 13.20 | 23.61 | 7.28 | 2.33 | 54.76 | 9.24 | 10.14 | 11.58 | 15.30 | 6.18 | 12.36 | 7.85 | 28.57 |

Event: From May 17, 2015 to June 03, 2015

Total horizontal rainfall : 62.0 mm

Average rainfall intensity : 0.90 mm/hr

Average air temperature : 14.16°C

Average relative humidity : 69.23%
 Average wind speed at 10 m height : 2.67 m/s
 Prevailing wind direction : South-west

| WDR gauge | SW1 | SW2 | SW3 | SW4 | SW5 | SW6 | W1 | N1 | N2 | E1 | E2 | E3 | E4 | E5 | E6 | SE1 |
|-------------------------|------|-------|-------|------|-------|------|-------|-------|-------|-------|------|-------|------|-------|------|------|
| Number of tips | 122 | 52 | 29 | 154 | 61 | 146 | 60 | 39 | 35 | 178 | 78 | 56 | 163 | 90 | 166 | 68 |
| Number of interruptions | 9 | 9 | 10 | 10 | 7 | 7 | 11 | 4 | 7 | 7 | 7 | 6 | 11 | 13 | 10 | 10 |
| Vbowl (g) | 5.5 | 5.5 | 5.5 | 5.5 | 5.5 | 5.5 | 5.5 | 5.5 | 5.5 | 5.5 | 5.5 | 5.5 | 5.5 | 5.5 | 5.5 | 5.5 |
| Swdr (mm) | 7.32 | 3.12 | 1.74 | 9.24 | 3.66 | 8.76 | 3.60 | 2.34 | 2.10 | 10.68 | 4.68 | 3.36 | 9.78 | 5.40 | 9.96 | 4.08 |
| EAW (mm) | 0.45 | 0.45 | 0.5 | 0.5 | 0.35 | 0.35 | 0.55 | 0.2 | 0.35 | 0.35 | 0.4 | 0.3 | 0.55 | 0.65 | 0.5 | 0.5 |
| EEVAP (mm) | 0 | 0 | 0 | 0 | 0 | 0 | 0 | 0 | 0 | 0 | 0 | 0 | 0 | 0 | 0 | 0 |
| EUC (mm) | 0 | 0 | 0 | 0 | 0 | 0 | 0 | 0 | 0 | 0 | 0 | 0 | 0 | 0 | 0 | 0 |
| ERW (g) | 5.5 | 5.5 | 5.5 | 5.5 | 5.5 | 5.5 | 5.5 | 5.5 | 5.5 | 5.5 | 5.5 | 5.5 | 5.5 | 5.5 | 5.5 | 5.5 |
| ETIP (g/tip) | 0 | 0 | 0 | 0 | 0 | 0 | 0 | 0 | 0 | 0 | 0 | 0 | 0 | 0 | 0 | 0 |
| ETOT (mm) | 0.51 | 0.51 | 0.56 | 0.56 | 0.41 | 0.41 | 0.61 | 0.26 | 0.41 | 0.41 | 0.41 | 0.36 | 0.61 | 0.71 | 0.56 | 0.56 |
| eTOT (%) | 6.97 | 16.35 | 32.18 | 6.06 | 11.20 | 4.68 | 16.94 | 11.11 | 19.52 | 3.84 | 8.76 | 10.71 | 6.24 | 13.15 | 5.62 | 13.7 |

HB Building, Montreal, QC

Event: From April 26, 2014 to May 04, 2014

Total horizontal rainfall : 79.40 mm
 Average rainfall intensity : 1.12 mm/hr
 Average air temperature : 8.84°C
 Average relative humidity : 76.99%
 Average wind speed at 10 m height : 2.60 m/s
 Prevailing wind direction : West-south-west

| WDR gauge | NW1 | NW2 | SW1 | SW2 | SW3 | SW4 | SW5 | SW6 | SW7 | SW8 | SW9 | SW10 | SE1 | SE2 | SE3 | SE4 |
|-------------------------|------|------|------|------|------|------|------|------|------|------|------|------|-------|------|-------|------|
| Number of tips | 49 | 54 | 115 | 27 | 50 | 21 | 46 | 22 | 56 | 36 | 0 | 32 | 169 | 86 | 228 | 53 |
| Number of interruptions | 5 | 6 | 11 | 11 | 6 | 10 | 9 | 9 | 8 | 9 | 0 | 7 | 5 | 9 | 5 | 6 |
| Vbowl (g) | 5.5 | 5.5 | 5.5 | 5.5 | 5.5 | 5.5 | 5.5 | 5.5 | 5.5 | 5.5 | 5.5 | 5.5 | 5.5 | 5.5 | 5.5 | 5.5 |
| Swdr (mm) | 2.94 | 3.24 | 6.90 | 1.62 | 3.00 | 1.26 | 2.76 | 1.32 | 3.36 | 2.16 | 0.00 | 1.92 | 10.14 | 5.16 | 13.68 | 3.18 |
| EAW (mm) | 0.25 | 0.3 | 0.55 | 0.55 | 0.3 | 0.5 | 0.45 | 0.45 | 0.4 | 0.45 | 0 | 0.35 | 0.25 | 0.45 | 0.25 | 0.3 |
| EEVAP (mm) | 0 | 0 | 0 | 0 | 0 | 0 | 0 | 0 | 0 | 0 | 0 | 0 | 0 | 0 | 0 | 0 |
| EUC (mm) | 0 | 0 | 0 | 0 | 0 | 0 | 0 | 0 | 0 | 0 | 0 | 0 | 0 | 0 | 0 | 0 |
| ERW (g) | 5.5 | 5.5 | 5.5 | 5.5 | 5.5 | 5.5 | 5.5 | 5.5 | 5.5 | 5.5 | 5.5 | 5.5 | 5.5 | 5.5 | 5.5 | 5.5 |
| ETIP (g/tip) | 0 | 0 | 0 | 0 | 0 | 0 | 0 | 0 | 0 | 0 | 0 | 0 | 0 | 0 | 0 | 0 |
| ETOT (mm) | 0.31 | 0.36 | 0.61 | 0.61 | 0.36 | 0.56 | 0.51 | 0.51 | 0.46 | 0.51 | 0.06 | 0.41 | 0.31 | 0.51 | 0.31 | 0.36 |
| eTOT (%) | 10.5 | 11.1 | 8.8 | 37.7 | 12.0 | 44.4 | 18.5 | 38.6 | 13.7 | 23.6 | | 21.4 | 3.1 | 9.9 | 2.3 | 11.3 |

Event: From June 11, 2014 to June 18, 2014

Total horizontal rainfall : 97.80 mm
 Average rainfall intensity : 2.0 mm/hr
 Average air temperature : 18.45°C
 Average relative humidity : 73.63%
 Average wind speed at 10 m height : 2.47 m/s
 Prevailing wind direction : East and South-east

| WDR gauge | NW1 | NW2 | SW1 | SW2 | SW3 | SW4 | SW5 | SW6 | SW7 | SW8 | SW9 | SW10 | SE1 | SE2 | SE3 | SE4 |
|-------------------------|-------|-------|-------|-------|-------|-------|-------|-------|-------|-------|------|-------|-------|------|-------|------|
| Number of tips | 5 | 6 | 168 | 35 | 45 | 20 | 36 | 26 | 37 | 31 | 0 | 14 | 317 | 144 | 347 | 125 |
| Number of interruptions | 1 | 3 | 10 | 7 | 7 | 4 | 6 | 9 | 8 | 9 | 0 | 5 | 7 | 7 | 7 | 10 |
| Vbowl (g) | 5.5 | 5.5 | 5.5 | 5.5 | 5.5 | 5.5 | 5.5 | 5.5 | 5.5 | 5.5 | 5.5 | 5.5 | 5.5 | 5.5 | 5.5 | 5.5 |
| Swdr (mm) | 0.30 | 0.36 | 10.08 | 2.10 | 2.70 | 1.20 | 2.16 | 1.56 | 2.22 | 1.86 | 0.00 | 0.84 | 19.02 | 8.64 | 20.82 | 7.50 |
| EAW (mm) | 0.05 | 0.15 | 0.5 | 0.35 | 0.35 | 0.2 | 0.3 | 0.45 | 0.4 | 0.45 | 0 | 0.25 | 0.35 | 0.35 | 0.35 | 0.5 |
| EEVAP (mm) | 0 | 0 | 0 | 0 | 0 | 0 | 0 | 0 | 0 | 0 | 0 | 0 | 0 | 0 | 0 | 0 |
| EUC (mm) | 0 | 0 | 0 | 0 | 0 | 0 | 0 | 0 | 0 | 0 | 0 | 0 | 0 | 0 | 0 | 0 |
| ERW (g) | 5.5 | 5.5 | 5.5 | 5.5 | 5.5 | 5.5 | 5.5 | 5.5 | 5.5 | 5.5 | 5.5 | 5.5 | 5.5 | 5.5 | 5.5 | 5.5 |
| ETIP (g/tip) | 0 | 0 | 0 | 0 | 0 | 0 | 0 | 0 | 0 | 0 | 0 | 0 | 0 | 0 | 0 | 0 |
| ETOT (mm) | 0.11 | 0.21 | 0.56 | 0.41 | 0.41 | 0.26 | 0.36 | 0.51 | 0.46 | 0.51 | 0.06 | 0.31 | 0.41 | 0.41 | 0.41 | 0.56 |
| eTOT (%) | 36.67 | 58.33 | 5.56 | 19.52 | 15.19 | 21.67 | 16.67 | 32.69 | 20.72 | 27.42 | | 36.90 | 2.16 | 4.75 | 1.97 | 7.47 |

Event: From August 12, 2014 to August 17, 2014

Total horizontal rainfall : 68.70 mm
 Average rainfall intensity : 1.53 mm/hr
 Average air temperature : 16.29°C
 Average relative humidity : 84.0%
 Average wind speed at 10 m height : 1.72 m/s
 Prevailing wind direction : West-south-west

| WDR gauge | NW1 | NW2 | SW1 | SW2 | SW3 | SW4 | SW5 | SW6 | SW7 | SW8 | SW9 | SW10 | SE1 | SE2 | SE3 | SE4 |
|-------------------------|-------|-------|-------|-------|-------|-------|-------|------|-------|-------|------|-------|------|------|-------|------|
| Number of tips | 7 | 7 | 10 | 58 | 82 | 37 | 72 | 61 | 80 | 47 | 0 | 41 | 148 | 53 | 176 | 63 |
| Number of interruptions | 2 | 1 | 2 | 6 | 9 | 5 | 8 | 6 | 10 | 8 | 0 | 7 | 5 | 4 | 5 | 6 |
| Vbowl (g) | 5.5 | 5.5 | 5.5 | 5.5 | 5.5 | 5.5 | 5.5 | 5.5 | 5.5 | 5.5 | 5.5 | 5.5 | 5.5 | 5.5 | 5.5 | 5.5 |
| Swdr (mm) | 0.42 | 0.42 | 0.60 | 3.48 | 4.92 | 2.22 | 4.32 | 3.66 | 4.80 | 2.82 | 0.00 | 2.46 | 8.88 | 3.18 | 10.56 | 3.78 |
| EAW (mm) | 0.1 | 0.05 | 0.1 | 0.3 | 0.45 | 0.25 | 0.4 | 0.3 | 0.5 | 0.4 | 0 | 0.35 | 0.25 | 0.2 | 0.25 | 0.3 |
| EEVAP (mm) | 0 | 0 | 0 | 0 | 0 | 0 | 0 | 0 | 0 | 0 | 0 | 0 | 0 | 0 | 0 | 0 |
| EUC (mm) | 0 | 0 | 0 | 0 | 0 | 0 | 0 | 0 | 0 | 0 | 0 | 0 | 0 | 0 | 0 | 0 |
| ERW (g) | 5.5 | 5.5 | 5.5 | 5.5 | 5.5 | 5.5 | 5.5 | 5.5 | 5.5 | 5.5 | 5.5 | 5.5 | 5.5 | 5.5 | 5.5 | 5.5 |
| ETIP (g/tip) | 0 | 0 | 0 | 0 | 0 | 0 | 0 | 0 | 0 | 0 | 0 | 0 | 0 | 0 | 0 | 0 |
| ETOT (mm) | 0.16 | 0.11 | 0.16 | 0.36 | 0.51 | 0.31 | 0.46 | 0.36 | 0.56 | 0.46 | 0.06 | 0.41 | 0.31 | 0.26 | 0.31 | 0.36 |
| eTOT (%) | 38.10 | 26.19 | 26.67 | 10.34 | 10.37 | 13.96 | 10.65 | 9.84 | 11.67 | 16.31 | | 16.67 | 3.49 | 8.18 | 2.94 | 9.52 |

Event: From October 04, 2014 to October 09, 2014

Total horizontal rainfall : 52.80 mm
 Average rainfall intensity : 1.32 mm/hr
 Average air temperature : 12.66°C
 Average relative humidity : 73.58%
 Average wind speed at 10 m height : 2.17 m/s
 Prevailing wind direction : West

| WDR gauge | NW1 | NW2 | SW1 | SW2 | SW3 | SW4 | SW5 | SW6 | SW7 | SW8 | SW9 | SW10 | SE1 | SE2 | SE3 | SE4 |
|-------------------------|-------|-------|-------|-------|-------|-------|------|-------|------|-------|------|-------|------|-------|------|------|
| Number of tips | 52 | 40 | 17 | 46 | 80 | 28 | 0 | 63 | 73 | 37 | 0 | 36 | 126 | 44 | 127 | 54 |
| Number of interruptions | 6 | 5 | 4 | 7 | 11 | 12 | 0 | 10 | 7 | 10 | 0 | 10 | 3 | 5 | 5 | 5 |
| Vbowl (g) | 5.5 | 5.5 | 5.5 | 5.5 | 5.5 | 5.5 | 5.5 | 5.5 | 5.5 | 5.5 | 5.5 | 5.5 | 5.5 | 5.5 | 5.5 | 5.5 |
| Swdr (mm) | 3.12 | 2.40 | 1.02 | 2.76 | 4.80 | 1.68 | 0.00 | 3.78 | 4.38 | 2.22 | 0.00 | 2.16 | 7.56 | 2.64 | 7.62 | 3.24 |
| EAW (mm) | 0.3 | 0.25 | 0.2 | 0.35 | 0.55 | 0.6 | 0 | 0.5 | 0.35 | 0.5 | 0 | 0.5 | 0.2 | 0.25 | 0.25 | 0.3 |
| EEVAP (mm) | 0 | 0 | 0 | 0 | 0 | 0 | 0 | 0 | 0 | 0 | 0 | 0 | 0 | 0 | 0 | 0 |
| EUC (mm) | 0 | 0 | 0 | 0 | 0 | 0 | 0 | 0 | 0 | 0 | 0 | 0 | 0 | 0 | 0 | 0 |
| ERW (g) | 5.5 | 5.5 | 5.5 | 5.5 | 5.5 | 5.5 | 5.5 | 5.5 | 5.5 | 5.5 | 5.5 | 5.5 | 5.5 | 5.5 | 5.5 | 5.5 |
| ETIP (g/tip) | 0 | 0 | 0 | 0 | 0 | 0 | 0 | 0 | 0 | 0 | 0 | 0 | 0 | 0 | 0 | 0 |
| ETOT (mm) | 0.36 | 0.31 | 0.26 | 0.41 | 0.61 | 0.66 | 0.06 | 0.56 | 0.41 | 0.56 | 0.06 | 0.56 | 0.21 | 0.31 | 0.31 | 0.31 |
| eTOT (%) | 11.54 | 12.92 | 25.49 | 14.86 | 12.71 | 39.29 | | 14.81 | 9.36 | 25.23 | | 25.93 | 2.78 | 11.74 | 4.07 | 9.57 |

Event: From November 22, 2014 to November 24, 2014

Total horizontal rainfall : 22.00 mm
 Average rainfall intensity : 1.69 mm/hr
 Average air temperature : 6.44°C
 Average relative humidity : 87.72%
 Average wind speed at 10 m height : 2.88 m/s
 Prevailing wind direction : West-south-west and East

| WDR gauge | NW1 | NW2 | SW1 | SW2 | SW3 | SW4 | SW5 | SW6 | SW7 | SW8 | SW9 | SW10 | SE1 | SE2 | SE3 | SE4 |
|-------------------------|-------|-------|------|------|-------|-------|------|-------|-------|-------|------|-------|------|------|------|------|
| Number of tips | 5 | 4 | 0 | 17 | 22 | 13 | 21 | 18 | 21 | 16 | 0 | 13 | 97 | 49 | 125 | 45 |
| Number of interruptions | 0 | 2 | 0 | 3 | 4 | 5 | 0 | 5 | 4 | 4 | 0 | 4 | 4 | 3 | 4 | 4 |
| Vbowl (g) | 5.5 | 5.5 | 5.5 | 5.5 | 5.5 | 5.5 | 5.5 | 5.5 | 5.5 | 5.5 | 5.5 | 5.5 | 5.5 | 5.5 | 5.5 | 5.5 |
| Swdr (mm) | 0.30 | 0.24 | 0.00 | 1.02 | 1.32 | 0.78 | 1.26 | 1.08 | 1.26 | 0.96 | 0.00 | 0.78 | 5.82 | 2.94 | 7.50 | 2.70 |
| EAW (mm) | 0 | 0.1 | 0 | 0.2 | 0.2 | 0.25 | 0 | 0.25 | 0.2 | 0.2 | 0 | 0.2 | 0.2 | 0.15 | 0.2 | 0.2 |
| EEVAP (mm) | 0 | 0 | 0 | 0 | 0 | 0 | 0 | 0 | 0 | 0 | 0 | 0 | 0 | 0 | 0 | 0 |
| EUC (mm) | 0 | 0 | 0 | 0 | 0 | 0 | 0 | 0 | 0 | 0 | 0 | 0 | 0 | 0 | 0 | 0 |
| ERW (g) | 5.5 | 5.5 | 5.5 | 5.5 | 5.5 | 5.5 | 5.5 | 5.5 | 5.5 | 5.5 | 5.5 | 5.5 | 5.5 | 5.5 | 5.5 | 5.5 |
| ETIP (g/tip) | 0 | 0 | 0 | 0 | 0 | 0 | 0 | 0 | 0 | 0 | 0 | 0 | 0 | 0 | 0 | 0 |
| ETOT (mm) | 0.06 | 0.16 | 0.06 | 0.21 | 0.26 | 0.31 | 0.06 | 0.31 | 0.26 | 0.26 | 0.06 | 0.26 | 0.26 | 0.21 | 0.26 | 0.26 |
| eTOT (%) | 20.00 | 66.67 | | 20.6 | 19.70 | 39.74 | 4.76 | 28.70 | 20.63 | 27.08 | | 33.33 | 4.47 | 7.14 | 3.47 | 9.63 |

Event: From May 25, 2015 to June 16, 2015

Total horizontal rainfall : 140.8 mm
 Average rainfall intensity : 1.68 mm/hr
 Average air temperature : 18.1°C
 Average relative humidity : 70.1%
 Average wind speed at 10 m height : 1.53 m/s
 Prevailing wind direction : West-south-west

| WDR gauge | NW1 | NW2 | SW1 | SW2 | SW3 | SW4 | SW5 | SW6 | SW7 | SW8 | SW9 | SW10 | SE1 | SE2 | SE3 | SE4 |
|-------------------------|------|------|------|------|------|------|------|------|------|------|------|------|-------|------|-------|------|
| Number of tips | 150 | 131 | 119 | 56 | 83 | 40 | 61 | 38 | 76 | 53 | 130 | 41 | 184 | 76 | 192 | 74 |
| Number of interruptions | 13 | 11 | 14 | 11 | 14 | 14 | 15 | 12 | 13 | 16 | 17 | 14 | 11 | 10 | 15 | 15 |
| Vbowl (g) | 5.5 | 5.5 | 5.5 | 5.5 | 5.5 | 5.5 | 5.5 | 5.5 | 5.5 | 5.5 | 5.5 | 5.5 | 5.5 | 5.5 | 5.5 | 5.5 |
| Swdr (mm) | 9.00 | 7.86 | 7.14 | 3.36 | 4.98 | 2.40 | 3.66 | 2.28 | 4.56 | 3.18 | 7.80 | 2.46 | 11.04 | 4.56 | 11.52 | 4.44 |
| EAW (mm) | 0.65 | 0.55 | 0.7 | 0.6 | 0.7 | 0.7 | 0.8 | 0.6 | 0.65 | 0.8 | 0.9 | 0.7 | 0.55 | 0.5 | 0.75 | 0.75 |
| EEVAP (mm) | 0 | 0 | 0 | 0 | 0 | 0 | 0 | 0 | 0 | 0 | 0 | 0 | 0 | 0 | 0 | 0 |
| EUC (mm) | 0 | 0 | 0 | 0 | 0 | 0 | 0 | 0 | 0 | 0 | 0 | 0 | 0 | 0 | 0 | 0 |
| ERW (g) | 5.5 | 5.5 | 5.5 | 5.5 | 5.5 | 5.5 | 5.5 | 5.5 | 5.5 | 5.5 | 5.5 | 5.5 | 5.5 | 5.5 | 5.5 | 5.5 |
| ETIP (g/tip) | 0 | 0 | 0 | 0 | 0 | 0 | 0 | 0 | 0 | 0 | 0 | 0 | 0 | 0 | 0 | 0 |
| ETOT (mm) | 0.71 | 0.61 | 0.76 | 0.61 | 0.76 | 0.76 | 0.81 | 0.66 | 0.71 | 0.86 | 0.91 | 0.76 | 0.61 | 0.56 | 0.81 | 0.81 |
| eTOT (%) | 7.9 | 7.8 | 10.6 | 18.2 | 15.3 | 31.7 | 22.1 | 28.9 | 15.6 | 27.0 | 11.7 | 30.9 | 5.5 | 12.3 | 7.0 | 18.2 |

FB Building, Montreal, QC

Event: From July 26, 2014 to August 07, 2014

Total horizontal rainfall : 53.40 mm
 Average rainfall intensity : 1.53 mm/hr
 Average air temperature : 21.11°C
 Average relative humidity : 70.20%
 Average wind speed at 10 m height : 1.80 m/s
 Prevailing wind direction : West-south-west

| WDR gauge | NE1 | NE2 | NE3 | NE4 | NE5 | NE6 | NE7 | NE8 | NE9 | NE10 | NW1 | SW1 | SW2 | SW3 | SW4 | SW5 | SW6 | SW7 | SE1 | SE2 | SE3 | SE4 | SE5 | SE6 |
|-------------------------|-------|------|-------|-------|------|-------|------|------|------|------|------|------|------|------|------|------|------|-------|-------|-------|------|------|-------|-------|
| Number of tips | 288 | 53 | 16 | 9 | 66 | 17 | 0 | 0 | 0 | 1 | 1 | 166 | 74 | 138 | 58 | 159 | 65 | 38 | 39 | 17 | 38 | 54 | 18 | 9 |
| Number of interruptions | 5 | 5 | 2 | 3 | 4 | 1 | 0 | 0 | 0 | 0 | 0 | 6 | 4 | 8 | 4 | 6 | 5 | 4 | 4 | 3 | 3 | 3 | 2 | 3 |
| Vbowl (g) | 5.5 | 5.5 | 5.5 | 5.5 | 5.5 | 5.5 | 5.5 | 5.5 | 5.5 | 5.5 | 5.5 | 5.5 | 5.5 | 5.5 | 5.5 | 5.5 | 5.5 | 5.5 | 5.5 | 5.5 | 5.5 | 5.5 | 5.5 | 5.5 |
| Swdr (mm) | 17.28 | 3.18 | 0.96 | 0.54 | 3.96 | 1.02 | 0.00 | 0.00 | 0.00 | 0.06 | 0.06 | 9.96 | 4.44 | 8.28 | 3.48 | 9.54 | 3.90 | 2.28 | 2.34 | 1.02 | 2.28 | 3.24 | 1.08 | 0.54 |
| EAW (mm) | 0.25 | 0.3 | 0.1 | 0.15 | 0.2 | 0.05 | 0 | 0 | 0 | 0 | 0 | 0.3 | 0.2 | 0.4 | 0.2 | 0.3 | 0.3 | 0.2 | 0.2 | 0.15 | 0.2 | 0.2 | 0.1 | 0.15 |
| EEVAP (mm) | 0 | 0 | 0 | 0 | 0 | 0 | 0 | 0 | 0 | 0 | 0 | 0 | 0 | 0 | 0 | 0 | 0 | 0 | 0 | 0 | 0 | 0 | 0 | 0 |
| EUC (mm) | 0 | 0 | 0 | 0 | 0 | 0 | 0 | 0 | 0 | 0 | 0 | 0 | 0 | 0 | 0 | 0 | 0 | 0 | 0 | 0 | 0 | 0 | 0 | 0 |
| ERW (g) | 5.5 | 5.5 | 5.5 | 5.5 | 5.5 | 5.5 | 5.5 | 5.5 | 5.5 | 5.5 | 5.5 | 5.5 | 5.5 | 5.5 | 5.5 | 5.5 | 5.5 | 5.5 | 5.5 | 5.5 | 5.5 | 5.5 | 5.5 | 5.5 |
| ETIP (g/tip) | 0 | 0 | 0 | 0 | 0 | 0 | 0 | 0 | 0 | 0 | 0 | 0 | 0 | 0 | 0 | 0 | 0 | 0 | 0 | 0 | 0 | 0 | 0 | 0 |
| ETOT (mm) | 0.31 | 0.31 | 0.16 | 0.21 | 0.26 | 0.11 | 0.06 | 0.06 | 0.06 | 0.06 | 0.06 | 0.36 | 0.26 | 0.46 | 0.26 | 0.36 | 0.31 | 0.26 | 0.26 | 0.21 | 0.21 | 0.21 | 0.16 | 0.21 |
| eTOT (%) | 1.79 | 9.75 | 16.67 | 38.89 | 6.57 | 10.78 | | | | 100 | 100 | 3.61 | 5.86 | 5.56 | 7.47 | 3.77 | 7.95 | 11.40 | 11.11 | 20.59 | 9.21 | 6.48 | 14.81 | 38.89 |

Event: From August 31, 2014 to September 06, 2014

Total horizontal rainfall : 27.90 mm
 Average rainfall intensity : 1.27 mm/hr

Average air temperature : 23.18°C
 Average relative humidity : 76.51%
 Average wind speed at 10 m height : 1.64 m/s
 Prevailing wind direction : West-south-west

| WDR gauge | NE1 | NE2 | NE3 | NE4 | NE5 | NE6 | NE7 | NE8 | NE9 | NE10 | NW1 | SW1 | SW2 | SW3 | SW4 | SW5 | SW6 | SW7 | SE1 | SE2 | SE3 | SE4 | SE5 | SE6 |
|-------------------------|------|-------|------|------|------|------|------|------|------|------|-------|------|-------|------|-------|------|-------|-------|-------|------|-------|-------|-------|------|
| Number of tips | 64 | 4 | 0 | 1 | 1 | 0 | 1 | 0 | 0 | 0 | 58 | 102 | 36 | 128 | 32 | 113 | 46 | 34 | 5 | 1 | 15 | 20 | 4 | 1 |
| Number of interruptions | 4 | 2 | 0 | 0 | 0 | 0 | 0 | 0 | 0 | 0 | 6 | 8 | 6 | 7 | 7 | 7 | 8 | 4 | 1 | 0 | 4 | 3 | 0 | 0 |
| Vbowl (g) | 5.5 | 5.5 | 5.5 | 5.5 | 5.5 | 5.5 | 5.5 | 5.5 | 5.5 | 5.5 | 5.5 | 5.5 | 5.5 | 5.5 | 5.5 | 5.5 | 5.5 | 5.5 | 5.5 | 5.5 | 5.5 | 5.5 | 5.5 | 5.5 |
| Swdr (mm) | 3.84 | 0.24 | 0.00 | 0.06 | 0.06 | 0.00 | 0.06 | 0.00 | 0.00 | 0.00 | 3.48 | 6.12 | 2.16 | 7.68 | 1.92 | 6.78 | 2.76 | 2.04 | 0.30 | 0.06 | 0.90 | 1.20 | 0.24 | 0.06 |
| EAW (mm) | 0.2 | 0.1 | 0 | 0 | 0 | 0 | 0 | 0 | 0 | 0 | 0.3 | 0.4 | 0.3 | 0.35 | 0.35 | 0.35 | 0.4 | 0.2 | 0.05 | 0 | 0.2 | 0.15 | 0 | 0 |
| EEVAP (mm) | 0 | 0 | 0 | 0 | 0 | 0 | 0 | 0 | 0 | 0 | 0 | 0 | 0 | 0 | 0 | 0 | 0 | 0 | 0 | 0 | 0 | 0 | 0 | 0 |
| EUC (mm) | 0 | 0 | 0 | 0 | 0 | 0 | 0 | 0 | 0 | 0 | 0 | 0 | 0 | 0 | 0 | 0 | 0 | 0 | 0 | 0 | 0 | 0 | 0 | 0 |
| ERW (g) | 5.5 | 5.5 | 5.5 | 5.5 | 5.5 | 5.5 | 5.5 | 5.5 | 5.5 | 5.5 | 5.5 | 5.5 | 5.5 | 5.5 | 5.5 | 5.5 | 5.5 | 5.5 | 5.5 | 5.5 | 5.5 | 5.5 | 5.5 | 5.5 |
| ETIP (g/tip) | 0 | 0 | 0 | 0 | 0 | 0 | 0 | 0 | 0 | 0 | 0 | 0 | 0 | 0 | 0 | 0 | 0 | 0 | 0 | 0 | 0 | 0 | 0 | 0 |
| ETOT (mm) | 0.26 | 0.16 | 0.06 | 0.06 | 0.06 | 0.06 | 0.06 | 0.06 | 0.06 | 0.06 | 0.36 | 0.46 | 0.36 | 0.41 | 0.41 | 0.41 | 0.46 | 0.26 | 0.11 | 0.06 | 0.26 | 0.21 | 0.06 | 0.06 |
| eTOT (%) | 6.77 | 66.67 | | 100 | 100 | | 100 | | | | 10.34 | 7.52 | 16.67 | 5.34 | 21.35 | 6.05 | 16.67 | 12.75 | 36.67 | 100 | 28.89 | 17.50 | 25.00 | 100 |

Event: From October 04, 2014 to October 09, 2014

Total horizontal rainfall : 65.10 mm
 Average rainfall intensity : 1.59 mm/hr
 Average air temperature : 12.87°C
 Average relative humidity : 74.52%
 Average wind speed at 10 m height : 2.19 m/s
 Prevailing wind direction : West-south-west

| WDR gauge | NE1 | NE2 | NE3 | NE4 | NE5 | NE6 | NE7 | NE8 | NE9 | NE10 | NW1 | SW1 | SW2 | SW3 | SW4 | SW5 | SW6 | SW7 | SE1 | SE2 | SE3 | SE4 | SE5 | SE6 |
|-------------------------|-------|-------|-------|-------|-------|-------|-------|-------|------|------|------|-------|------|------|------|-------|------|-------|-------|------|------|-------|------|-------|
| Number of tips | 190 | 13 | 5 | 8 | 25 | 2 | 26 | 12 | 0 | 0 | 39 | 233 | 79 | 0 | 63 | 251 | 109 | 70 | 206 | 96 | 141 | 201 | 71 | 31 |
| Number of interruptions | 6 | 5 | 2 | 5 | 5 | 0 | 3 | 3 | 0 | 0 | | 9 | 8 | 11 | 0 | 10 | 8 | 10 | 6 | 5 | 5 | 6 | 4 | 5 |
| Vbowl (g) | 5.5 | 5.5 | 5.5 | 5.5 | 5.5 | 5.5 | 5.5 | 5.5 | 5.5 | 5.5 | 5.5 | 5.5 | 5.5 | 5.5 | 5.5 | 5.5 | 5.5 | 5.5 | 5.5 | 5.5 | 5.5 | 5.5 | 5.5 | 5.5 |
| Swdr (mm) | 11.40 | 0.78 | 0.30 | 0.48 | 1.50 | 0.12 | 1.56 | 0.72 | 0.00 | 0.00 | 2.34 | 13.98 | 4.74 | 0.00 | 3.78 | 15.06 | 6.54 | 4.20 | 12.36 | 5.76 | 8.46 | 12.06 | 4.26 | 1.86 |
| EAW (mm) | 0.3 | 0.25 | 0.1 | 0.25 | 0.25 | 0 | 0.15 | 0.15 | 0 | 0 | 0 | 0.45 | 0.4 | 0.55 | 0 | 0.5 | 0.4 | 0.5 | 0.3 | 0.25 | 0.25 | 0.3 | 0.2 | 0.25 |
| EEVAP (mm) | 0 | 0 | 0 | 0 | 0 | 0 | 0 | 0 | 0 | 0 | 0 | 0 | 0 | 0 | 0 | 0 | 0 | 0 | 0 | 0 | 0 | 0 | 0 | 0 |
| EUC (mm) | 0 | 0 | 0 | 0 | 0 | 0 | 0 | 0 | 0 | 0 | 0 | 0 | 0 | 0 | 0 | 0 | 0 | 0 | 0 | 0 | 0 | 0 | 0 | 0 |
| ERW (g) | 5.5 | 5.5 | 5.5 | 5.5 | 5.5 | 5.5 | 5.5 | 5.5 | 5.5 | 5.5 | 5.5 | 5.5 | 5.5 | 5.5 | 5.5 | 5.5 | 5.5 | 5.5 | 5.5 | 5.5 | 5.5 | 5.5 | 5.5 | 5.5 |
| ETIP (g/tip) | 0 | 0 | 0 | 0 | 0 | 0 | 0 | 0 | 0 | 0 | 0 | 0 | 0 | 0 | 0 | 0 | 0 | 0 | 0 | 0 | 0 | 0 | 0 | 0 |
| ETOT (mm) | 0.36 | 0.31 | 0.16 | 0.31 | 0.31 | 0.06 | 0.21 | 0.21 | 0.06 | 0.06 | 0.06 | 0.51 | 0.46 | 0.61 | 0.06 | 0.56 | 0.46 | 0.56 | 0.36 | 0.31 | 0.31 | 0.36 | 0.26 | 0.31 |
| eTOT (%) | 3.16 | 39.74 | 53.33 | 64.58 | 20.67 | 50.00 | 13.46 | 29.17 | | | 2.56 | 3.65 | 9.70 | | 1.59 | 3.72 | 7.03 | 13.33 | 2.91 | 5.38 | 3.66 | 2.99 | 6.10 | 16.67 |

Event: From November 22, 2014 to November 24, 2014

Total horizontal rainfall : 20.80 mm

Average rainfall intensity : 2.08 mm/hr

Average air temperature : 6.91°C

Average relative humidity : 90.07%

Average wind speed at 10 m height : 2.34 m/s

Prevailing wind direction : South-south-west

| WDR gauge | NE1 | NE2 | NE3 | NE4 | NE5 | NE6 | NE7 | NE8 | NE9 | NE10 | NW1 | SW1 | SW2 | SW3 | SW4 | SW5 | SW6 | SW7 | SE1 | SE2 | SE3 | SE4 | SE5 | SE6 |
|-------------------------|------|-------|-------|-------|------|-------|------|-------|------|------|-------|------|-------|------|-------|------|-------|-------|------|------|------|------|------|------|
| Number of tips | 83 | 5 | 3 | 3 | 19 | 5 | 19 | 11 | 1 | 0 | 6 | 45 | 21 | 55 | 24 | 78 | 21 | 17 | 140 | 72 | 94 | 134 | 118 | 36 |
| Number of interruptions | 2 | 2 | 2 | 2 | 1 | 2 | 1 | 2 | 0 | 0 | 3 | 3 | 4 | 4 | 3 | 3 | 3 | 3 | 3 | 3 | 4 | 4 | 5 | 3 |
| Vbowl (g) | 5.5 | 5.5 | 5.5 | 5.5 | 5.5 | 5.5 | 5.5 | 5.5 | 5.5 | 5.5 | 5.5 | 5.5 | 5.5 | 5.5 | 5.5 | 5.5 | 5.5 | 5.5 | 5.5 | 5.5 | 5.5 | 5.5 | 5.5 | 5.5 |
| Swdr (mm) | 4.98 | 0.30 | 0.18 | 0.18 | 1.14 | 0.30 | 1.14 | 0.66 | 0.06 | 0.00 | 0.36 | 2.70 | 1.26 | 3.30 | 1.44 | 4.68 | 1.26 | 1.02 | 8.40 | 4.32 | 5.64 | 8.04 | 7.08 | 2.16 |
| EAW (mm) | 0.1 | 0.1 | 0.1 | 0.1 | 0.1 | 0.1 | 0.1 | 0.1 | 0 | 0 | 0.15 | 0.2 | 0.2 | 0.2 | 0.15 | 0.15 | 0.15 | 0.15 | 0.15 | 0.15 | 0.2 | 0.2 | 0.25 | 0.15 |
| EEVAP (mm) | 0 | 0 | 0 | 0 | 0 | 0 | 0 | 0 | 0 | 0 | 0 | 0 | 0 | 0 | 0 | 0 | 0 | 0 | 0 | 0 | 0 | 0 | 0 | 0 |
| EUC (mm) | 0 | 0 | 0 | 0 | 0 | 0 | 0 | 0 | 0 | 0 | 0 | 0 | 0 | 0 | 0 | 0 | 0 | 0 | 0 | 0 | 0 | 0 | 0 | 0 |
| ERW (g) | 5.5 | 5.5 | 5.5 | 5.5 | 5.5 | 5.5 | 5.5 | 5.5 | 5.5 | 5.5 | 5.5 | 5.5 | 5.5 | 5.5 | 5.5 | 5.5 | 5.5 | 5.5 | 5.5 | 5.5 | 5.5 | 5.5 | 5.5 | 5.5 |
| ETIP (g/tip) | 0 | 0 | 0 | 0 | 0 | 0 | 0 | 0 | 0 | 0 | 0 | 0 | 0 | 0 | 0 | 0 | 0 | 0 | 0 | 0 | 0 | 0 | 0 | 0 |
| ETOT (mm) | 0.16 | 0.16 | 0.16 | 0.16 | 0.11 | 0.16 | 0.11 | 0.16 | 0.06 | 0.06 | 0.21 | 0.21 | 0.26 | 0.26 | 0.21 | 0.21 | 0.21 | 0.21 | 0.21 | 0.21 | 0.26 | 0.26 | 0.31 | 0.21 |
| eTOT (%) | 3.21 | 53.33 | 88.89 | 88.89 | 9.65 | 53.33 | 9.65 | 24.24 | 100 | | 58.33 | 7.78 | 20.63 | 7.88 | 14.58 | 4.49 | 16.67 | 20.59 | 2.50 | 4.86 | 4.61 | 3.23 | 4.38 | 9.72 |

Event: From December 23, 2014 to December 28, 2014

Total horizontal rainfall : 35.30 mm
 Average rainfall intensity : 1.14 mm/hr
 Average air temperature : 4.96°C
 Average relative humidity : 84.24%
 Average wind speed at 10 m height : 2.12 m/s
 Prevailing wind direction : West-south-west

| WDR gauge | NE1 | NE2 | NE3 | NE4 | NE5 | NE6 | NE7 | NE8 | NE9 | NE10 | NW1 | SW1 | SW2 | SW3 | SW4 | SW5 | SW6 | SW7 | SE1 | SE2 | SE3 | SE4 | SE5 | SE6 |
|-------------------------|-------|-------|-------|-------|-------|-------|-------|-------|------|-------|-------|-------|-------|------|-------|------|-------|-------|-------|------|------|-------|------|------|
| Number of tips | 200 | 6 | 3 | 4 | 22 | 4 | 25 | 12 | 1 | 3 | 7 | 77 | 21 | 0 | 19 | 158 | 24 | 17 | 206 | 80 | 127 | 179 | 97 | 32 |
| Number of interruptions | 5 | 5 | 2 | 3 | 5 | 3 | 4 | 4 | 0 | 2 | 4 | 9 | 3 | 0 | 4 | 7 | 4 | 3 | 4 | 2 | 6 | 5 | 2 | 1 |
| Vbowl (g) | 5.5 | 5.5 | 5.5 | 5.5 | 5.5 | 5.5 | 5.5 | 5.5 | 5.5 | 5.5 | 5.5 | 5.5 | 5.5 | 5.5 | 5.5 | 5.5 | 5.5 | 5.5 | 5.5 | 5.5 | 5.5 | 5.5 | 5.5 | 5.5 |
| Swdr (mm) | 12.00 | 0.36 | 0.18 | 0.24 | 1.32 | 0.24 | 1.50 | 0.72 | 0.06 | 0.18 | 0.42 | 4.62 | 1.26 | 0.00 | 1.14 | 9.48 | 1.44 | 1.02 | 12.36 | 4.80 | 7.62 | 10.74 | 5.82 | 1.92 |
| EAW (mm) | 0.25 | 0.25 | 0.1 | 0.15 | 0.25 | 0.15 | 0.2 | 0.2 | 0 | 0.1 | 0.2 | 0.45 | 0.15 | 0 | 0.2 | 0.35 | 0.2 | 0.15 | 0.2 | 0.1 | 0.3 | 0.25 | 0.1 | 0.1 |
| EEVAP (mm) | 0 | 0 | 0 | 0 | 0 | 0 | 0 | 0 | 0 | 0 | 0 | 0 | 0 | 0 | 0 | 0 | 0 | 0 | 0 | 0 | 0 | 0 | 0 | 0 |
| EUC (mm) | 0 | 0 | 0 | 0 | 0 | 0 | 0 | 0 | 0 | 0 | 0 | 0 | 0 | 0 | 0 | 0 | 0 | 0 | 0 | 0 | 0 | 0 | 0 | 0 |
| ERW (g) | 5.5 | 5.5 | 5.5 | 5.5 | 5.5 | 5.5 | 5.5 | 5.5 | 5.5 | 5.5 | 5.5 | 5.5 | 5.5 | 5.5 | 5.5 | 5.5 | 5.5 | 5.5 | 5.5 | 5.5 | 5.5 | 5.5 | 5.5 | 5.5 |
| ETIP (g/tip) | 0 | 0 | 0 | 0 | 0 | 0 | 0 | 0 | 0 | 0 | 0 | 0 | 0 | 0 | 0 | 0 | 0 | 0 | 0 | 0 | 0 | 0 | 0 | 0 |
| ETOT (mm) | 0.31 | 0.31 | 0.16 | 0.21 | 0.31 | 0.21 | 0.26 | 0.26 | 0.06 | 0.16 | 0.26 | 0.51 | 0.21 | 0.06 | 0.26 | 0.41 | 0.26 | 0.21 | 0.26 | 0.16 | 0.36 | 0.31 | 0.16 | 0.11 |
| eTOT (%) | 2.58 | 86.11 | 88.89 | 87.50 | 23.48 | 87.50 | 17.33 | 36.11 | 100 | 88.89 | 61.90 | 11.04 | 16.67 | | 22.81 | 4.32 | 18.06 | 20.59 | 2.10 | 3.33 | 4.72 | 2.89 | 2.75 | 5.73 |

Event: From May 30, 2015 to June 10, 2015

Total horizontal rainfall : 45.2 mm
 Average rainfall intensity : 0.9 mm/hr
 Average air temperature : 15.98°C
 Average relative humidity : 69.03%

Average wind speed at 10 m height : 1.72 m/s

Prevailing wind direction : West

| WDR gauge | NE1 | NE2 | NE3 | NE4 | NE5 | NE6 | NE7 | NE8 | NE9 | NE10 | NW1 | SW1 | SW2 | SW3 | SW4 | SW5 | SW6 | SW7 | SE1 | SE2 | SE3 | SE4 | SE5 | SE6 |
|-------------------------|-------|-------|-------|-------|-------|-------|-------|-------|-------|------|------|-------|------|-------|-------|-------|------|------|------|-------|------|------|-------|-------|
| Number of tips | 75 | 25 | 6 | 7 | 34 | 4 | 26 | 13 | 4 | 0 | 115 | 186 | 77 | 232 | 67 | 296 | 106 | 108 | 84 | 34 | 104 | 130 | 36 | 14 |
| Number of interruptions | 11 | 10 | 5 | 6 | 9 | 3 | 9 | 7 | 2 | 0 | 10 | 9 | 7 | 11 | 9 | 10 | 3 | 3 | 6 | 3 | 7 | 10 | 4 | 3 |
| Vbowl (g) | 5.5 | 5.5 | 5.5 | 5.5 | 5.5 | 5.5 | 5.5 | 5.5 | 5.5 | 5.5 | 5.5 | 5.5 | 5.5 | 5.5 | 5.5 | 5.5 | 5.5 | 5.5 | 5.5 | 5.5 | 5.5 | 5.5 | 5.5 | 5.5 |
| Swdr (mm) | 4.50 | 1.50 | 0.36 | 0.42 | 2.04 | 0.24 | 1.56 | 0.78 | 0.24 | 0.00 | 6.90 | 11.16 | 4.62 | 13.92 | 4.02 | 17.76 | 6.36 | 6.48 | 5.04 | 2.04 | 6.24 | 7.80 | 2.16 | 0.84 |
| EAW (mm) | 0.55 | 0.5 | 0.25 | 0.3 | 0.45 | 0.15 | 0.45 | 0.35 | 0.1 | 0 | 0.5 | 0.45 | 0.35 | 0.55 | 0.45 | 0.5 | 0.15 | 0.15 | 0.3 | 0.15 | 0.35 | 0.5 | 0.2 | 0.15 |
| EEVAP (mm) | 0 | 0 | 0 | 0 | 0 | 0 | 0 | 0 | 0 | 0 | 0 | 0 | 0 | 0 | 0 | 0 | 0 | 0 | 0 | 0 | 0 | 0 | 0 | 0 |
| EUC (mm) | 0 | 0 | 0 | 0 | 0 | 0 | 0 | 0 | 0 | 0 | 0 | 0 | 0 | 0 | 0 | 0 | 0 | 0 | 0 | 0 | 0 | 0 | 0 | 0 |
| ERW (g) | 5.5 | 5.5 | 5.5 | 5.5 | 5.5 | 5.5 | 5.5 | 5.5 | 5.5 | 5.5 | 5.5 | 5.5 | 5.5 | 5.5 | 5.5 | 5.5 | 5.5 | 5.5 | 5.5 | 5.5 | 5.5 | 5.5 | 5.5 | 5.5 |
| ETIP (g/tip) | 0 | 0 | 0 | 0 | 0 | 0 | 0 | 0 | 0 | 0 | 0 | 0 | 0 | 0 | 0 | 0 | 0 | 0 | 0 | 0 | 0 | 0 | 0 | 0 |
| ETOT (mm) | 0.61 | 0.56 | 0.31 | 0.36 | 0.51 | 0.21 | 0.51 | 0.41 | 0.16 | 0.06 | 0.56 | 0.51 | 0.41 | 0.61 | 0.51 | 0.56 | 0.21 | 0.21 | 0.36 | 0.21 | 0.41 | 0.56 | 0.26 | 0.21 |
| eTOT (%) | 13.56 | 37.33 | 86.11 | 85.71 | 25.00 | 87.50 | 32.69 | 52.56 | 66.67 | | 8.12 | 4.57 | 8.87 | 4.38 | 12.69 | 3.15 | 3.30 | 3.24 | 7.14 | 10.29 | 6.57 | 7.18 | 12.04 | 25.00 |